GEM TN-91-25

GEM PAC Review

October 2, 1991

Abstract:
Transparencies from the GEM PAC Review at the SSCL on October 2, 1991 are presented.

B. Barish

GEM

(PAC - Oct 2, 1991)

GEM

(Outline - Morning)

1. Overview (Barish)

2. Magnet (Stroynowski)
   (Deis)

3. Calorimeters (Willis)
   (Newman)
   (Gordon)

4. Muons (Ahlen)

5. Inner Tracking (Baltay)

- Menu -

1. Electronics / DAQ / Computers (Marlow)
2. Engineering / Cost Methodology (Sanders)
3. Physics Performance (Lane)

An Expression of Interest to Construct a Major SSC Detector

July 8, 1991

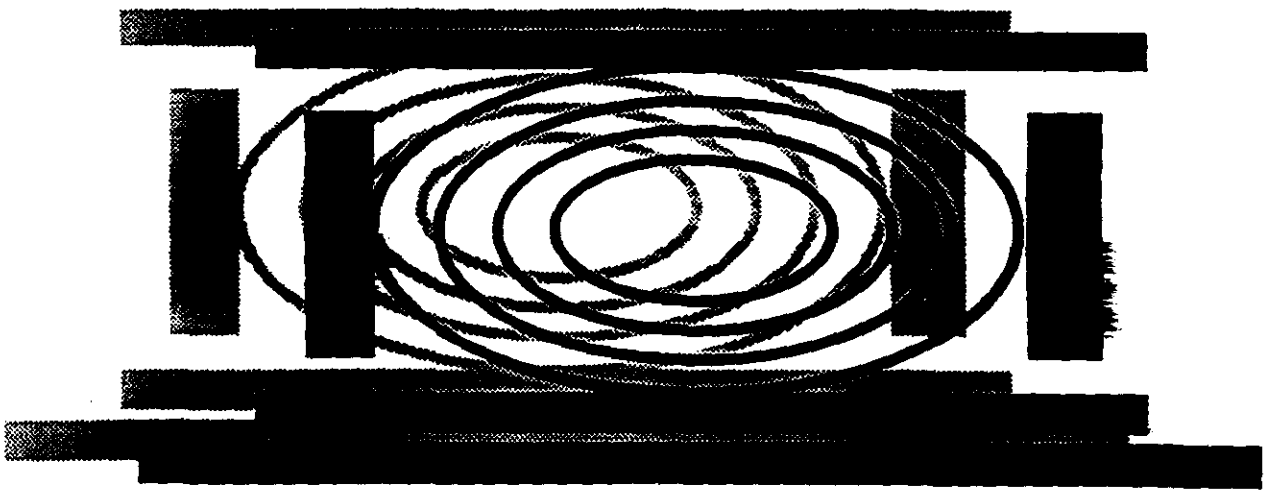

July 91 PAC

SDC, L*, E/T LOIs ⇒ *NO SINGLE DETECTOR* can guarantee that *ALL* 1 TeV physics possibilties and ***realities*** are covered with *PRECISION* !

Detector deficiencies are a direct consequence of ***detector design philosophy*** & ***emphasis***:

SDC: large tracking volume and surrounding solenoid with intervening material ⇒ degraded EM and Muon precision, much reduced capability at $\mathcal{L} > 10^{33}$.

Our Detector: open geometry emphasizing precision EM and Muon measurement ⇒ reduced central tracking ability.

⇓

⇓

COMPLEMENTARY DETECTORS !

PROPOSED PLAN

JULY 91
PAC

JUNE 91 - Collaboration Forms

JULY 91 - Submit EOI

Name Detector
Define Detector
Choose Technologies
} DECISIONS!

Nov 91 - Submit LOI

R+D
Engineering
Test Beams
(April 92 - Report for Hall Title II)

Nov 92 - Submit Eng/Design Report

This schedule stays on critical path!

- Hall kept on schedule
- Single Coil SC Magnet
- Needs R+D; Engineering Support

F

testf

gem

Gamma's

gem

Electrons

Muons

gem

July 91
PAC

Decisions before LOI

1) **HALL** to keep on schedule

2) **MAGNET** to proceed with Engineering Design.

3) **MUONS** - design tracking system
- pursue ≤ 2 technologies for FY92

4) **CALORIMETERS**

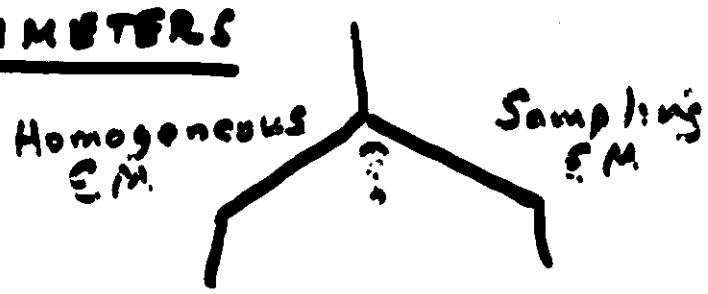

- pursue ≤ 2 techologies for calorimeter subsystems
- design, location, techologies for Forward Calorimeters

5) **TRACKER** - goals
- technologies to pursue.

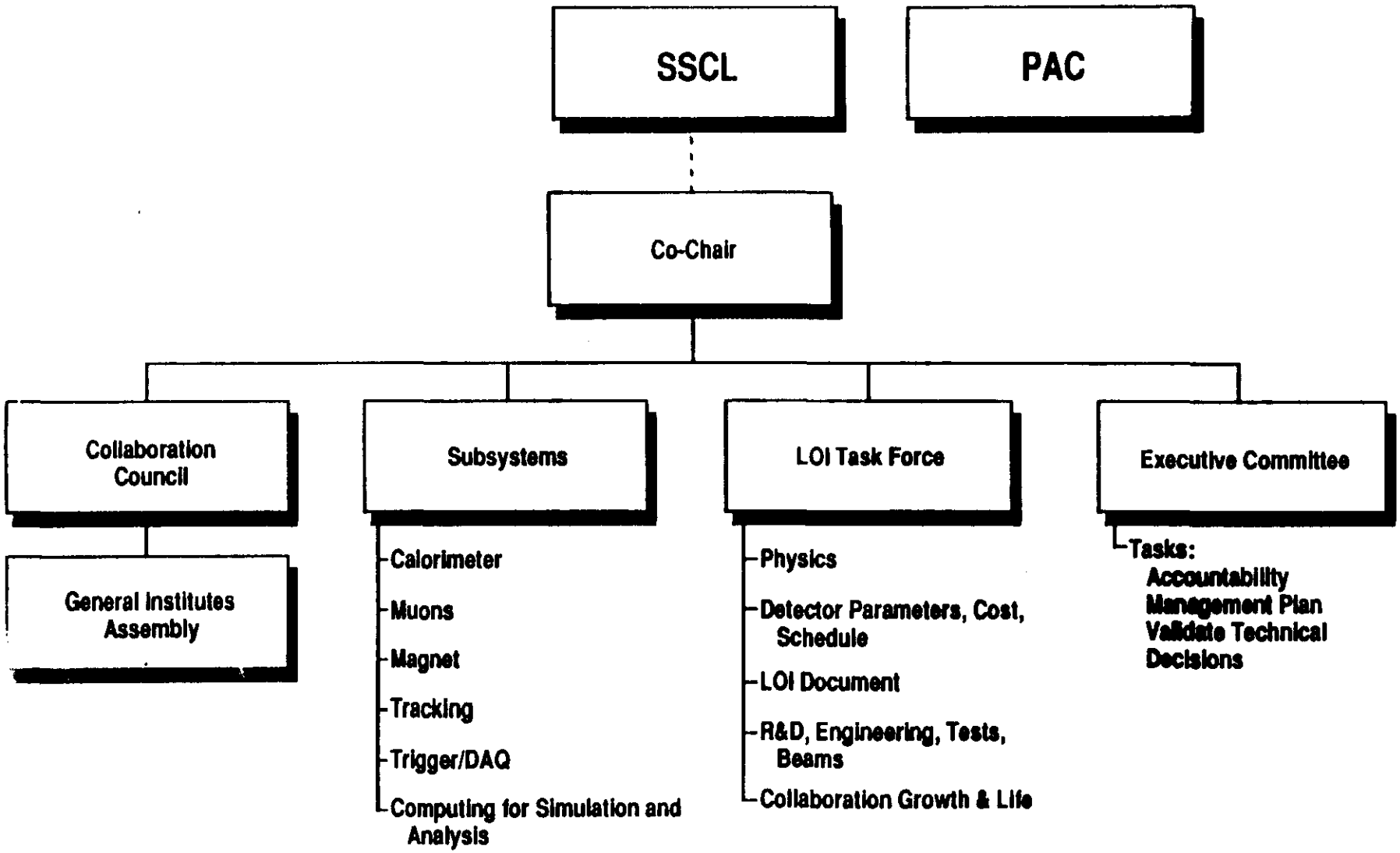
SSCL
PAC
Co-Chair
Collaboration Council
General Institutes Assembly
Subsystems
Calorimeter
Muons
Magnet
Tracking
Trigger/DAQ
Computing for Simulation and Analysis
LOI Task Force
Physics
Detector Parameters, Cost, Schedule
LOI Document
R&D, Engineering, Tests, Beams
Collaboration Growth & Life
Executive Committee
Tasks:
Accountability
Management Plan
Validate Technical Decisions

hd/7-17-91

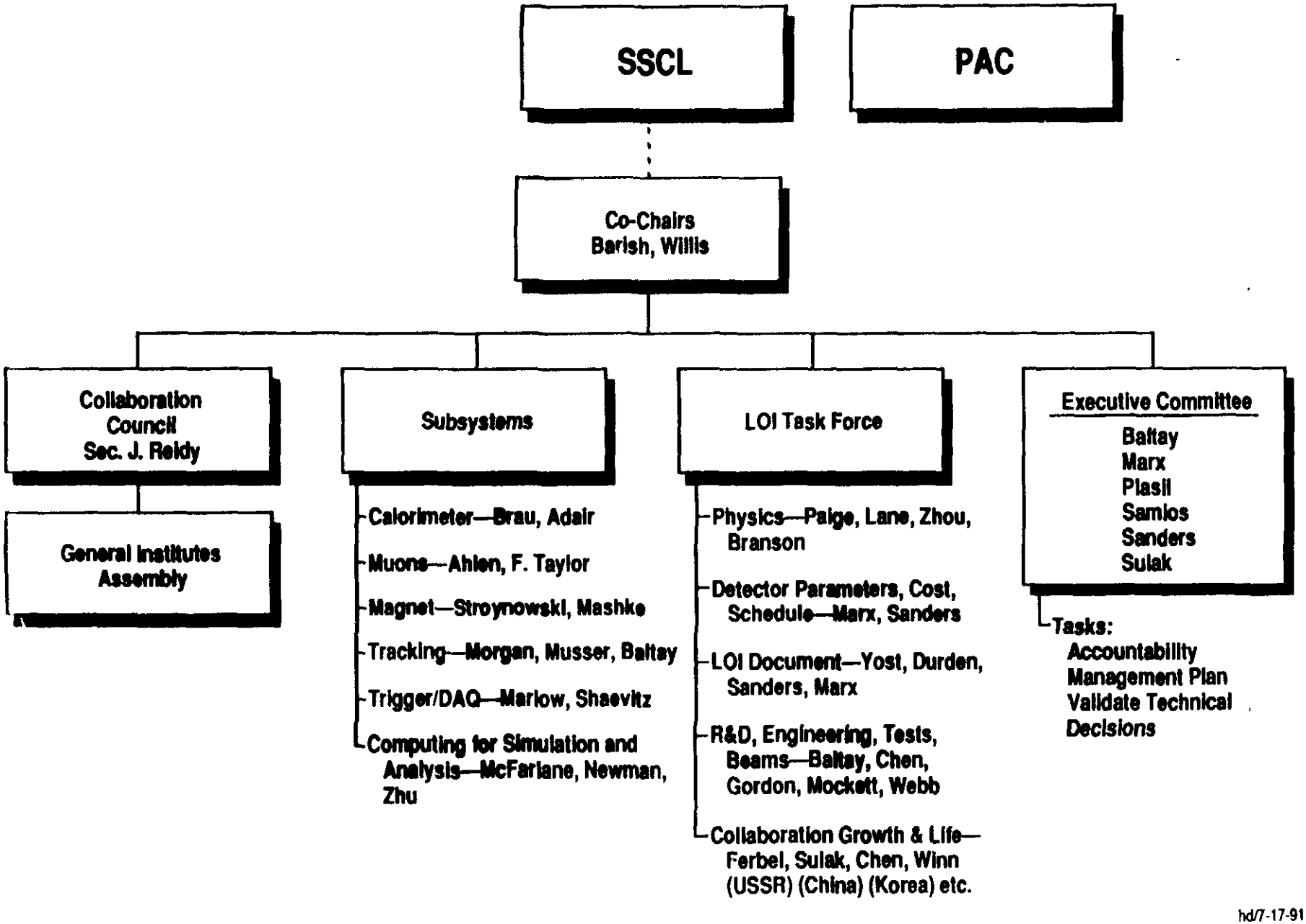
SSCL
PAC
Co-Chairs
Barish, Willis
Collaboration Council
Sec. J. Reidy
General Institutes Assembly
Subsystems
Calorimeter—Brau, Adair
Muons—Ahlen, F. Taylor
Magnet—Stroynowski, Mashke
Tracking—Morgan, Musser, Baltay
Trigger/DAQ—Marlow, Shaevitz
Computing for Simulation and Analysis—McFarlane, Newman, Zhu
LOI Task Force
Physics—Paige, Lane, Zhou, Branson
Detector Parameters, Cost, Schedule—Marx, Sanders
LOI Document—Yost, Durden, Sanders, Marx
R&D, Engineering, Tests, Beams—Baltay, Chen, Gordon, Mockett, Webb
Collaboration Growth & Life—Ferbel, Sulak, Chen, Winn (USSR) (China) (Korea) etc.
Executive Committee
Baltay
Marx
Plasil
Samios
Sanders
Sulak
Tasks:
Accountability
Management Plan
Validate Technical Decisions

hd/7-17-91

BASEPIE.XLC

GEM COST TARGETS (29 JULY 1991)
($ MILLIONS)

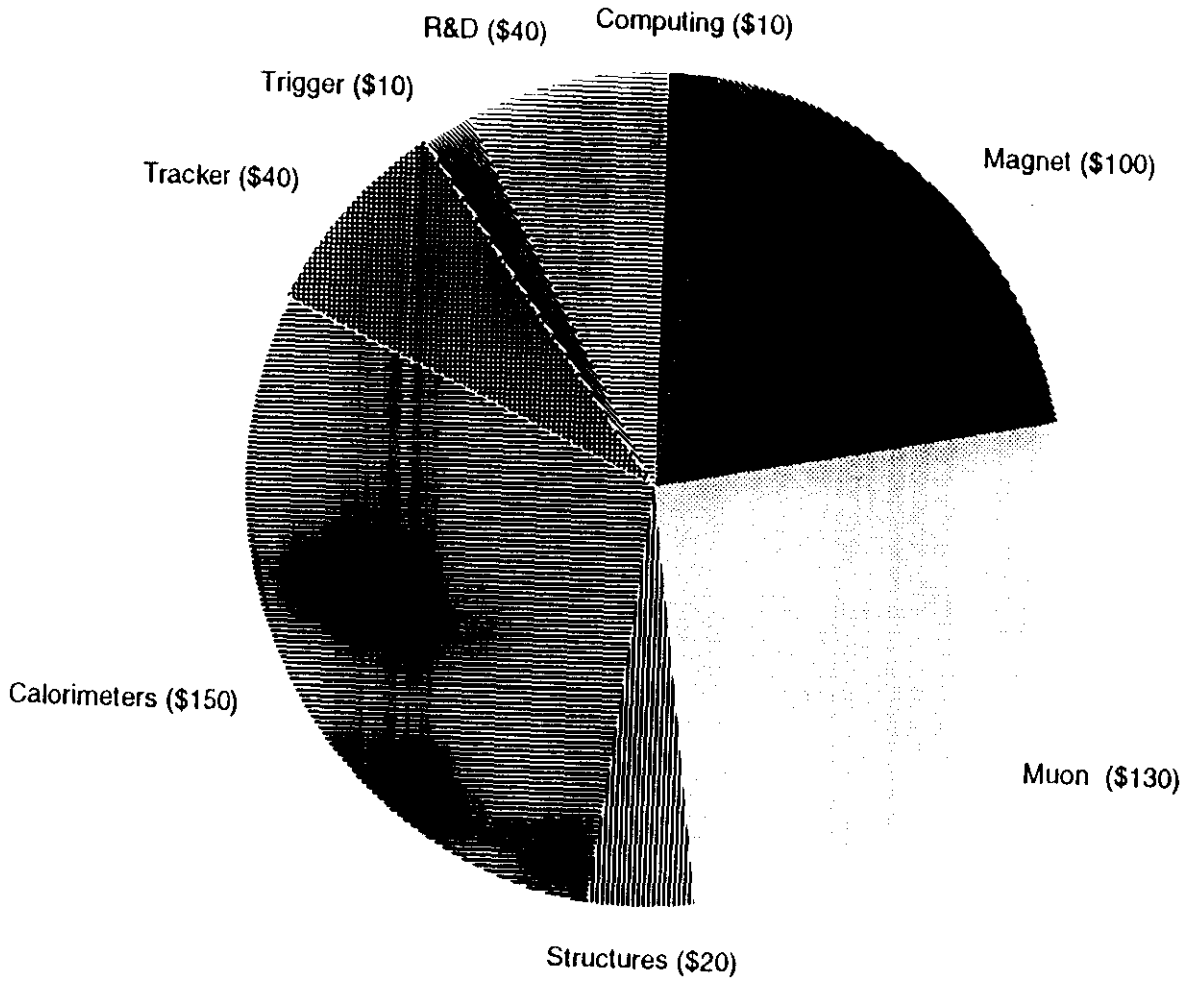

RIGHT VIEW
CABLE SHAFT
30.0 m
CRANE 100 T
26.2 m
ASSEMBLY SHAFT
2.95 m
8.0 m
SUPPORT CRADLE FOR DETECTOR

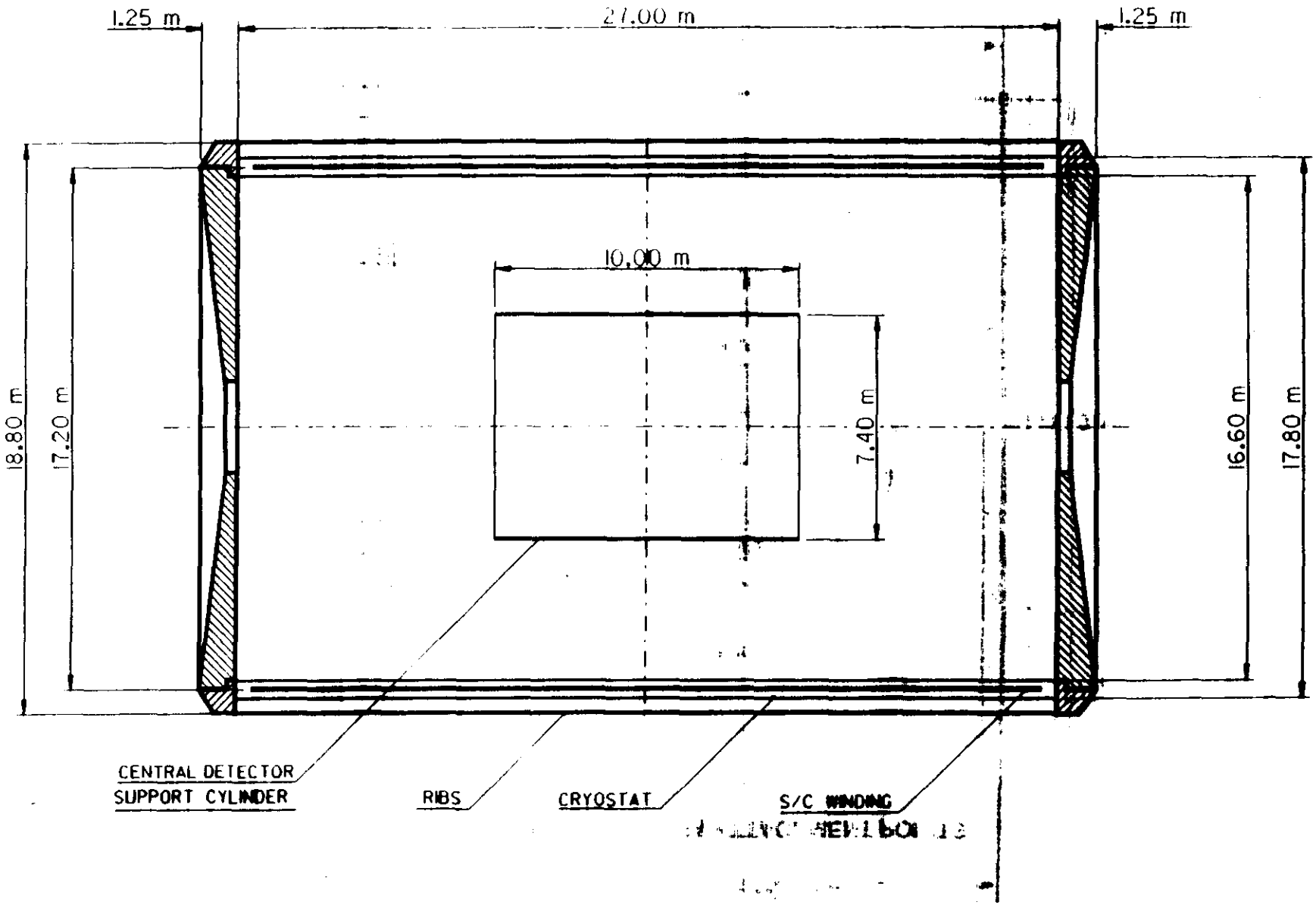
1.25 m
27.00 m
1.25 m
10.00 m
18.80 m
17.20 m
7.40 m
16.60 m
17.80 m
CENTRAL DETECTOR
SUPPORT CYLINDER
RIBS
CRYOSTAT
S/C WINDING

Magnet

1) Proceed with <u>Single</u> Superconducti
Coil Option

- Less Expensive (vs. Shielded)
- Minimal Technical Risk
- Can Build on Schedule

- - - - - - -

- Future Upgrades possible
(outside measurements)

- Improve Forward Direction
(shape field)

2) HFO Back-up

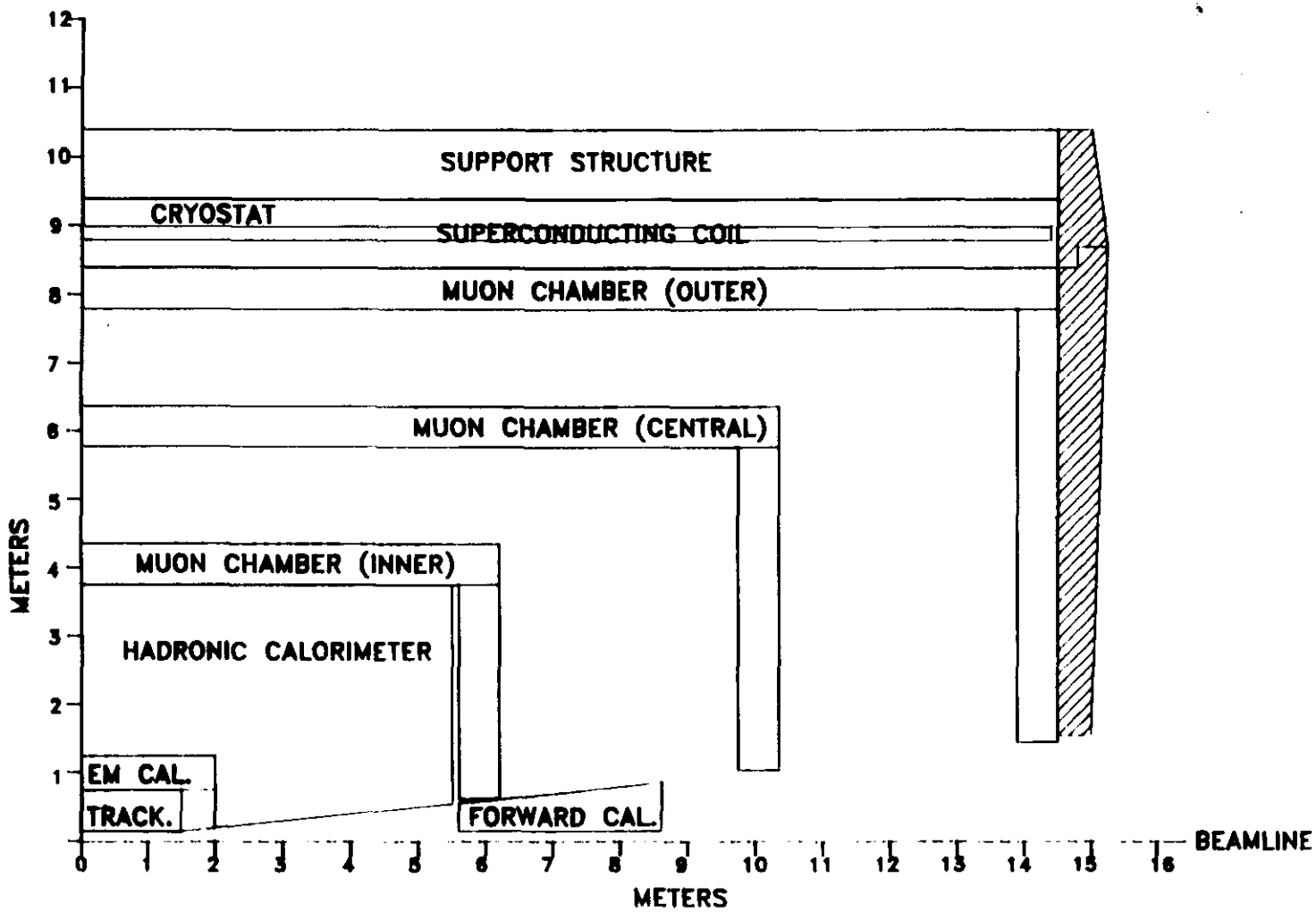

QUADRANT VIEW OF THE DETECTOR CONCEPT

Muons

- Evaluated various technologies

- Propose –

  Barrel: Drift Tubes
  (R+D to decide between)
  LSDT, PDT

  End Caps: Cathode Strip read-out
  Chambers (CSC's)

  Beam Cross Tag: RPC's
  (scintillator backup)

TECHNIQUE	ATTRIBUTES	DISADVANTAGES	R&D EFFORTS	REF.
		HOMOGENEOUS ELECTROMAGNETIC		
BaF_2 Crystals	Ultra-high resolution-stochastic term ~ 1.3%	Untested technology	Calibration & monitoring	1
	Fast – 3 ns peaking tail $<10^{-4}$ after 35 ns	Radiation damage unless pure to ppb level	Refining materials	
		Suppression of slow, dominant light-K-Cs-Te Photocathodes necessary	Photocathodes under development	
		Low density high Moliere radius = 2 - 4.7 cm degrades isolation cut		
		Expensive		
		Piping of 220 mm UV light to PM's axial to B-Field	UV prisms	
		Requires external preradiator		
Liquid Xenon	3 depth segmentation-angular resolution	Untested technology	Large area photodiodes	2
	Very high light production 10^7 γ/GeV	Expensive Availability- 8 yrs. of U.S. supply		
	Ultra-high resolution-stochastic term ~1%	Cryogenic dewar		
	Fast	Low density high Moliere radius = 2.7-5.6 cm degrades isolation cut	Light attenuation length Wall reflectivity	
	Potential γ/π^0 separation	VUV Light - 170 nm - reflective wall quality		
	Calibration with α's			

TECHNIQUE	ATTRIBUTES	DISADVANTAGES	R&D EFFORTS	REF.
		EM/HADRONIC		
Silicon	Ultra-high spatial/angular resolution	Very expensive	New production techniques	3
Liquid Argon	Mature technology	Dewar walls, supports etc.-degrade hermeticity	Detailed design	4
	Experience with construction of large systems	Speed/noise tradeoff-isolation cuts		
	Uniform response	Integration time-≥40ns; pileup	Fast shaping preamps	
	10^5 dynamic range	Preamps inside dewar-reliability/maintenance/hardness	Under test	
	Gain = 1	Cryogenic system	Detailed design	
	Simple calibration	Large sampling fraction e/h ~ 1.5 Positive ion buildup at high luminosity	1 mm Pb plate to be tested	
EM only:	$7\%/\sqrt{E} \oplus 0.5\%$ resolution for plate geometry	"Accordion" mechanics nontrivial for projective geometry. Large sampling fraction-long Lrad	Needs detailed design	5
Scintillating Fiber	Fast - σ_E and e/π in 16 ns trigger, 32 ns integration time	10 Mrad sensitivity i.e., lives 2 years @ 10^{34} @ $\eta <$ 3	O_2 influence Rate dependence	6
	Hermetic - no walls/supports/cracks	No intrinsic depth segmentation Short L_{rad} and L_{abs}	Fiber hardening	
	π/e rejection 10^3 via "electronic" segmentation Demonstrated performance		Construction techniques, cost effectiveness	
	Simple construction, modular, inexpensive	Calibration/monitoring	Detailed design	
	Uniform response ~ 0.5% over face			
EM only:	$6\%/\sqrt{E}$ demonstrated (JETSET) resolution for 50% fiber	Compensating 0.5 mm fiber Must tilt fibers at 3°	Under test	7

Calorimetry

- Highest achievable EM resolution
  - Two prong approach
    - ① BaF_2 + Scint. Hadronic
    - ② Liquid Argon/Krypton Accordian + Plate Hadronic

- Forward Calorimetry
- Preradiators

} = under study

INNER TRACKER

- Baseline = descoped L^* tracker (EOI)

1) Defined <u>Physics</u> Goals of Tracker

2) Technological Implications

3) Solutions under Investigation

FY92 - Engineering > Requests
R + D

Item	Engineering	R & D
Integration,Coordination,Costing	1.25	
Magnet	1.25	1.5
Muon System	.5	2.0
Calorimetry	.5	3.0
Tracking	.5	2.0
Trigger/ACQ		0.5
Reserve		1.0
Total	4.0	10.0

Assumes ability to <u>redistribute</u> R+D toward 'chosen' systems for FY92!

Plans

Goal: Techological Choices and Engineering/Design Report by Nov. '92.

R+D/Engineering Required

- Determined + Proposed by Novem
- Present Estimate (Eng + R+D)

Magnet	~6.0 M
Muons	~3.0 M
Calorimetry	~6.0
Tracker	~1.0
Elect.	~1.0
	~17.0 M

{~½ R+D
~½ Eng

Reliable Design to Cost

~ FEB/MARCH '92.

R. STROYNOWSKI /SMU

MAGNET

1. BASE-LINE DESIGN

SINGLE COIL SUPERCONDUCTING SOLENOID

INNER DIAMETER	[illegible] m
LENGTH	2.9 m
FIELD	[illegible] T

- DESIGN TEAM

  LLNL - LAWRENCE LIVERMORN NATIONAL LABORATORY

  MIT PLASMA FUSION MAGNET LABORATORY

  NATIONAL HIGH MAGNETIC FIELD LABORATORY (FLORIDA)

  + EXTENSIVE CONSULTATIONS FROM GEM MAGNET ADVISORY PANEL (MAGNET DESIGN EXPERTS FROM EUROPE, NATIONAL LABORATORIES AND INDUSTRY)

2. PARAMETERS

OPERATING CURRENT	52.5 kA
STORED ENERGY	[illegible] GJ
OVERALL OUTER DIAMETER	[illegible] m
CHARGE / DISCHARGE TIME	~2 h
EMERGENCY DISCHARGE TIME	~5 [illegible]

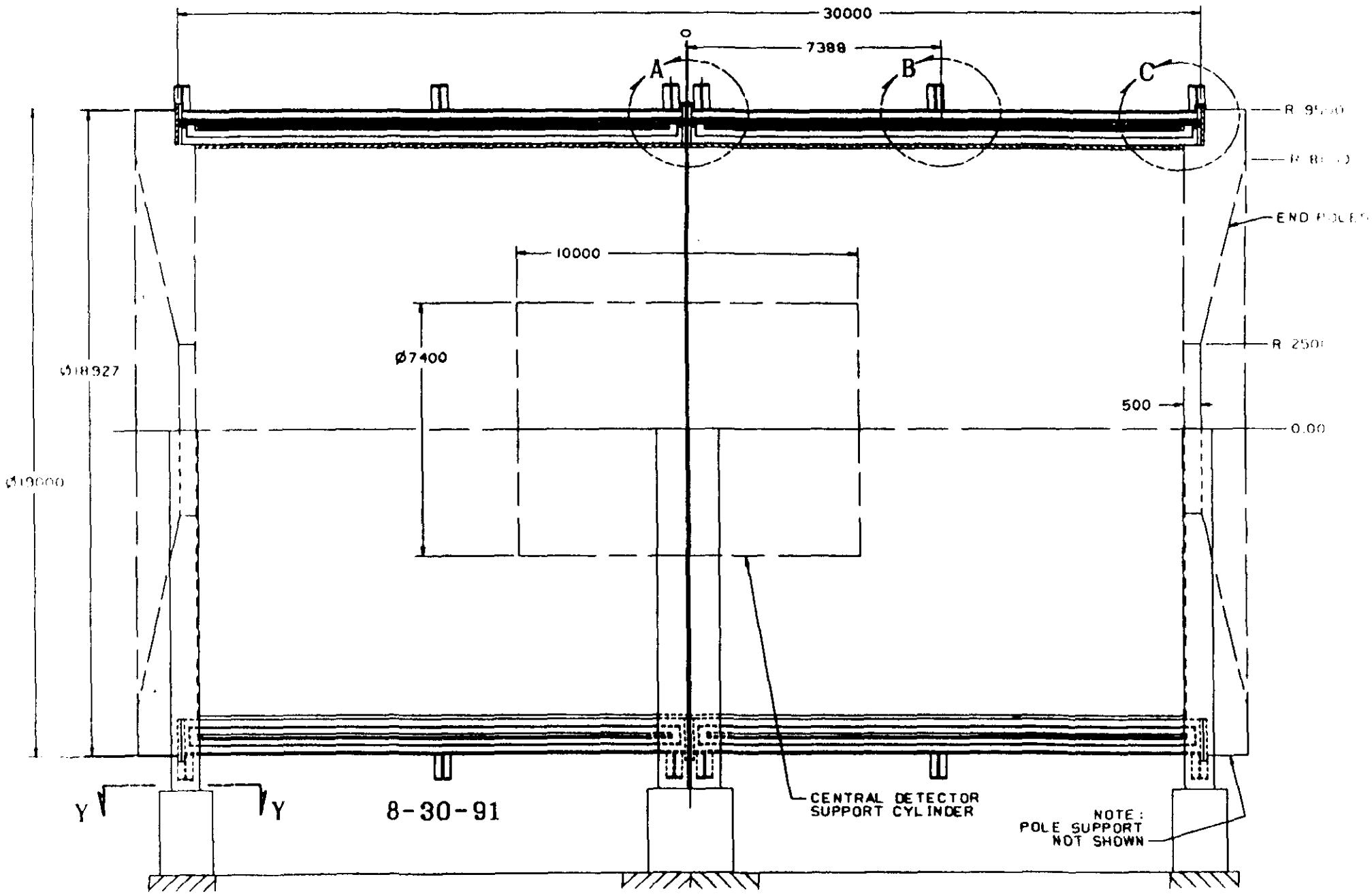
30000
7388
A
B
C
R 9500
R 8500
END POLES
10000
Ø7400
Ø18927
Ø19000
R 2500
500
0.00
Y
Y
8-30-91
CENTRAL DETECTOR
SUPPORT CYLINDER
NOTE:
POLE SUPPORT
NOT SHOWN

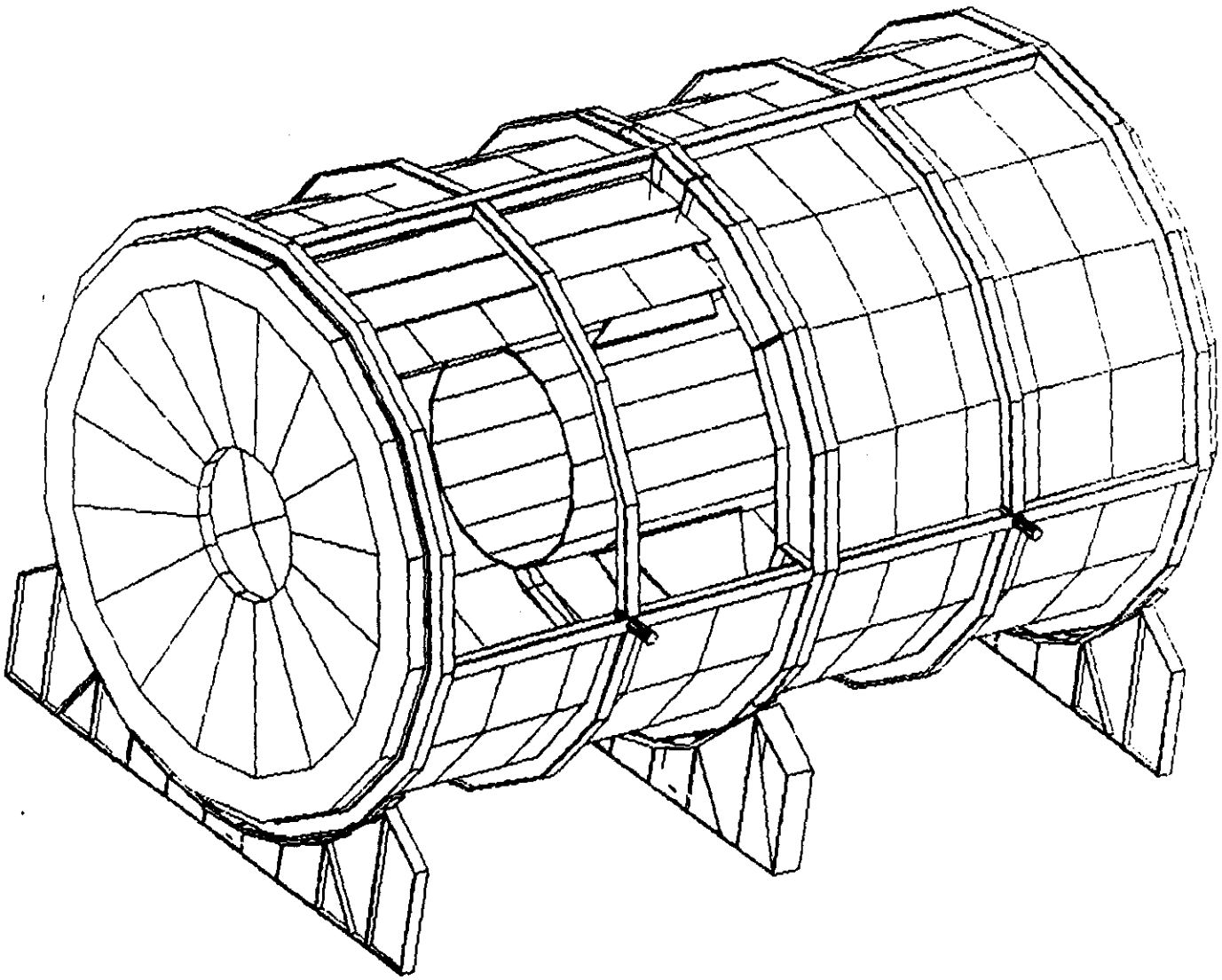

CONTOURS OF CONSTANT FLUX

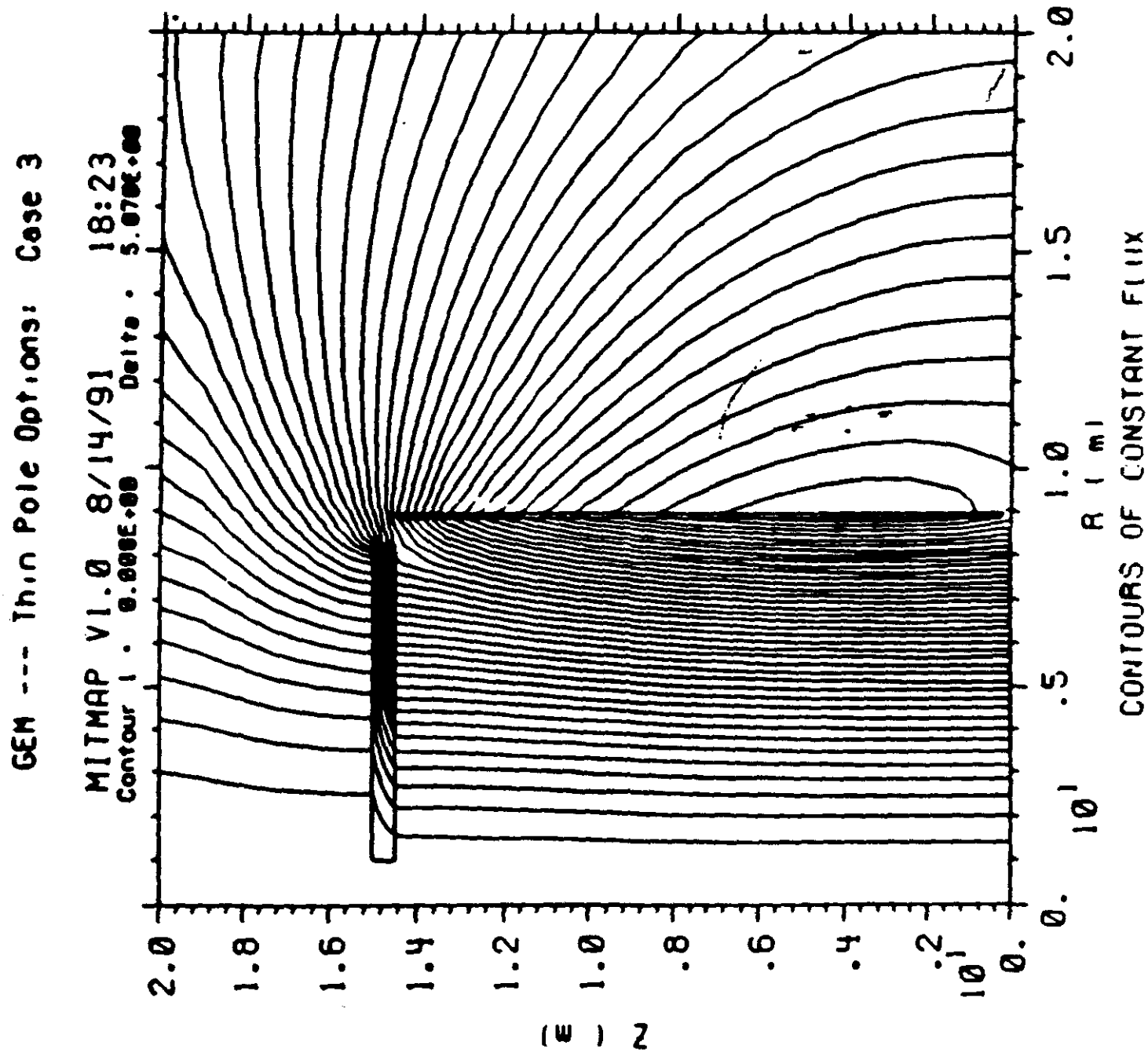

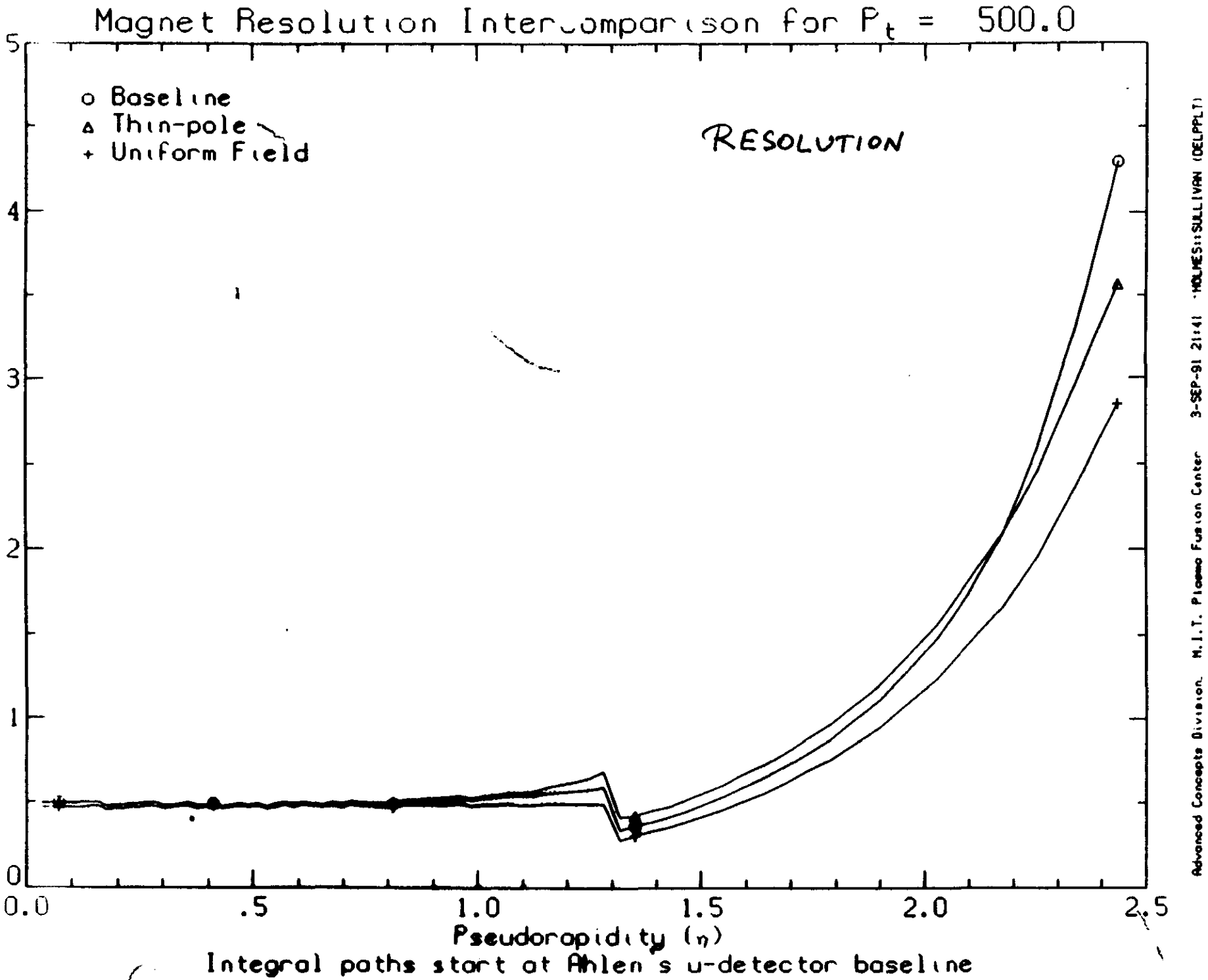
Magnet Resolution Intercomparison for P_t = 500.0
o Baseline
Δ Thin-pole
+ Uniform Field
RESOLUTION
0
1
2
3
4
5
0.0
.5
1.0
1.5
2.0
2.5
Pseudorapidity (η)
Integral paths start at Ahlen's u-detector baseline
Advanced Concepts Division M.I.T. Plasma Fusion Center 3-SEP-91 21:41 HOLMES::SULLIVAN (DELPPLT)

BASE LINE DESIGN

GEM Magnet Subsystem

Single-coil Design

Major Parameters List
Rev. 2
8/28/91

	Parameter	Symbol	Unit	Value	Ref.	Note	Rev
1.	Central Induction	Bi	T	0.80	-	1	1
2.	Mean radius of windings	Rw	m	8.9	6	2	1
3.	Outer Radius of outer cryostat vessel	Rv,o	m	9.463	6	2	1
4.	Inner Radius of inner cryostat vessel	Rv,i	m	8.4	6	2	1
5.	Inner Radius, magnet subsystem		m	8.3	1	2	1
6.	Coil length, end-to-end	Li	m	28.5	1	2	1
7.	Pole-to-pole inside length	L	m	29.0	1	-	1
8.	Cryostat vessel length (end-to-end)	Lv	m	30.0	1	2	1
9.	Conductor Length	Lc	km	24	1	2	1
10.	Total mass of windings	Mw	t	440	1	2	1
11.	Total mass cold structure (per half)	Mcs	t	330	6	2	1
12.	Total mass cryostat vessel(each half)	Mv	t	555	6	2	1
13.	Total mass iron end poles (each pole)	Mp	t	2950	1	2	1
14.	Radial pressure on windings	Pr	kPa	255	1	2	1
15.	Operating current	I	kA	52.5	9	3	2
16.	Stored Energy	Es	GJ	1.84	1	2	1
17.	Inductance	H	H	1.47	1	2	1
18.	Number of turns	Nt	#	408	9	3	2
19.	Thickness, inner thermal shield		m	0.100	6	-	1
20.	Thickness, inner cryostat	tv,i	m	0.019	6	-	1
21.	Outer radius, inner cryostat vessel	Rvi,o	m	8.419	6	-	1
22.	Inner radius, inner LN shield		m	8.649	6	-	1
23.	Outer radius, inner LN shield		m	8.651	6	-	1
24.	Inner radius, conductor		m	8.850	6	-	1
25.	Mean radius, conductor		m	8.900	6	-	1
26.	Outer radius, conductor		m	8.950	6	-	1
27.	Inner radius, bobbin		m	8.950	6	-	1
28.	Outer radius, bobbin		m	9.000	6	-	1
29.	Inner radius, outer LN shield		m	9.199	6	-	1
30.	Outer radius, outer LN shield		m	9.201	6	-	1
31.	Thickness, outer cryostat vessel	tv,o	m	0.0635	6	-	1
32.	Inner radius, outer cryostat vessel	Rvo,i	m	9.400	6	-	1
33.	Overall outer radius (outside ribs)	Ro	m	9.4635	-	-	1
34.	Depth of outer ribs		m	0.000	-	-	1
35.	Number of coil/cryostat assemblies		#	2	-	-	1
36.	Number of ribs per coil assembly		#	0	-	-	1
37.	Thickness of cryostat vessel ends		m	0.010	6	-	1
38.	Actual axial winding length per assembly		m	14.25	6	-	1
39.	Central membrane maximum z		m	0.025	6	-	1
40.	Cryostat inner end minimum z		m	0.025	6	-	1
41.	Cryostat inner end maximum z		m	0.125	6	-	1

	Parameter	Symbol	Unit	Value	Ref.	Note	Rev
42.	LN shield minimum z		m	0.162	6	-	1
43.	Bobbin minimum z		m	0.200	6	-	1
44.	Winding minimum z		m	0.250	6	-	1
45.	Winding maximum z		m	14.500	6	-	1
46.	Bobbin maximum z		m	14.600	6	-	1
47.	LN shield maximum z		m	14.750	6	-	1
48.	Cryostat outer end minimum z		m	14.900	6	-	1
49.	Cryostat outer end maximum z		m	15.000	6	-	1
50.	Pole face minimum z		m	14.500	1	-	1
51.	Number of turns		#	?	-	-	1
52.	Axial force on poles		N	63.5e6	3	-	1
53.	Axial force on conductor		N	27.9e6	7	-	1
54.	Mass of one muon sector		t	11.4	5	-	1
55.	Number of central muon sectors per half		#	16	5	-	1
56.	Radius of CG of central muon sectors		m	6.22	5	-	1
57.	Z-location of CG of central muon sectors		m	3.89	5	-	1
57.	Magnet axis height above hall floor		m	13.0	8	-	2

References

9. P Martson calculation 8/27/91
8. GCD - 000002 (7/25/91 version)
7. G. Dels notes, "Axial Force on Coil" 8/13/91
6. P Marston notes, 8/12/91
5. F. Nimblett estimates, 8/9/91
4. Obsolete
3. P. Marston calculation, per G. Dels
2. Obsolete
1. Second Detector EOI

Notes

3. 8/28/91 - Values revised from Ref1 values, based on more detailed design and calc's by P Martson.
2. 8/8/91 - Value revised from Ref1 value, based on more detailed design and calc's.
1. 8/8/91 - Ref 1 actually shows 0.823T, and historical number is 0.83T.

GEM Magnet Review Panel Members and Participants

September 25, 1991

September 4-6
September 25-27
October 10-11

Members

Peter Clee, Rutherford Appleton Laboratoy (second & third session)
Gary Deis, Lawrence Livermore National Laboratory
Mike Harris, SSC Laboratory
Alain Herve, CERN (only third session)
Coleman Johnson, Lawrence Livermore National Laboratory
Robert Johnson, JBc Associates
E. Klimenko, Kurchatov IAE
Dennis Lieurance, General Dynamics Space Systems
Peter Marston, Massachusetts Institute of Technology
Nickolai Martovetsky, Kurchatov IAE
John Miller, Lawrence Livermore National Laboratory
Bruce Montgomery, Massachusetts Institute of Technology (first session only)
Dr. Roberto Penco, Ensaldo Compontenti
Tom Prosapio, SSC Laboratory
Robert Richardson, SSC Laboratory
Dr. Gary Sanders, Los Alamos National Laboratory
Dr. Ray Stefanski, SSC Laboratory
Dr. Richard Stroynowski, Caltech High Energy Physics
Francois Wittgenstein, CERN (only second session)
Ronn Wooley, SSC Laboratory
Phil Sanger, SSC Laboratory
Don Edwards, SSC Labortory
Jon Ives, SSC Laboratory
George Mulholland, SSC Laboratory
Ted Kozman, SSC Laboratory

Participants

Howard Shaffer, Westinghouse Science & Technology Center
Sharad K. Singh, Westinghouse Science & Technology Center
Robert Swinderman, Pitt-Des Moines, Inc.
Yehia Eyssa, Babcox and Wilcox
Joe Heim, LLNL
Z. John Stekly, Intermag. Gen. Corp.

SHIELDED VS UNSHIELDED MAGNET OPTIONS

	COST	TIME SCALE	RISK
SINGLE COIL	1.0	END OF 1996	
DOUBLE COIL	1.5	+1 YEAR	FORCES BETWEEN COIL
SINGLE COIL + IRON	1.9	+1 YEAR	STRESSES + ACCESS

ISSUES OF UNSHIELDED MAGNET

HEALTH AND SAFETY (R. WOOLLEY REPORT)

a) NO REGULATORY LIMITS FOR WORKING IN FIELDS < 20 KGAUSS FOR SHORT PERIODS OF TIME (LIMITS ON WEEKLY EXPOSURES)

b) PEOPLE WITH PACEMAKERS AND METALLIC PROSTHESES CAN NOT BE EXPOSED TO FIELDS > 10 GAUSS

c) OPERATION OF SOME EQUIPMENT MAY BE AFFECTED. LOCAL SHIELDING MAY BE REQUIRED.

d) FAA SHOULD BE NOTIFIED OF POSSIBLE MAGNETIC ANOMALY

Safety & Health Effects

R.P.Woolley

Table 4. Sensitivity of Equipment and Component

	>5 G	>10 G	>100 G	>1000 G
Data Acquisition System				
Computer	x			
Monitors				
Black & white		x		
Color	x			
Instrumentation & Control				
Relay			x	
Solid-state device			x	
Magnetic solenoids, valves			x	
Safety device				x
Analog display			x	
Vacuum & Refrigerator				
Mechanical pump			x	
Turbo pump			x	
Electric motors			x	
Ferro-fluidic seals				x

x: shielding is needed

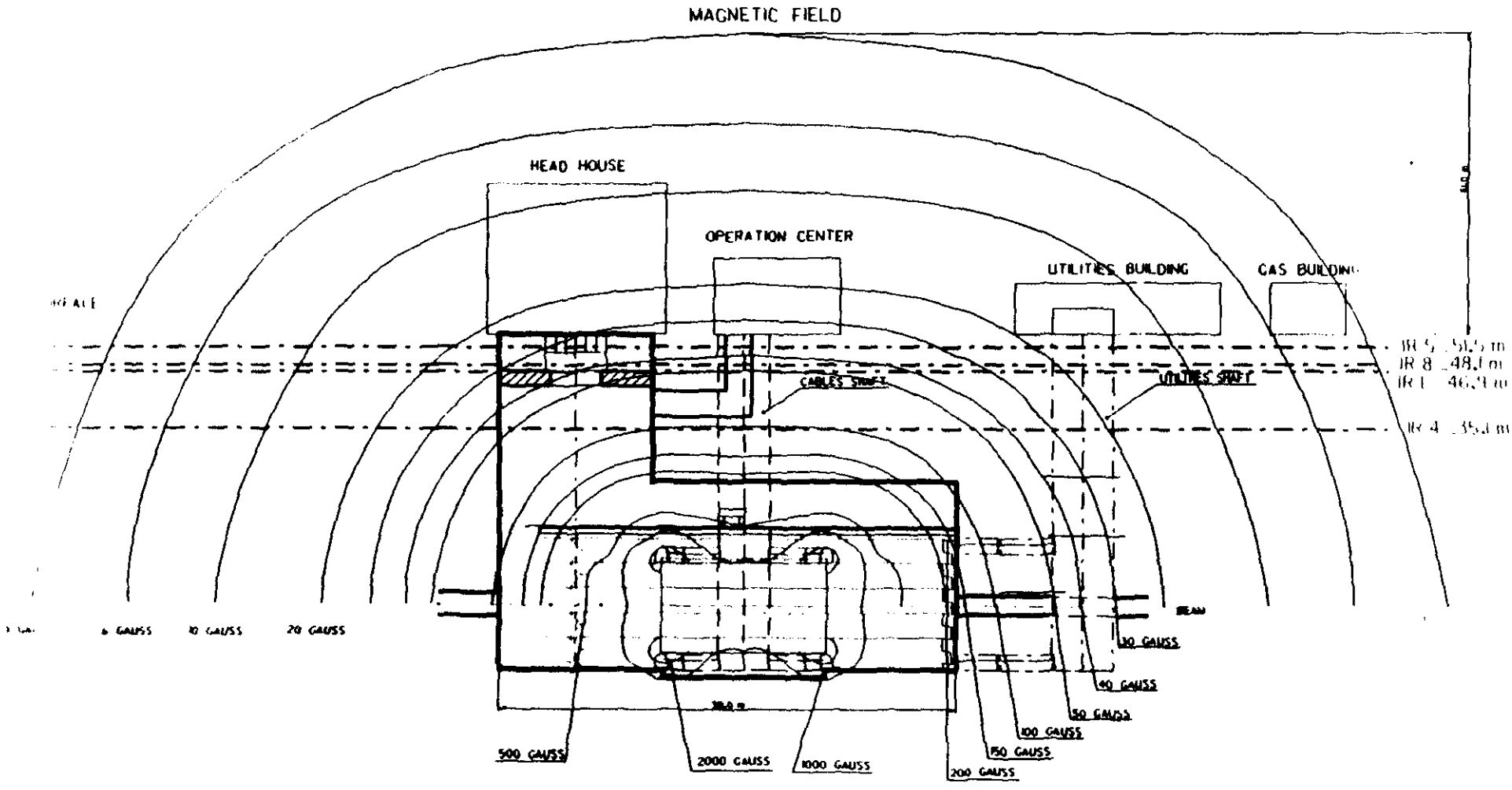
MAGNETIC FIELD
HEAD HOUSE
OPERATION CENTER
UTILITIES BUILDING
GAS BUILDING
CABLES SHAFT
UTILITIES SHAFT
BEAM
6 GAUSS
10 GAUSS
20 GAUSS
30 GAUSS
40 GAUSS
50 GAUSS
100 GAUSS
150 GAUSS
200 GAUSS
500 GAUSS
2000 GAUSS
1000 GAUSS

- [illegible]

- AREA WITH FIELD >10 GAUSS [illegible]
  [illegible]
  [illegible]
  [illegible]
  HFTF, MFTF, FENIX AT LLNL
  ALCATOR C-MOD AT MIT
  15' BUBBLE CHAMBER AT FNAL
  LCT AT OAK RIDGE NL
  MRI FACILITIES AT HOSPITALS

- FIELD ~1 GAUSS AT HIGHT OF ~60 m
- NO OBVIOUS OTHER HEALTH HAZARDS

• OPTIONS UNDER STUDY
  - FENCE AROUND 5 GAUSS PERIMETER
  - RESTRICTED ACCESS FOR PEOPLE WITH PACEMAKERS
  - SHIELDING OF THE COUNTING HOUSE (~$150k)

  - SHIELDING OF SURFACE WITH IRON PLATES
    [illegible] ~$5M
    (BACKUP OPTION, CAN BE PUT IN LATER)

  - BUILD A HILL ~50 m HIGH

Thick pole design

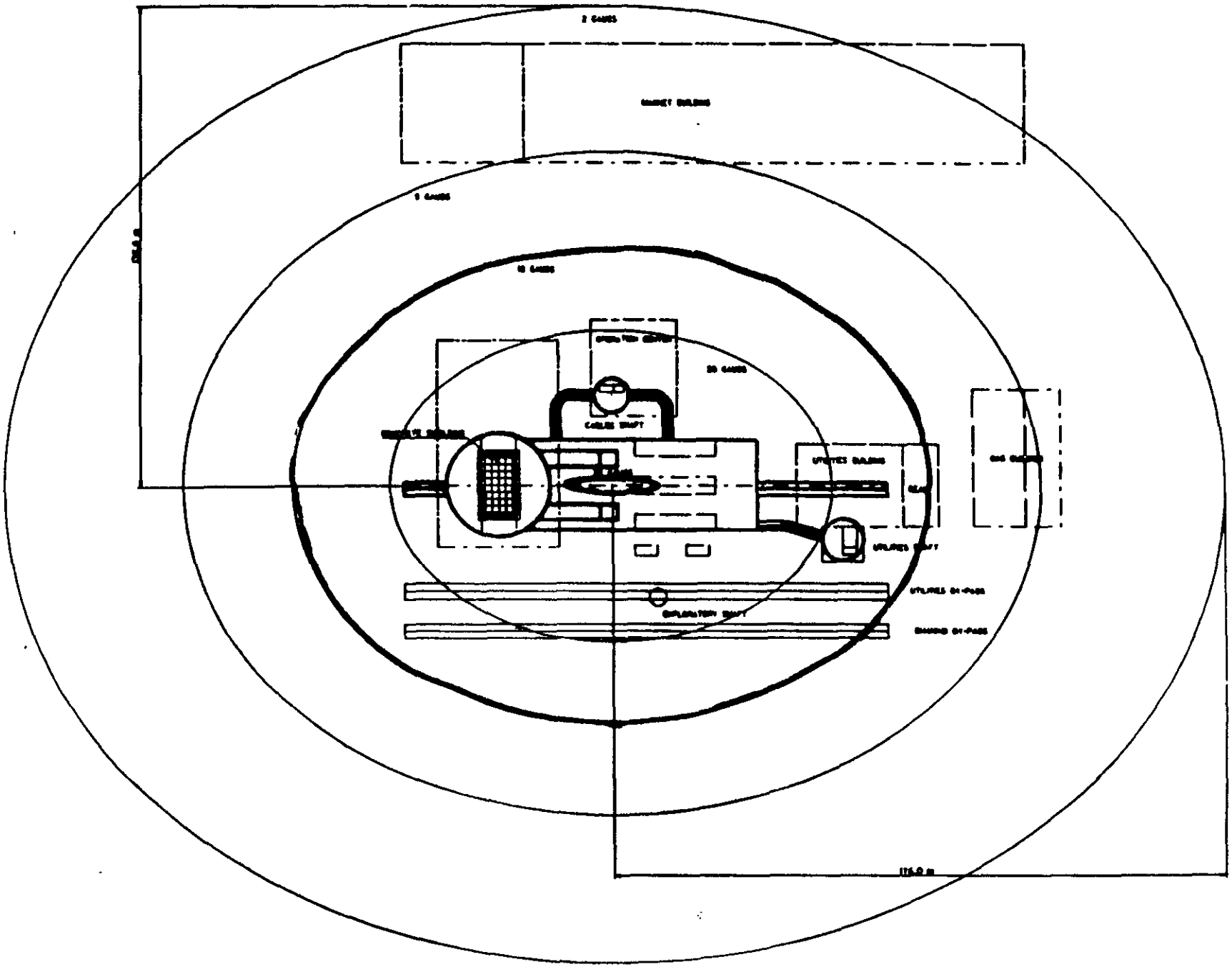

FIELD SIZE COMPARISON

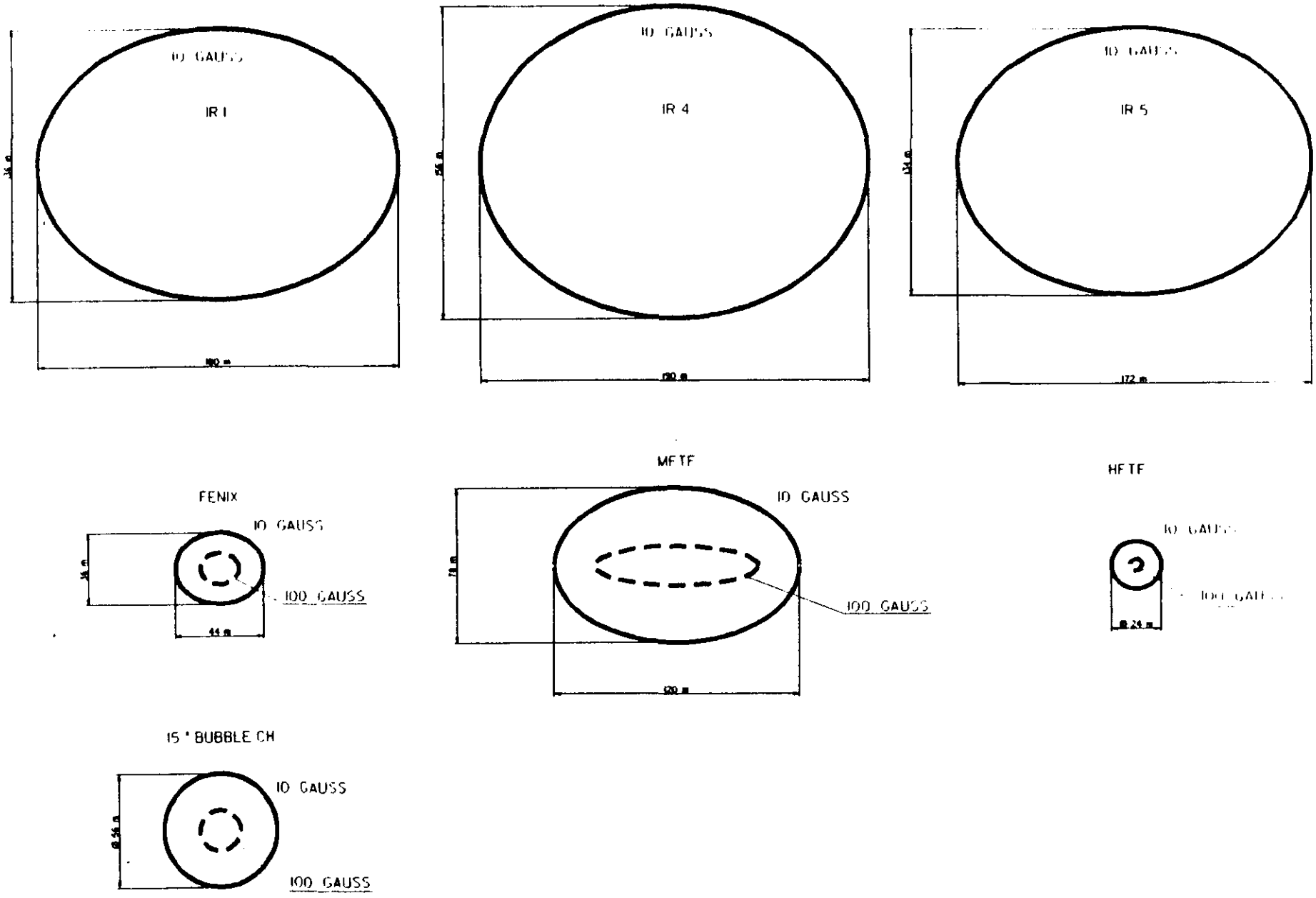

MFTF

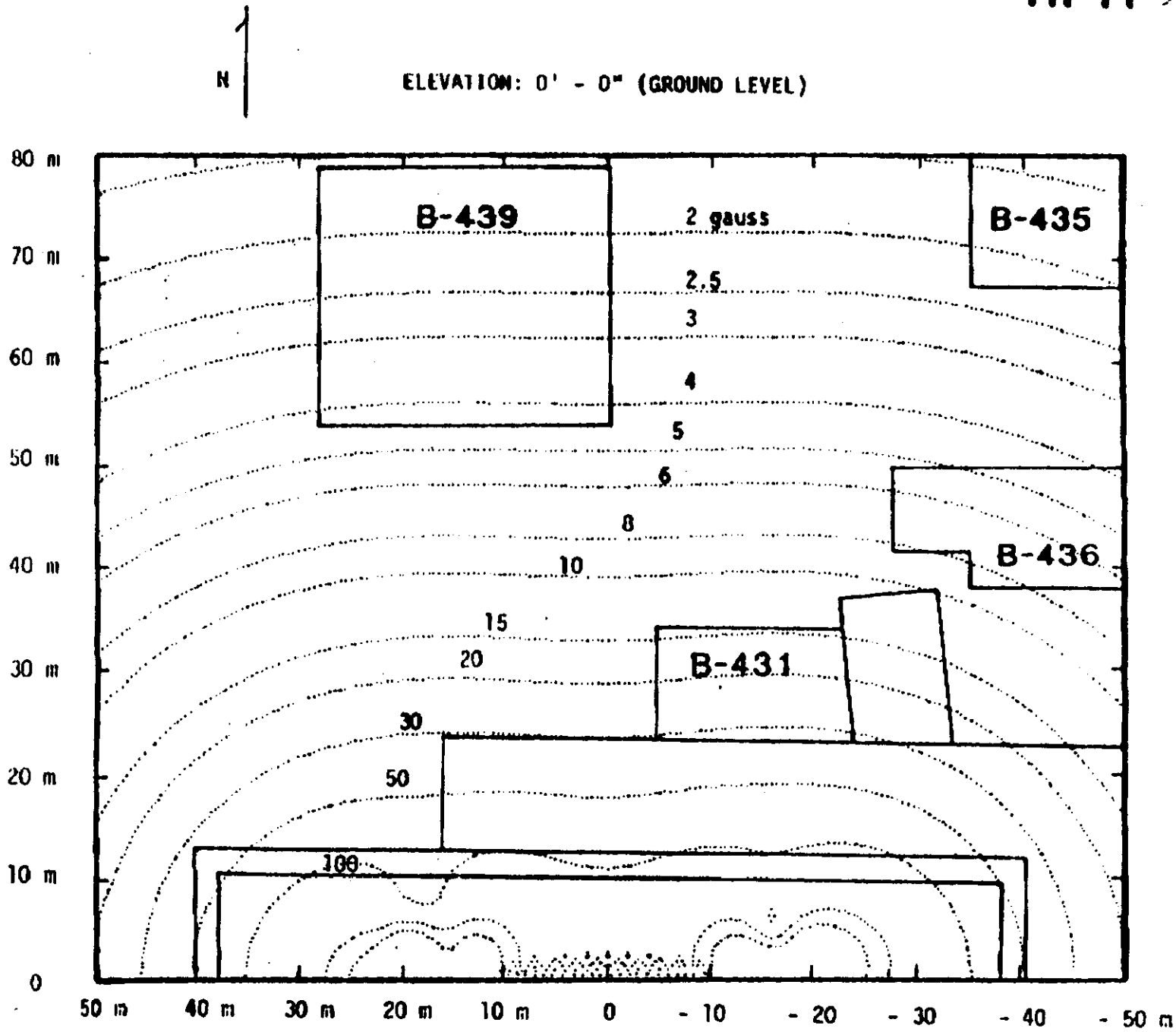
N
ELEVATION: 0' - 0" (GROUND LEVEL)
B-439
B-435
B-436
B-431
2 gauss
2.5
3
4
5
6
8
10
15
20
30
50
100
80 m
70 m
60 m
50 m
40 m
30 m
20 m
10 m
0
50 m
40 m
30 m
20 m
10 m
0
- 10
- 20
- 30
- 40
- 50 m

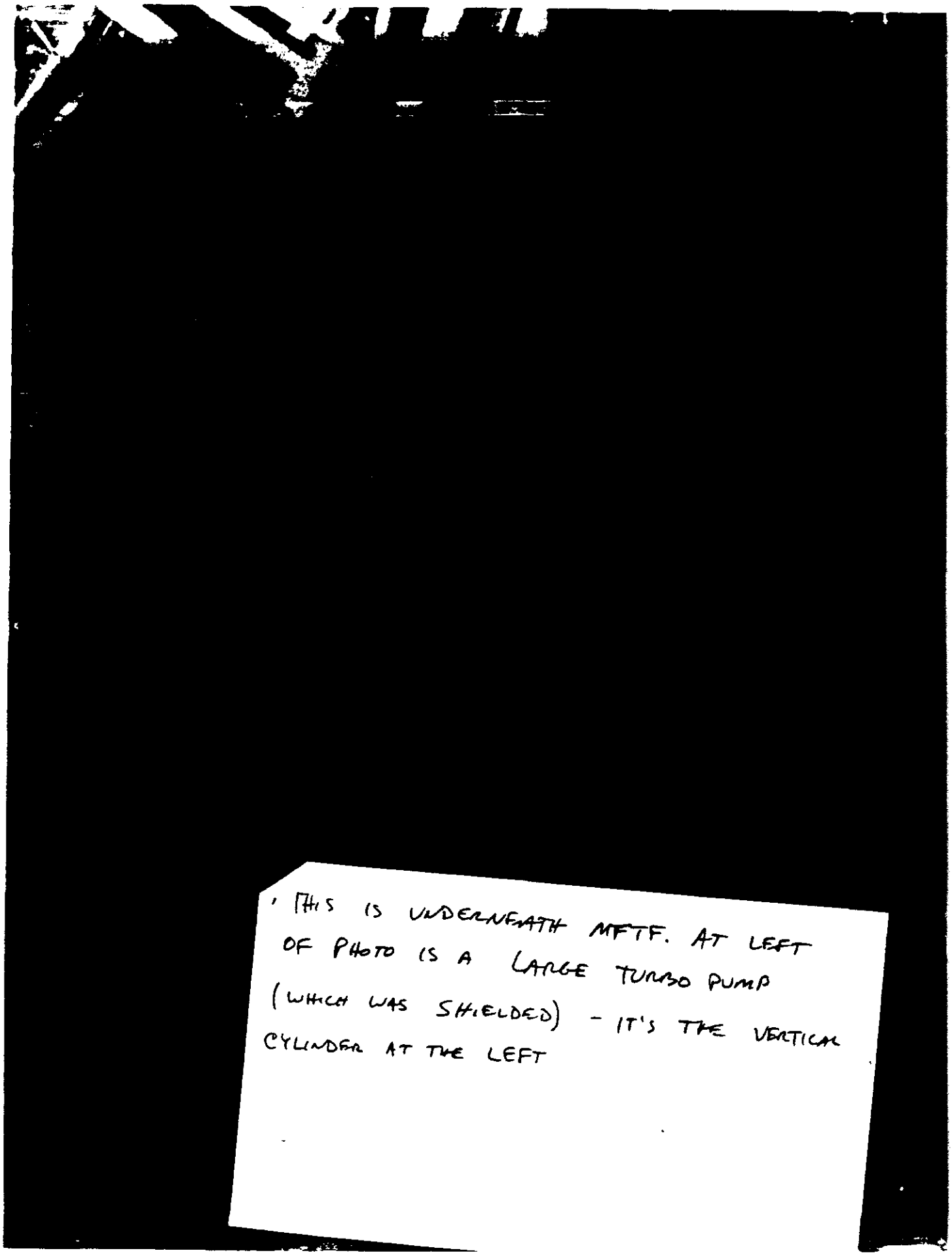

THIS IS UNDERNEATH MFTF. AT LEFT OF PHOTO IS A LARGE TURBO PUMP (WHICH WAS SHIELDED) - IT'S THE VERTICAL CYLINDER AT THE LEFT

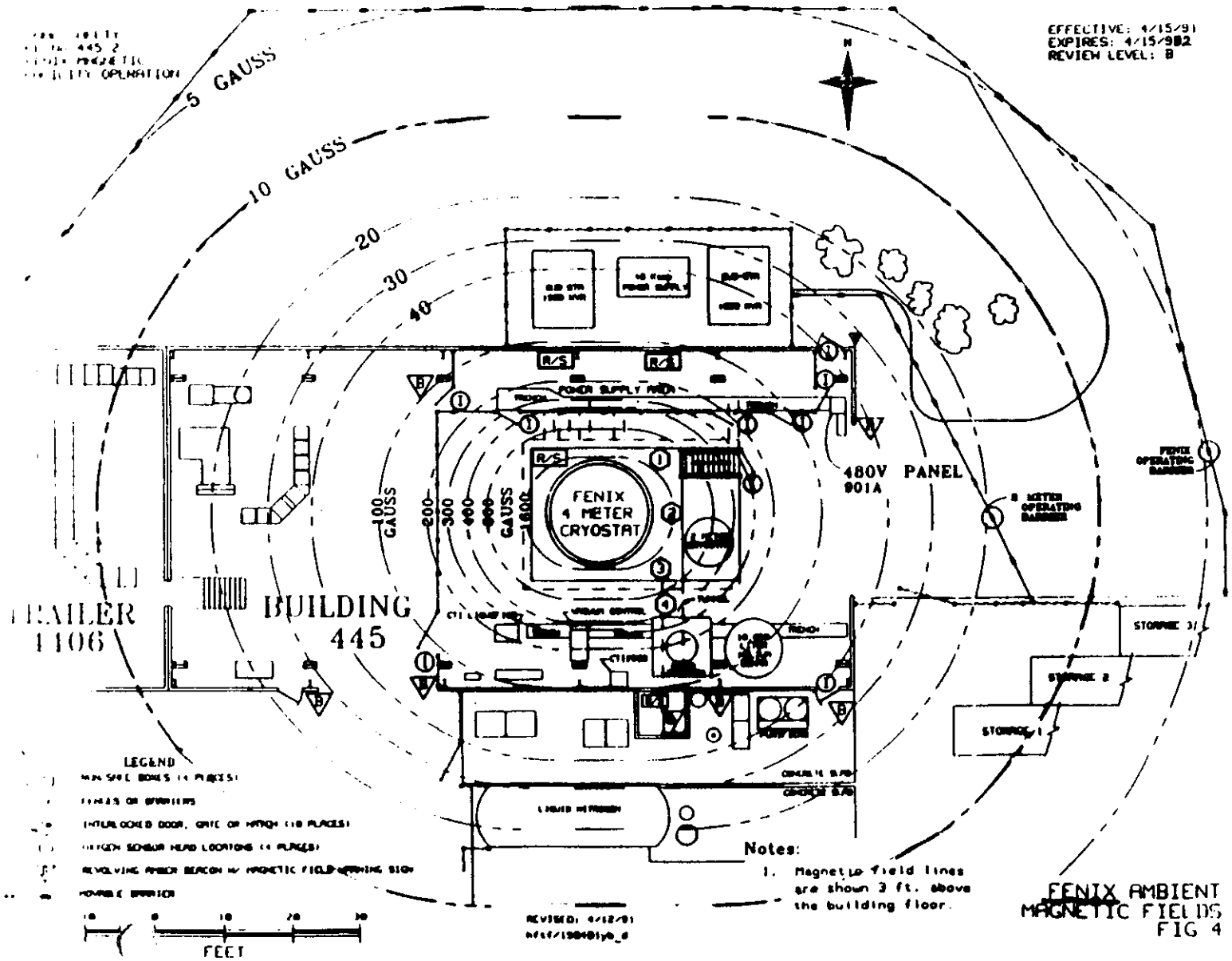

FENIX AMBIENT MAGNETIC FIELDS
FIG 4

PHENIX

See plot for field levels.

NOTE He plant ~~xx~~ at Left (Blue cylinder)
Power supply @ right. Controlroom at far end
through window.

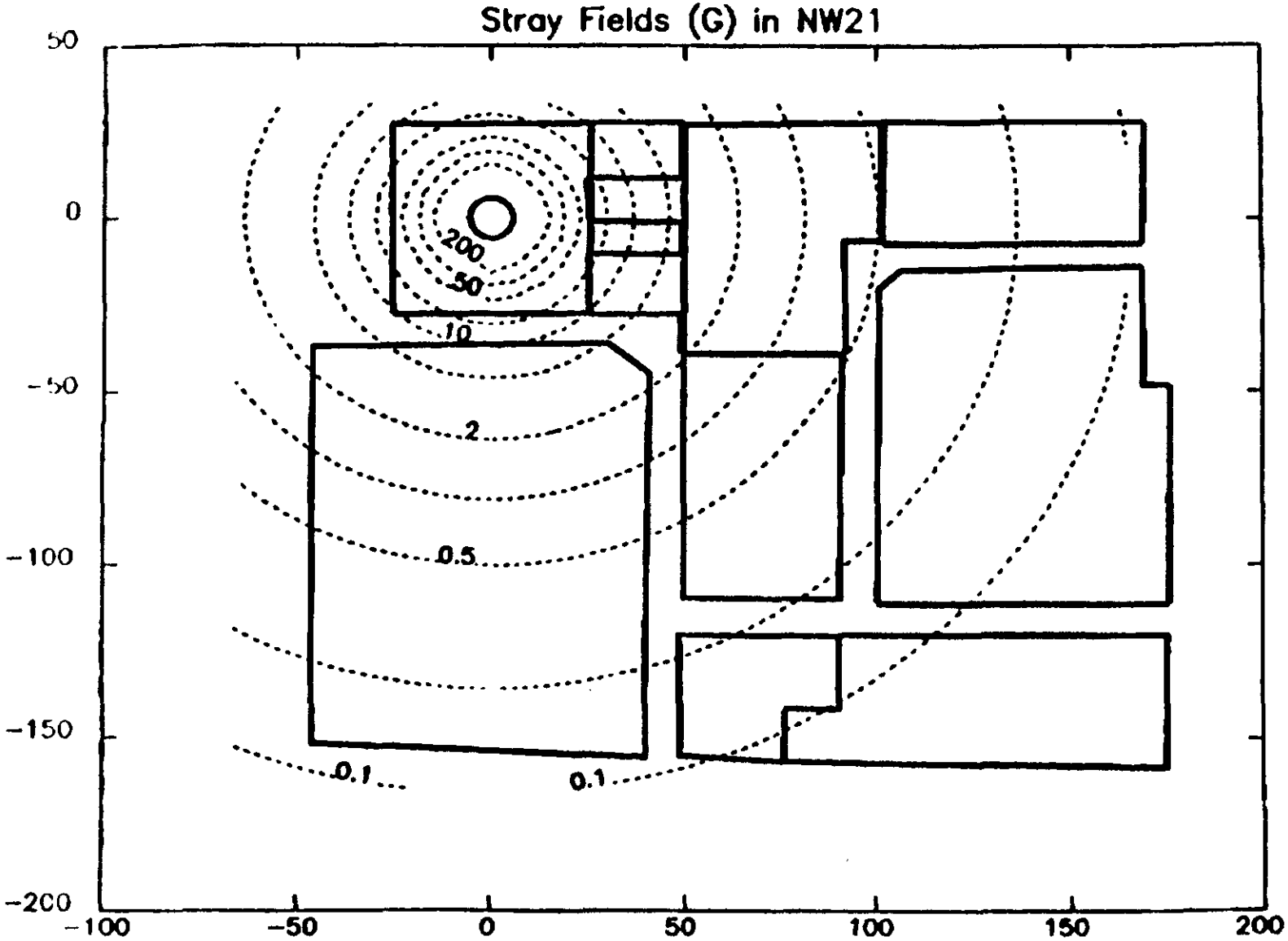

MIT
ALCATOR MOD-C

- FRINGE FIELD IN THE HALL

LARGE 1 ÷ 2 KGAUSS NEAR THE DETECTOR
200 ÷ 300 GAUSS NEAR LOWER COUNTING HOUSE

OPERATIONAL ISSUES ADDRESSED/SOLVED IN OTHER FACILITIES

PERSONNEL PROTECTION SYSTEM HAS TO BE IN PLACE
NO GENERAL ACCESS WITH FIELD ON
PERSONNEL TRAINING MAY BE NEEDED

SENSITIVE EQUIPMENT HAS TO BE SHIELDED
MOTORS, FANS, PUMPS, ...

FERROMAGNETIC OBJECTS HAVE TO BE SECURED
Be Cu TOOLS FOR WORK IN THE FIELD

ASSESSMENT OF GEM MAGNET ADVISORY PANEL

- MAGNET - FEASIBLE
- RISKS - ACCEPTABLE

} STATE OF THE ART MAGNET WITH SUBSTANTIAL ENGINEERING CHALLENGE

- TIME SCHEDULE - TIGHT BUT POSSIBLE
  STRONGLY DEPENDS ON PROCUREMENT AND MANUFACTURING SCHEME

- COST - $ 94.1 M INCLUDING 25% CONTINGENCY

Current Magnet Cost Estimate

	Tech Panel Estimate ($M)
Subsystem Design	10.1
Coil Forms	5.6
Conductor	6.1
Winding (incl tooling)	9.5
Thermal radiation shields	1.8
Vacuum vessels	6.5
Cold mass supports	5.8
Coil assembly	5.1
Poles	8.9
Power/protection system	4.6
Cryogenics & vacuum	8.9
Installation	1.7
Management/integration	1.0
Contingency (25%)	19.0
TOTAL	$94.1M

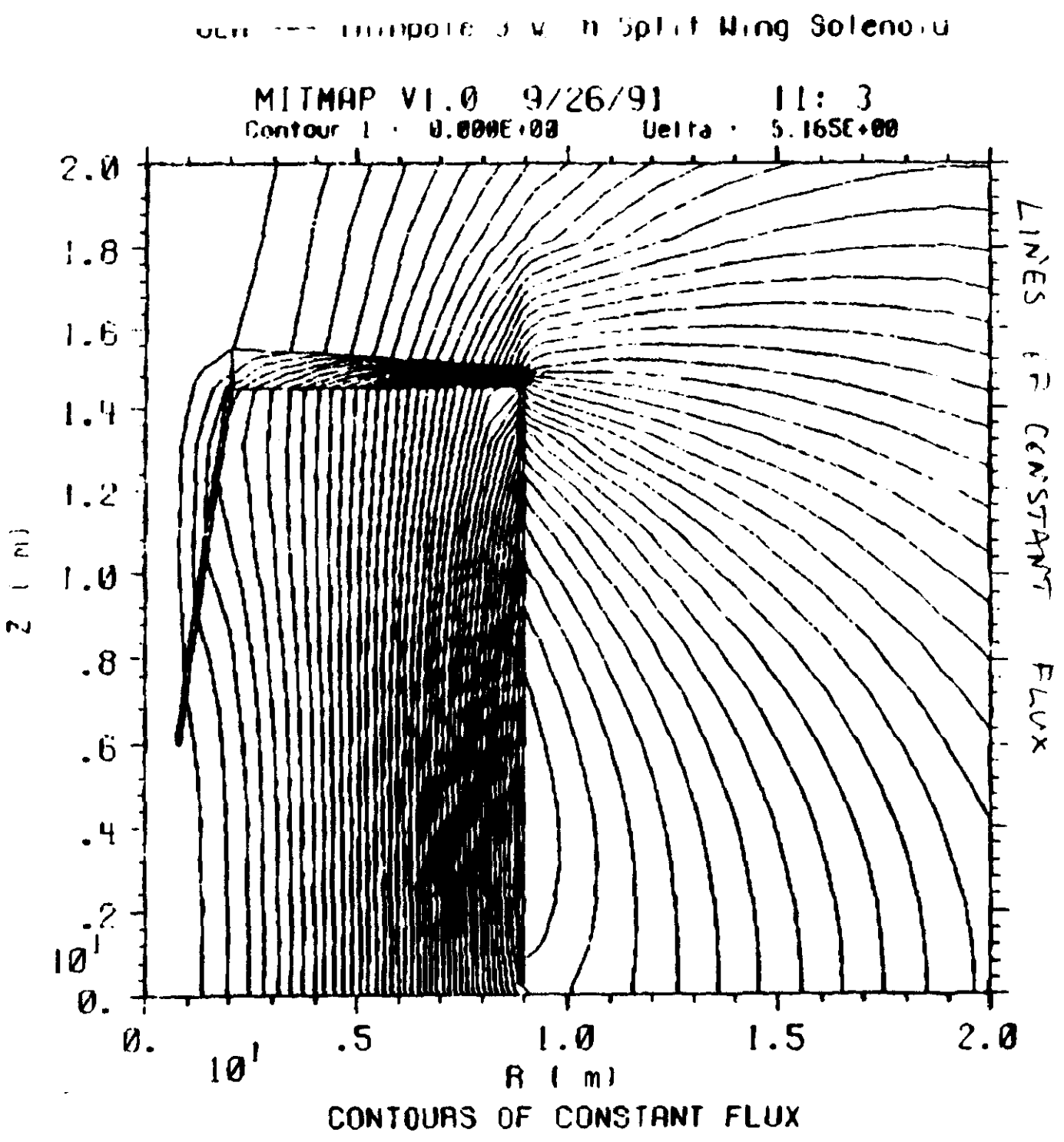
MITMAP V1.0 9/26/91 II: 3
Contour 1 : 0.000E+00 Delta : 5.165E+00
2.0
1.8
1.6
1.4
1.2
1.0
.8
.6
.4
.2
0.
Z (m)
0.
.5
1.0
1.5
2.0
R (m)
LINES OF CONSTANT FLUX
CONTOURS OF CONSTANT FLUX

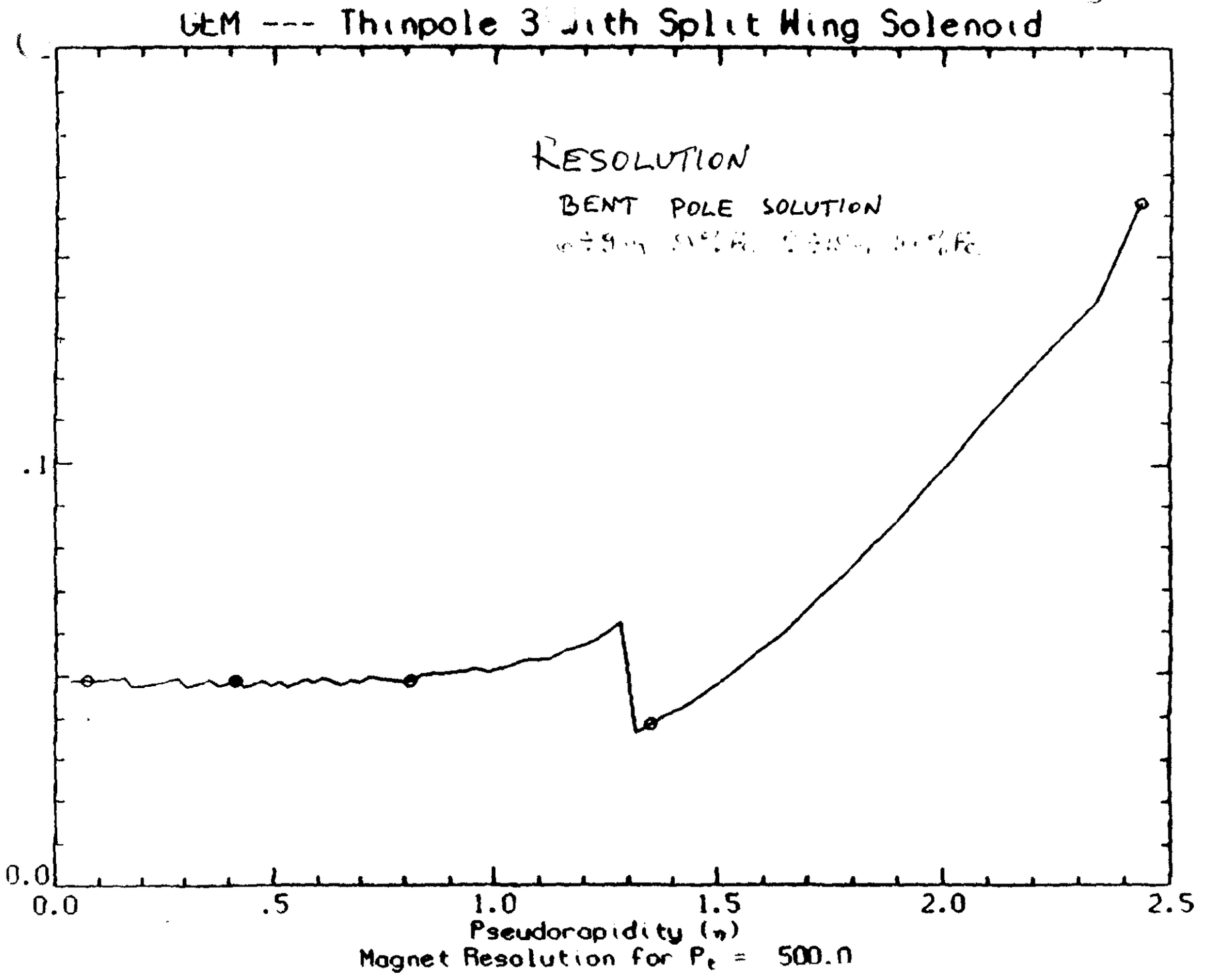
GEM --- Thinpole 3 with Split Wing Solenoid
RESOLUTION
BENT POLE SOLUTION
.1
0.0
0.0
.5
1.0
1.5
2.0
2.5
Pseudorapidity (η)
Magnet Resolution for P_t = 500.0

6. FORWARD DIRECTION - POSSIBLE IMPROVEMENTS

- RESOLUTION AS PROPOSED NOW -.-% AT y = 2.-
- ISSUE PUT ON BACK BURNER DUE TO LACK OF TIME AND MONEY FOR WELL ENGINEERED SOLUTION
- IDEAS EXIST

  BENT POLE

  ADD-ON SOLENOID

- WILL COST > $5 M PER END

PAGE.002

The GEM Magnet Subsystem

Design Status

Gary A. Deis, LLNL

SSCL Program Advisory Committee Meeting
3-4 October, 1991

OCT 1 '91 14:40 FROM GFED

Outline

In this talk, I will discuss the present design for the GEM magnet, currently being developed by LLNL and MIT:

- **Present design status**
- **Conductor design options**
- **Coil form design**
- **Vacuum vessel design, structural supports**
- **Cold mass supports, radial and axial**
- **Manufacturing approach, facility considerations**
- **Industrial involvement**
- **Overall schedule**
- **Summary**

The present engineering design is only two months old

Since August, we have focused on developing a conceptual design in sufficient detail to support the LOI and to permit a good cost estimate

- As a minimum, we have addressed each system or component at a very coarse level of detail, e.g. cryogenics, power/protection
- Where we felt it important for feasibility, cost, or schedule considerations, we have worked in considerably more detail, e.g. vacuum vessels, conductor/winding design
- We are working with vendors on high-cost items, both to get their design recommendations, and to furnish us with a good basis for costing

BUT - few detailed design aspects have been optimized, and some are undergoing rapid changes at this time

The design is driven by requirements on performance, cost, and schedule

Basic requirements:

- **Performance :** ~5% $\Delta P_t/P_t$ at 90°, 500 GeV~
  good low-angle resolution
- **Cost (goal):** under $80M total
- **Schedule :** ready to install Jan 96, done by Oct 96

Overall Specifications:

- **Internal size** 16.6m ID x 29m long
- **Field** 0.8T
- **Concept** "unshielded" superconducting solenoid, with field-shaping steel end poles
- **External size** ~20m OD x ~32m long

gdxxxxx 1
10/1/91

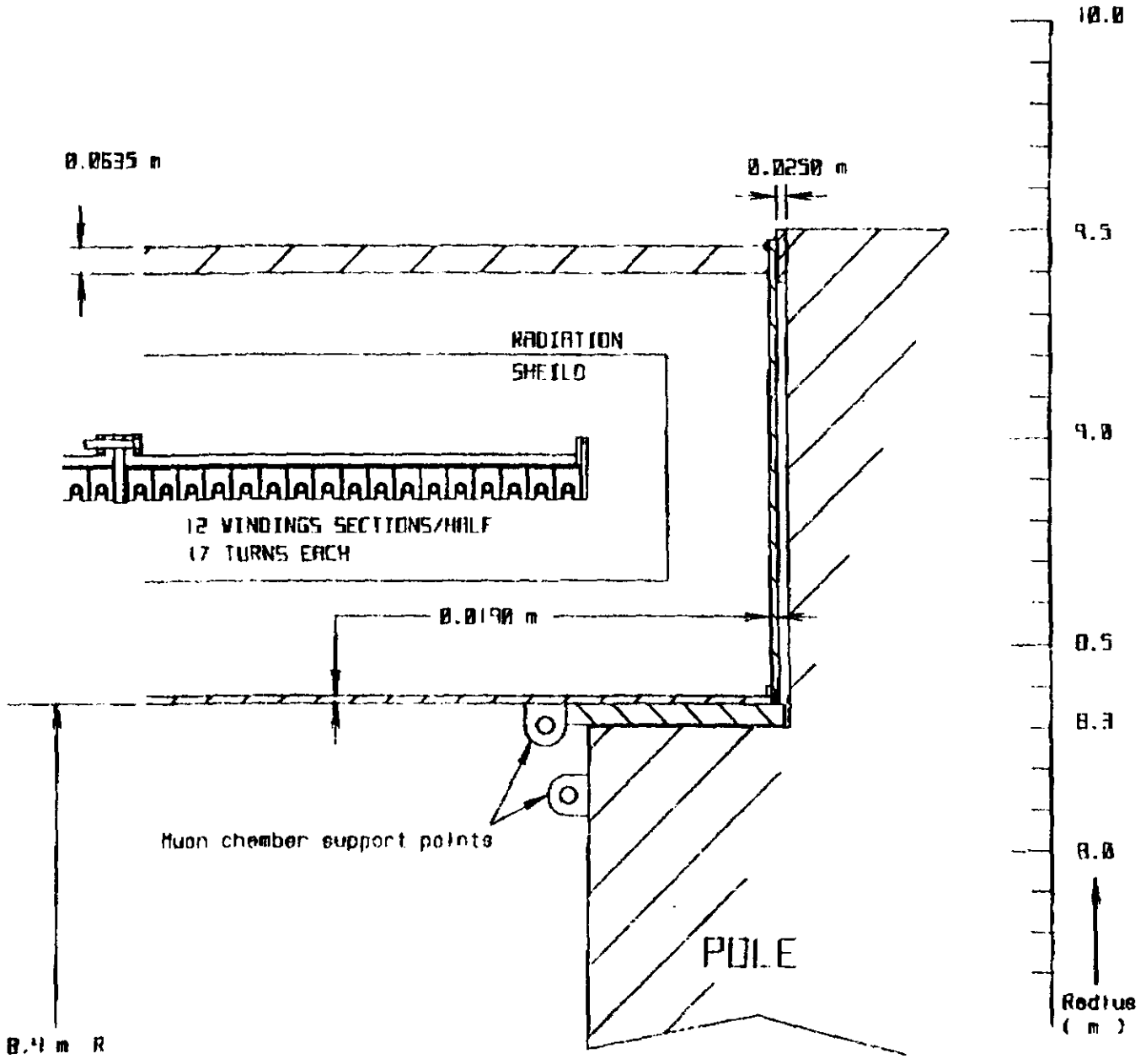

COIL DETAIL AT POLE

MAGNET NATURAL CONVECTION (THERMAL SYPHON) LOOP

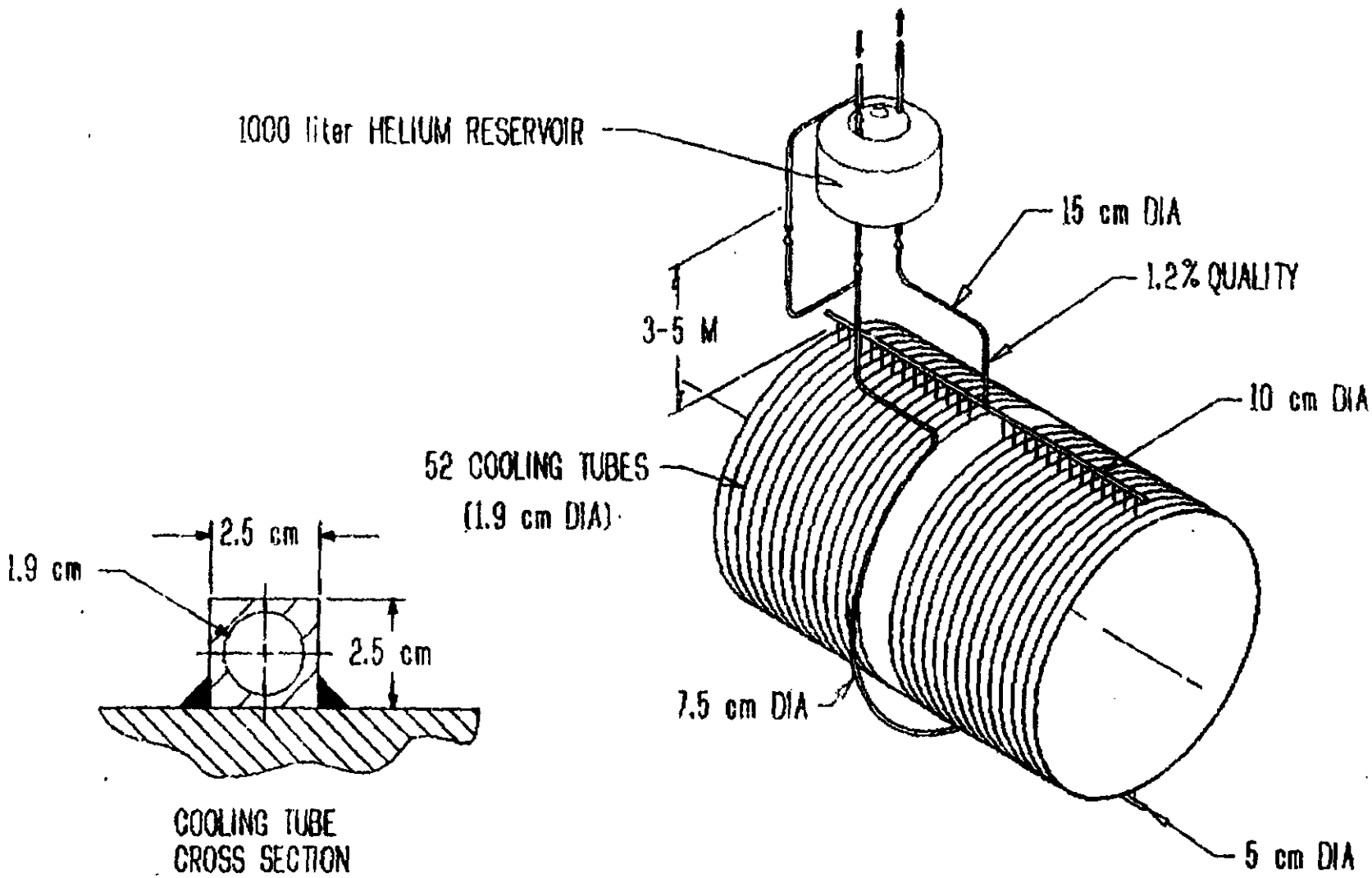

FIG 2

OCT 1 '91 14:45 FROM ARED

Coil/bobbin design

(not shown)

Outline - use Peter's drawing

- bobbin in 12 sections for schedule reasons
- 5cm thick bobbin, ground plane insulation, then windings
- 1/4 sections of bobbin built off-site, assembled on-site

current break??? not too sure how to do this yet (ID'd by magnet panel last week)

thermosyphon loop on outside (show LLNL picture)

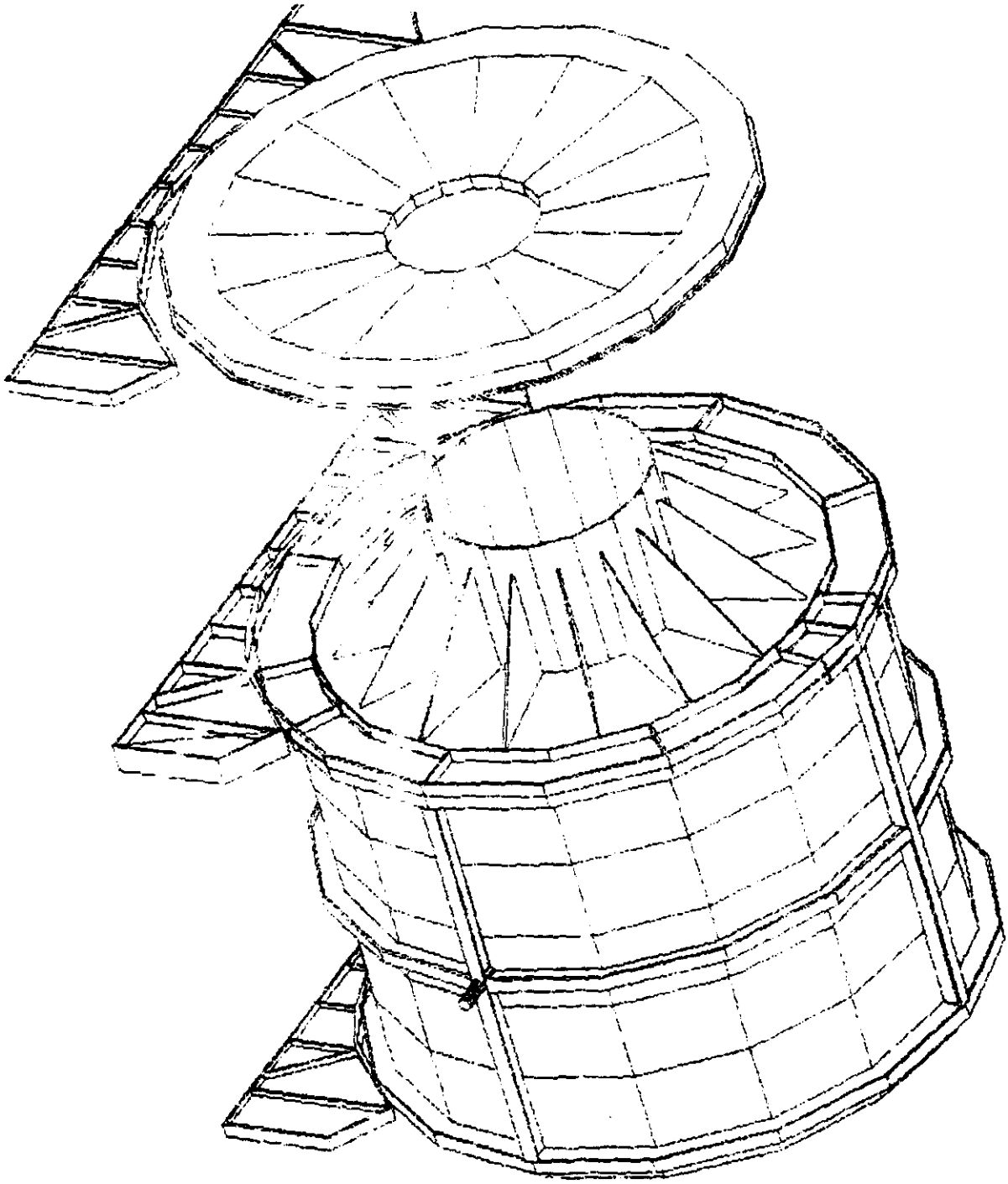

Vacuum vessel/structural supports (Not shown)

Outline - use LLNL overall iso dwg

- Vac vessels - outer is LCS external-pressure vessel, 5cm thick, stiffened 3 places axially, 4 longitudinal stiffeners to take pole load
  - -inner is 304SST, 2cm thick, "stress-free" ex for vac
- Intersection of axial, ring beams provides good spot for rotation of vessel during assembly
- Vessel supported on normal 120° saddles, fixed at midplane, with rollers to accomodate axial length change
- Hydraulic jacks used to lift assembly (underneath saddles) for insertion of shims to compensate for ground motion. Support points located on caissons,

OCT 1 '91 14:46 FROM ARED

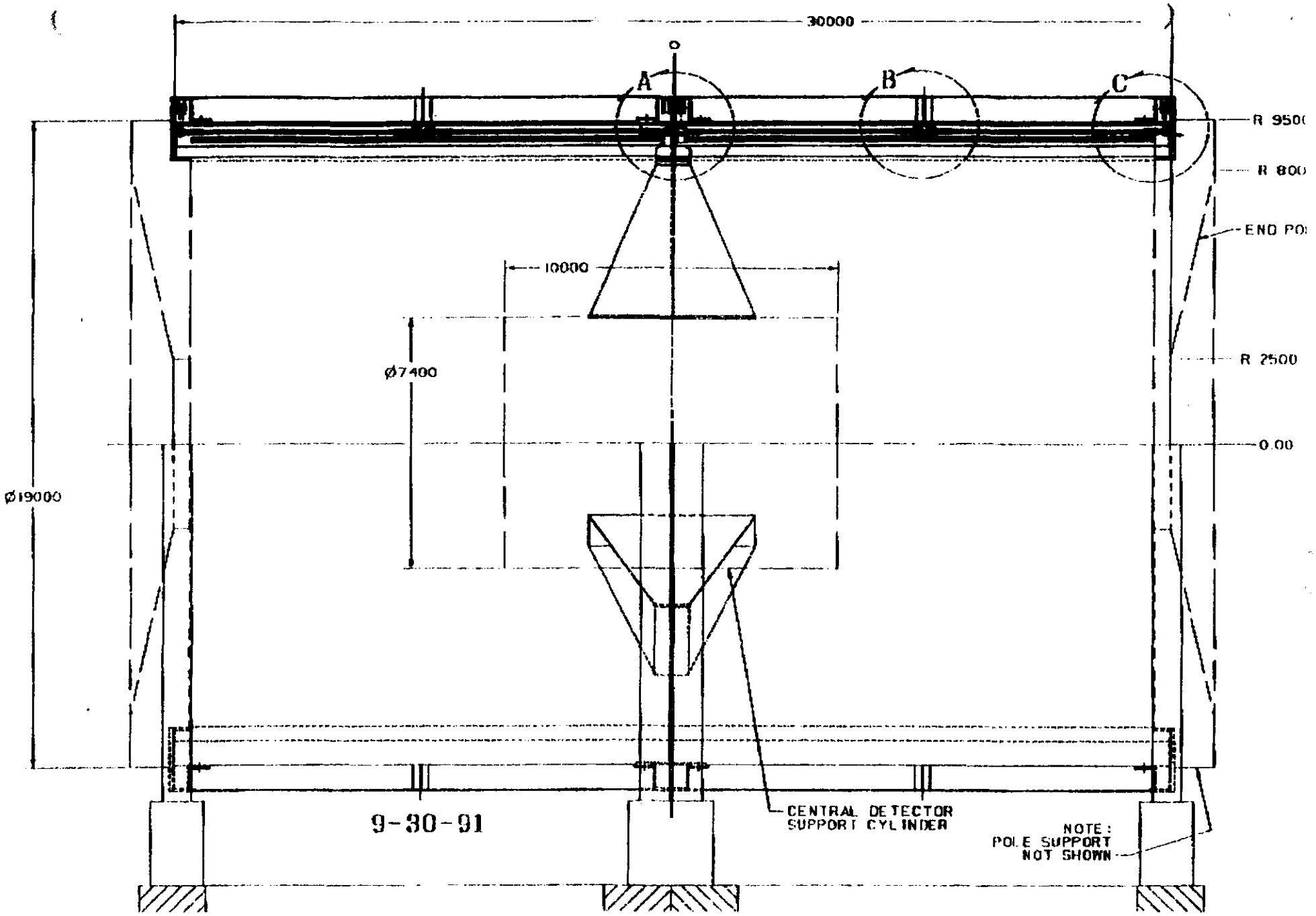
30000
A
B
C
R 9500
R 800
END PO
10000
Ø7400
R 2500
0.00
Ø19000
9-30-91
CENTRAL DETECTOR
SUPPORT CYLINDER
NOTE:
POLE SUPPORT
NOT SHOWN

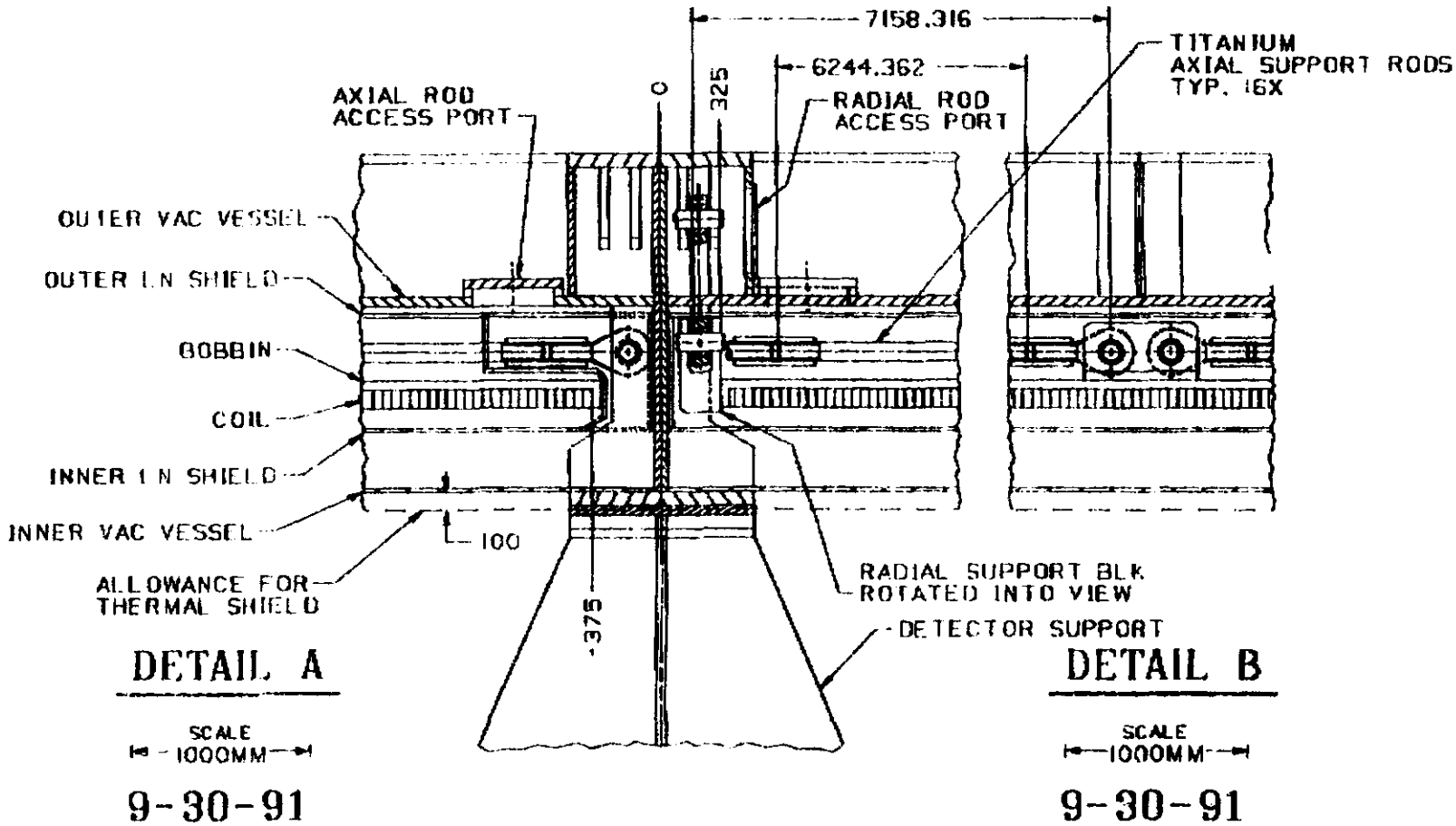
7158.316
6244.362
0
325
AXIAL ROD ACCESS PORT
RADIAL ROD ACCESS PORT
TITANIUM AXIAL SUPPORT RODS TYP. 16X
OUTER VAC VESSEL
OUTER LN SHIELD
BOBBIN
COIL
INNER LN SHIELD
INNER VAC VESSEL
100
ALLOWANCE FOR THERMAL SHIELD
-375
RADIAL SUPPORT BLK ROTATED INTO VIEW
DETECTOR SUPPORT
DETAIL A
SCALE 1000MM
9-30-91
DETAIL B
SCALE 1000MM
9-30-91

(NOT SHOWN)

Vacuum vessel/integration with cold mass supports and central detector support

Outline - use LLNL section dwg at midplane

- Vessel stiffeners connected @ midplane to form solid structure, connected directly to ground.
- This also provides room for cold mass radial supports
- Central detector support connects to stiff midplane structure

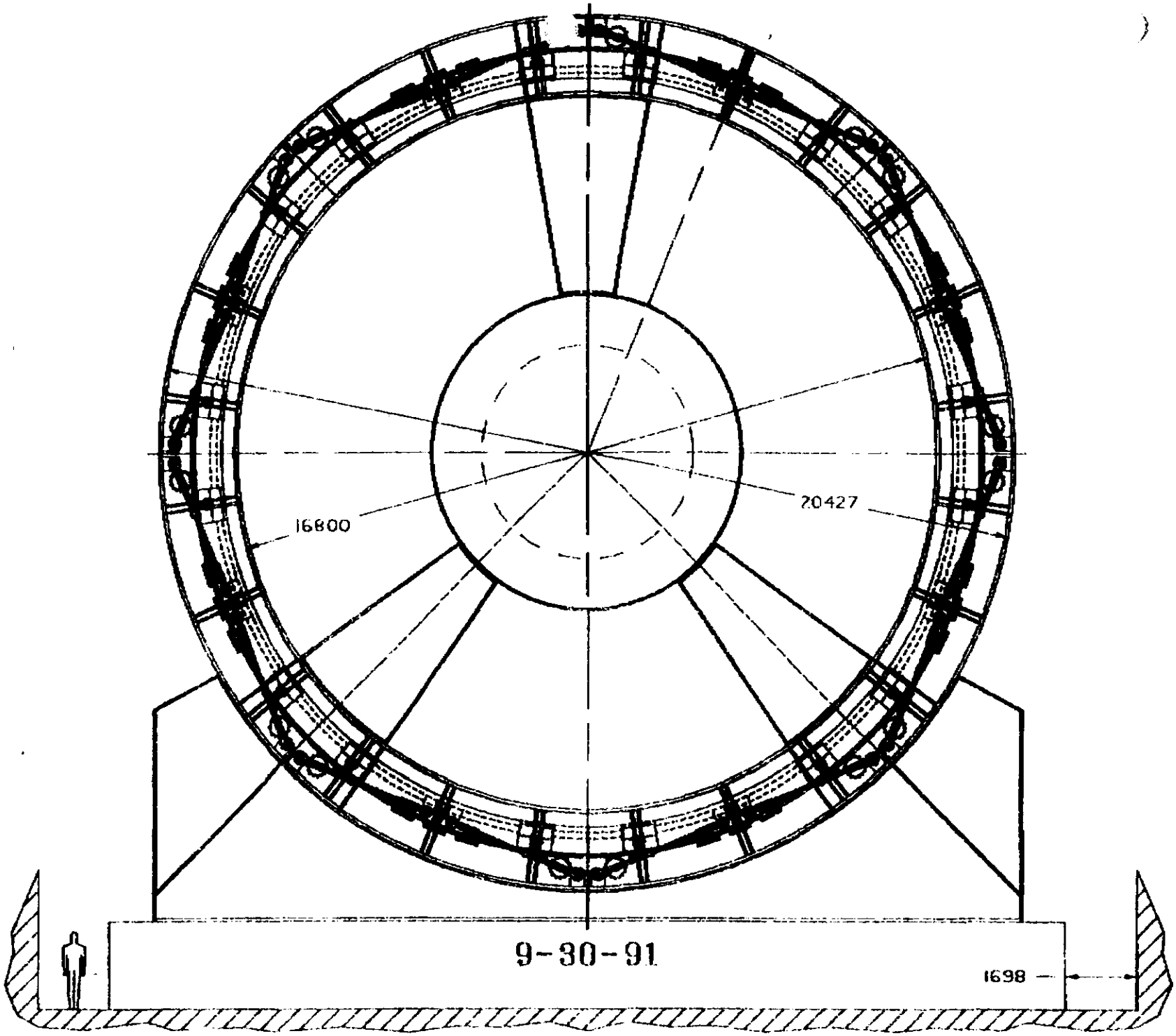
16800
20427
9-30-91
1698

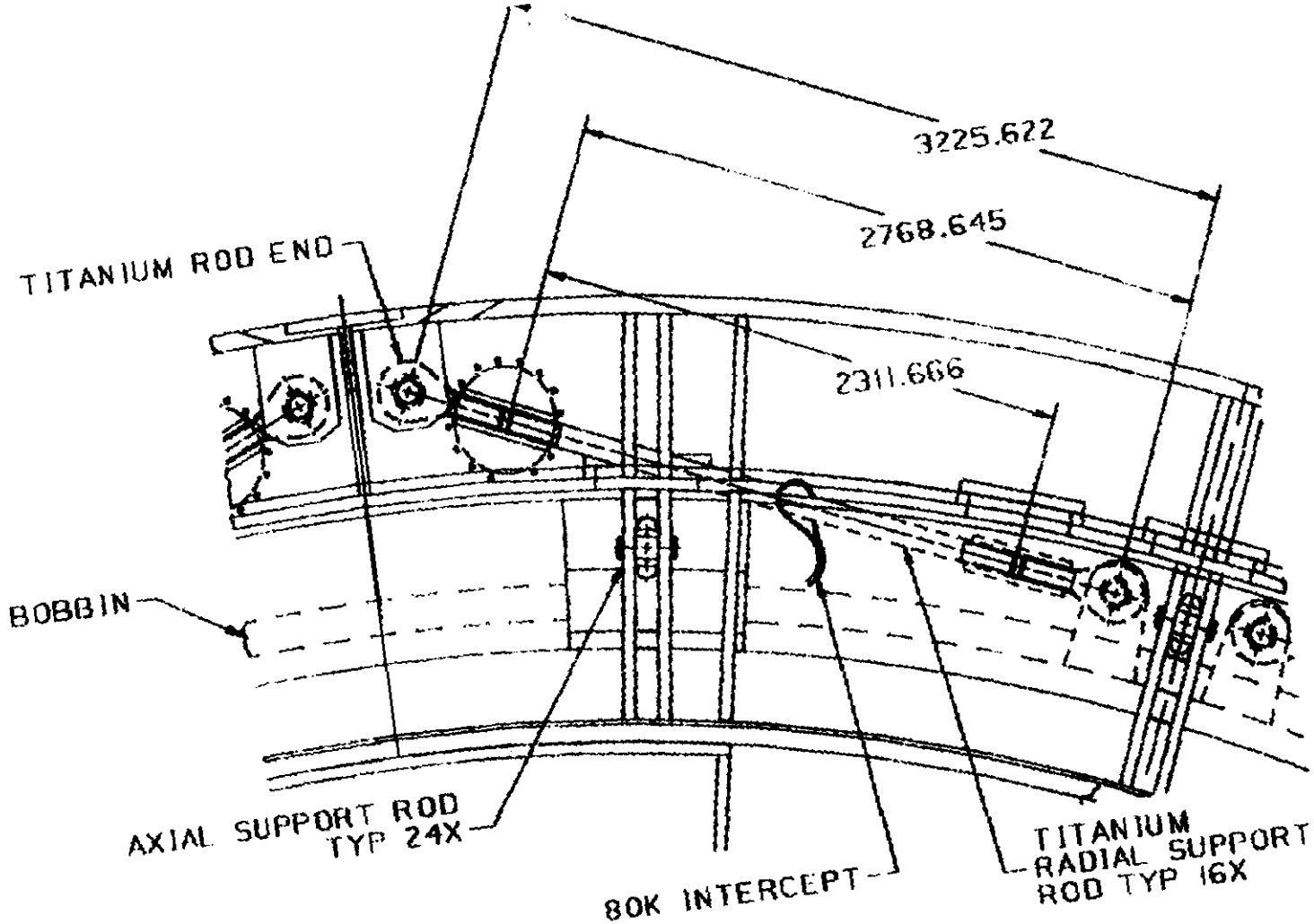

SECTION X-X

SCALE
1000M

9-30-91

CT 1 '91 14:48 FROM AREO

Cold mass supports-radial

(NOT SHOWN)

Outline - use end view and section xx

- Radial supports are 5cm dia titanium rods, 8 pairs at each end of each coil half (64 rods total). These hold up the coil form while allowing cooldown contraction. Minimal heat leak, due to length/diameter
- Access ports are being designed in to allow assy and adjustment of rod lengths
- Coil roundness maintained primarily by flanges on coil form

Several interfaces affect the end pole design

For now, we are assuming the "thick" pole, with simple axial translation to access the interior of the magnet

- **Physics performance vs. cost is the primary consideration between "thick" and "thin" pole options**
- **The specific pole design must incorporate means of access into the detector; options include:**
  - **roll it back in one piece (current baseline)**
  - **roll it back in more than one piece**
  - **open two doors**
- **Pole must not interfere with quadrupole when opened**
- **The design is also affected by support scheme for muon endcaps**
- **There may be other ways to shape the field (winding pitch)**

The manufacturing scheme must be an integral part of the design (for an object this size!)

Much of the design is driven by abilities to ship large, heavy parts, as well as abilities of industrial field-fabricators

- Vacuum vessels will supplied as complete units. Each shell will be made up of ~20 factory-fabricated pieces, assembled on site (through leak-checking)
- Coil forms are also assembled on-site from factory-fabricated pieces (4 per form, 96 parts total)
- Conductor will be fabricated off-site in ~1 km lengths
- Stabilizer may need to be joined into 1km lengths on-site.
- Stabilizer/conductor unit is wound into 1-meter-long coil forms on-site, in two parallel winding areas

Manufacturing approach, cont'd

- One-meter coils are joined into 12-meter coil halves in an assembly stand. Insulation, plumbing, and thermal shields are completed.
- Coil assembly is lifted into vacuum vessel, and assembly is completed.
- Assembly is rotated to horizontal, cold-leak testing is performed.
- Coils and poles are then lowered into position in underground hall and mounted

SSC DETECTOR 2 MA .NET FABRICATION FACILITY

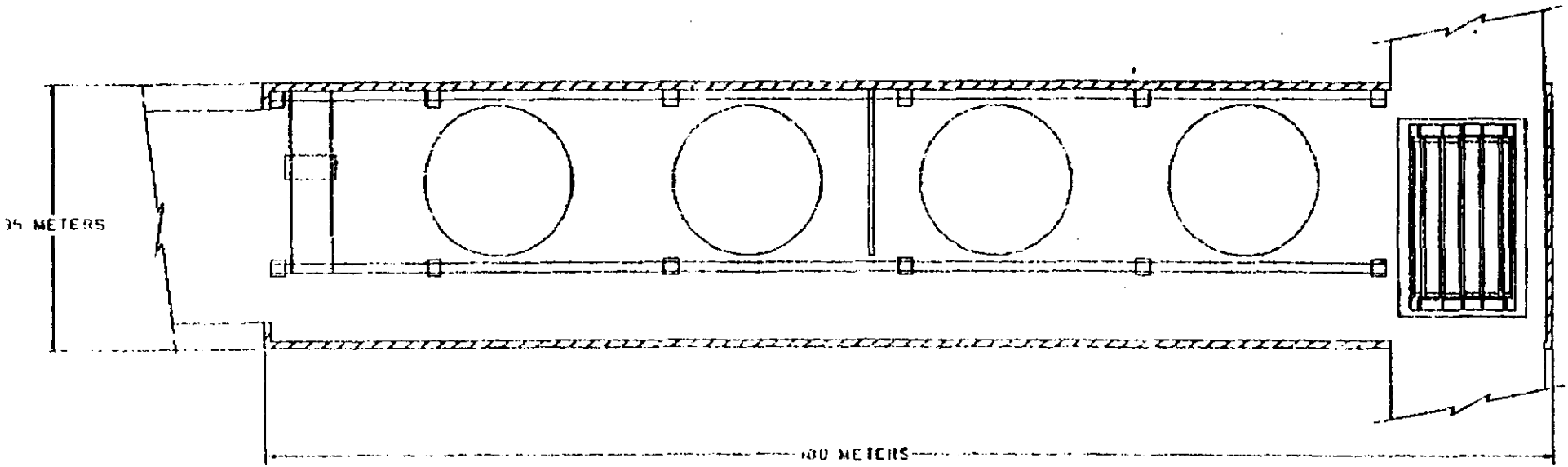

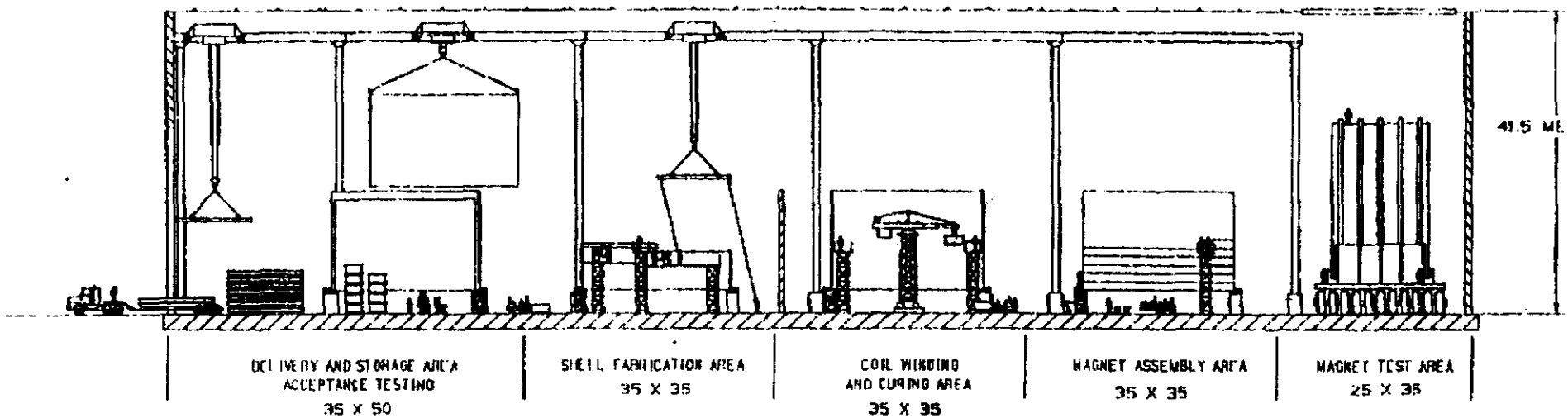

AREA 1

DELIVERY AND STORAGE AREA/ACCEPTANCE TESTING

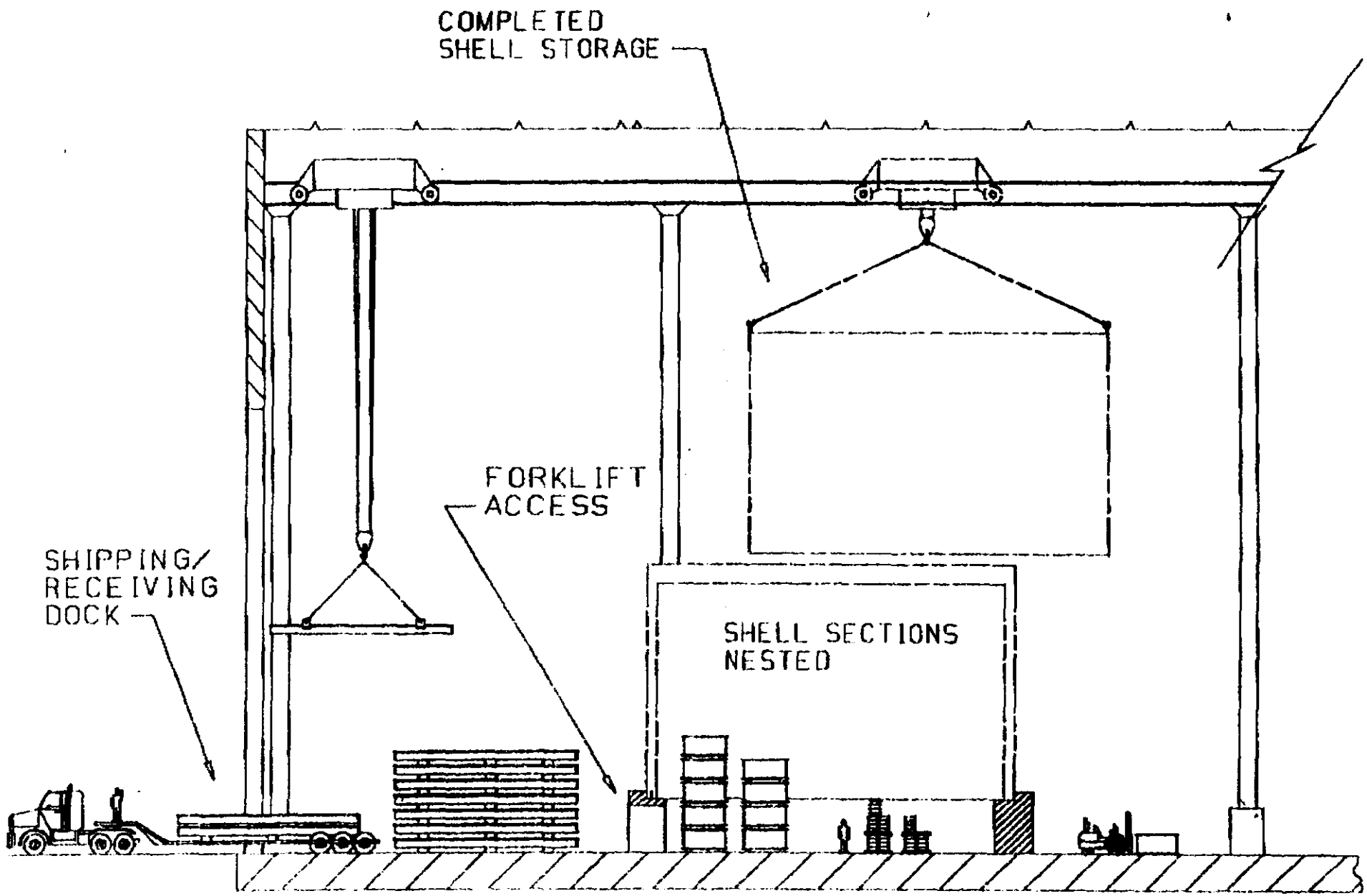

AREA 2

SHELL FABRICATION AREA

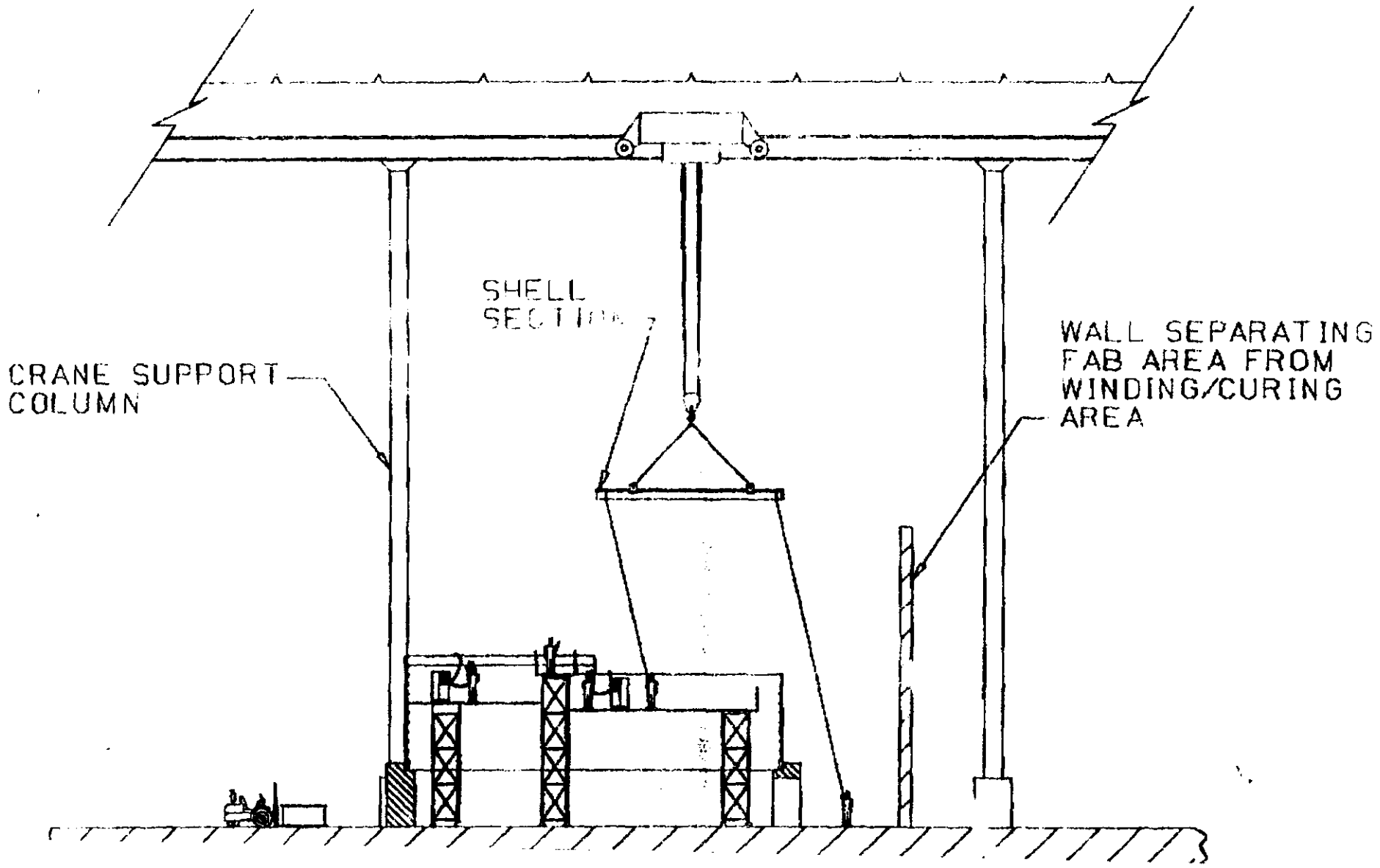

ARLA 3

COIL WINDING AND CURING AREA

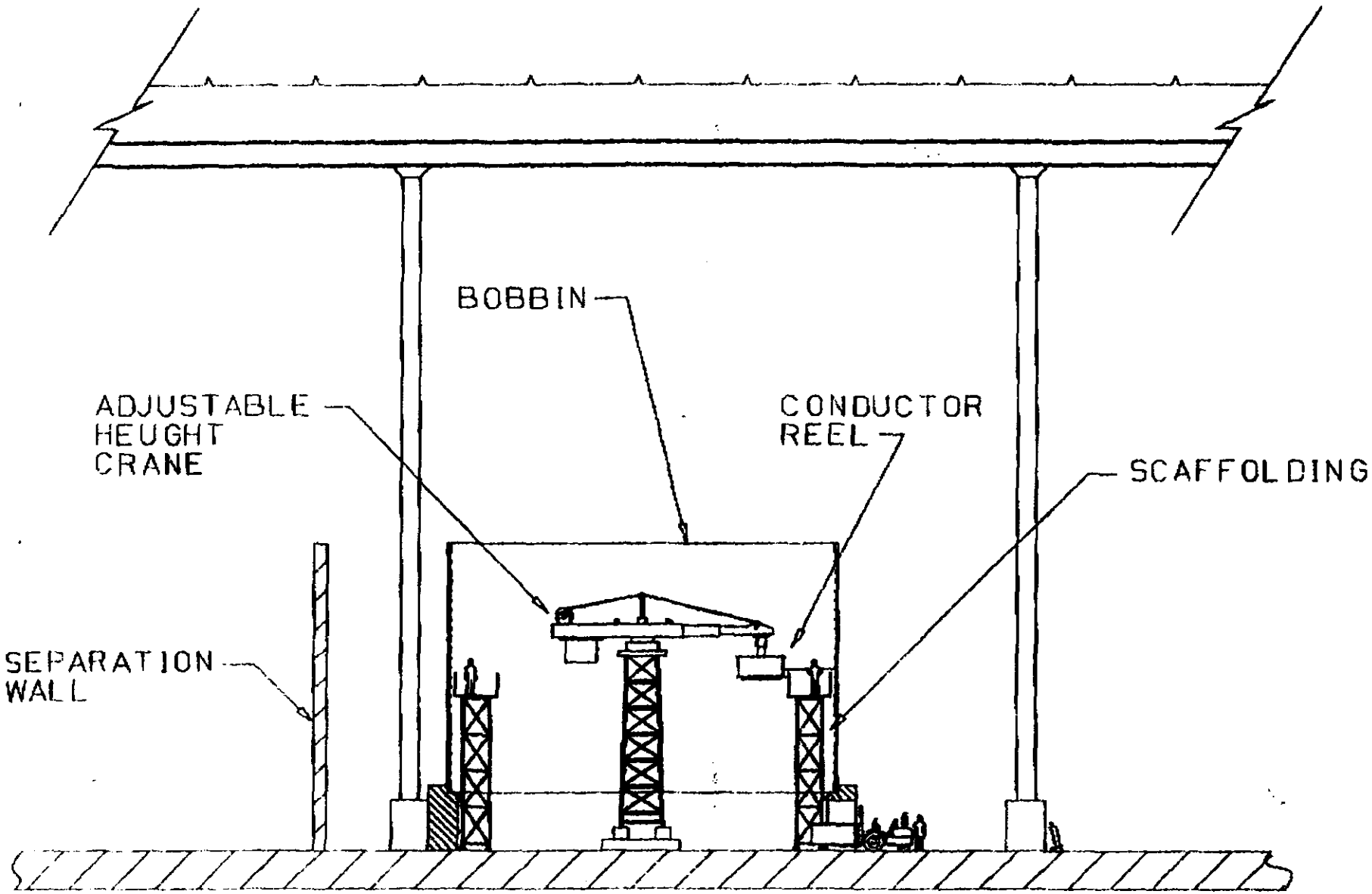

ARLA 4

MAGNET ASSEMBLY AREA

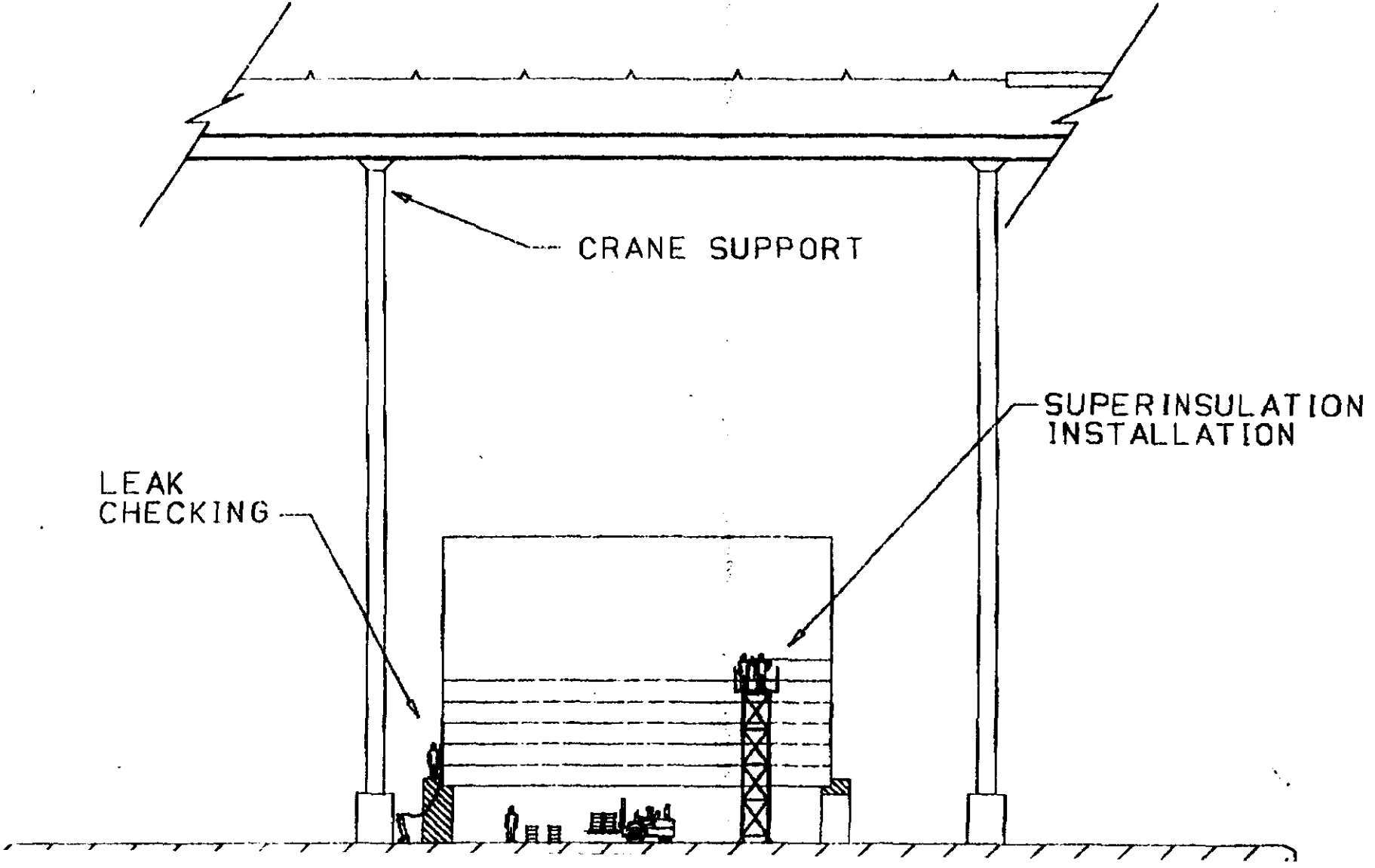

AREA 5

MAGNET TEST AREA/ROLLOVER TRANSPORT PREP

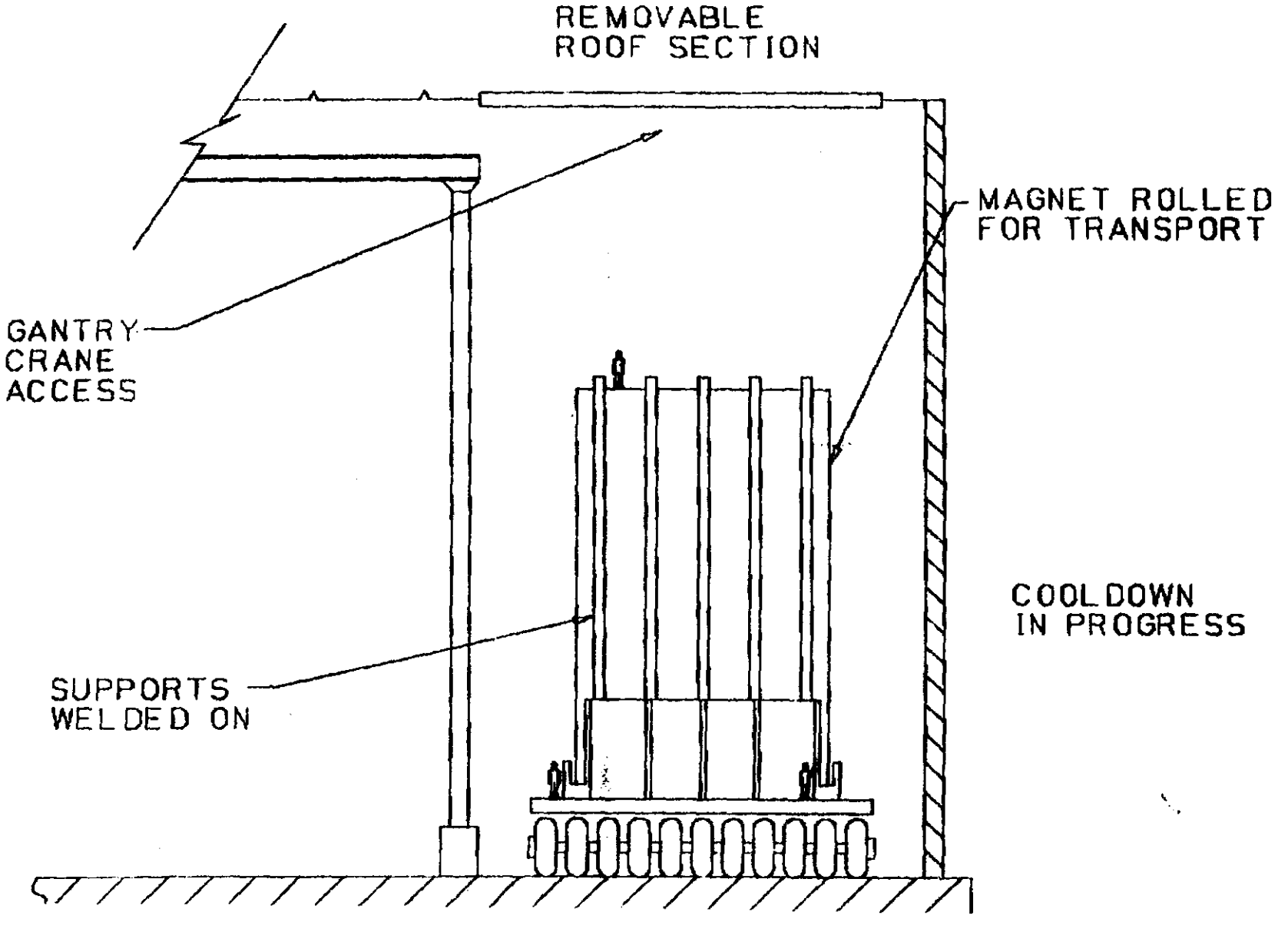

We are already working with industry in most areas

We are informally soliciting input on the design, and we are requesting cost/schedule estimates to serve as the basis of our cost estimate

- **Heavy field-fabricators for vessels, coil forms, radiation shields: CBI, PDM, Nooter, and others**
- **Conductor/stabilizer fabricators: 25 copper extruders, 6 aluminum extruders, several conductor manufacturers**
- **Transportation: Santa Fe and Southern Pacific railroads, Tri–State Trucking**
- **Titanium fabricators (for cold-mass supports): 6 companies**

Also: aluminum/steel suppliers, high-speed welding machines, field machining, cryogenic lines and valves, heavy jacks and transporters

GEM Magnet Subsystem Schedule

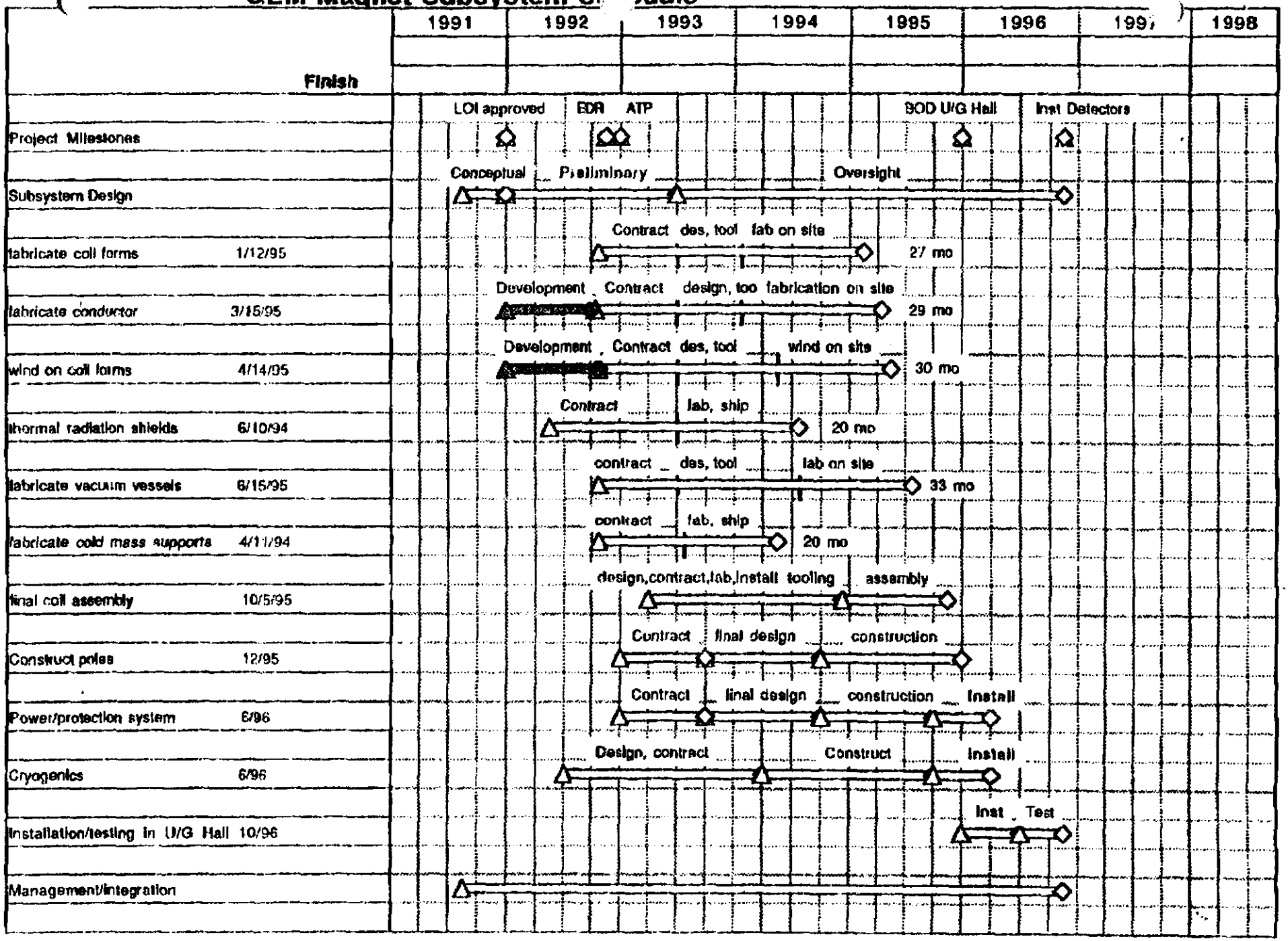

Sunday, September 22, 1991

OCT 1 '9: 14:52 FROM ARED

Gem Magnet Subsystem - Near-term Schedule

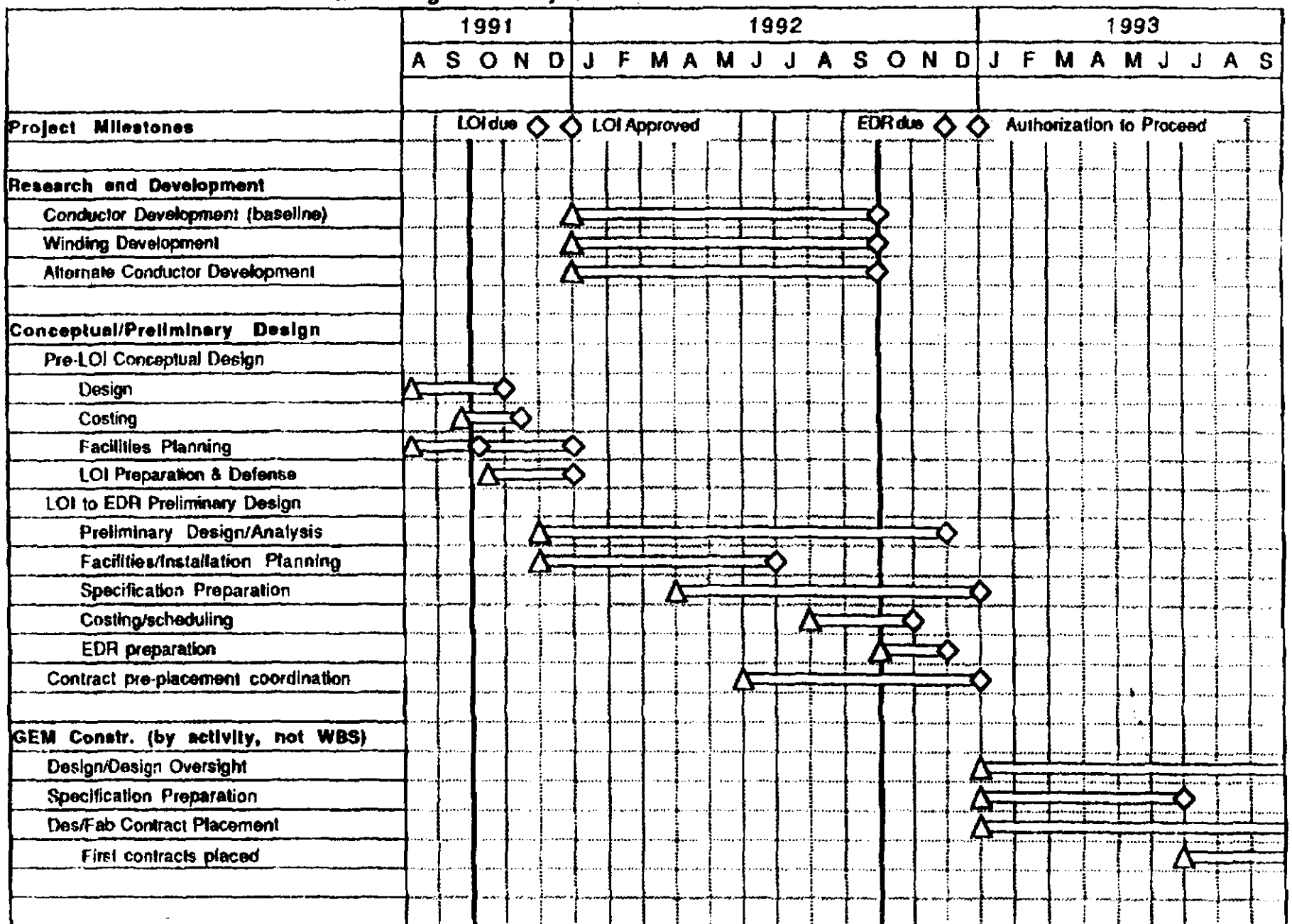

Sunday, September 22, 1991

NOT SHOWN

Schedule

Outline - show schedule slide without funding profile

- Rough schedule has been worked out, and it is tight, but definitely possible
- The key areas are the conductor and winding, and we need to get development going ASAP.
- This schedule assumes a procurement plan in which LLNL/MIT team oversees various vendors, who have "design and build to spec" contracts. Approximately $70-80M will be spent in industry

Summary

The LLNL/MIT team is working the GEM magnet design in both breadth and depth.

- **For the LOI, we are covering <u>all</u> design areas to identify problems, propose solutions, assemble a complete conceptual design, and produce a credible cost estimate**

- **For the "long run" we are analyzing the details of a few specific features, such as field shapes, conductor stability, and winding design, to lead into the preliminary design, and to identify areas for near-term development effort**

- **Industrial participation will be vital to the realization of this magnet, and we are already working to develop the required relationships to ensure success**

Summary of the 2nd Meeting of the GEM Magnet Technical Panel

SSC Laboratory
Dallas, Texas

The GEM Magnet Technical Panel has completed two of its three scheduled meetings and has studied issues related to the technical credibility of the magnet concept, the cost estimate, proposed schedule, and issues related to the proposed operation of a solenoid with substantial return flux outside of the magnet.

The Panel finds that the proposed unshielded solenoid is technically credible and has very substantial cost, schedule and technical risk advantages relative to possible shielded solenoid options. The Panel recommends that the unshielded solenoid shall be the baseline magnet configuration for the GEM detector.

Studies carried out by the Panel and the Laboratory find no environmental, safety, or operational considerations which require containing the GEM magnet return flux. Operational issues related to this magnet have been identified for further detailed development of operational procedures. These issues have been based upon the experience on numerous past and current physics research and medical diagnostic magnets operated with uncontained return flux.

The collaboration team has presented an initial design concept for the magnet conductor, coil, fabrication, cryostat and supports. The design appears to be within the range of credible options and we have reviewed with the collaboration a broad range of additional options. Final choices will depend upon the results of further design and development.

The magnet schedule is very tight and we considered several possible procurement plans and possible initial design and development strategies which may avoid schedule delays. We recommend that early and intensive discussions between the collaboration, the Laboratory and the Department of Energy shall be initiated to identify a preferred procurement strategy. We further recommend rapid commencement of the conductor development.

The cost estimate presented by the Collaboration team has been reviewed. For most subsystems of the magnet, our estimated costs are consistent with those presented by the Collaboration. However, variations in several areas lead us to conclude that the estimated $80 million cost may be low by approximately $15 million.

The Panel has reviewed the proposed surface facilities. Industrial advice to the collaboration has permitted substantial descoping of the initial facility concept.

Studies of magnet forces on structural steel in the underground hall have been recommended. These studies will determine whether

any of the structural steel should be replaced by aluminum or stainless steel.

It should be noted that, the participation in the second meeting of the Panel included representatives of large magnet industrial contractors, conductor suppliers, vessel manufacturers and members with experience in high-energy research magnet construction and operation. Our meeting also included representatives of the SSC magnet and procurement groups.

GEM Magnet Technical Panel Report on the Choice of the Unshielded Single Solenoid Magnet for the GEM Detector

SSC Laboratory

Dallas, Texas

The GEM Magnet Technical Panel recommends that the unshielded solenoid shall be the baseline magnet configuration for the GEM detector. The recommendation is made on the following basis:

1) The cost of an unshielded single-coil magnet is significantly less than a two-coil system or an iron-shielded system of equal performance. Either alternative would cost 50% to 100% more than the single-coil, unshielded option which is currently estimated at $95M. Additionally, both alternatives would have an impact on the underground facility, either increasing the size of the detector hall or its floor loading requirement. These considerations may add $1M to $5M to the hall cost and may also increase the technical and construction complexity of the facility.

2) The technical risk associated with the single-coil version is significantly less than in the more complex two-coil approach. The magnetic forces between the two coils are very high, and represent a significant challenge to structural design of the system. The iron shielded magnet also has challenging structural issues that must be solved for the return yoke. The installation of about 40 K tonnes of steel below ground also presents a serious scheduling problem.

3) The single-coil version avoids the technical and schedule impact of either constructing the more complex double coil or placing a large quantity of iron below ground. The Panel feels that the construction of either shielded option would not be feasible within the schedule constraints set by the project.

4) The Panel believes that the unshielded coil can be used without violating any existing environmental and safety regulatory requirements for workers or for the general public as documented in the report by Ronn Woolley[1]. It will be necessary only to place warning signs in those areas of personnel access where the field exceeds 10 Gauss. This is an at-surface elliptical area of about 26,800 m^2. The area can be posted by fence or even hedge, with pacemaker warning signs.

Also, the effect of the magnetic field on local aviation should be minimal. The solenoid will be housed in the detector hall 54 meters

[1]"SSC GEM Magnetic Field Safety and Health Effects," R. Woolley, September 1991

below ground. The magnetic field at a height of 60 m above ground will be near the 1 Gauss level, and therefore should not precipitate any action from the FAA.

5) There is ample precedent for safe operation of unshielded facilities. Bubble chambers, magnetic fusion confinement devices, and many MRI[2] hospital installations serve as examples:

1) HFTF, MFTF, and FENIX at LLNL
2) LCT (ISMTF) at ORNL
3) 15-ft. Bubble Chamber[3] and the CCM at FNAL
4) ALCATOR C-MOD at MIT Frank Bitter Magnet Laboratory
5) MRI solenoid at the MIT F.B.M.L.

Fringe field comparisons with existing facilities have been made, and although the extent of GEM's 10 Gauss field is about 3.5 times that of the LLNL-MFTF, their safety considerations are the same. One can make a quantitative comparison between existing facilities and GEM. For example, a number of safe, successful years of operation of unshielded magnet facilities, with no injuries or mishaps, have been documented, and this is summarized in the Table. The larger surface-area 10 Gauss field of GEM (shown in the Figure) does not present any additional safety issues, beyond those already addressed by existing facilities. Because of the larger GEM field, additional local equipment shielding may be required, but this issue is not safety related.

---

[2]Ferromagnetic Screening Around a Superconducting Magnetic Resonance Imager, *Health Physics* Vol. 51, No. 4 (October), pp 545-550, 1986.
[3]See for example, memo from L Coulson dated July 30, 1991, *Magnetic Field measurements Around Bubble Chambers*.

Safety personnel at LLNL and FNAL state that their operational experience indicates no adverse effects to employees or equipment, when normal safeguards are applied.[4]

6) Local shielding for sensitive equipment is probably feasible if required, over substantial volumes (10x10x10 m counting rooms) or local regions (scopes, terminals or turbopumps).

7) Surface shielding is feasible as a backup against unlikely future changes in regulatory requirements. For example, a reinforced concrete pad of ~ 160 x 200 meters, carrying the equivalent of ~ 12 cm of solid steel in the central region, tapering toward the edges, could reduce the surface field to the 10 Gauss level.

8) Facilities with large fringe fields (as cited) have been successfully operated. Issues associated with the use of ferromagnetic materials in the hall, magnetic shielding requirements, and the affect of the field on the operability of the GEM detector present some interesting problems, all of which have been addressed and solved in existing facilities. In order to avoid problems with operations, the magnet will be designed for a normal discharge time of two hours, so that work in the hall during maintenance periods

[4]Taken from private communication with Gordon Miller and Phil Dean at LLNL, Tim Miller and Tom Peterson at FNAL, and Larry Coulson at SSCL, on September 24-25, 1991.

can proceed safely. For emergency discharge, as might occur in the event of fire, the magnet will discharge within a few minutes to avoid hampering the emergency response effort. As such, no extraordinary fire containment techniques will be necessary in the hall.

These eight considerations form the basis for the Panel's recommendation. To be succinct, the unshielded option is the only large coil option that can meet cost and schedule constraints, and the methods associated with operating in an unshielded area appear tenable.

FACILITIES FRINGE FIELDS COMPARISON

Date: September 23, 1991 - R. Woolley

	LAB FACILITY	Years In Operation	Magnet Strength	Altitude of 5 gauss Field	Magnet Elevation	Surface Area 10 gauss (pacemaker)	Surface Area 5 gauss (instrumentation sensitivity)	Health Effects Reported
1	SSC - GEM	New	0.8 T	71m	<47m>	~26,800m2	~43,000m2	n/a
2	LLNL - FENIX	~0.5	14.0 T	23m	<3 m>	4,976m2	6,464m2	none
3	LLNL - HFTF	~10	~11 T	16m	<2 m>	452m2	804m2	none
4	LLNL - MFTF	<1 week	~ 7 T	50m	~3.5 m	7,350m2	~13,000m2	none
5	15'BBL.CH-FNAL	15	~3.2 T	~40m	2 m	2,463m2	~5,000m2	one suture move
6	LCT - ORNL	2	8 T	n/a	3m	n/a	n/a	no verifiable
7	Tohoku/Chicago Sync.-FNAL	~20-25	~ 3.0 T ea.	?	?	?	?	?

FIELD SIZE COMPARISON

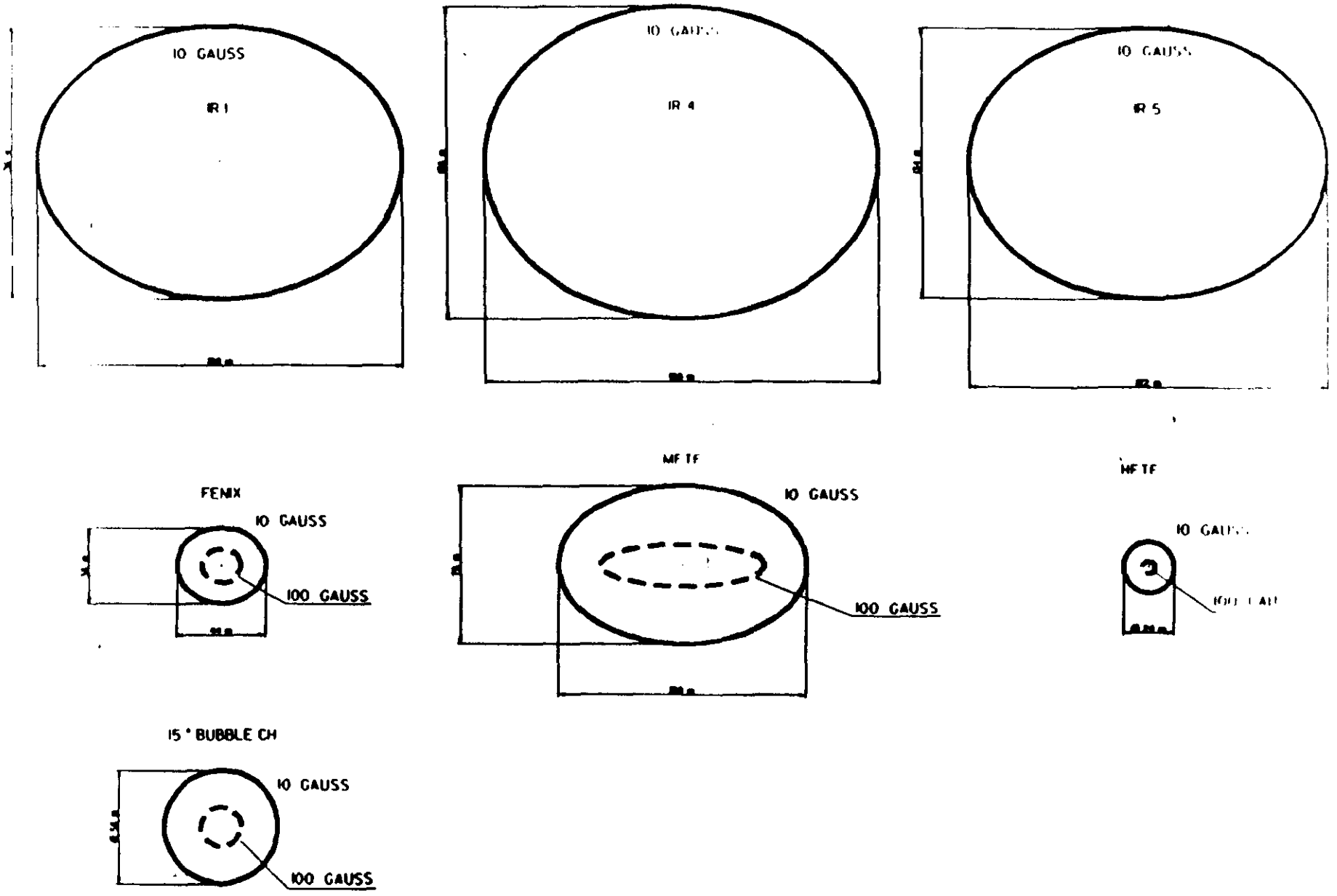

DRAFT

SSC GEM Magnetic Field Safety & Health Effects

R.P. Woolley

GEM Safety Coordinator
Experimental Facilities
Physics Research
Superconducting Super Collider Lab

September 22, 1991

TABLE of CONTENTS

1.0	INTRODUCTION AND SCOPE	1
2.0	DETECTOR OVERVIEW	2
3.0	PROBLEM STATEMENT	3
4.0	MAGNETIC FIELD EFFECTS	4-5
5.0	REGULATORY STANDARDS	6
6.0	SUMMARY/DISCUSSION	7-8
7.0	REFERENCES	9
Fig. 1	Magnetic Fringe Field	10
Fig. 2	Magnetic Field (lateral view)	11
Fig. 3-4	Facilities Fringe Field Comparisons	12-13
Tab. 1	Magnetic Field Exposure Limits	14
Tab. 2	Sensitivity of Equipment and Component	15
Figs.5-10	Magnetic 'B' Contour Plots	16-21

1.0 INTRODUCTION AND SCOPE

This report focuses upon the safety concerns associated with the fringe magnetic field, generated by the unshielded GEM Detector design. The report's purpose is to present the GEM Collaboration and SSC Directoral management with the regulatory requirements, and background information on human and equipment fringe field effects. Safety issues associated with the effects of the magnetic field upon personnel and equipment will be discussed, with the applicable regulatory requirements noted. The intent then is for SSC management to determine the nature and extent of application of the appropriate safeguarding, in mitigating the risk.

2.0 DETECTOR OVERVIEW

The GEM Collaboration is proposing a large solenoidal detector for lepton, photon, and muon measurement/detection. To accomplish this objective, the detector will have hermetic electromagnetic and hadronic calorimetry and central tracking in a magnetic field. This field is generated from the proposed detector magnet system, and consists of a 16.6-meter bore and a 8,300 gauss single-coil (unshielded) superconducting solenoid oriented concentric to the beam axis. The coil has iron poles at both ends but no flux return (coils or iron) in the barrel region. Steel poles cover each end of the solenoid. Reductions in cost and manufacturing time result from elimination of the outer shield winding, however this produces a large external fringe field.

3.0 PROBLEM STATEMENT

Preliminary safety studies of the effect of the detector's external static magnetic field have been made. The personnel at risk from GEM's fringe magnetic field are those associated with implanted cardiac pacemakers, blood disorders (ex: sickle-cell anemia), or (at higher flux densities) implanted ferromagnetic medical devices, e.g., suture staples, aneurism clips, prostheses, etc.[2] These restrictions point toward prohibiting access of these personnel to surface buildings and surrounding areas, within the 5-10 gauss field boundary. Based upon recent human exposure data, limited potential exists for personnel health effects.

Indications are that there is a definite potential for interference with the normal electro-mechanical operation of 'magnetically sensitive' equipment, within the hall and on the surface. The high (8,300 gauss) magnetic field, generated at the muon and central tracking areas during conductor tests, is an uncommon safety and environmental risk caused by the large unshielded superconducting solenoid.

Significant stray fields will occur due to the absence of controlled flux return paths. Maps of this field are shown in Figures 1 & 2.[1] Based upon this data, shielding or design modifications will need to be applied to nullify any operational-interference effects upon hall and surface components. The fringe field level in the 'counting room' area of the Operations Center represents the worst-case stray dc field of ~ 25 gauss, with a transient time constant of 0.17 gauss/second (higher during 70 sec. quench) during a magnet discharge.[1] A < 40 gauss field would be present in the Operations Center, having a single-level basement.

Sensitive control and data processing equipment may require shielding or removal from the field, in order to nullify the adverse effects of magnetic flux densities > 5 gauss.

Existing regulatory magnetic field limits have incorporated a safety factor. It is management's decision to define a magnetic field exposure limit and the methodology of attaining compliance.

4.0 MAGNETIC FIELD EFFECTS

Field strength contour maps are shown in Figures 1 & 2. Recent U.S. epidemiological surveys have shown no significant health effects upon man associated with long term exposure to static magnetic fields. Available knowledge indicates the absence of any adverse health effects due to exposure to static magnetic fields up to 20,000 gauss[4]. One study inferred that the white blood cells of workers exposed to an average field of 76 gauss and a maximum of 146 gauss, were slightly changed (yet, still within the normal range). At a U.S. accelerator laboratory 792 employees worked in fields of 50 gauss for long durations and up to 20,000 gauss for periods of several hours. No significant change in 19 disease categories was found between the exposed and control groups[4]. The preliminary indication from limited experimental data is that short-term exposure to static fields > 50,000 gauss may produce significant adverse health effects, such as a ~7% reduction in aortic blood flow velocity[4].

A survey is required to verify that all equipment or components in the detector, underground hall and some surface buildings, are suitably shielded or designed to avoid the operationally disruptive influence of the field (See Table 2). Techniques for accomplishing this have been successfully applied in other high field unshielded magnet facilities[1]. Equipment and components that could cause injury or major detector damage, if field influenced, must be protected. The magnetic field affects dc motors (their armatures, commutators, and brushes) and other magnetically-coupled devices. The dc magnetic field strength is ~ 1,000 (R) and 2,000 (Z) gauss immediately external to the operating detector's support structure[3]. Comparisons of existing unshielded magnet facilities to GEM, are presented in Figs. 3-4. Fringe field strength decreases with the cube of the distance from the source. Field strength contours of constant 'B' are illustrated in Figures 5-10,[6] where 'Z' is the beam axis and 'R' is the vertical axis.

At a level of ≥ 100 gauss ferrous tools may begin to be transported[4]. This indictates that an interlock system should power-down the magnet prior to personnel access of the underground hall, and patrols of the hall wil be required to ensure that all personnel and loose magnetic materials are removed.

The U/G hall and surface operations building(s) (especially the Counting Room) will require that their magnetically-sensitive safety systems, components and instrumentation (ex: fire detection, computers, monitors, software, etc.) have iron shielding or field shaping coils. The shielding, to attenuate the fringe 'B' (magnetic) field to 5-10 gauss, is currently being reviewed as to thickness, magnetic saturation, permeability, and cost. Shielding to a ≤ 10 gauss level meets the current regulatory pacemaker requirement. Fences and barriers with pacemaker-warning signs could be located just beyond the 10 gauss (OSHA) field line, and inside and outside of any buildings within this field to notify and warn personnel. A site survey should be done and general access restricted during the first full-field operation.

The FAA currently has no regulations for static magnetic fields. Of primary concern is the field's influence upon aircraft that would penetrate the above-ground magnetic field 'bubble'. The FAA indicated that a significantly stronger and higher (than GEM's) elevation field, would be required before being considered a potential air-traffic hazard[7]. The FAA suggested that after the field is surveyed and measured, SSC should inform them of the field strength/gradient characteristics in order for FAA to decide upon navigational map inclusion.

Additional areas of concern are electromagnetic interference and compatibility with transmission and communication systems within the field of influence. Also, SSC Management should anticipate the public's reaction to knowledge of this field.

Static magnetic fields are not within the jurisdiction of the Federal Communications Commission (FCC), the Environmental Protection Agency (EPA), and the Texas Department of Health, Radiation Control (TDHRC).

5.0 REGULATORY STANDARDS

Following are currently accepted magnetic fields exposure guidelines, based upon the best available data from several official sources[4,9] :

Maximum Exposure: Workers must never be exposed to fields > 20,000 Gauss, regardless of the duration of the exposure or the body part exposed.

Fields > 5,000 G: If the peak exposure is > 5,000 G, workers should be exposed to a daily maximum average field strength of ≤ 600 G (measured at the torso) or 6,000 G (measured at the extremities).

Fields < 5,000 G: If the peak field to which workers are exposed is < 5,000 G, personnel may be exposed to a week-long maximum average field strength of ≤ 600 G (measured at the torso) or 6,000 G (measured at the extremities)[2].

Medical Restrictions: Personnel with medical electronic implants (such as artificial cardiac pacemakers) and metallic prosthetic implants cannot be exposed to fields > 10 G.* Personnel with sickle-cell anemia or similar hemoglobin-related conditions (but not carriers) cannot be exposed to fields > 500 G.

* The 10 G level is from the American Conference of Governmental Industrial Hygienists (ACGIH), a standards-setting group recognized by OSHA.

Agencies involved with the regulation or standard-setting of magnetic field radiation include:

- Department of Energy (DOE)
- Occupational Safety & Health Administration (OSHA)
- Food and Drug Administration- Center for Devices and Radiological Health (FDA)
- Environmental Protection Agency (EPA)
- Federal Aeronautics Administration (FAA)
- National Institute of Safety & Health (NIOSH)
- Texas Department of Health, Radiation Control (TDHRC)
- Amer. Conf. of Gov't. Ind. Hygienists (ACGIH)
- Electric Power Research Institute (EPRI)
- World Health Organization (WHO) - EHC 69

Table 1 provides a summary of all applicable regulatory agency's magnetic field exposure limits.

6.0 SUMMARY/DISCUSSION

The FDA's field exposure limit of 5 gauss only applies to cardiac pacemaker manufacturers, while the FNAL[8], ACGIH and OSHA have determined that their pacemaker safety limit is 10 gauss. This is certainly several orders of magnitude below the level at which health may begin to be affected. Some data acquisition systems (computers, monitors, software) are influenced at the 5-10 gauss level, so consideration should be given to shielding or relocation. Additional consideration must be given to aircraft instrumentation affectation. The initial indication from two sources is that magnetically-sensitive instrumentation CAN be disrupted at ≥ ~5 gauss, however, no pertinent regulation currently exists.

The FDA regulation requires controlled access to all areas with > 5 gauss. New-design pacemakers can be affected at 15-17 gauss[5]. The FDA was cautious and incorporated a large safety factor, due to the liability aspect and questionable confidence levels on input from pacemaker manufacturers. For SSC and consortium personnel, a questionnaire on body metal content and a written legal warning should effectively screen those affected from controlled access areas.

The unshielded single-coil magnet is significantly less expensive than either the two-coil or iron-shielded systems. If surface shielding is considered, the Final Supplemental Environmental Impact Statement (FSEIS) won't allow SSC to pave a large (hectares) area with steel plate, without reopening the environmental impact assessment process. For access protection of the field perimeter, fencing or even hedges with proper warning signs is acceptable.

No applicable magnetic field data was contained within the following sources:

- TRNLC/URA Contract - DEAR 970.5704-2
- SEIS for SSC-Main Report, 12/90
- FCC - OST Bulletin #65, 10/85
- Texas Regulations for Control of Radiation-Part 35, 9/88
- PPPL - Practices and Procedures RF and Microwave, Sec.4, 1/82
- SSC ES&H Manual
- FNAL Radiation Guide
- Various SSC Radiation TaskForce Reports,1/86-11/88
- LBL Safety Manual
- TU Electric - Safety Policy
- Microwave News-Report on Non-Ionizing Radiation-89-91.

The preliminary indication from the FAA is that SSCL would need to notify them, when the actual field size and strength is measured, to allow the FAA to determine if flight navigation maps require revision. A draft is being prepared that would advise them of our GEM intentions.

Operational experience from several unshielded dc magnet systems indicates that an effective personnel safety protocol can be established[1]. These safe-operation facilities include bubble chambers, magnetic fusion confinement devices, and many MRI[10] hospital installations:

- HFTF at LLNL
- MFTF at LLNL
- FENIX at LLNL
- LCT (ISMTF) at ORNL
- 15-ft. Bubble Chamber[11]/CCM at FNAL
- ALCATOR C-MOD at MIT Francis Bitter Magnet Laboratory
- MRI Solenoid at the MIT F.B.M.L.

Please refer to Figures 3 & 4 for simple quantitative comparisons between GEM and these existing facilities. Although the extent of GEM's 10 gauss field is ~3.5x that of LLNL-MFTF, their safety considerations are the same. No new safety issues are represented by GEM's sizeable fringe field. A significant number of safe, successful years of operation have been logged, by existing unshielded magnet facilities, with no indication of accidents or injuries. The larger GEM fringe field will probably necessitate additional localized equipment shielding, to maintain operability.

7.0 REFERENCES

[1] *Shielding Scheme for the SSC SC Magnet Stray Field Environment*, Shen, Patrick, Heim, & Chaplin (7/91).

[2] *Threshold Limit Values for Chemical Substances and Physical Agents - 1990-1991*, ACGIH, ('90).

[3] *An Expression of Interest to Construct a Major SSC Detector*, SSC EOI-0020, Barish & Willis, (7/91).

[4] *Environmental Health Criteria 69 - Magnetic Fields*, UN, WHO, & IRPA, (1987).

[5] *DC Magnetic Field Limits*(memo), Jay Benesch, (8/14/91).

[6] *Magnetic Contours of Constant B*, Peter Marston, MIT, (8/16/91).

[7] *Private telcon with Dick Kirsch at FAA*, (8/14/91)

[8] *Fermilab ES&H Manual, Static Magnetic Fields* - 5062.2, (11/87).

[9] *LLNL Health & Safety Manual*, Supplement 26.12, "Working in Magnetic Fields," ('85)

[10] *Ferromagnetic Screening Around a Superconducting Magnetic Resonance Imager*, Health Physics Vol.51, No. 4 (Oct.'86), pp 545-550.

[11] *Magnetic Field Measurements Around Bubble Chambers*. Memo from L. Coulson dated 7-30-91.

FIELD ON THE SURFACE IR 1 , IR 8

IR 1 : BEAM 46.9 m /surface

IR 8 : BEAM 48.1 m /surface

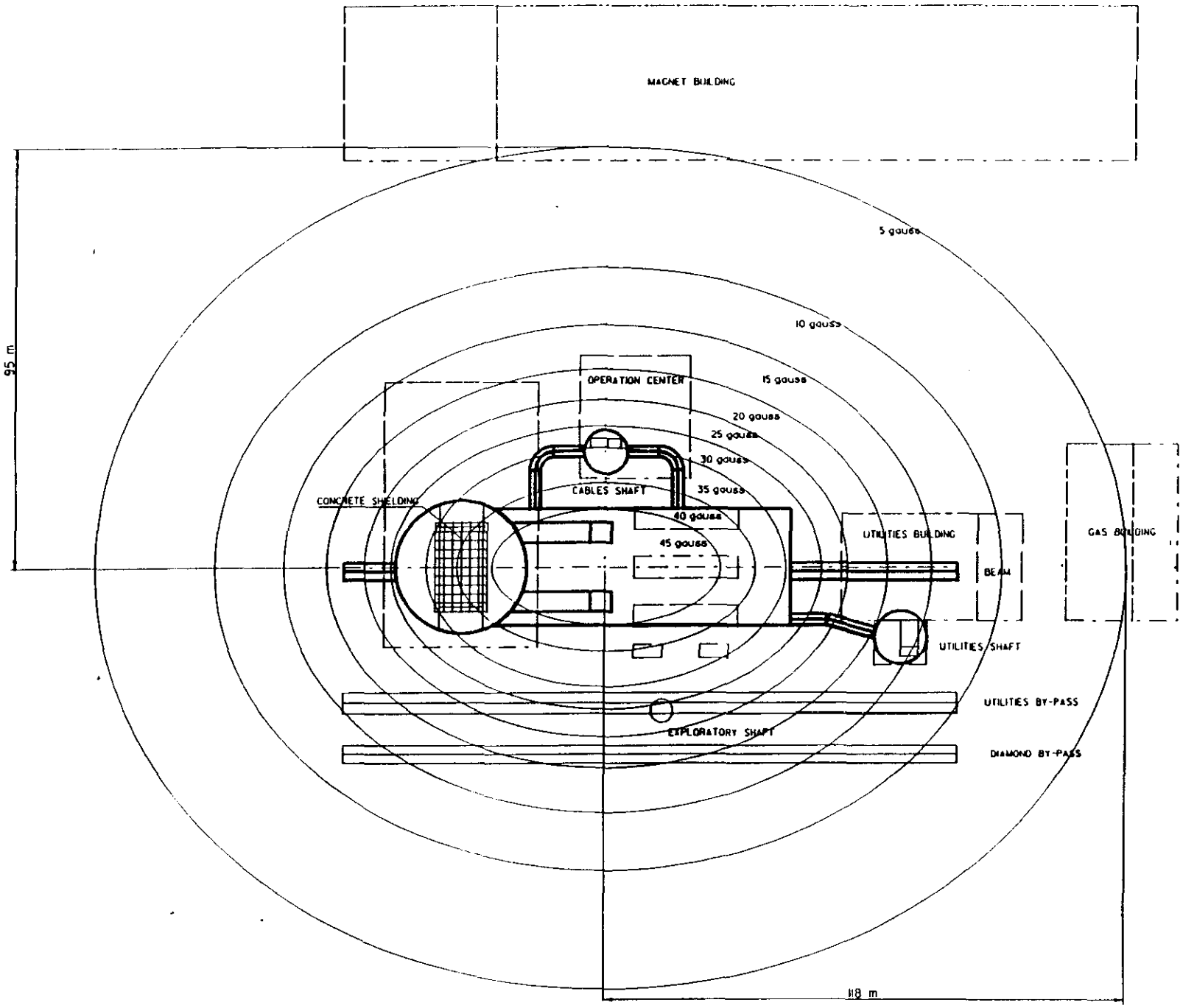

FIGURE

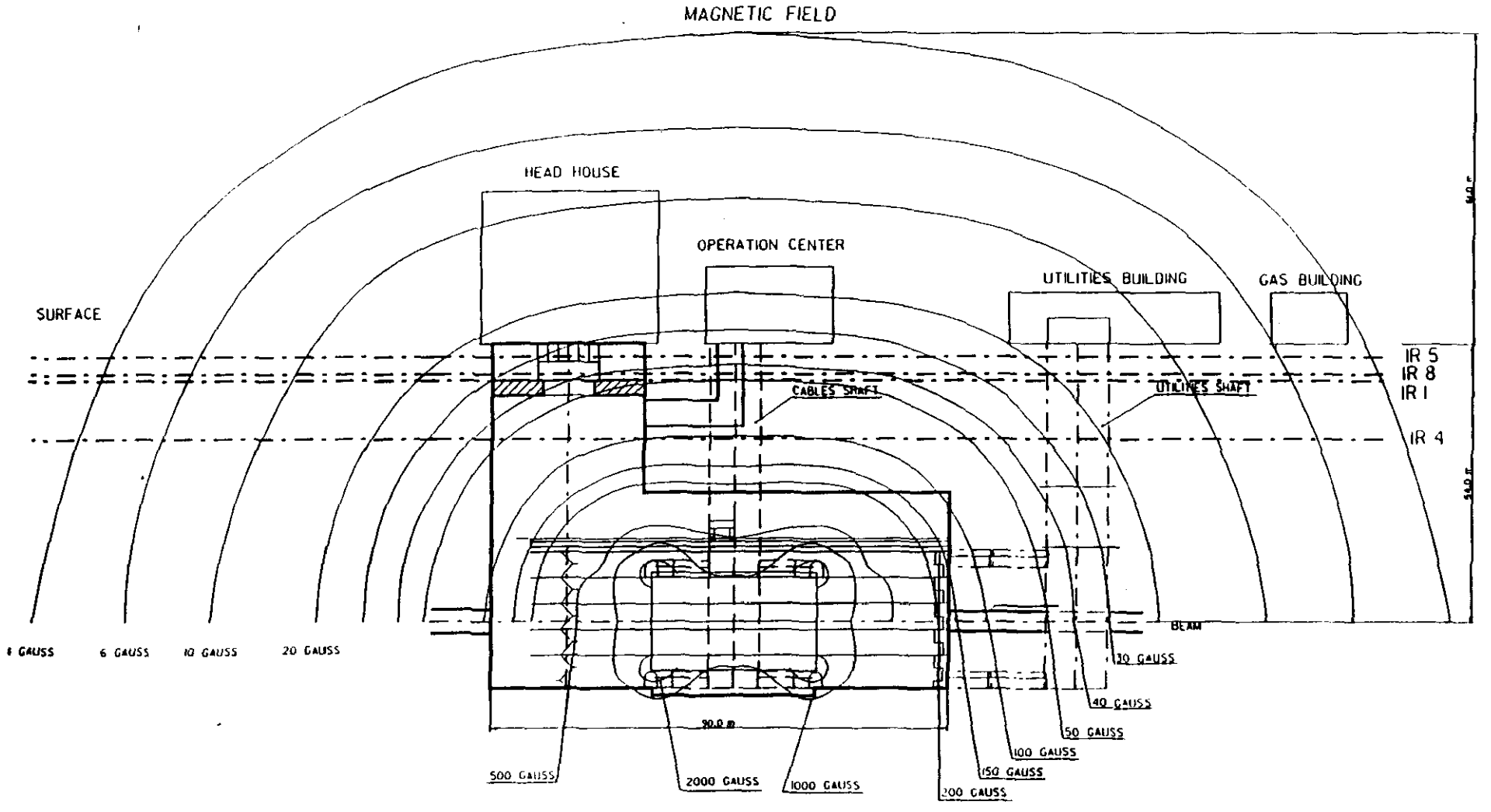
MAGNETIC FIELD
HEAD HOUSE
OPERATION CENTER
UTILITIES BUILDING
GAS BUILDING
SURFACE
IR 5
IR 8
IR 1
IR 4
CABLES SHAFT
UTILITIES SHAFT
BEAM
4 GAUSS
6 GAUSS
10 GAUSS
20 GAUSS
30 GAUSS
40 GAUSS
50 GAUSS
100 GAUSS
150 GAUSS
200 GAUSS
500 GAUSS
2000 GAUSS
1000 GAUSS
90.0 m

FIGURE 2

FACILITIES FRINGE FIELDS COMPARISON

Date: September 23, 1991 - R. Woolley

	LAB FACILITY	Years in Operation	Magnet Strength	Altitude of 5 gauss Field	Magnet Elevation	Surface Area 10 gauss (pacemaker)	Surface Area 5 gauss (instrumentation sensitivity)	Health Effects Reported
1	SSC - GEM	New	0.8 T	71m	<47m>	~26,800m2	~43,000m2	n/a
2	LLNL - FENIX	~0.5	14.0 T	23m	<3 m>	4,976m2	6,464m2	none
3	LLNL - HFTF	~10	~11 T	16m	<2 m>	452m2	804m2	none
4	LLNL - MFTF	<1 week	~ 7 T	50m	~3.5 m	7,350m2	~13,000m2	none
5	15'BBL.CH-FNAL	15	~3.2 T	~40m	2 m	2,463m2	~5,000m2	one suture move
6	LCT - ORNL	2	8 T	n/a	3m	n/a	n/a	no verifiable
7	Tohoku/Chicago Sync.-FNAL	~20-25	~ 3.0 T ea.	?	?	?	?	?

FIGURE

FIELD SIZE COMPARISON

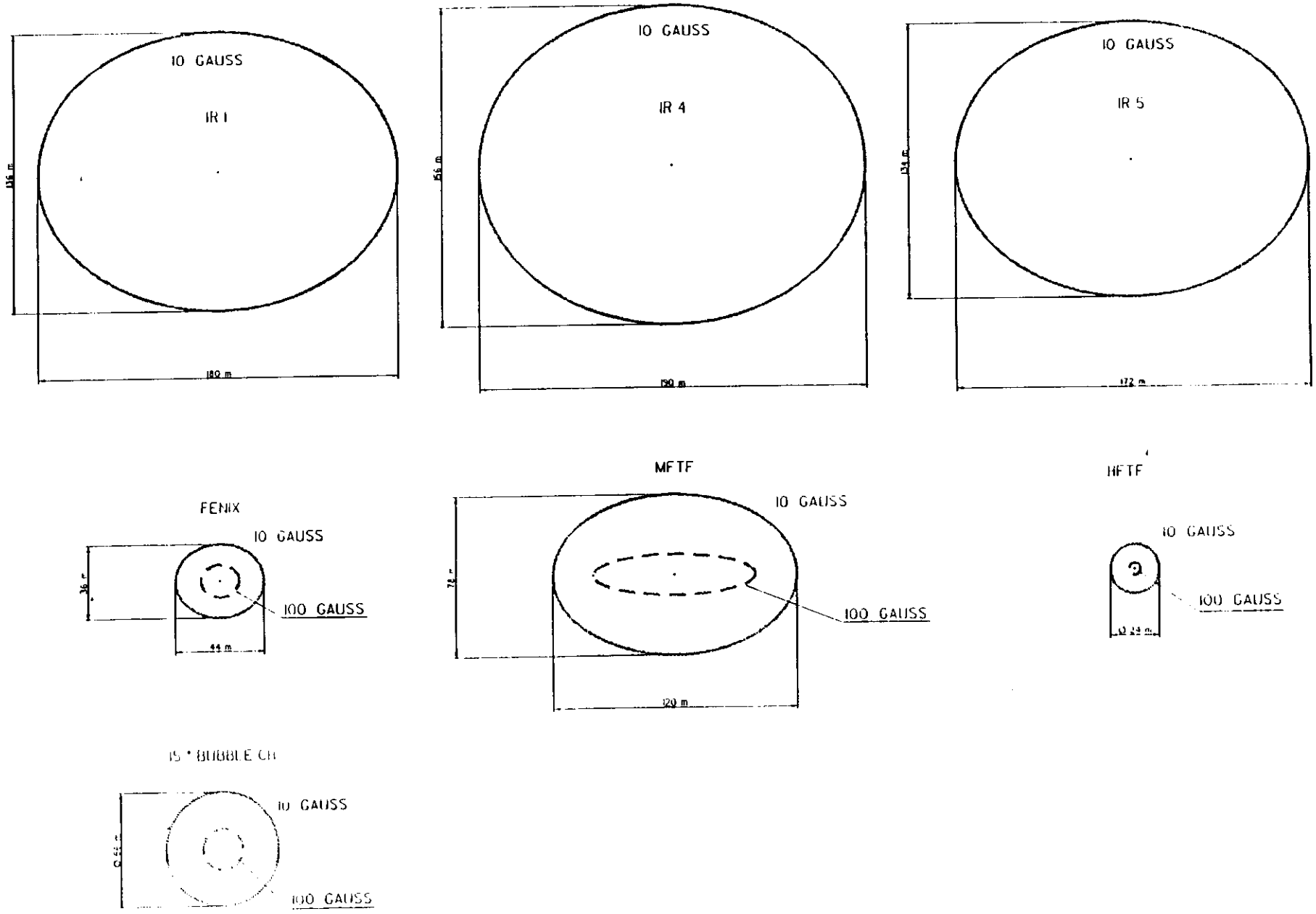

FIGURE 4

Table 1. Magnetic Field Exposure Limits[4]

Agency	Field	Exposure Time	Body Region	Comments
SLAC (1970)	200 G	extended (h)	whole body	unofficial, occupational
	2,000 G	short (min.)	whole body	
	2,000 G	extended (h)	arms, hands	
	20,000 G	short (min.)	arms, hands	
USSR (1978)	100 G	8 hours	whole body	regulation issued by Ministry of Health
DOE (Alpen, 1979)	100 G	8 hours	whole body	recommended to DOE contractors
	1,000 G	<= 1 hour	whole body	
	5,000 G	<= 10 min.	whole body	
FDA (1980)	5 G	none	pacemaker	limit is dictated by pacemaker mnfr. only
CERN (NRPB, 1981)	2,000 G	minutes	whole body	recommended practice
	20,000 G	short	hands, arms, feet	
LLNL (1985)	600 G	day	torso	max. ave./day in peak field > 5 kG
	600 G	day	torso	max. ave./week in peak field < 5 kG
	6,000 G	day	extremities	max. ave./wk.(<5kG) max. ave./day(>5kG)
	20,000 G	short (min.)	whole body	peak exposure limit
ACGIH (1990)	10 G	none	pacemaker	current 15-17G limit of mech. interference
	600 G	8 hours	whole body	time-weighted average
	6,000 G	8 hours	extremities	time-weighted average
	20,000 G	ceiling limit	whole body	never exceed

Table 2. Sensitivity of Equipment and Component

	>5 G	>10 G	>100 G	>1000 G
Data Acquisition System				
Computer	x			
Monitors				
Black & white		x		
Color	x			
Instrumentation & Control				
Relay			x	
Solid-state device			x	
Magnetic solenoids, valves			x	
Safety device				x
Analog display			x	
Vacuum & Refrigerator				
Mechanical pump			x	
Turbo pump			x	
Electric motors			x	
Ferro-fluidic seals				x

x: shielding is needed

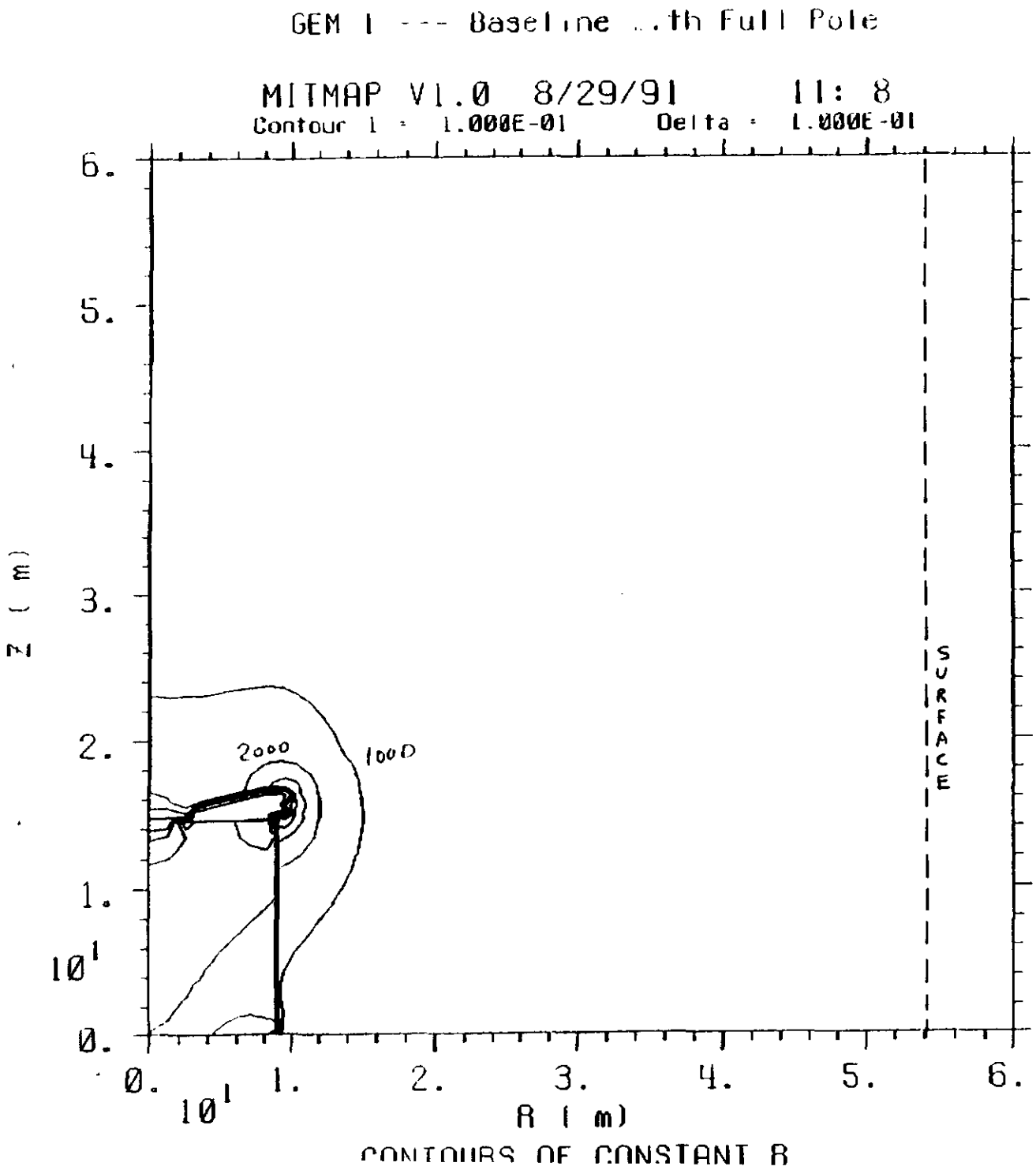
GEM I --- Baseline ...th Full Pole
MITMAP V1.0 8/29/91 11: 8
Contour 1 = 1.000E-01 Delta = 1.000E-01
6.
5.
4.
3.
2.
1.
10¹
0.
Z (m)
2000
1000
SURFACE
0.
10¹
1.
2.
3.
4.
5.
6.
R (m)
CONTOURS OF CONSTANT B

FIGURE 5

GEM I -- Baseline w/h Full Pole

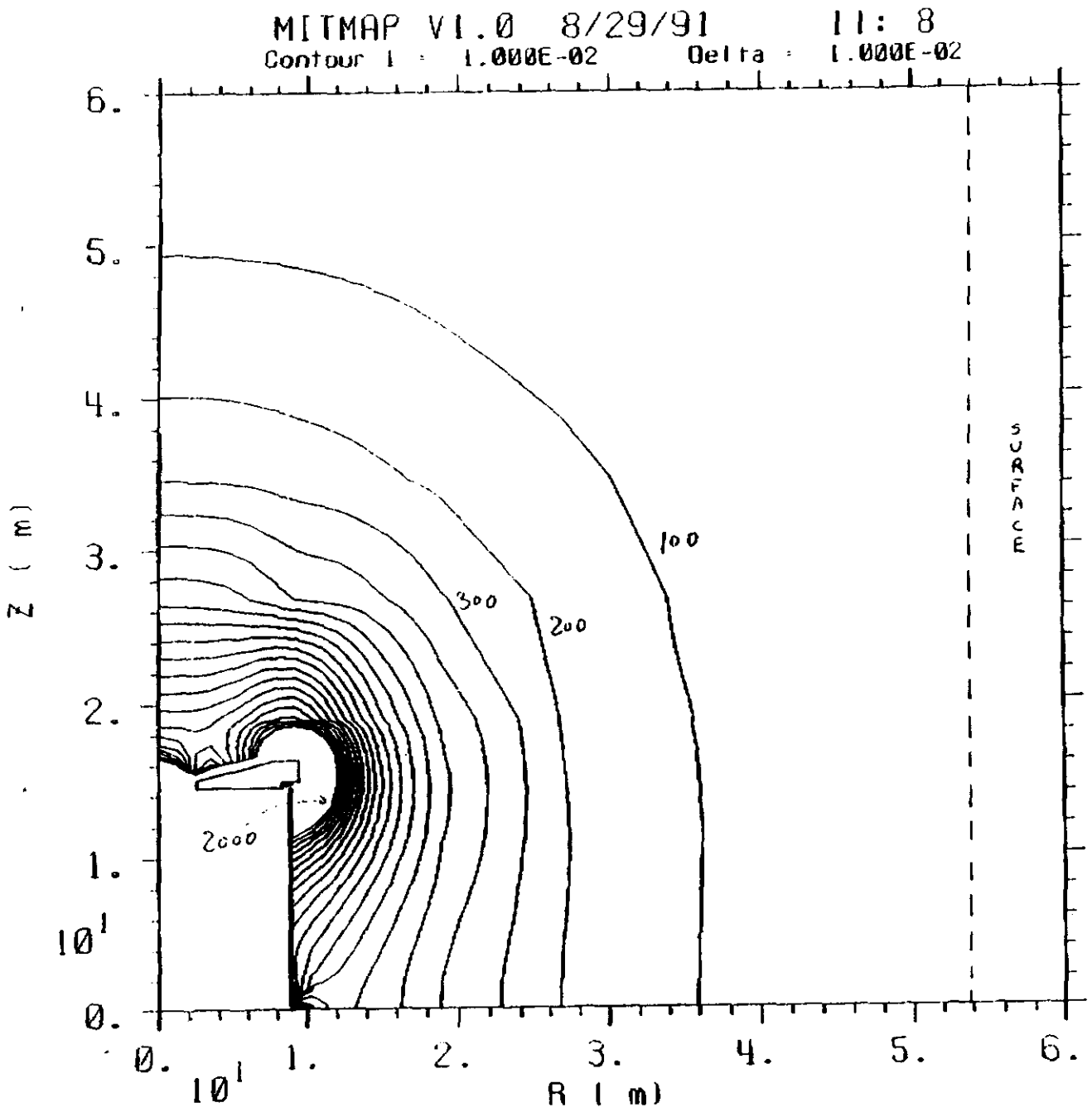

CONTOURS OF CONSTANT B

FIGURE 6

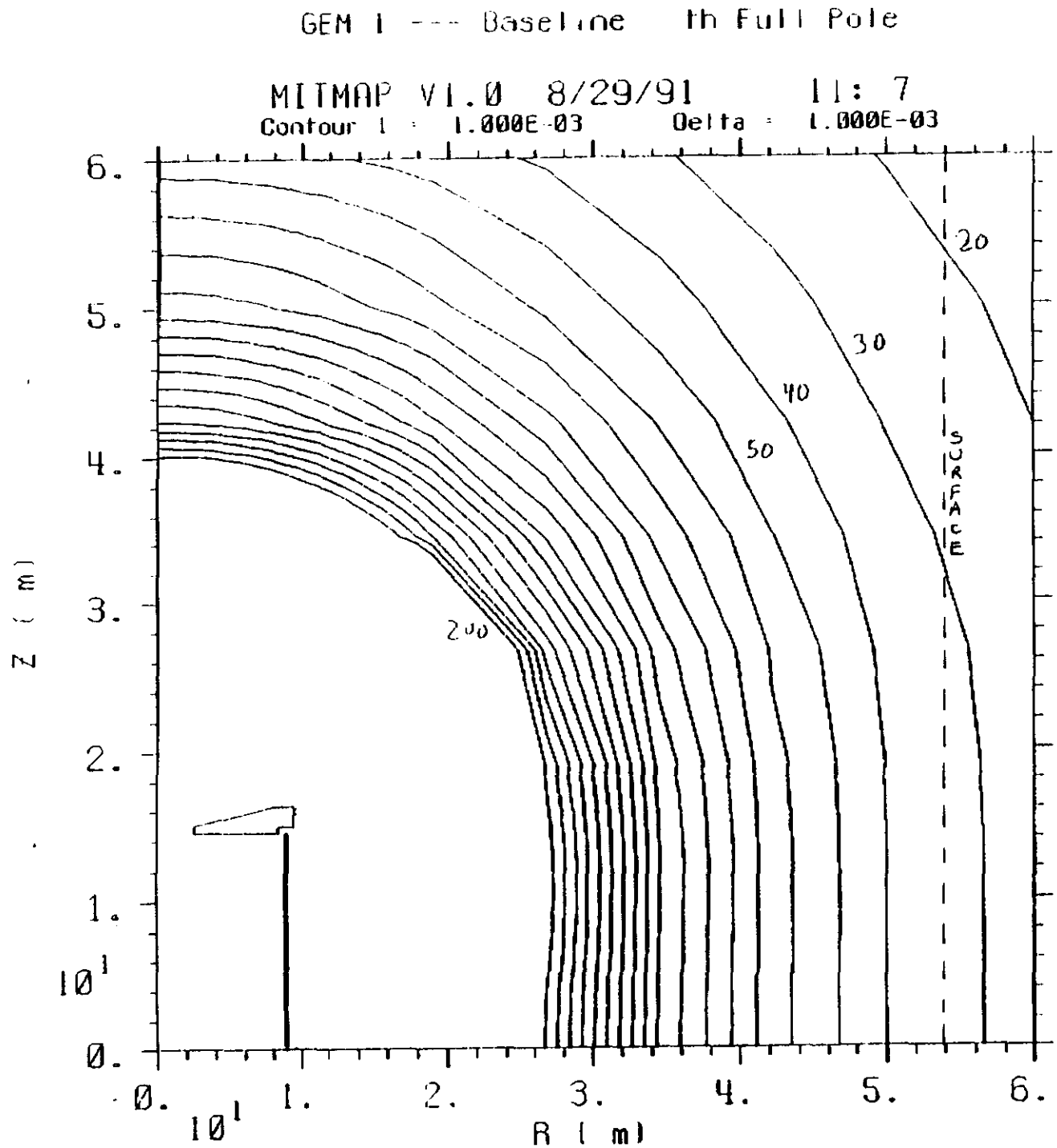

CONTOURS OF CONSTANT B

FIGURE 7

FLUX DENSITY AT GROUND ELEVATION*, NO SHIELDING

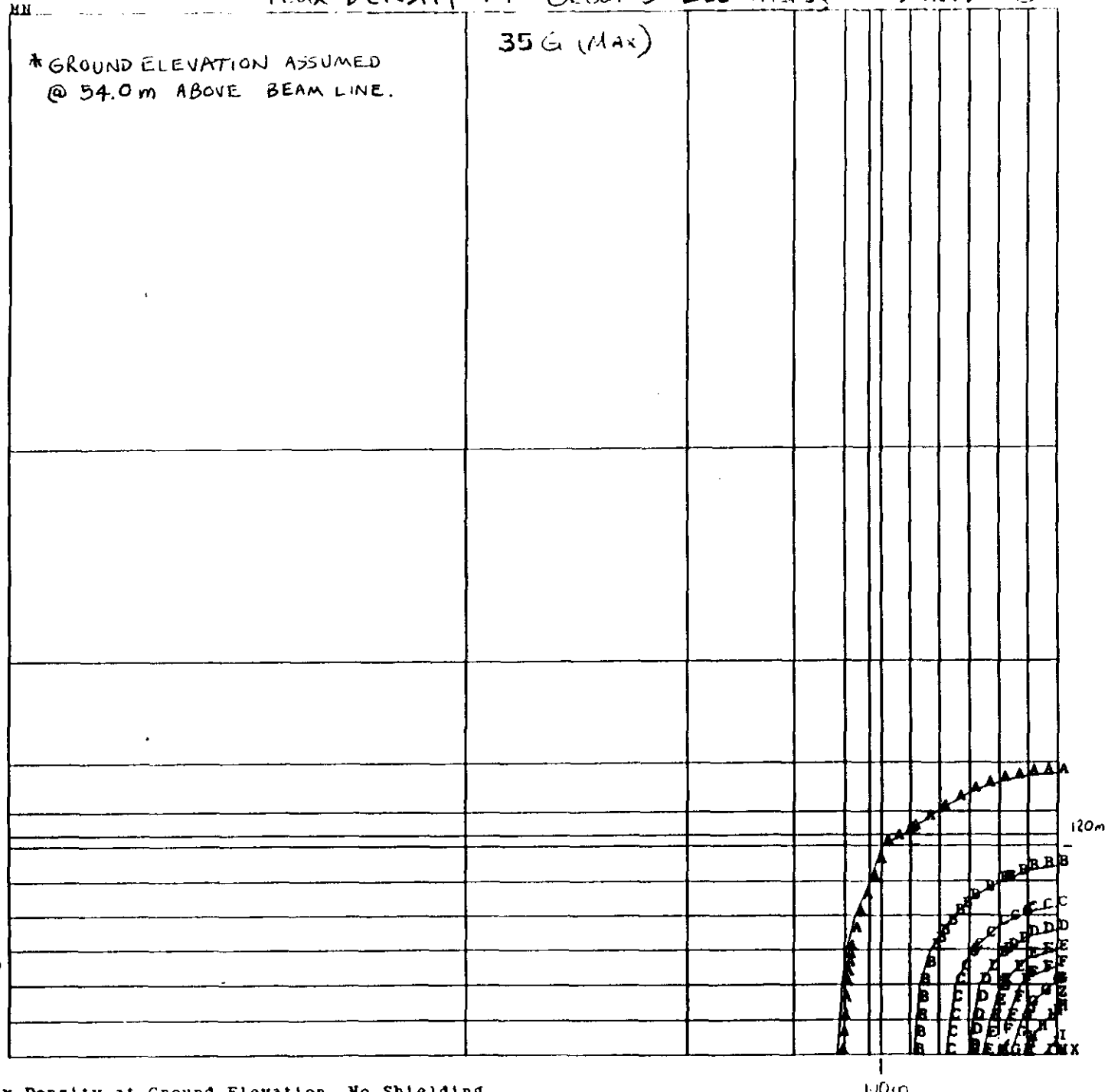

ANSYS 4.4A
AUG 28 1991
14:30:37
PLOT NO. 1
POST1 STRESS
STEP=1
ITER=1
BSUM (AVG)
SMN =0.300E-05
SMX =0.003976

YV =1
DIST=330
XF =300
ZF =300
VUP =Z
A =0.224E-03 [T]
B =0.665E-03
C =0.001107
D =0.001548
E =0.00199
F =0.002431
G =0.002873
H =0.003314
I =0.003755

PROPOSED PIT SIZE
200m WIDE
x
240m LONG
x
THK
(TO BE DETERMINED)

FIGURE 8

Flux Density at Ground Elevation, No Shielding

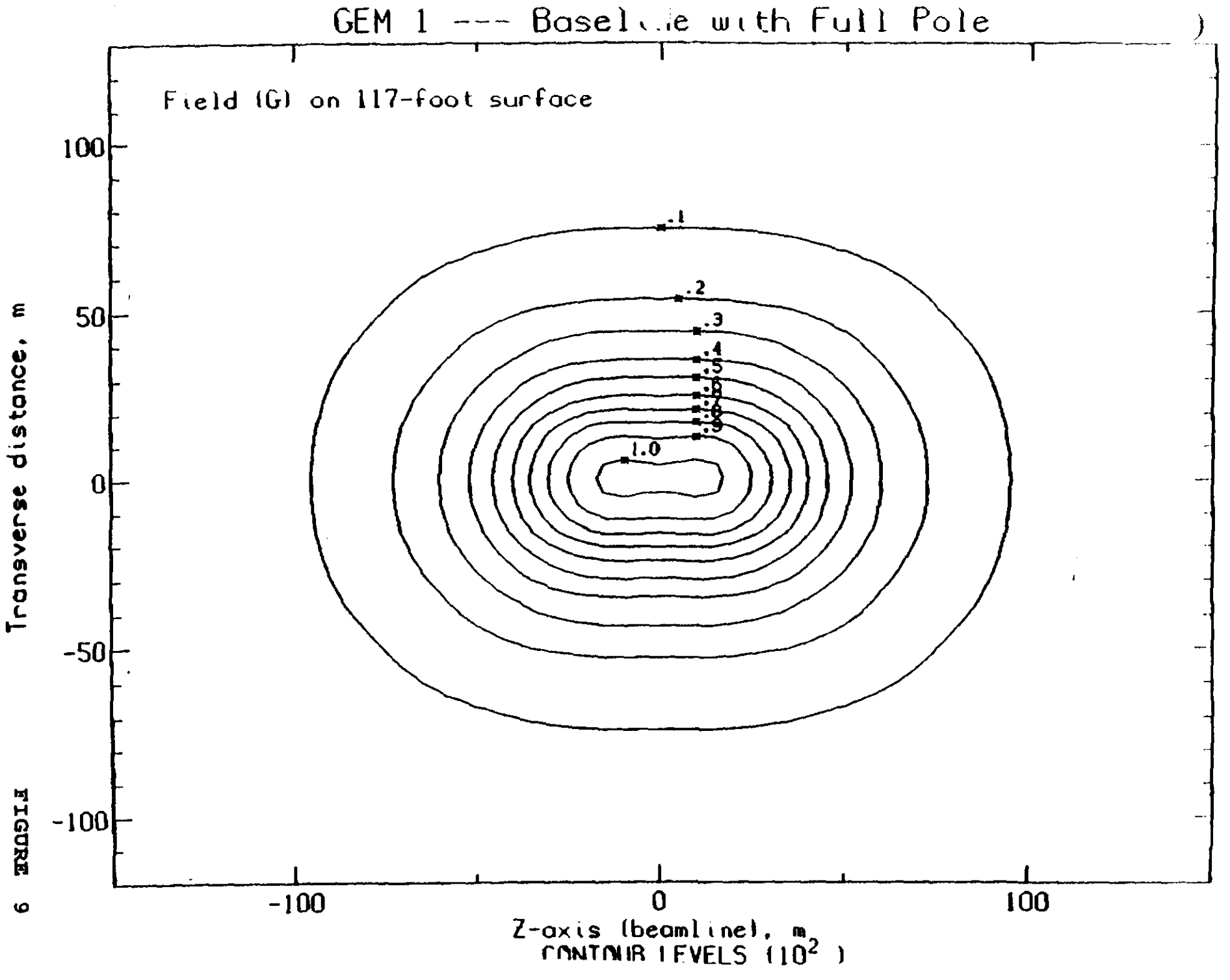
GEM 1 --- Baseline with Full Pole
Field (G) on 117-foot surface
.1
.2
.3
.4
.5
.6
.7
.8
.9
1.0
100
50
0
-50
-100
Transverse distance, m
-100
0
100
Z-axis (beamline), m
CONTOUR LEVELS (10^2)

FIGURE 9

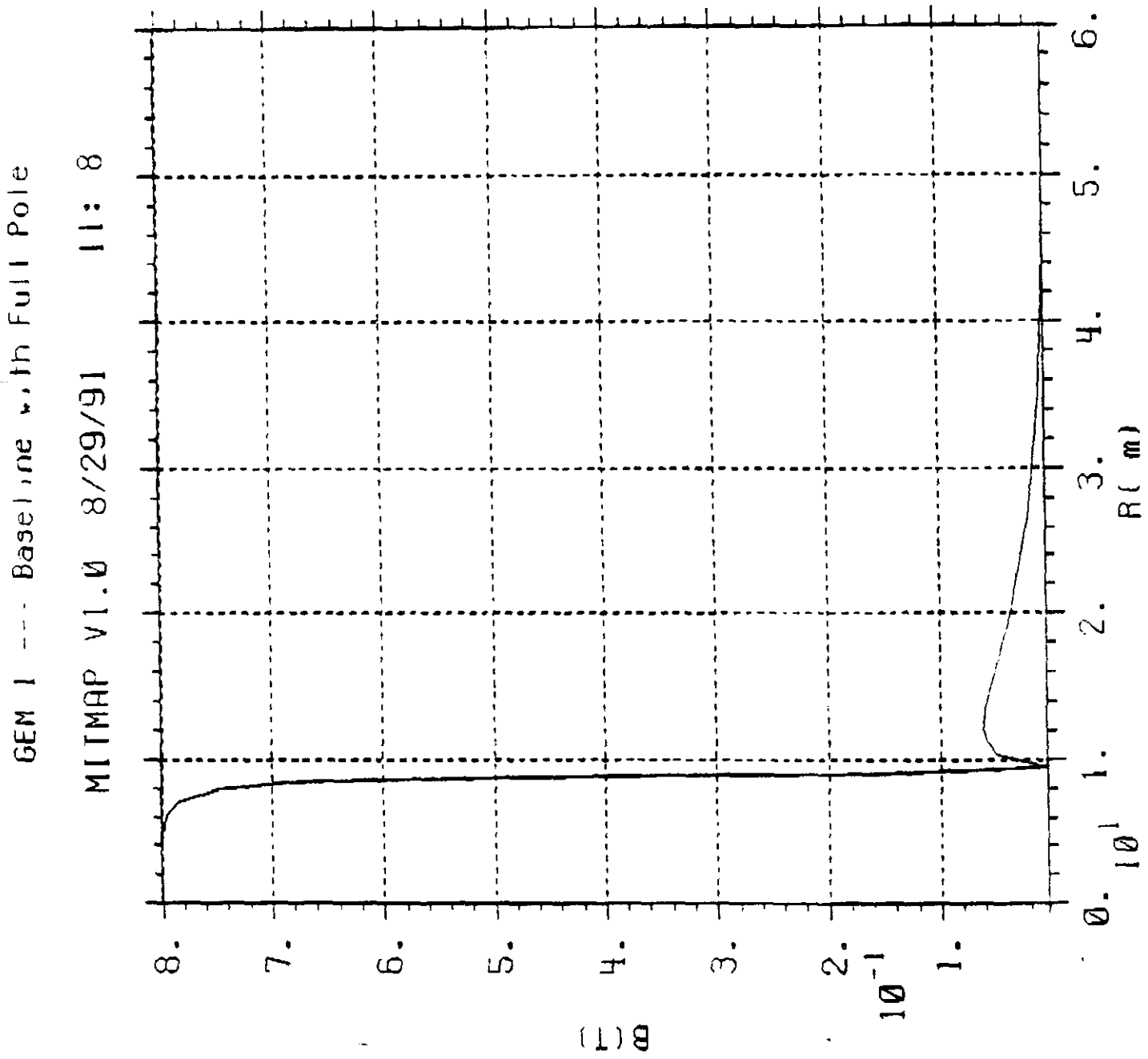
GEM I --- Baseline with Full Pole
MITMAP V1.0 8/29/91 11: 8
B(T)
8.
7.
6.
5.
4.
3.
2.
1.
10^{-1}
0.
1.
2.
3.
4.
5.
6.
10^{1}
R(m)

FIGURE 10

MUON PHYSICS OF GEM DETECTOR AT THE SSC

— **Higgs search for 140 < M_{H^0} < 800 GeV**

$$H^0 \rightarrow ZZ/ZZ^* \rightarrow \mu^+\mu^-\mu^+\mu^-$$

— **$Z_L Z_L / W_L W_L$ interactions**

— **New Gauge Boson Searches**

$$Z' \rightarrow \mu^+\mu^-, \qquad W' \rightarrow \nu\mu$$

— **Top/heavy Quark Searches**

$$t \rightarrow W + b \rightarrow \mu_{iso} + \nu + \mu_{inc} + jet$$

— **SUSY: like-sign μ-pairs**

— **Unpredicted phenomena**

Design Principle

Measure muons precisely outside of the calorimetry, in a large volume magnetic field.

Advantages:

– Most clean & reliable signal in TeV collider;

– Low rate and low radiation;

– Only way to measure the charge asymmetry for TeV Z';

– Working at 10^{34}.

Design Criteria :

- $\Delta p/p = a \times p \bigoplus b$

  $b \leq 1\%$, for $ZZ^* \rightarrow \mu^+\mu^-\mu^+\mu^-$;

  $X_{mid} < 10\% X_R$

  $a \leq 10\%$, for charge asymmetry

  measurement (6 TeV Z').

- $\eta \geq 2.5$ for 4μ acceptance.

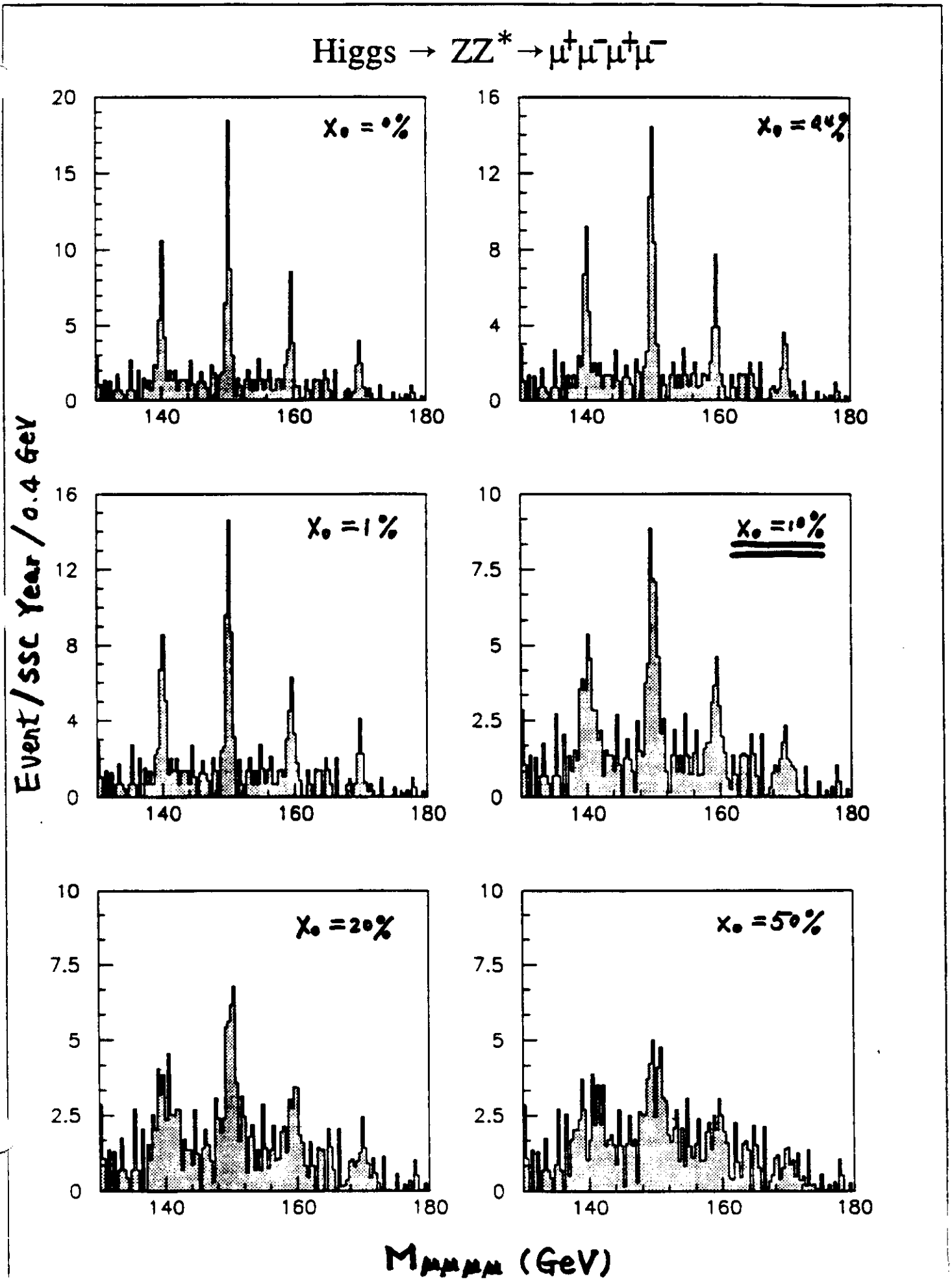
Higgs → ZZ* → μ+μ−μ+μ−
X₀ = 0%
X₀ = 0.4%
X₀ = 1%
X₀ = 10%
X₀ = 20%
X₀ = 50%
Event/SSC Year/0.4 GeV
M_μμμμ (GeV)

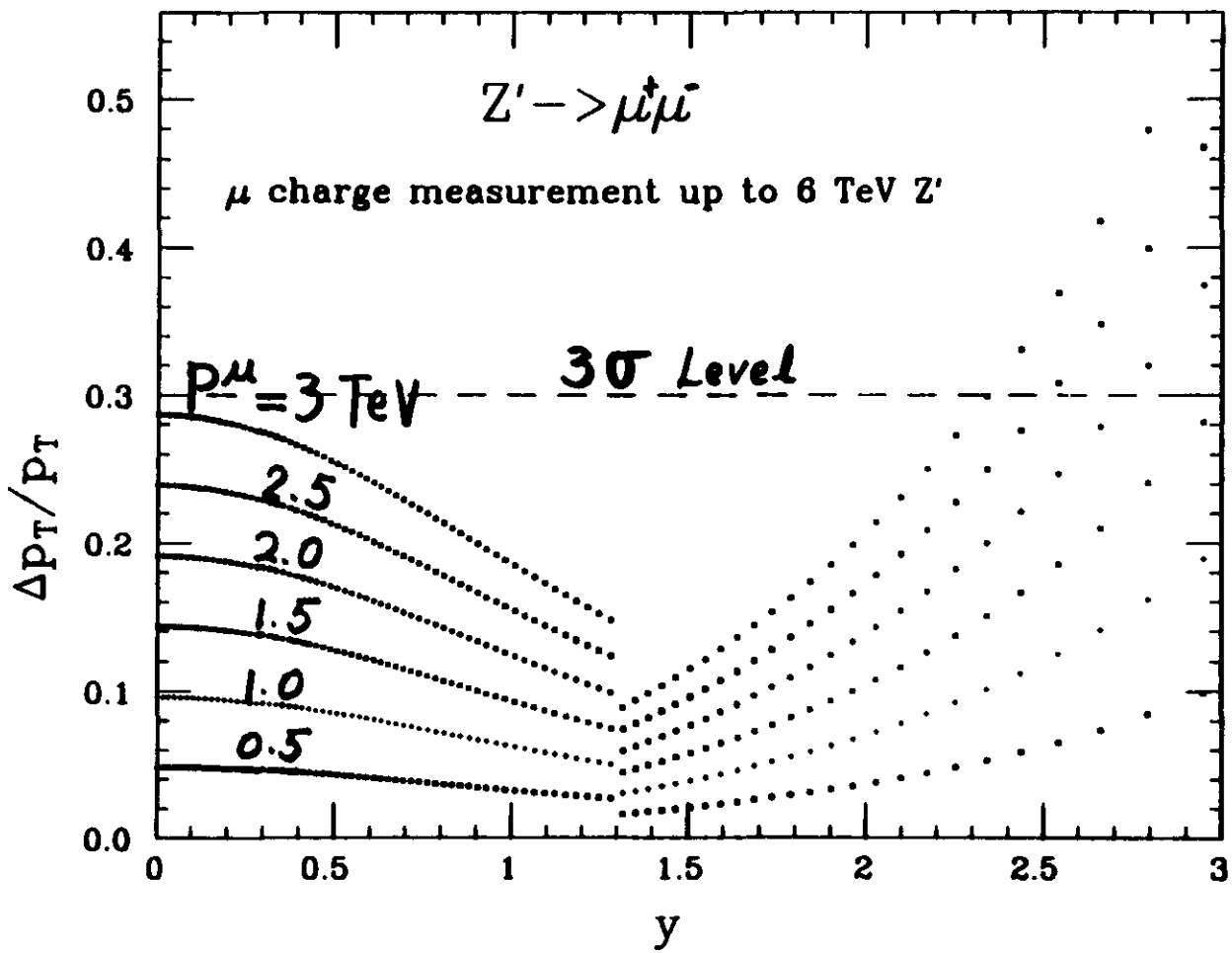
$Z' \to \mu^+\mu^-$
μ charge measurement up to 6 TeV Z'
3σ Level
$P^{\mu}=3$ TeV
2.5
2.0
1.5
1.0
0.5
$\Delta p_T/p_T$
y
0.0
0.1
0.2
0.3
0.4
0.5
0
0.5
1
1.5
2
2.5
3

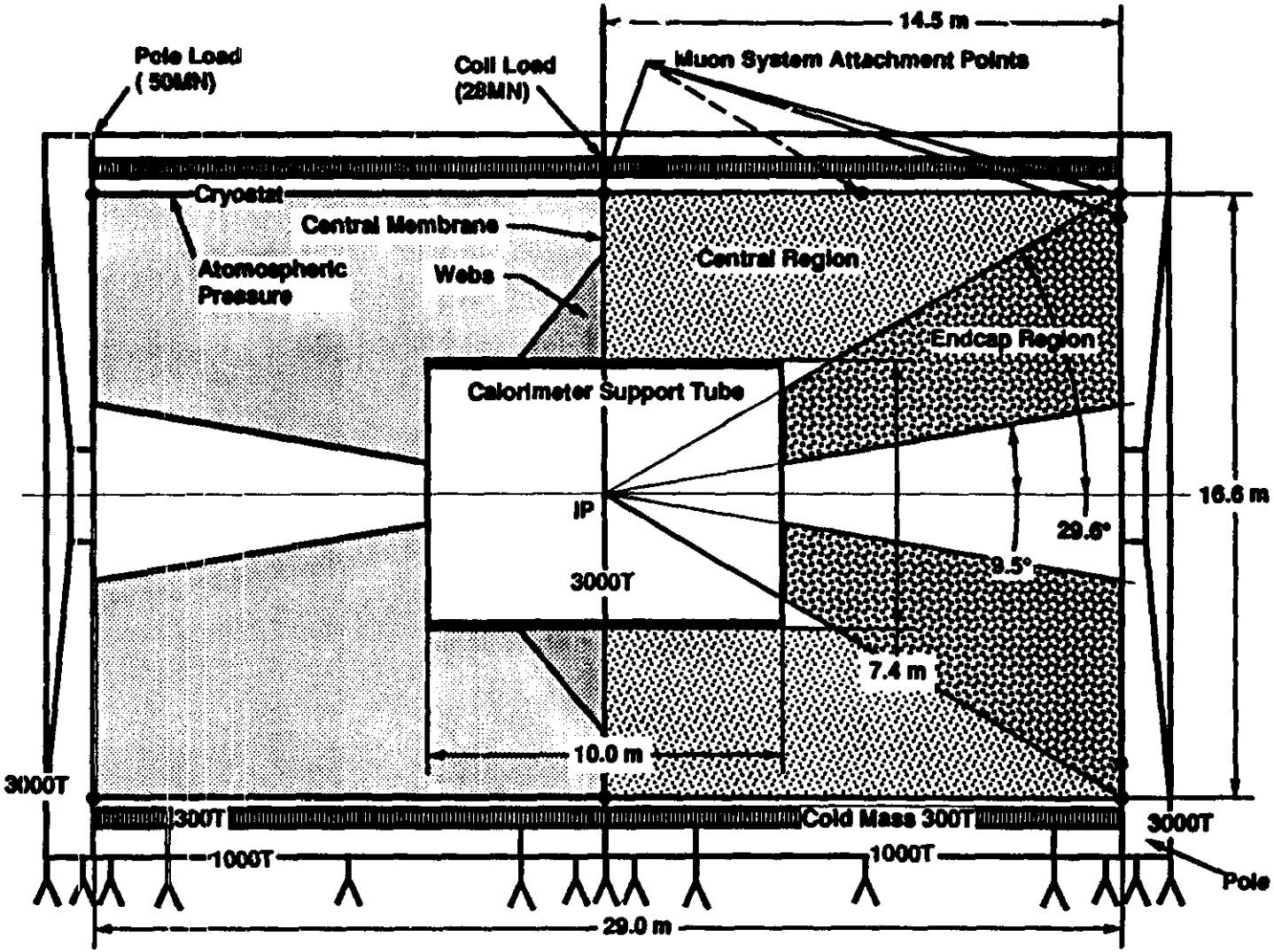

Elevation of GEM Magnet/ Muon System

F. Nimblett 8/21/91

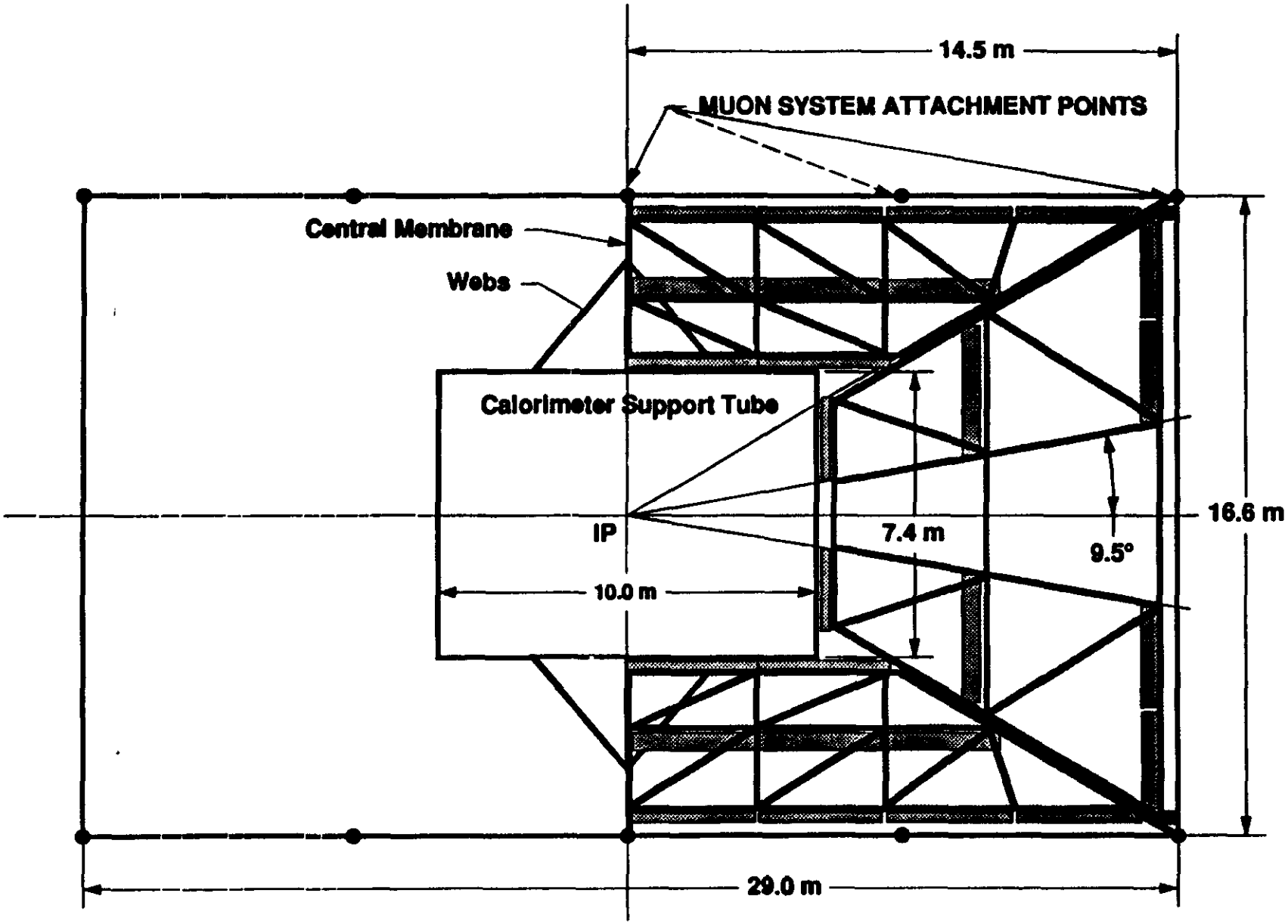

ELEVATION OF PDT MUON SYSTEM

F. Nimblett
21 August 1991

	END CAP	BARREL
• AREA (inner)	17 m^2	392 m^2
• AREA (middle)	71 m^2	852 m^2
• AREA (outer)	181 m^2	1475 m^2
• $\vec{B}$ ORIENTATION	⊥ Chamber	∥ Chamber
• MECHANICS	TOUGH	EASY
• PARTICLE RATE (10^{34})	200 Hz/cm^2	1 Hz/c
• CELL SIZE FOR MOMENTUM TRIGGER	3 mm	3 cm
• GEOMETRY FOR TRIGGER SENSE ELEMENT	RADIAL (z, φ const.)	Longitudina (r, φ const

CONCLUSIONS (~ Consensus) of 9/6/91 mtng.

BARREL : LARGE AREA BUT RELATIVELY EASY - CHOOSE INEXPENSIVE, ROBUST TECHNOLOGY (Tubes/RPC's?

END-CAP: VERY DIFFICULT, BUT AREA NOT SO LARGE - CHOOSE "HIGH PERFORMANCE" (may be expensive / m^2) TECHNOLOGY (Strips?)

Proposed GEM Muon System

Momentum Determination and Trigger:

Central Region:

1) Pressurized Drift Tubes (PDT)

OR 2) Limited Streamer Drift Tubes (LSDT)

Endcap Region: Detector and Trigger

1) Cathode Strip Chambers (CSC)

OR Limited Streamer Tubes (backup)

Beam Crossing Tag:

Central region: Resistive Plate Chambers (RPC)

Endcap region: Cathode Strip Chambers (CSC)

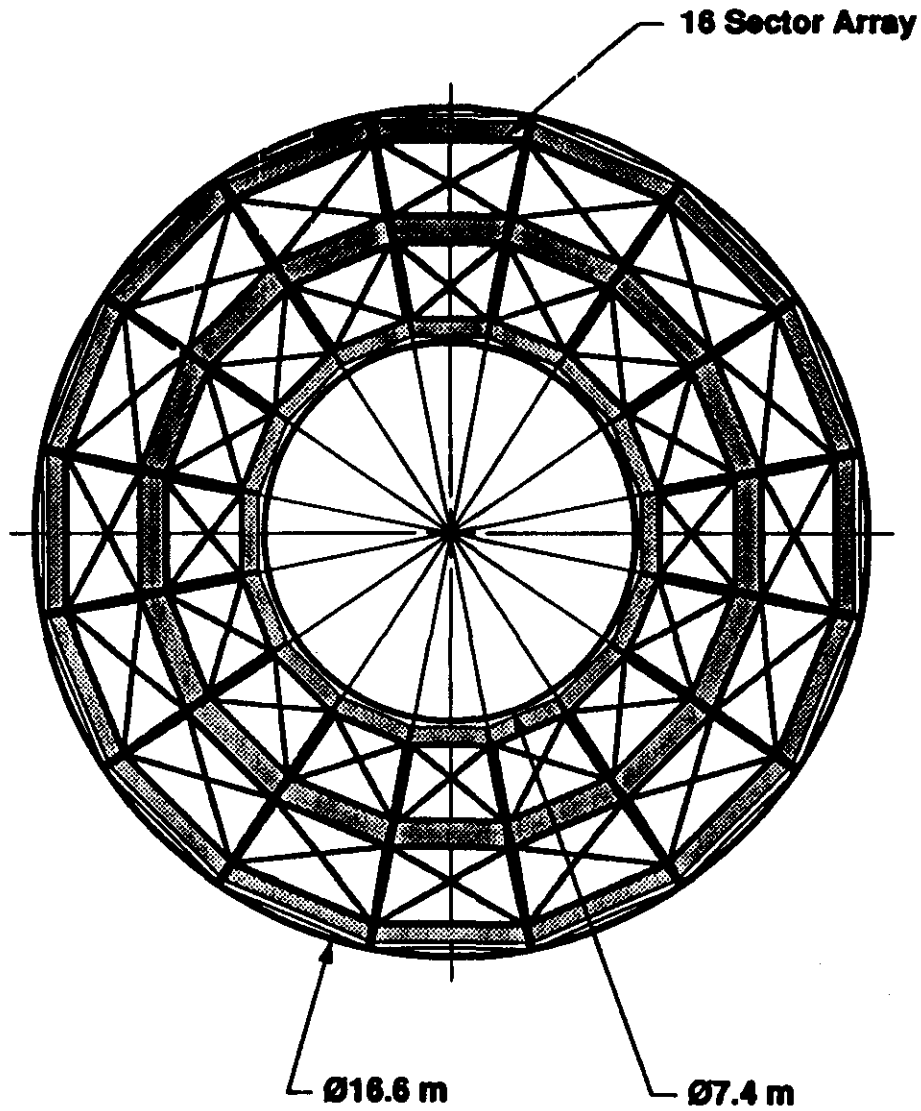

END VIEW PDT MUON SYSTEM
(Central Region shown with support structure)

F. Nimblett
21 August 1991

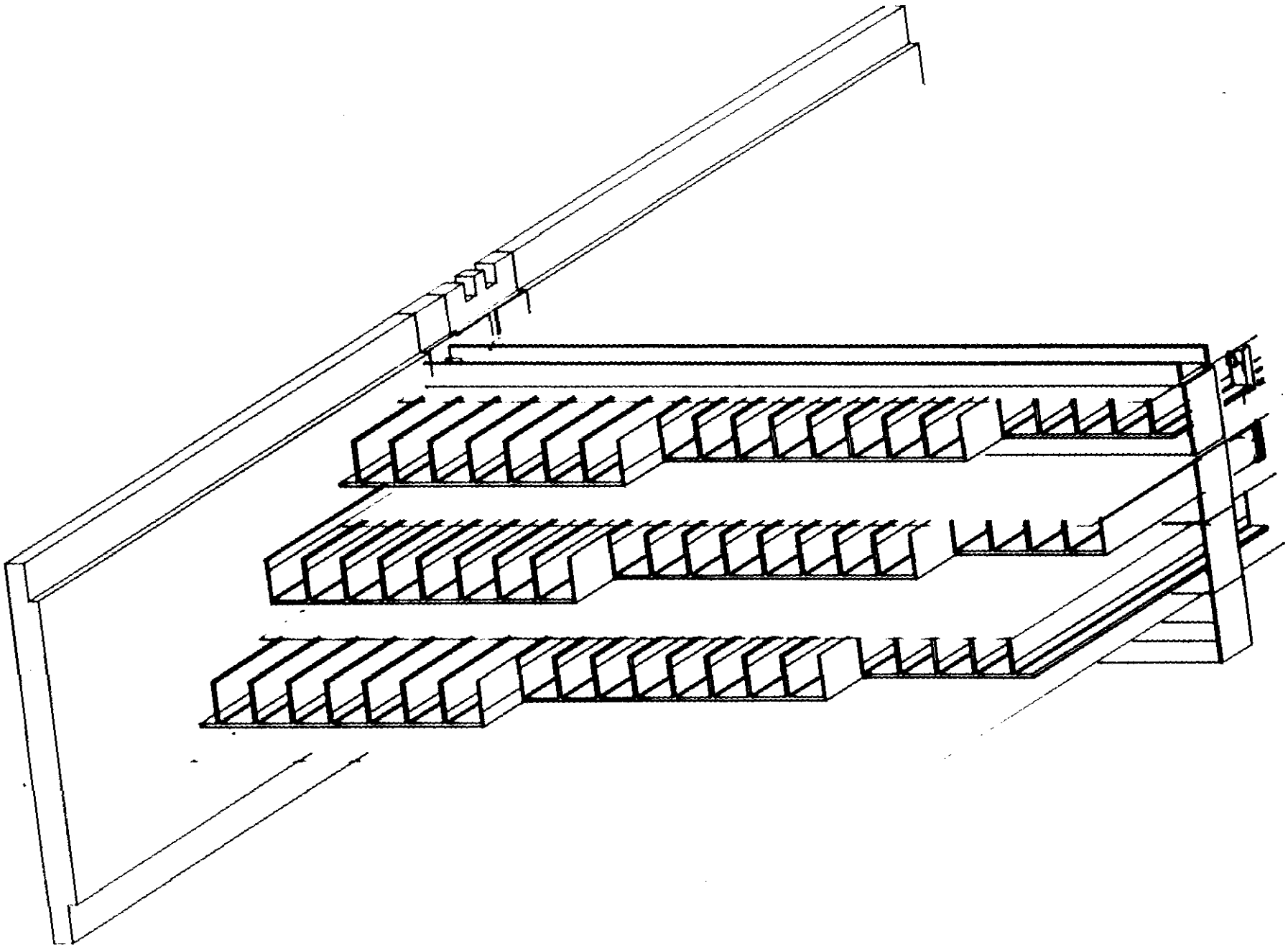

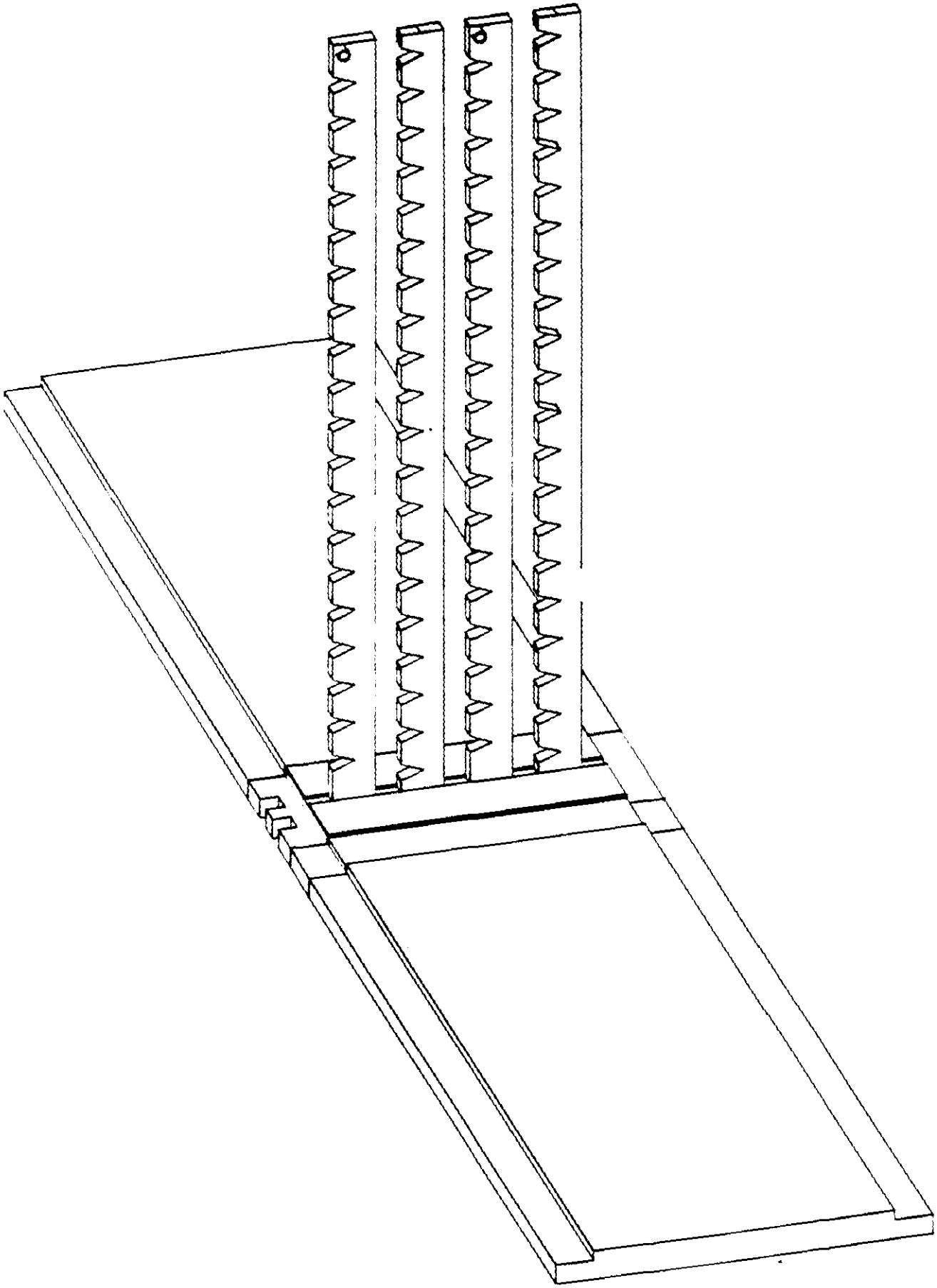

Cosmic Rays - A + Isobutane

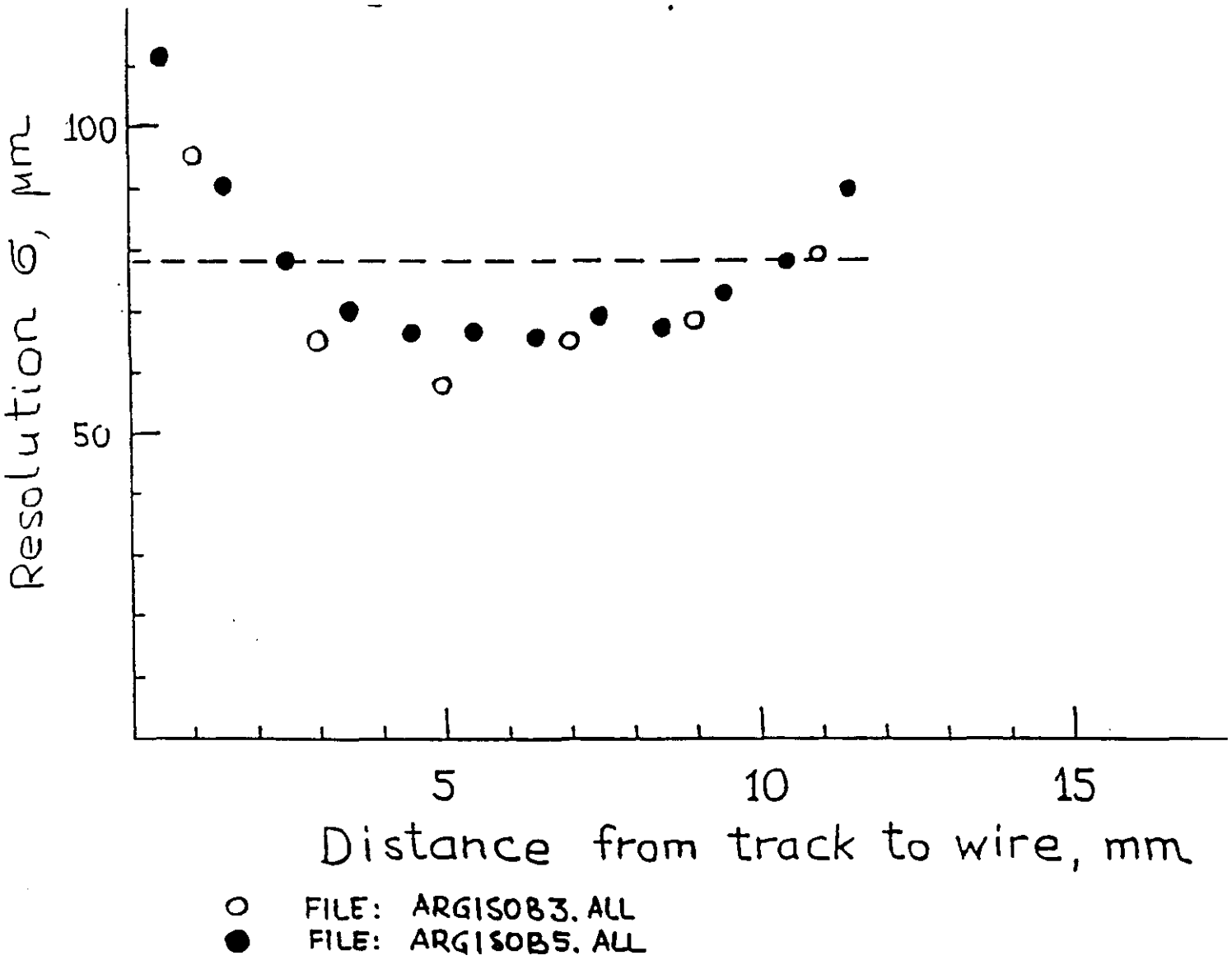

Fig. A.4

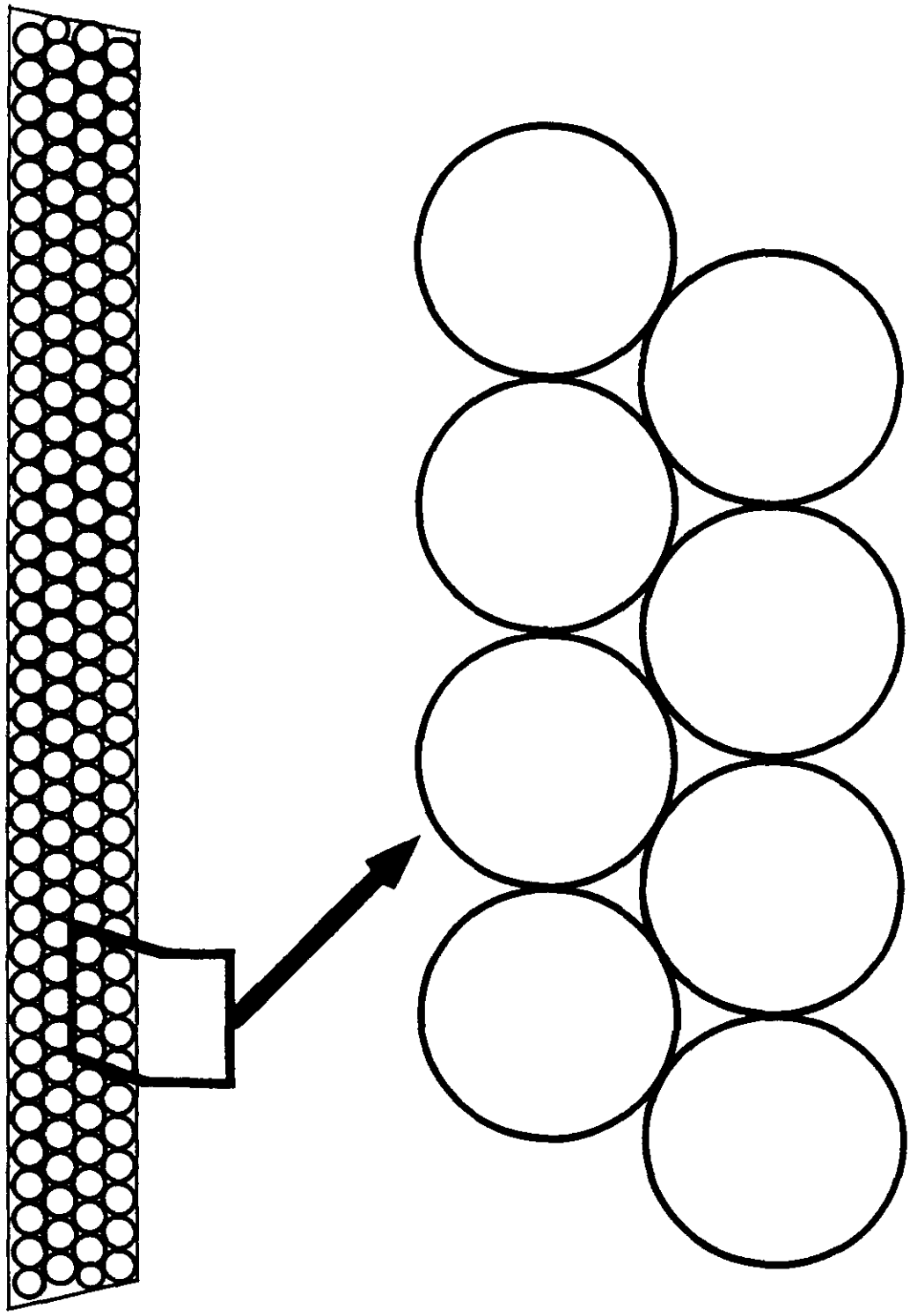

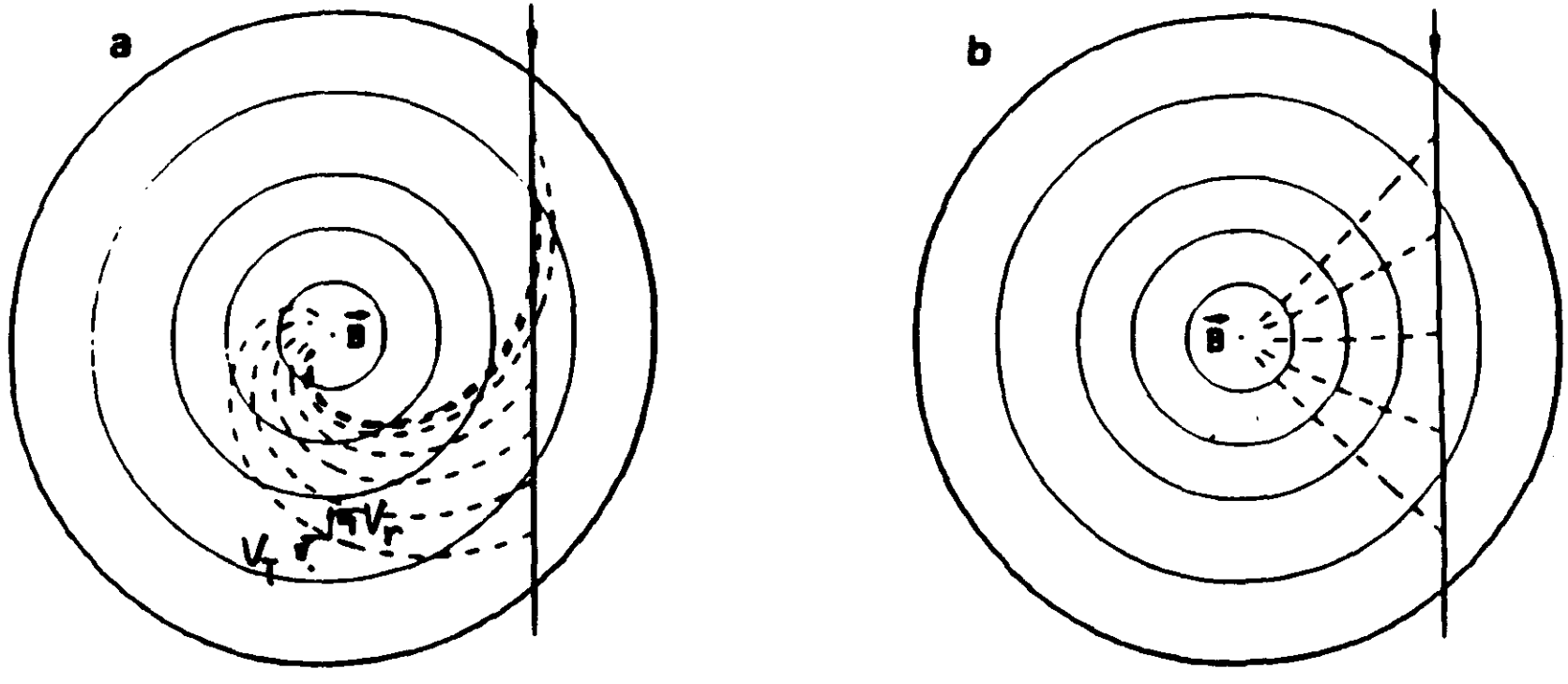

Fig. 8. Electron drift trajectories (dashed lines) in a 1 in. diameter drift tube at 15 kG B-field. The solid line with the arrow is the particle track and the thin solid circles inside the tube represent the E-field potentials. (a) for 50–50 argon–ethane gas, (b) for DME gas.

raw data

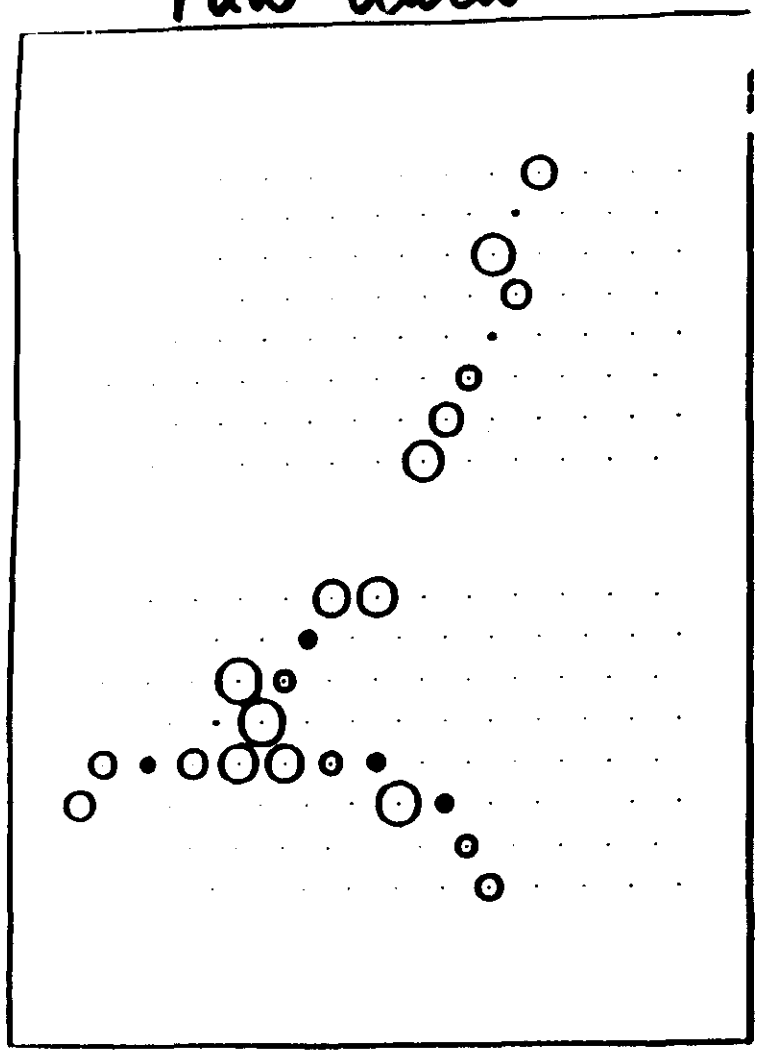

event reconstruction

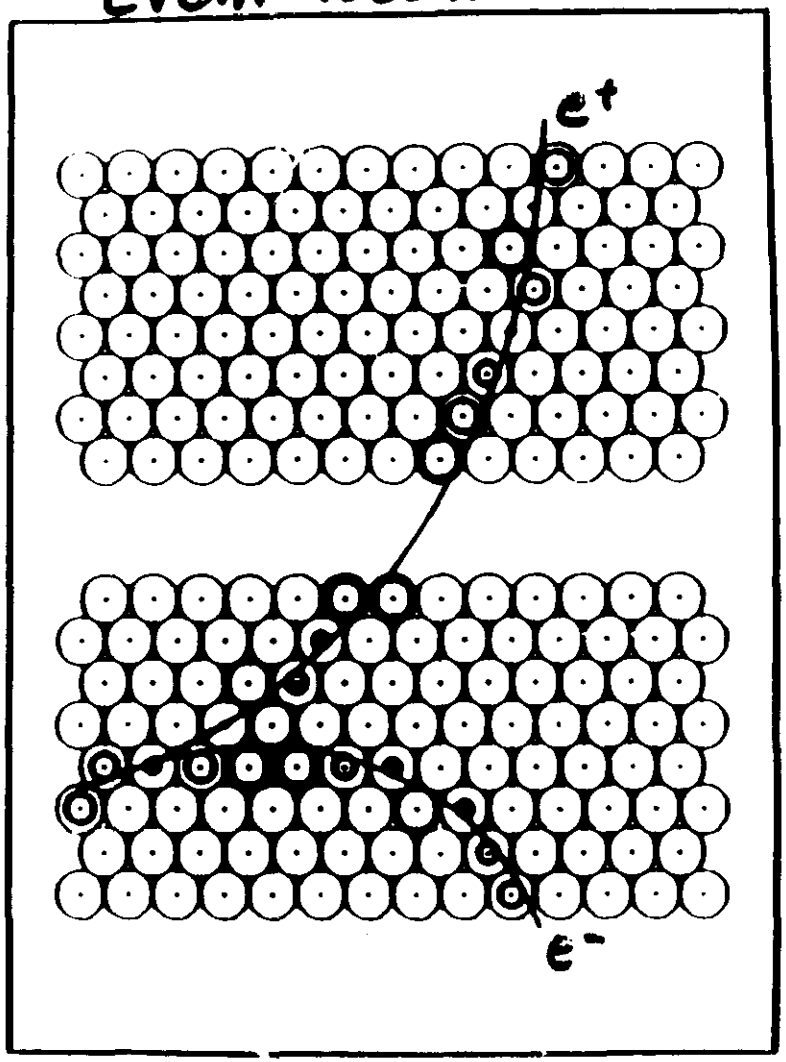

$\bar{p}$ experiment data display

EVENT # 5

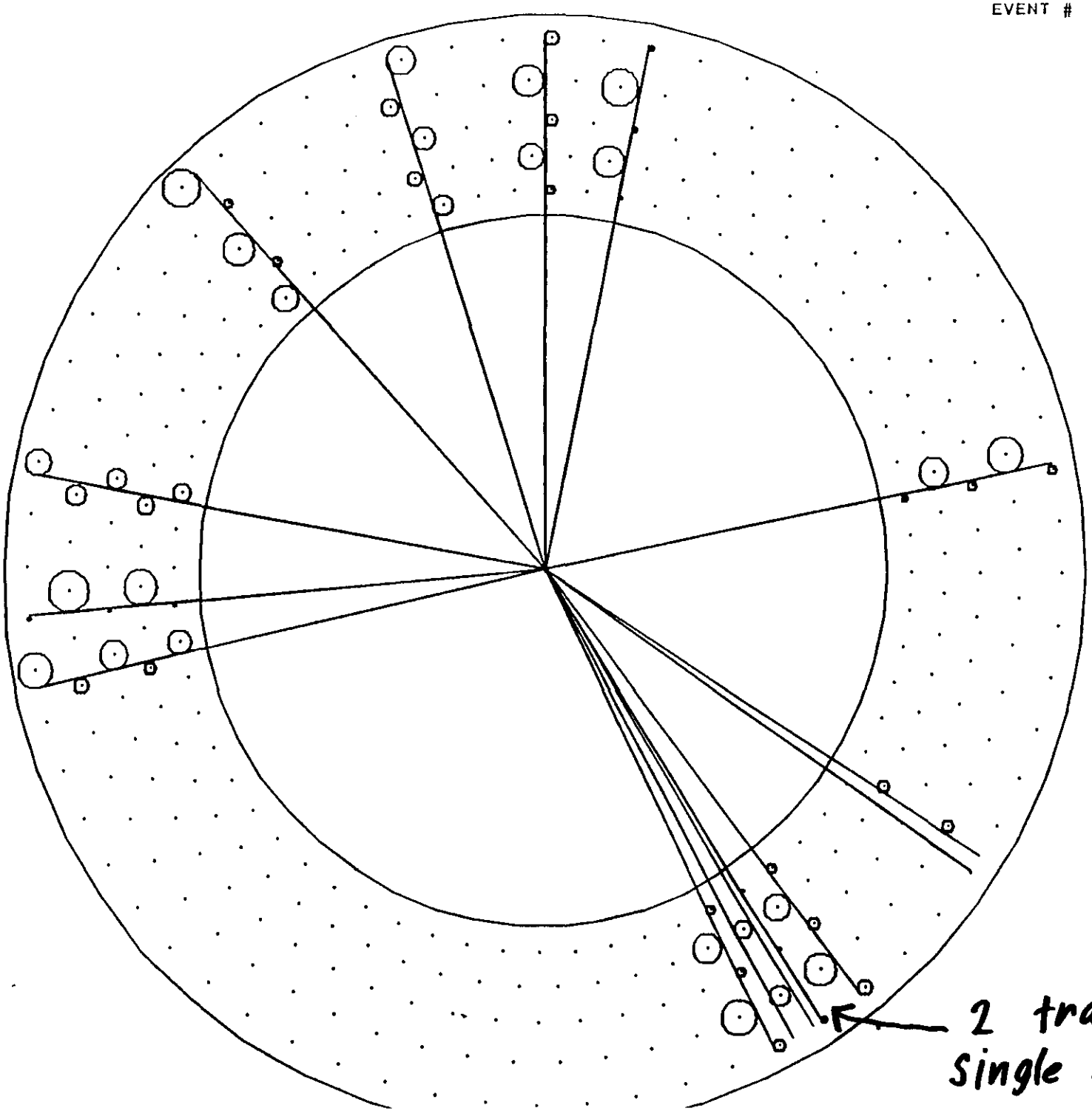

DRIFT TUBE DETECTORS

Expt., Field, Pressure	Wall Thick. (μm)	# of tubes	Diam. (mm)	Length (cm)	Gas	σ (μm)
BU SSC Proto.	25 (P)	23	3.8	30	Ar-ethane	89
CLEO IVD	25 (P)	192	4-6	50	Ar-ethane	90
					DME	37
AMY ITC (3T)	25 (P)	576	4-6	57	Ar-ethane	80
PBAR (1T)	25 (P)	332	12	20	Ar-ethane	84
					DME	34
HRS (1.6T)	150 (SS)	996	25	360	Ar-CO2(9:1)	150
CDF (1.5T)	200 (SS)	2016	25	300	LST mode	200
EXAM (cosmic)	150 (SS)	600	38	370	Ar-CO2(9:1)	175
MAC (4 atm)	100 (P)	320	6.9	10	Ar-CO2(1:1)	45
DUKE SSC	50 (P)	60	4	270	Ar-ethane	110

P = plastic
SS = stainless steel

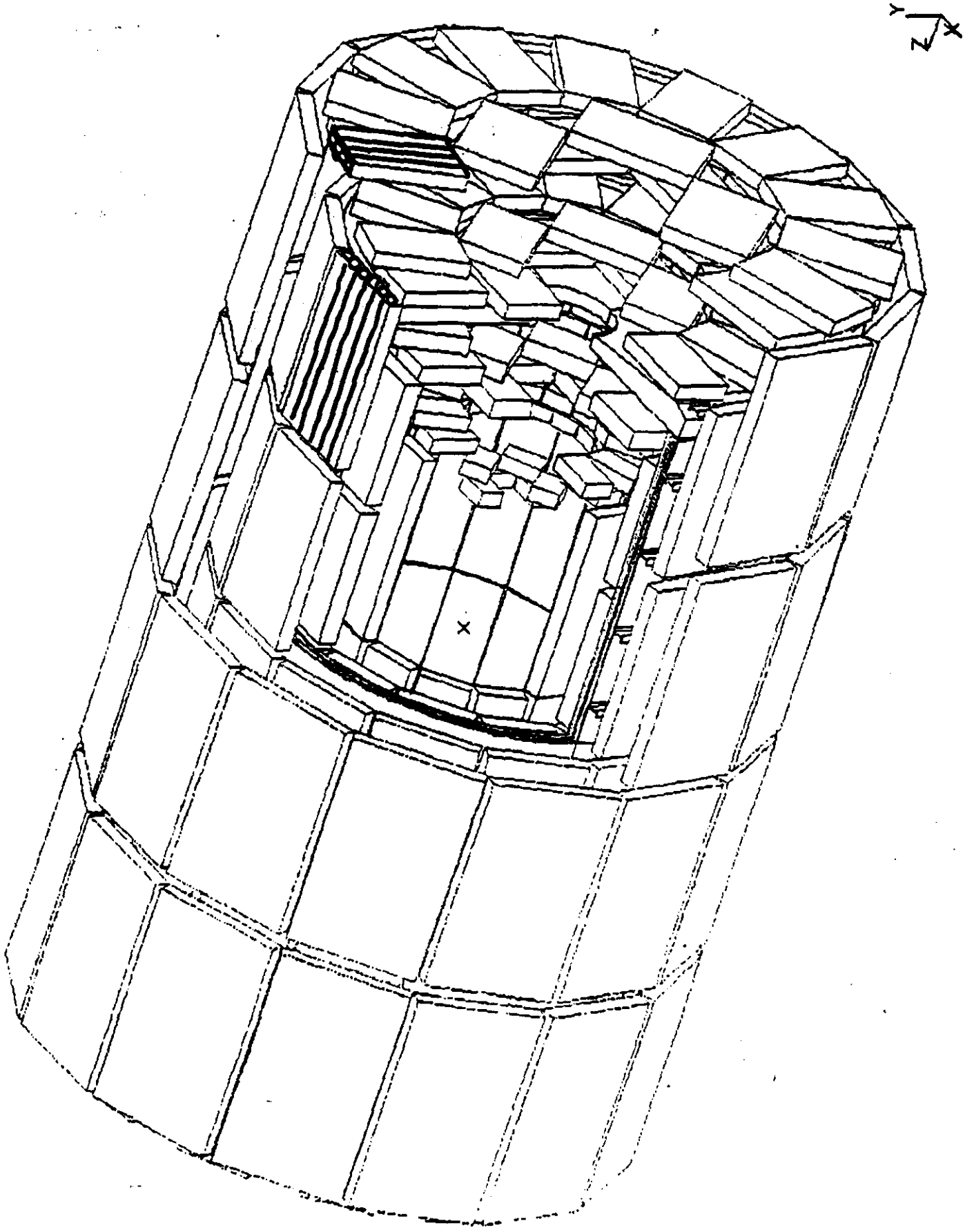
Y
X
Z

CATHODE STRIP CHAMBERS IN ENDCAPS

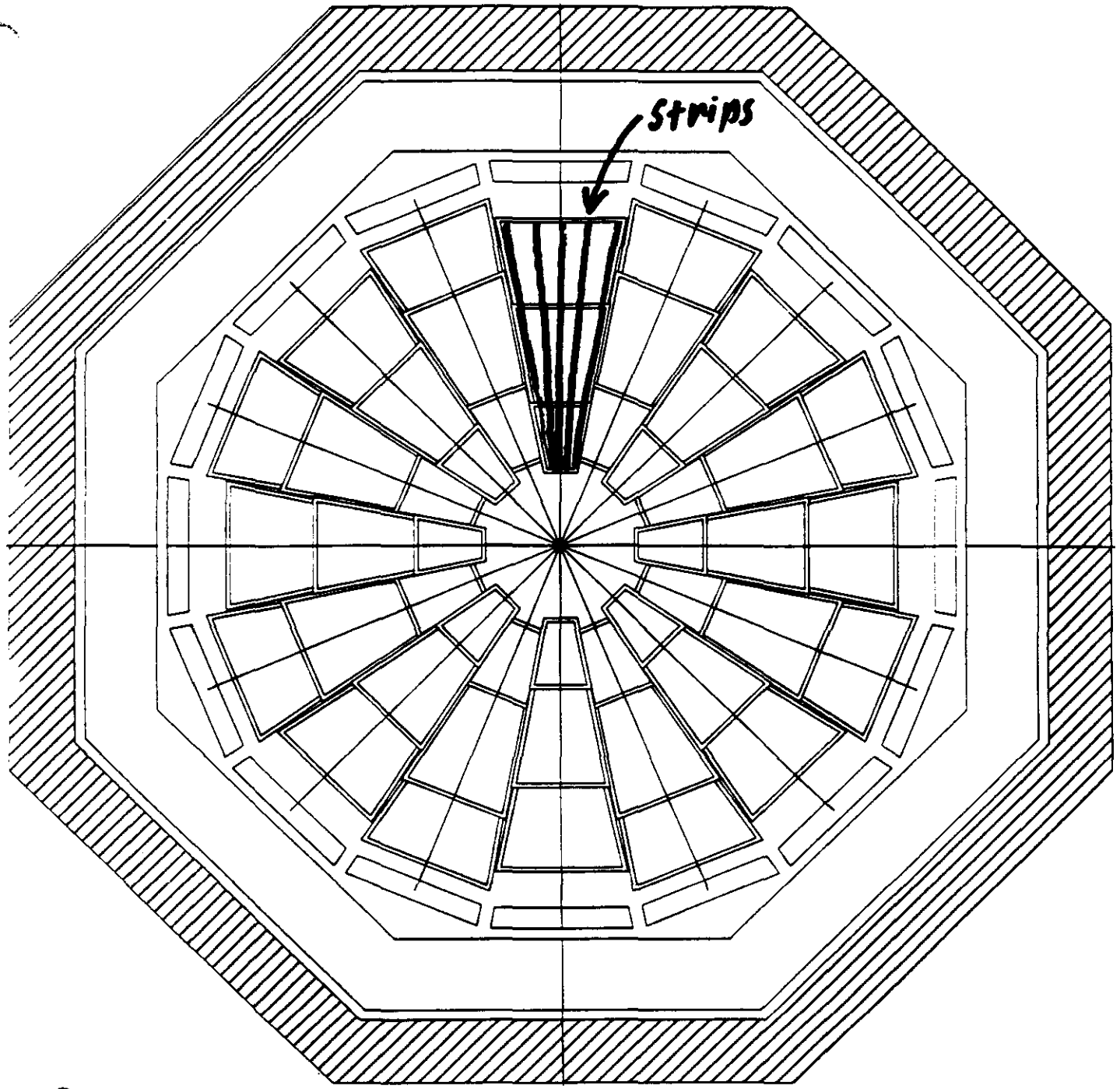

① Strips can be layed out radially - ideal for p measurement and trigger

② Wire pitch can be made small enough to enable beam cross tagging

L* 20MW Magnet Version/4

Muon Spectrometer Volume

C. Grinnell
scale 1:100
version 4.5 14.02.90
from 20MW/4 13.10.89

View from top of detector

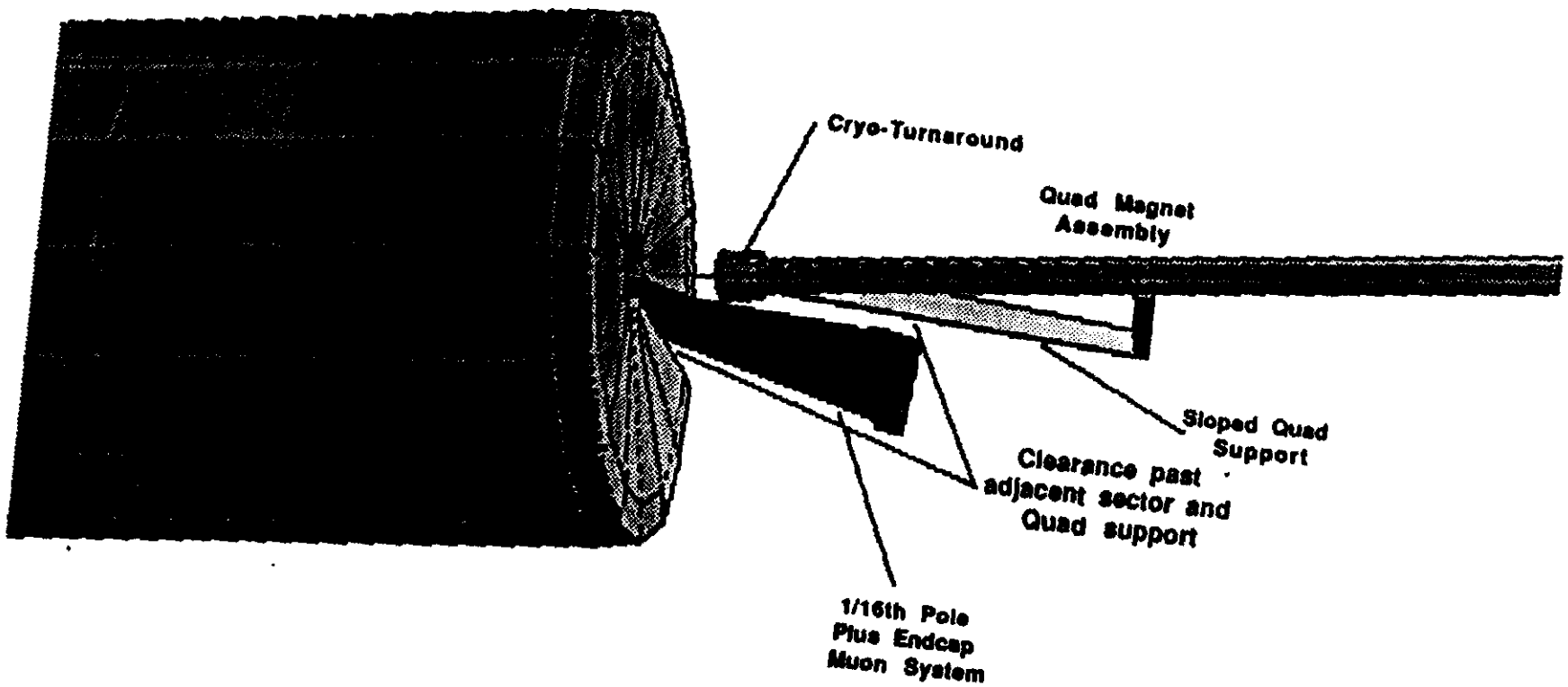

GEM Muon System
(1/16th pole option)

F.Nimblett
9/17/91

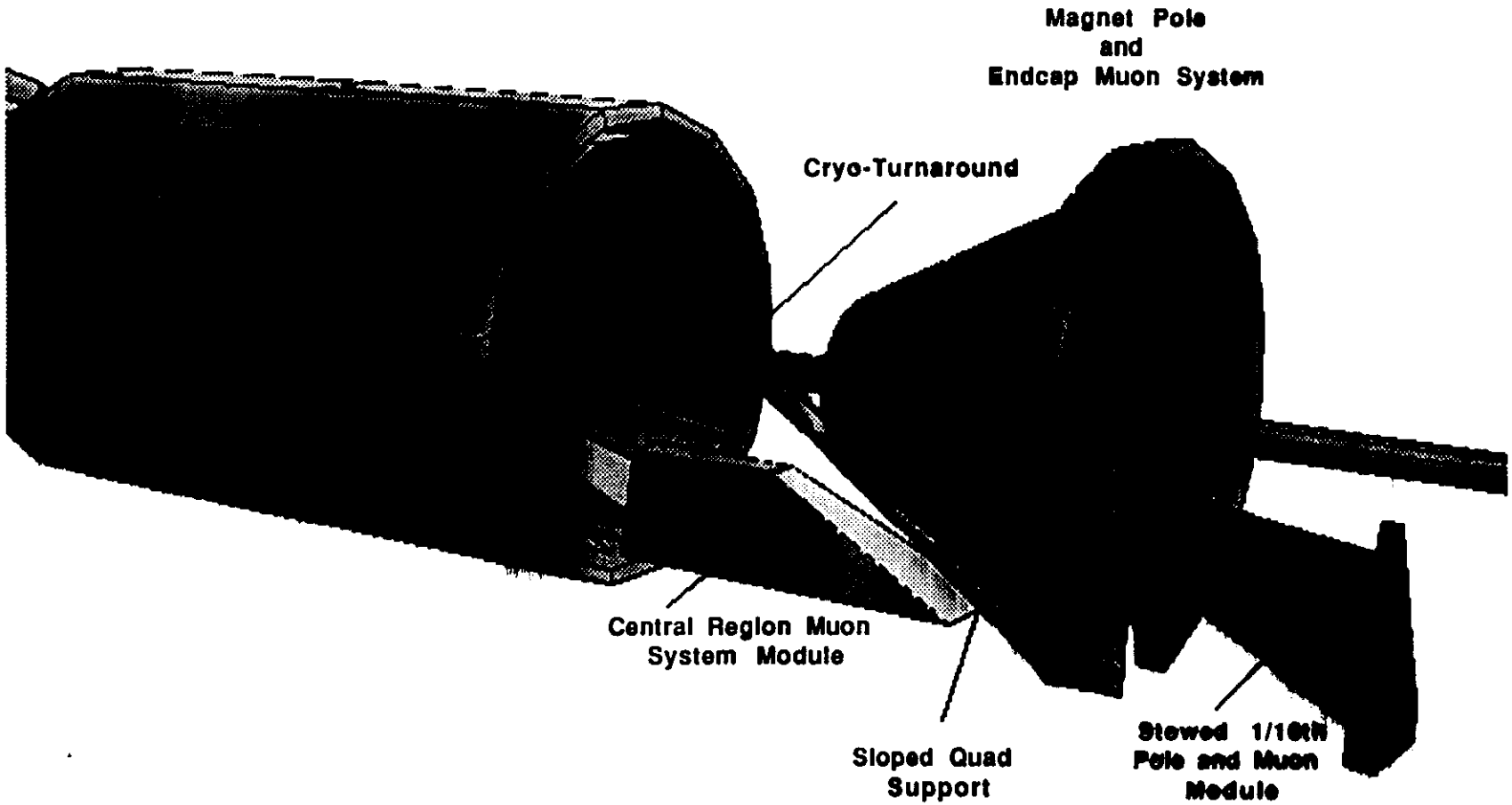

GEM
Muon System
Access

F. Nimblett
9/17/91

BASICS OF PAD CHAMBERS

Proportional chambers:

- 5 mm gas gap
- 2.5 mm anode wire pitch
- CO_2 / CF_4 mixture

  -> small Lorentz angle

  -> adequate drift velocity max drift time ~ 40 ns
- Gas gain 10,000 -- 20,000

Good resolution achieved by precise measurement of image charge sharing between cathode strips

- Precise cathode structure
- Charge measurement to 1%
- Integration times ~ 1 μsec to reduce noise
- Precision achieved < 1% of strip width
- Space-point -- no L/R ambiguity
- Two-track resolution 3--4 strip widths

For the present exercise: 5 mm strip width

assume 1 -- 2 % resolution -> 50 -- 100 μm

Position Resolution vs. Anode Charge
for a Single Chevron Cathode

(5.4 keV X-rays, 12mm readout spacing, 50% Ar + 50% C_2H_6 gas mixture)

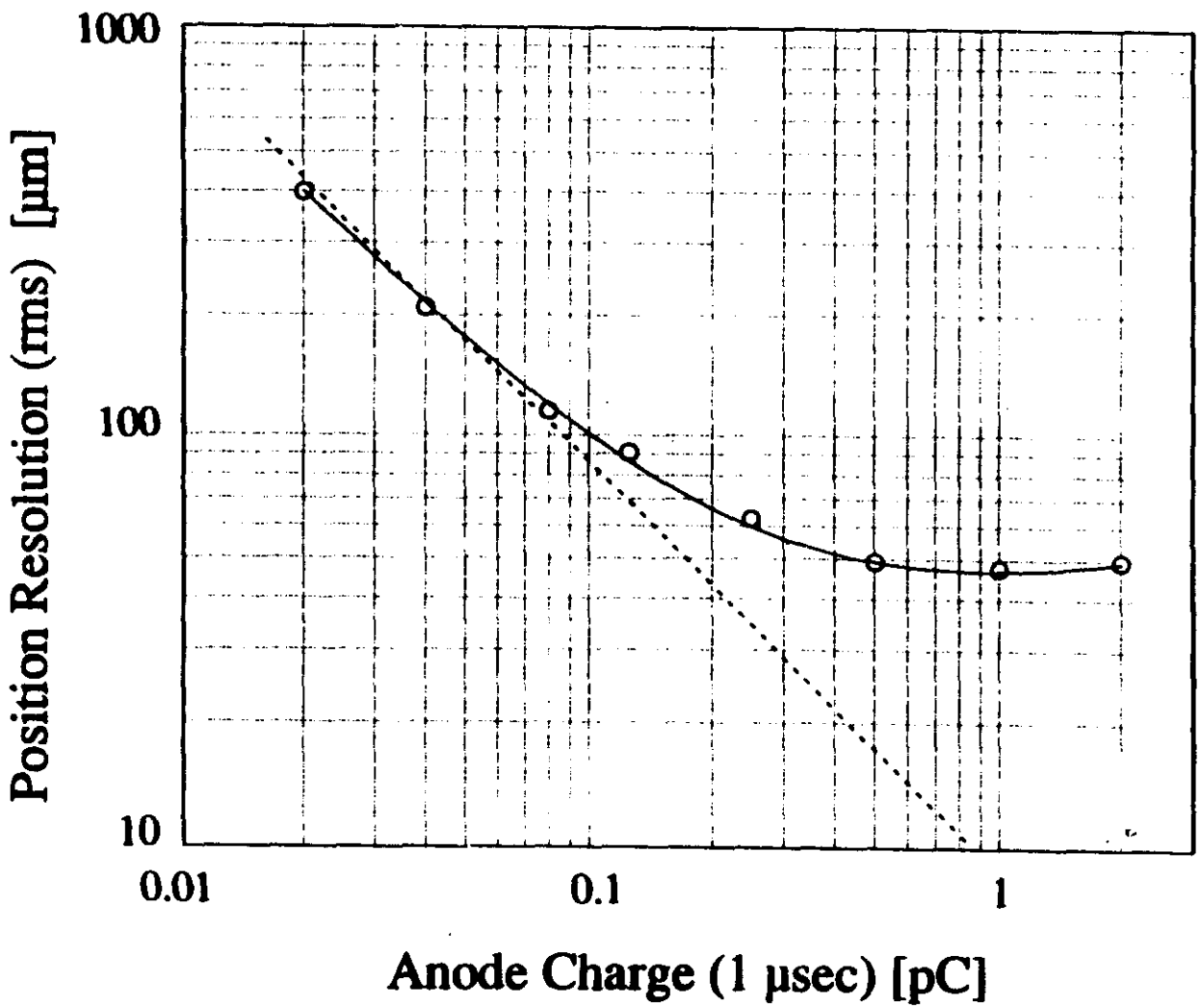

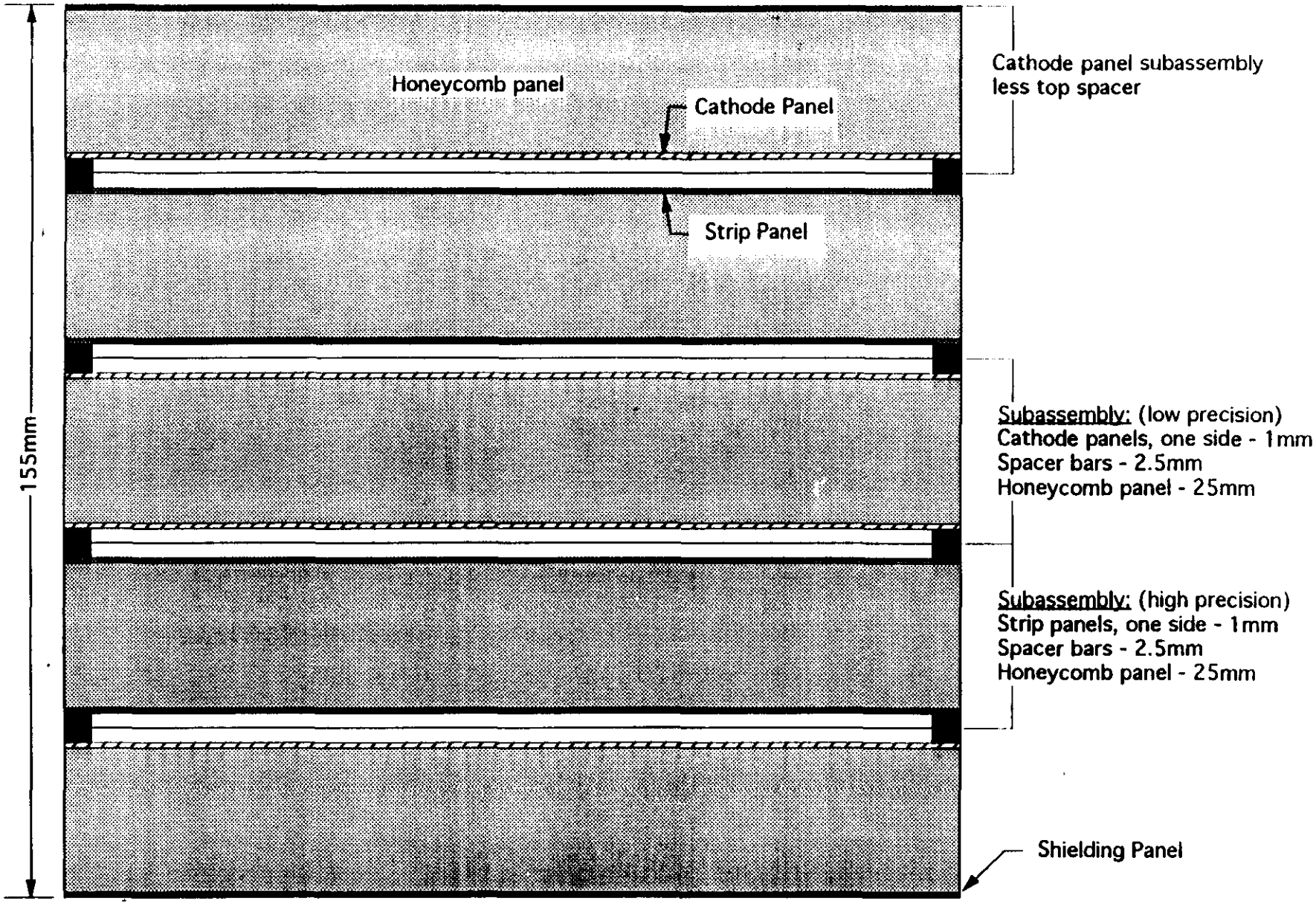

Gas Pad Chambers Study.2
C. Grinnell 09.08.91 page 1/2

OPTIMAL MUON CHAMBER CONFIGURATION

A_3 = area / layer ———— N_3 layers

A_2 ———— N_2 layers

A_1 —— N_1 layers

- Sagitta Error = $\sigma\left[\frac{1}{4N_1} + \frac{1}{N_2} + \frac{1}{4N_3}\right]^{1/2} = \delta$

- Fix Total Area, A_T (i.e. <u>cost</u>)

$$A_T = N_1 A_1 + N_2 A_2 + N_3 A_3$$

- δs is minimized for:

$$N_1 = \frac{A_T}{\sqrt{A_1 A_3} + 2\sqrt{A_1 A_2} + A_1}$$

$$N_2 = 2 N_1 \sqrt{\frac{A_1}{A_2}}$$

$$N_3 = A_T/A_3 - N_1 A_1/A_3 - N_2 A_2/A_3$$

① $A_1 = A_2 = A_3 \Rightarrow N_1 = \frac{A_T}{4A_1}$, $N_2 = 2N_1$, $N_3 = N_1$

② GEM BARREL : $\boxed{N_1 : N_2 : N_3 = 1.9 : 2.6 : 1}$

③ GEM ENDCAP : $\boxed{N_1 : N_2 : N_3 = 3.3 : 3.2 : 1}$

Cost Model: N = 8:8:4 in barrel; N = 4:4:3 in endcap; endcap muon cost = 1/2 of barrel muon cost; muon cost proportional to chamber area; magnet cost proportional to (stored energy)^(2/3); resolution = 5% at 90 degrees at 500 GeV

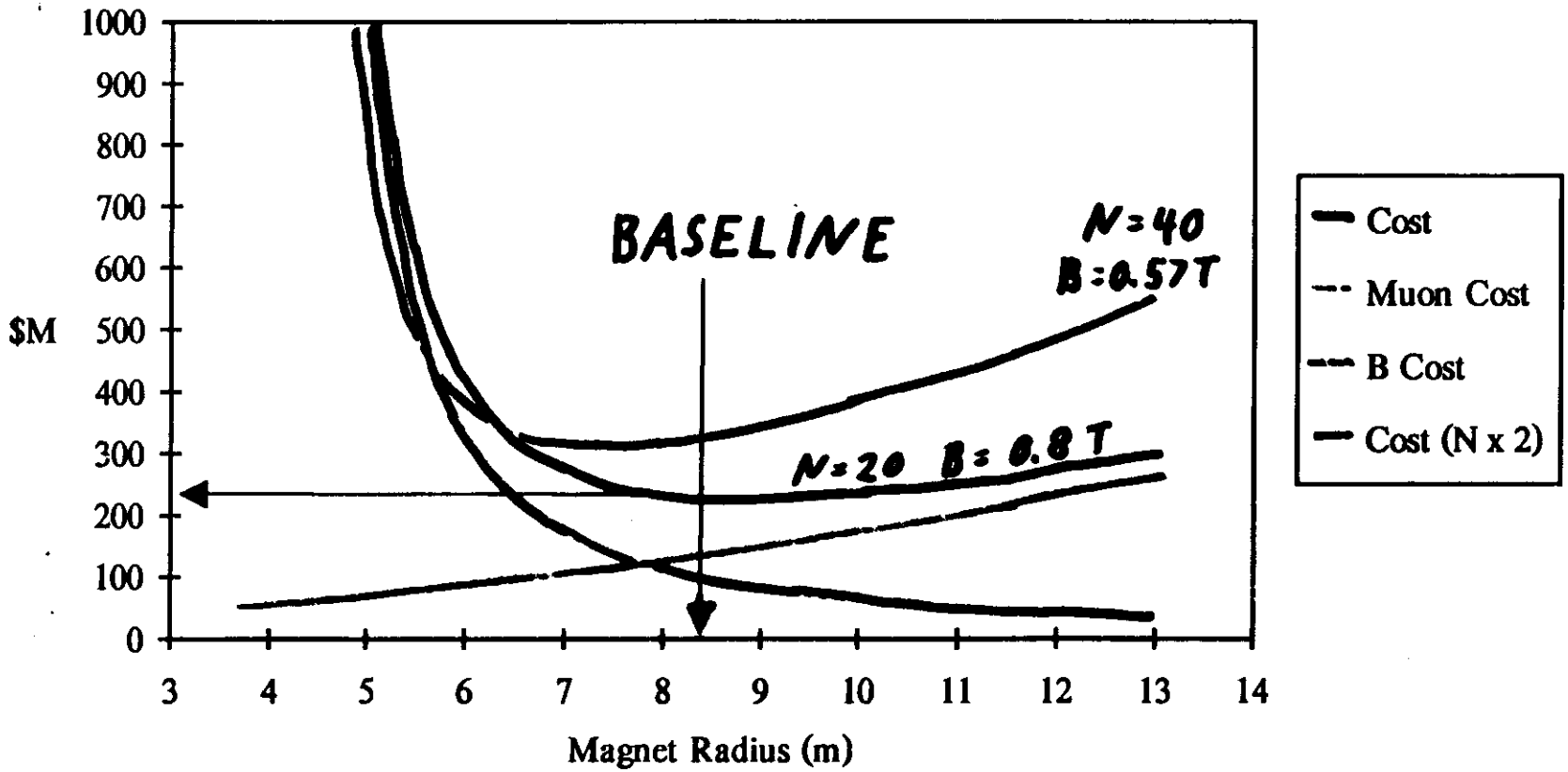

GEM Muon Momentum Resolution at p = 500 GeV: 8:8(10% X):4 @ 100 microns in Barrel; 4:4(8% X):3 @ 75 microns in EndCaps; systematic sagitta error = 25 microns, and B = 0.8 Tesla

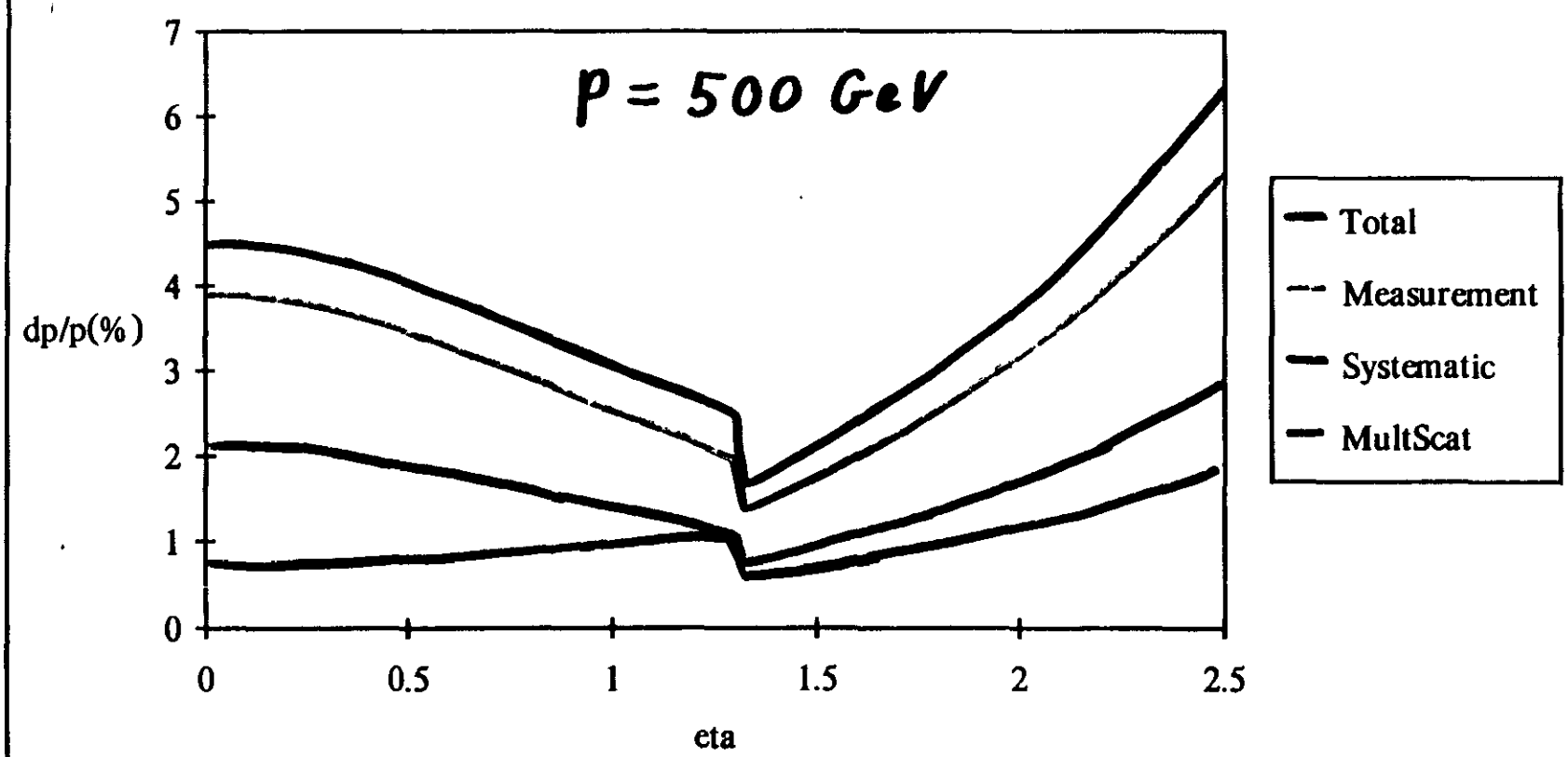

GEM Muon Momentum Resolution at p = 50 GeV: 8:8(10% X):4 @ 100 microns in Barrel; 4:4(8% X):3 @ 75 microns in EndCaps; systematic sagitta error = 25 microns, and B = 0.8 Tesla

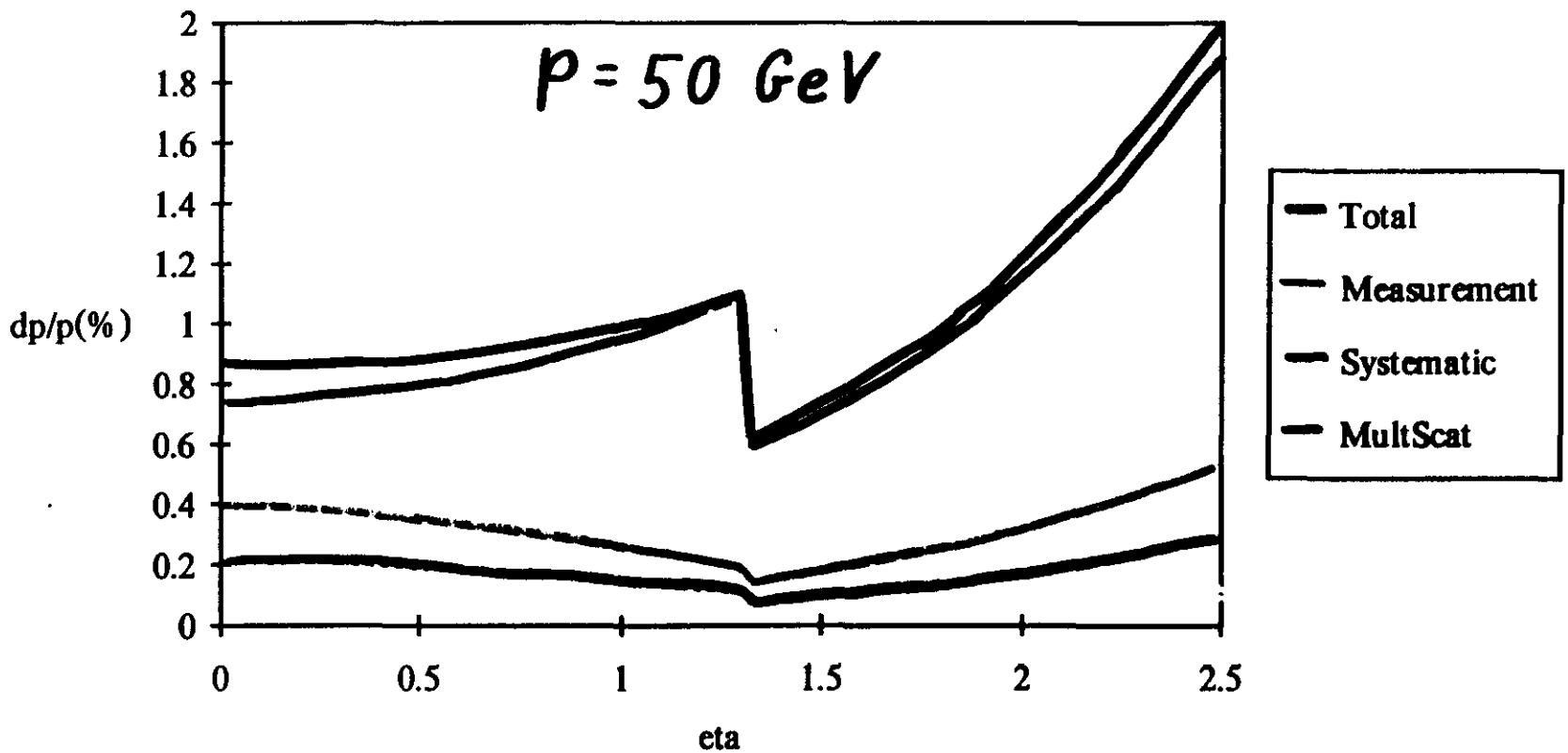

Possible improvements to baseline resol'n:

(a) Constrain the primary vertex in trajectory fit:

For σ vertex = 100 μm:

$\delta P\mu/P\mu$ at 5 TeV/c improves by factor of 0.5 to 0.8.
Less improvement at lower momentum.

(b) Adding planes external to coil:

For 3 planes at ΔR = 3 m and ΔZ = 5 m:

$\delta P\mu/P\mu$ improves at 1 TeV/c by factor of 0.65 at 90^0.
Less improvement at lower momentum and angle.

(c) B-field shaping at forward angles:

Cusp option improves $\delta P\mu/P\mu$ by 0.5 at η = 2.5

Note: Thin Pole versus Thick Pole:

$\Delta(\delta P\mu/P\mu)$ < 20 % between options

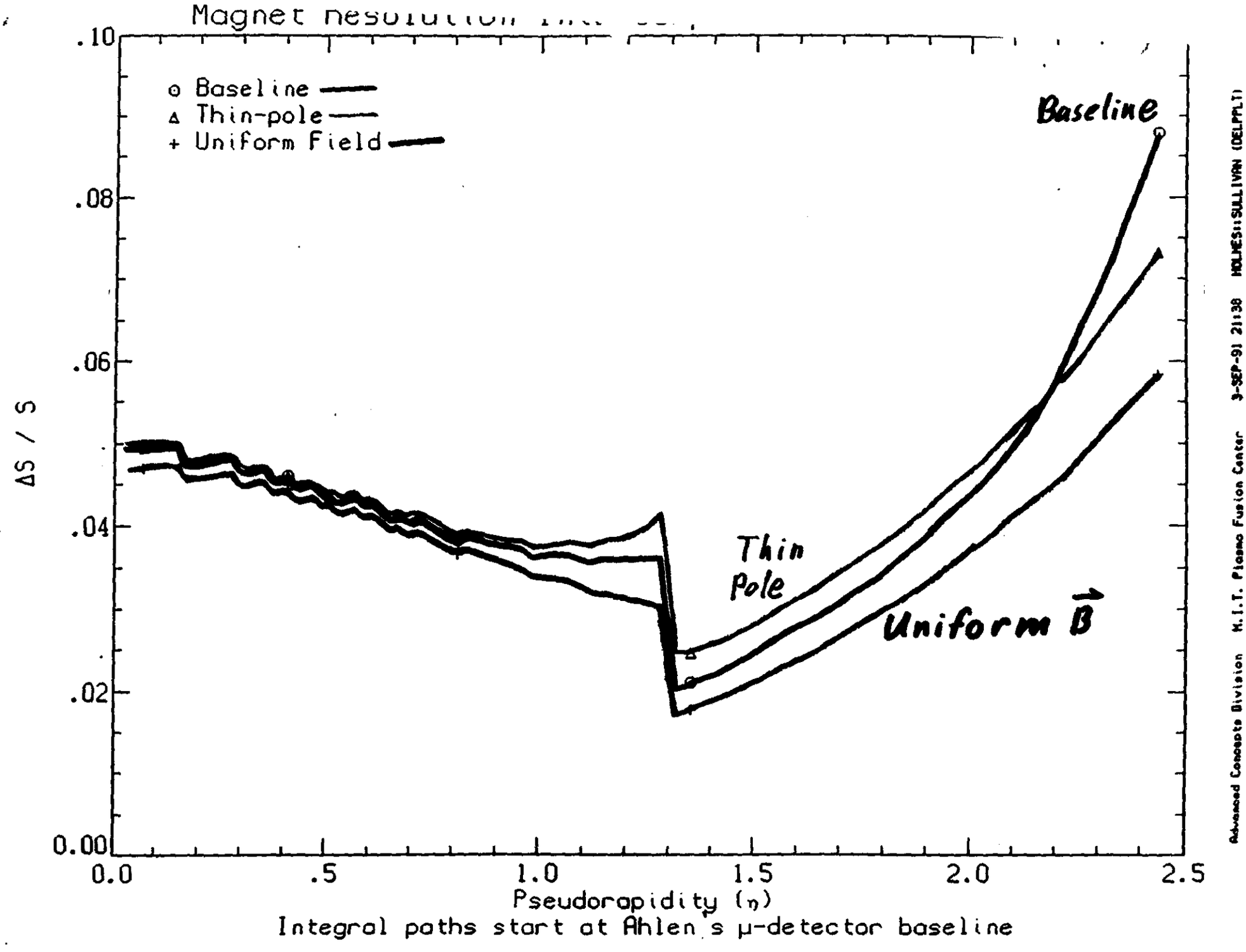
Magnet Resolution
Baseline
Thin-pole
Uniform Field
Baseline
Thin Pole
Uniform $\vec{B}$
ΔS / S
.10
.08
.06
.04
.02
0.00
0.0
.5
1.0
1.5
2.0
2.5
Pseudorapidity (η)
Integral paths start at Ahlen's μ-detector baseline
Advanced Concepts Division M.I.T. Plasma Fusion Center 3-SEP-91 21:38 HOLMES::SULLIVAN (DELPHI)

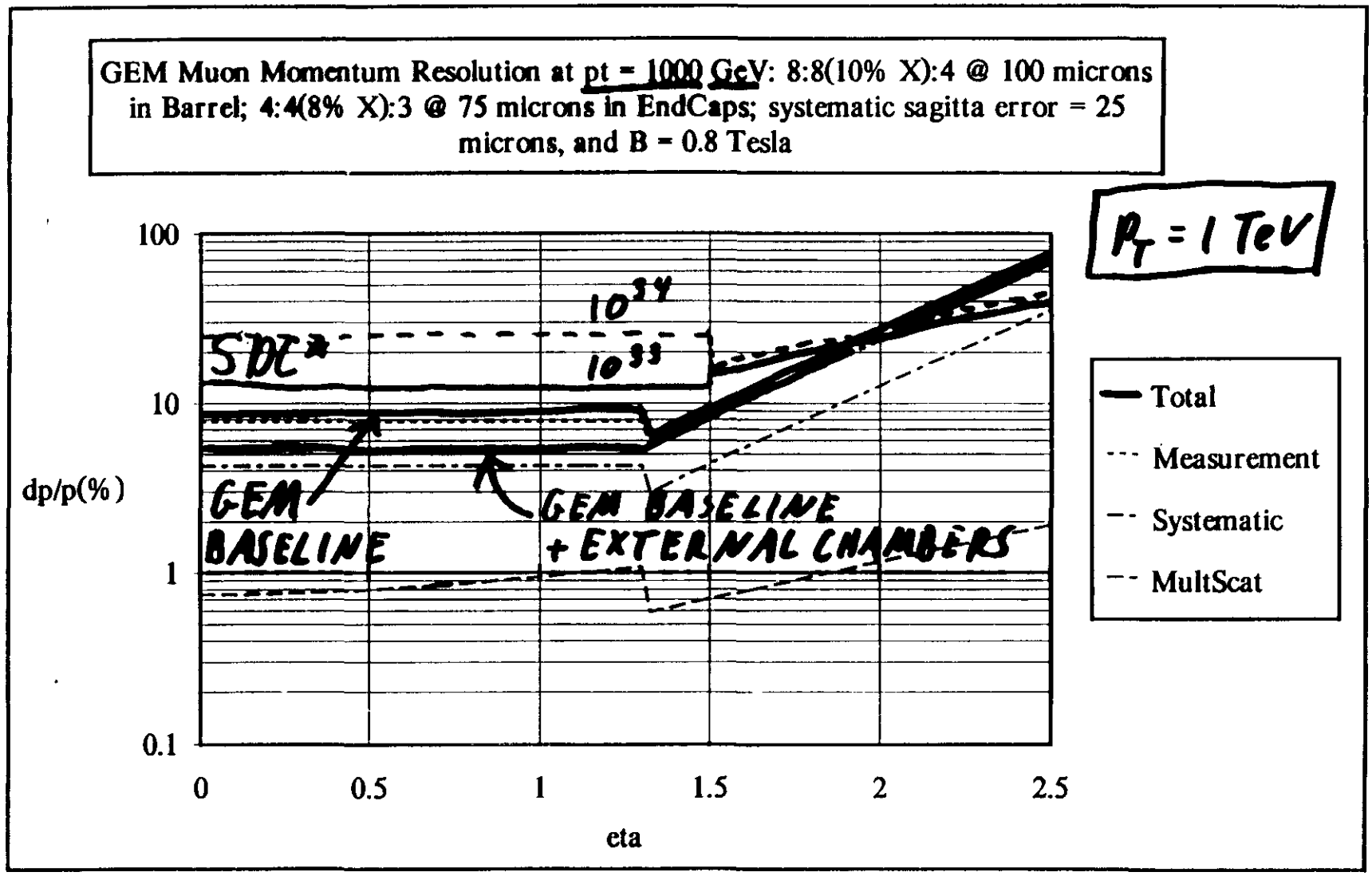

* Fig. 13 (10^{33}) and Fig. 14 (10^{34}) from SDC LoI

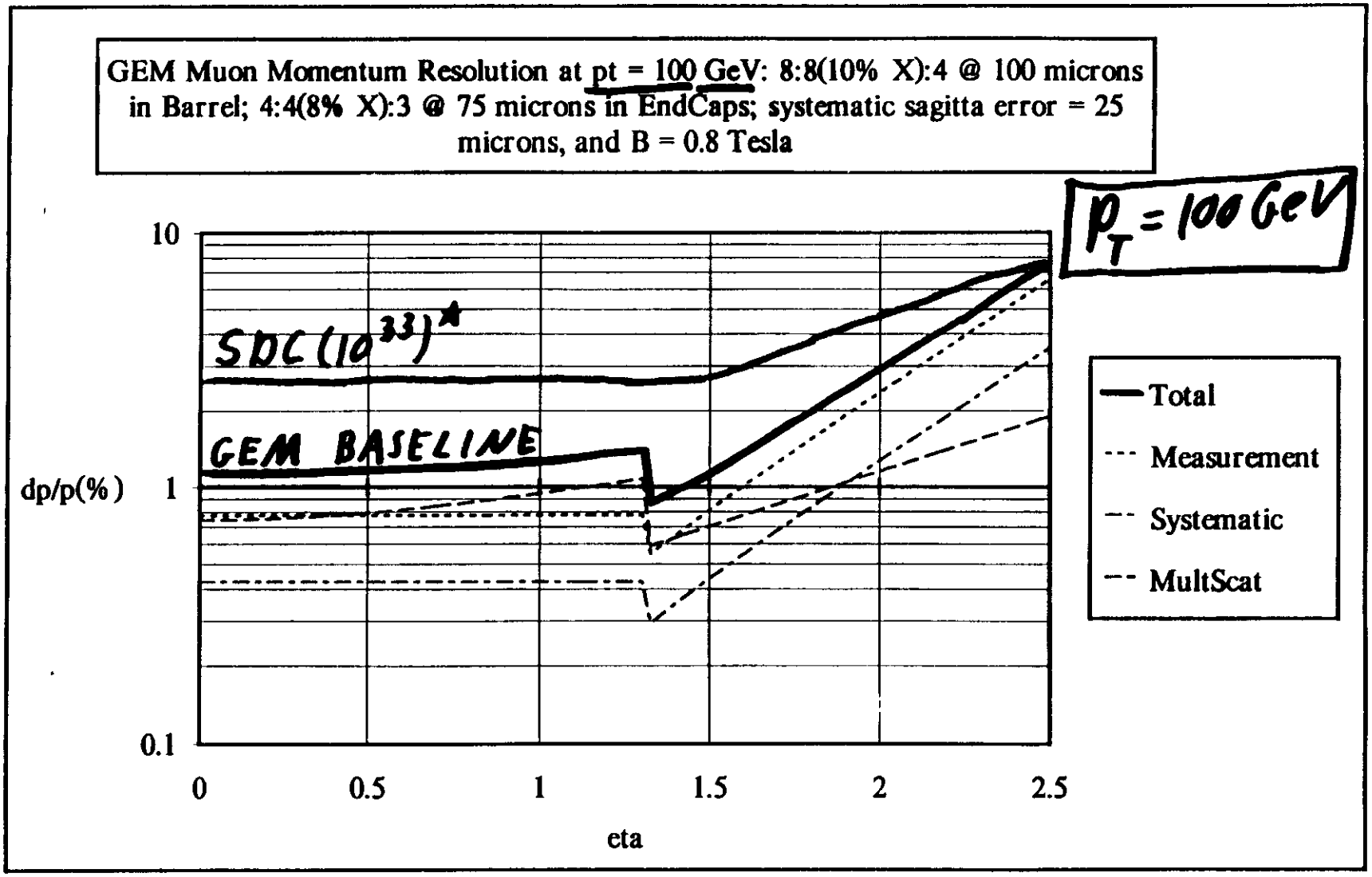

* Fig. 13 - SDC LoI

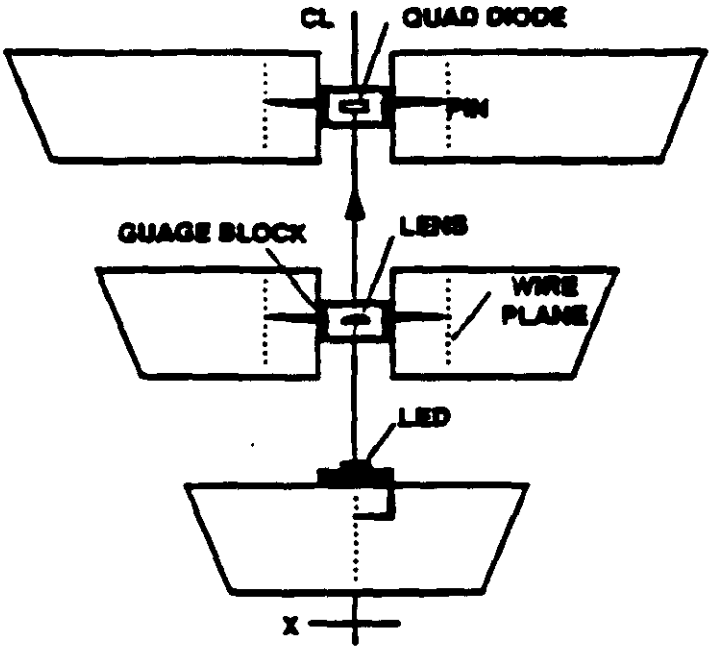

Stability of L3 Alignment for 3 Layers of Chambers

4μm

Reproduces after 1 Year

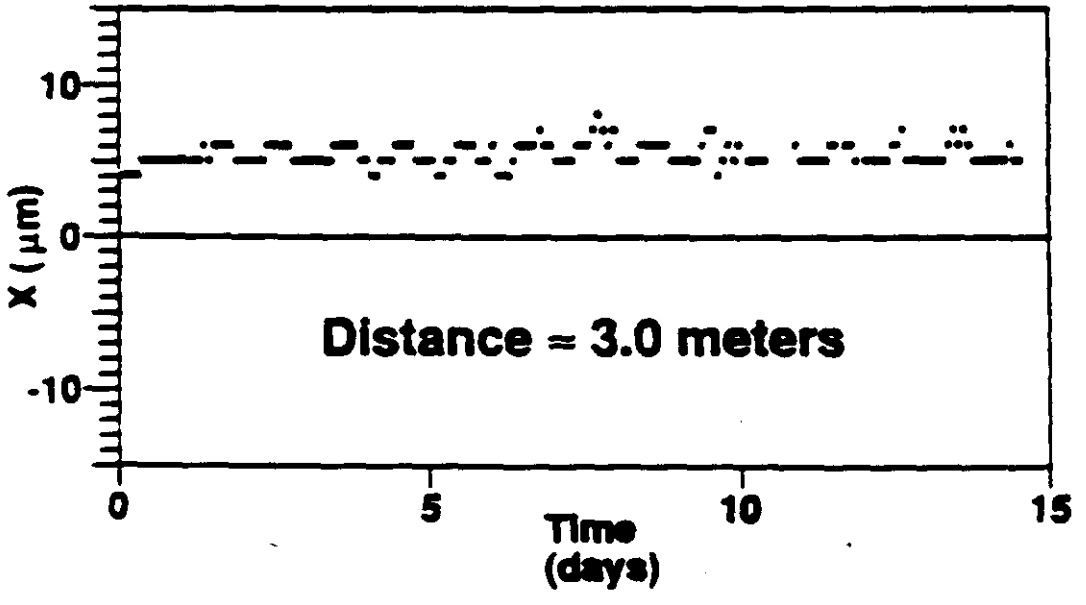

L3 AND L★
WIRE POSITIONING ACCURACY

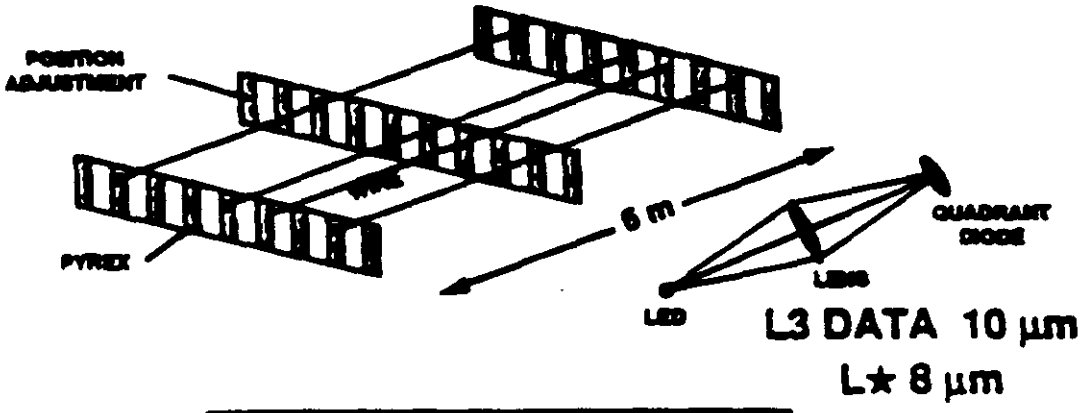

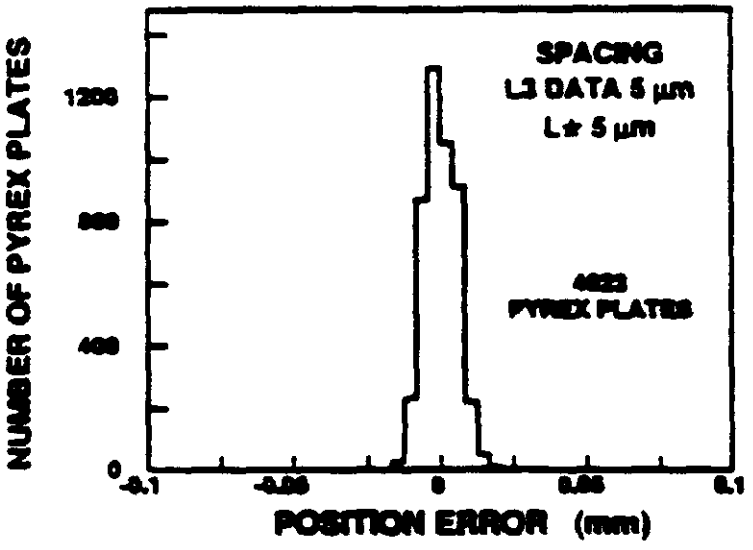

X STRAIGHTNESS MONITOR

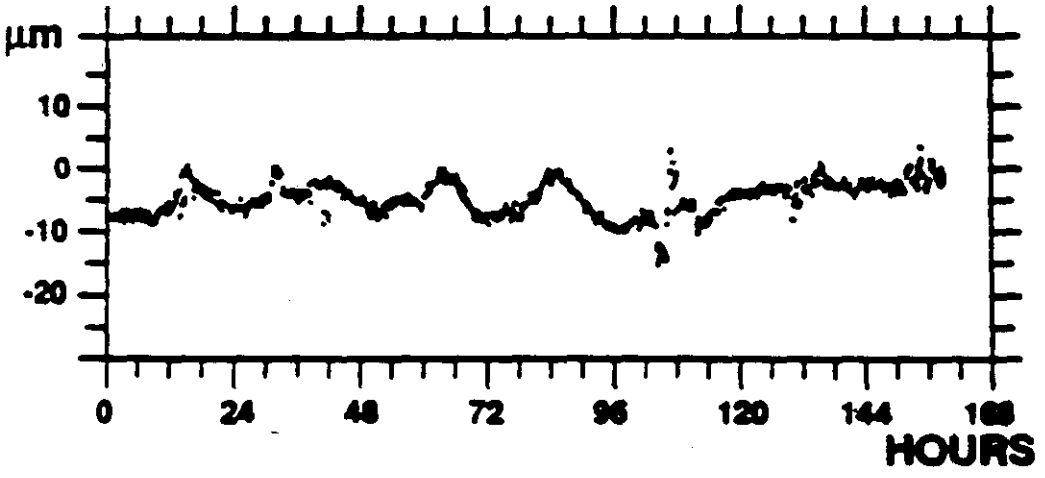

Module Alignment Strategies for GEM

① Limited Streamer Drift Tubes

a) Precision Machined Micalex Bridges

b) Fiducials at Sides of Bridges for alignment to external world

② Pressurized Drift Tubes

a) Precision Machined End Plates

b) Knowledge of wire resonant frequency to correct for 200 μm sag of unsupported wire

③ Cathode Strip Chambers

a) Precision Strip Placement on Printed Circuit Boards

b) Stable support by Hexcell

c) Fiducials at edge of module for alignment to external world

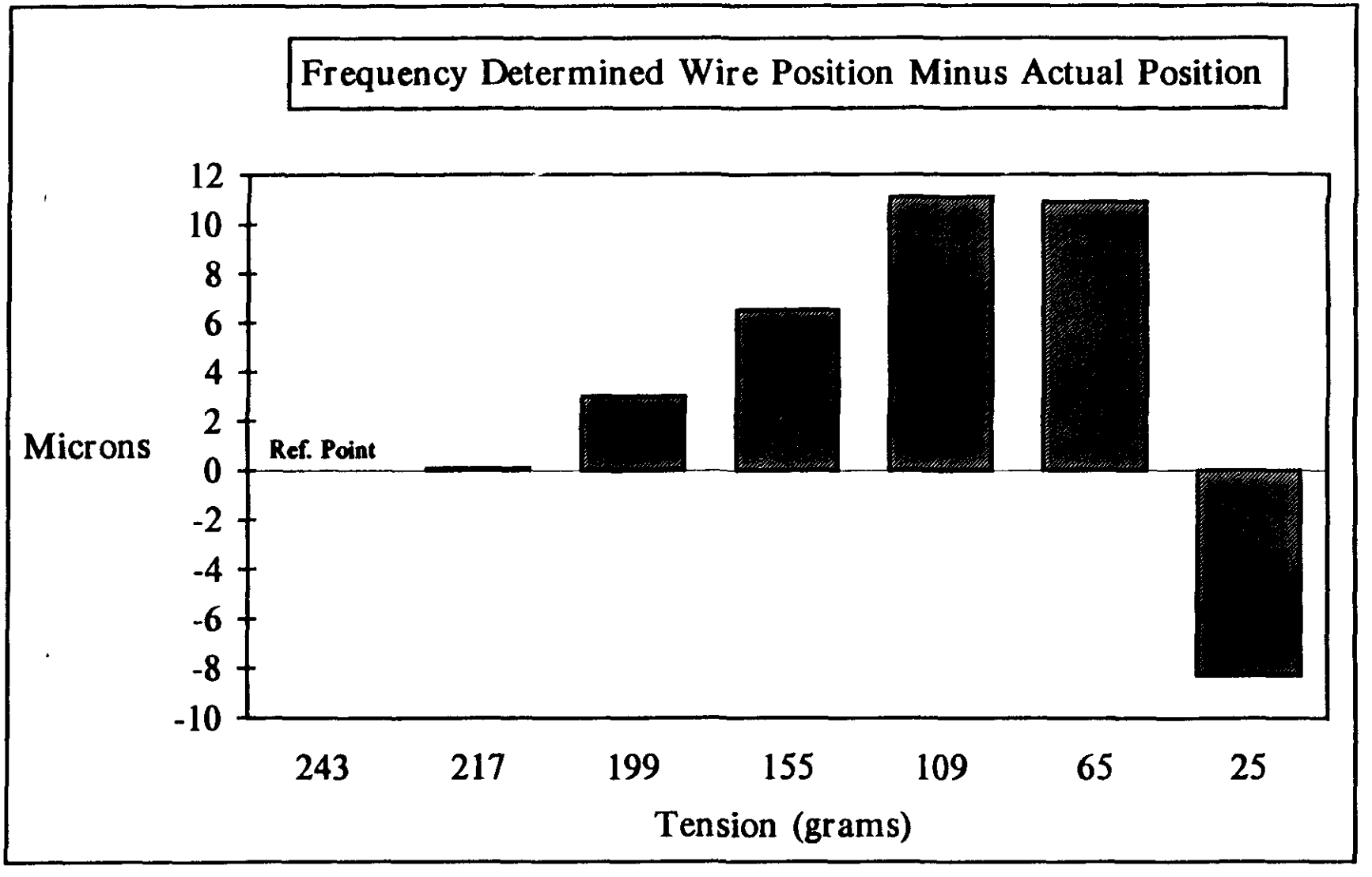
Frequency Determined Wire Position Minus Actual Position
Microns
12
10
8
6
4
2
0
-2
-4
-6
-8
-10
Ref. Point
243
217
199
155
109
65
25
Tension (grams)

R&D and Engineering needs for FY92

Structure and Alignment R&D :

1) Design, fabricate and assemble Large Support Prototype (LSP) to serve as a uniform test bed for the various technology options for large scale chamber prototypes. This test fixture will accommodate three separate layers of muon chambers, an RPC layer, a silicon detector, two scintillator layers and 30 cm of lead as filter for the second layer of scintillators.
2) Design, Fabricate and test GEM Alignment system (straight-line monitor)
3) Design, Fabrication and Test a Small Prototype Structure to evaluate construction concepts for Sector Test Fixture to be proposed in GFY93
4) Design, Fabricate and Test interface hardware prototypes (chamber/structure/magnet)
5) Provide engineering support to produce a credible design of muon chambers and structures as well as the costing analysis for the Muon System for the GEM LoI.

Pressurized Drift Tubes (PDT):

1) Design, Fabrication and Evaluation of End Plug/Manifold/Alignment Plate concept.
2) Design, Fabrication and Evaluation of "Large Prototype" to evaluate assembly procedures, handling, structural integrity and resolution in LSP fixture.
3) Safe gas versus pressure and resolution studies with the LSP.

Limited Streamer Drift Tubes (LSDT):

1) Safe gas versus resolution studies with the a Small Prototype in a representative 0.8T magnetic field.
2) Design, Fabrication and Evaluation of "Large Prototype" to evaluate assembly procedures, handling, structural integrity and long term stability as well as resolution in LSP fixture.

Cathode Strip Chambers (CSC):

1) Design, Fabrication and Test a Small Prototype in a representative 0.8T magnetic field to determine resolution, evaluate safe, low Lorentz angle gases and Radiation Hardness evaluation.
2) Development of electronics suitable for the 1% accuracy requirements as well as for improved multiplexing should be carried out.
3) Design, Fabrication and Evaluation of "Large Prototype" to evaluate assembly procedures handling, structural integrity.and resolution in the LSP fixture.
4) Evaluation of wire tensioning problems in a non-rectangular frame
5) Rate capabilities study for luminosity of 10^{34}.

Resistive Plate Chambers (RPC):

1) Design, Fabrication and Test a Small Prototype in a representative 0.8T magnetic field.
2) Develop materials for high rate low noise capability.
3) Design, Fabrication and Evaluation of "Large Prototype" to evaluate assembly procedures handling, structural integrity, and resolution in the LSP fixture.

GEM

A PRECISION LEPTON-PHOTON DETECTOR FOR THE SSC

- **CALORIMETRY GOALS: DRIVEN By PHYSICS**
  - **The Highest Resolution Calorimetry System for Leptons and Photons**
  - **Within Budget and Schedule**
  - **Radiation Hard**
  - **Complementary to SDC**

15 ran

GEM

PHYSICS GOALS LEAD To TWO SYSTEM APPROACHES

- LOWER RISK SOLUTION EXISTS; NEEDS HIGHER EM RESOLUTION:

  ⇒ LIQUID ARGON With Fine Sampling Accordion EM

- HIGHER RISK SYSTEM, With POTENTIAL LARGE PERFORMANCE GAIN:

  ⇒ BaF_2 CRYSTAL EM, With SCINTILLATOR HCAL

  - NOTE: Radiation Hard Production Not Yet Achieved
    - Requires One Year of R&D
    - Expert Review Panel

GEM

TWO COMPLEMENTARY APPROACHES

RESULTING IN THE HIGHEST FEASIBLE RESOLUTION

- **LIQUID ARGON With ACCORDION EM; Liquid Krypton Option**
  - **Intrinsic Stability**
    ⇒ Ease of Calibration
  - **Tested in Large Systems (With Plates)**
    ⇒ Small Systematics
  - **Radiation Resistant**
  - **Uniform**
- **BaF_2 CRYSTAL EM, With SCINTILLATOR HCAL**
  - **Intrinsic Higher EM Resolution**
  - **Higher HCAL Speed:**
    ⇒ Lower Noise in Isolation Cone
  - **Effective Compensation:**
    ⇒ Small Constant Term for Jets
    With HCAL $e/\pi \approx 1$
  - **More λ for a Given Radius**

GEM CALORIMETRY

- **COMPLEMENTARY STRENGTHS:**

  INTRINSIC RESOL'N and SPEED $\Longleftrightarrow$ **LOWER RISK TECHNOLOGY**

- **COMPLEMENTARY TASKS for EM:**

  $\sigma_E/E = (a/\sqrt{E} \oplus b)\%$

  BaF_2 + SCINT. HCAL $\Longleftrightarrow$ **LIQUID ARGON**

  Reduce b $\leq$ 0.5% — **Reduce a $\leq$ 7%**

  ↑

  → DESIGN and SIMULATE AS a SUBDETECTOR of GEM

BaF_2 + CALORIMETER SYSTEM:

Scintillating Fiber (SF) or Liquid Scintillator (LS); Liquid Argon Study

Choice of One Scintillator HCAL By Early November

HCAL SUBSYSTEM GOALS:

- Complement the BaF_2:
  $\Delta\eta \times \Delta\phi \approx 0.08 \times 0.08$

  $\Rightarrow$ Good Jet Resolution

  $\Rightarrow$ Missing E_T Resolution, (With Forward HCAL)

  $\Rightarrow$ Improved Lepton ID and Measurement

- Rapid Development: Ready for GEM System Choice By Design Report

  $\Rightarrow$ Beam Test By Summer 1992

- Maximize GEM's Physics Capability

BaF_2 + HCAL CHOICE: GENERAL QUESTIONS:

Answers In October

- **Conceptual Design Layouts With Dimensions:**
  - ⇒ LS: Module, Layer Structure, Fiber Readout
  - ⇒ SF: Module Structure, Fiber Readout
  - ⇒ LAr: Segmentation, Cryostat, Readout
  - ⇒ ALL: Mechanical Structures and Supports; Access/Assembly/Disassembly Scheme
- **HCAL Depth (λ); Dead Spaces**

Liquid Scintillator Hadron Calorimeter (Version 0.08-1)
Barium Fluoride EM Calorimeter

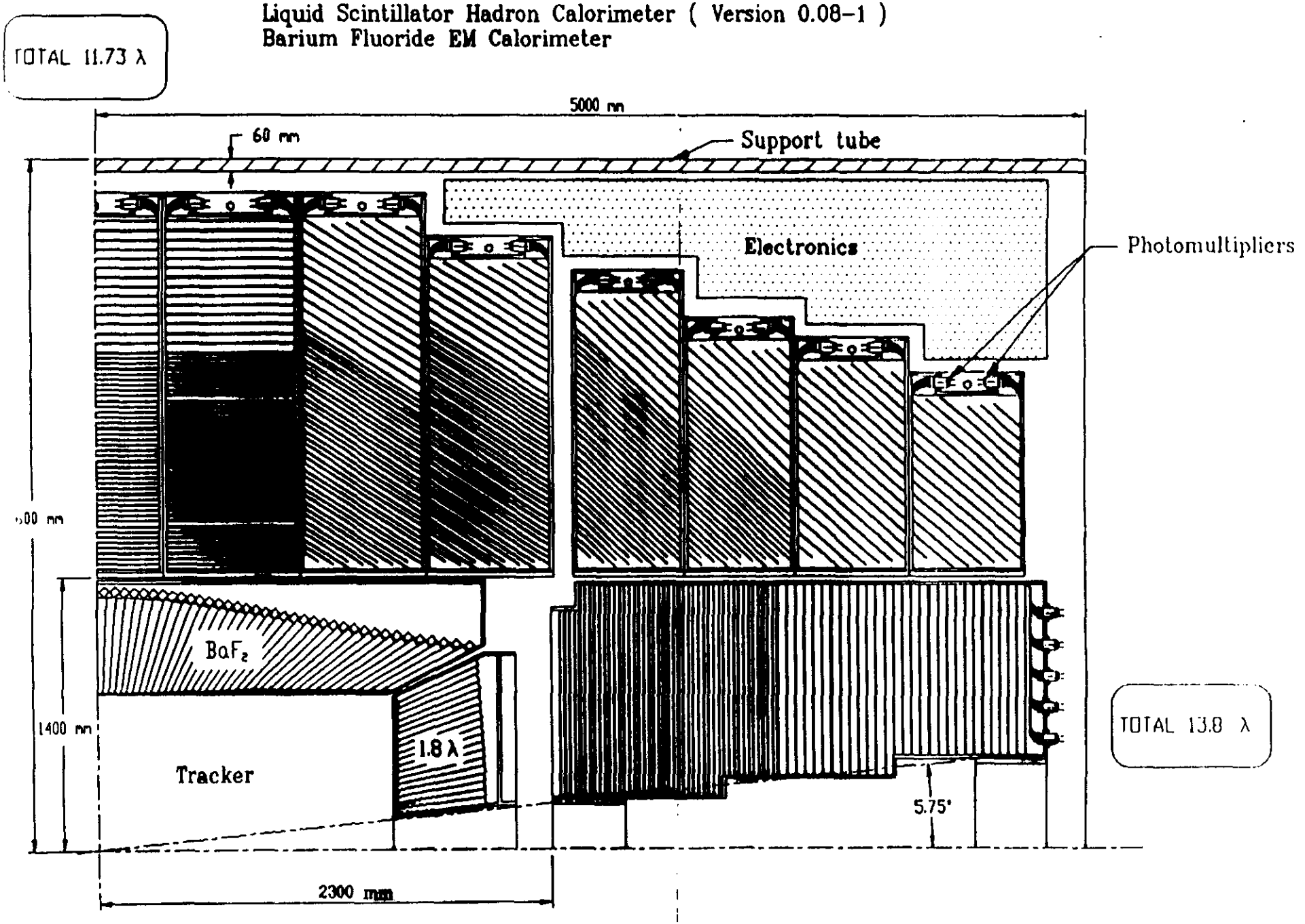

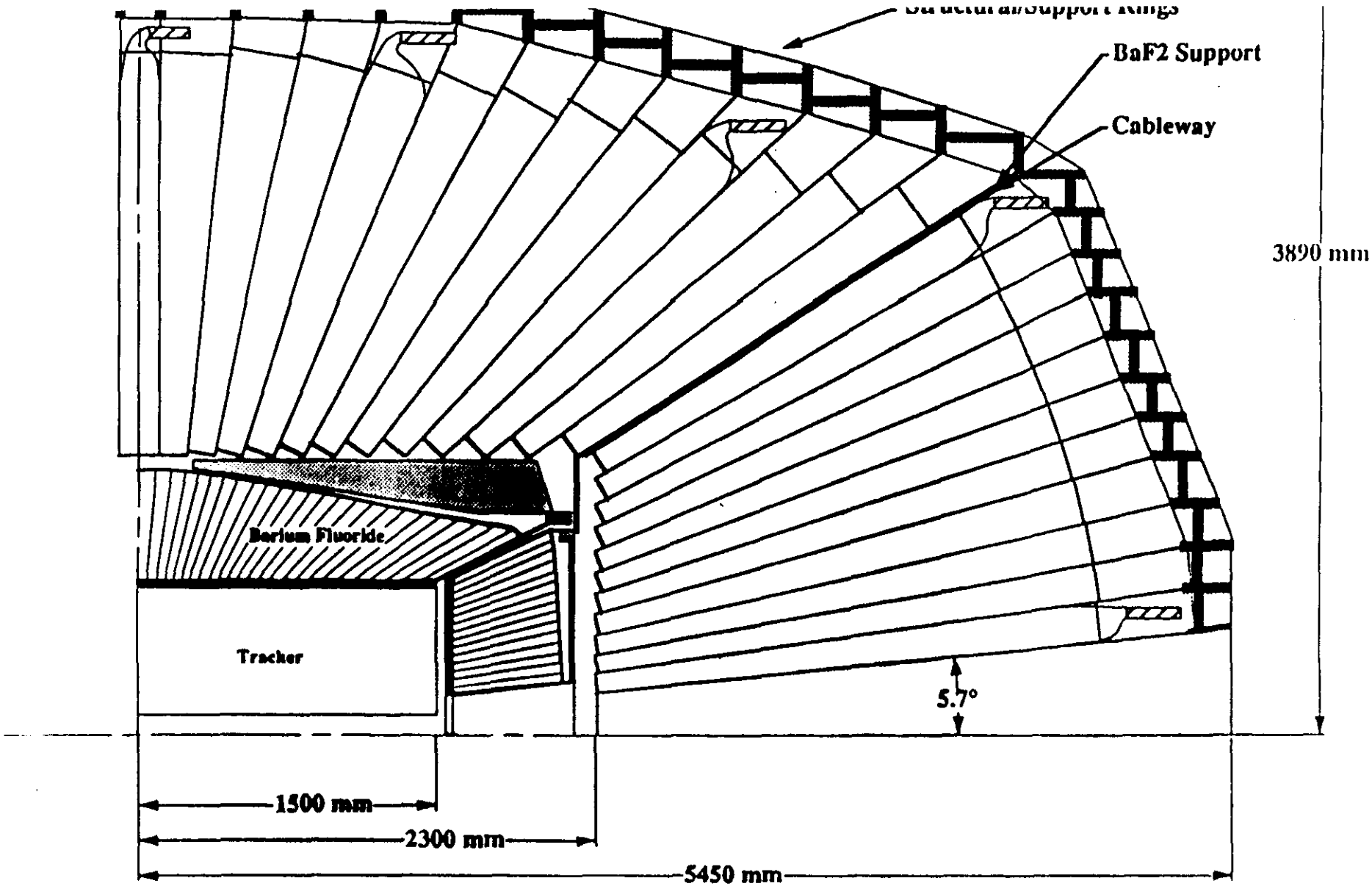

Spaghetti Hadron Calorimeter
Lead Shot Filled/ 0.10 Segmentation
Barium Fluoride EM Calorimeter

G.03.SC.00038

Rennich

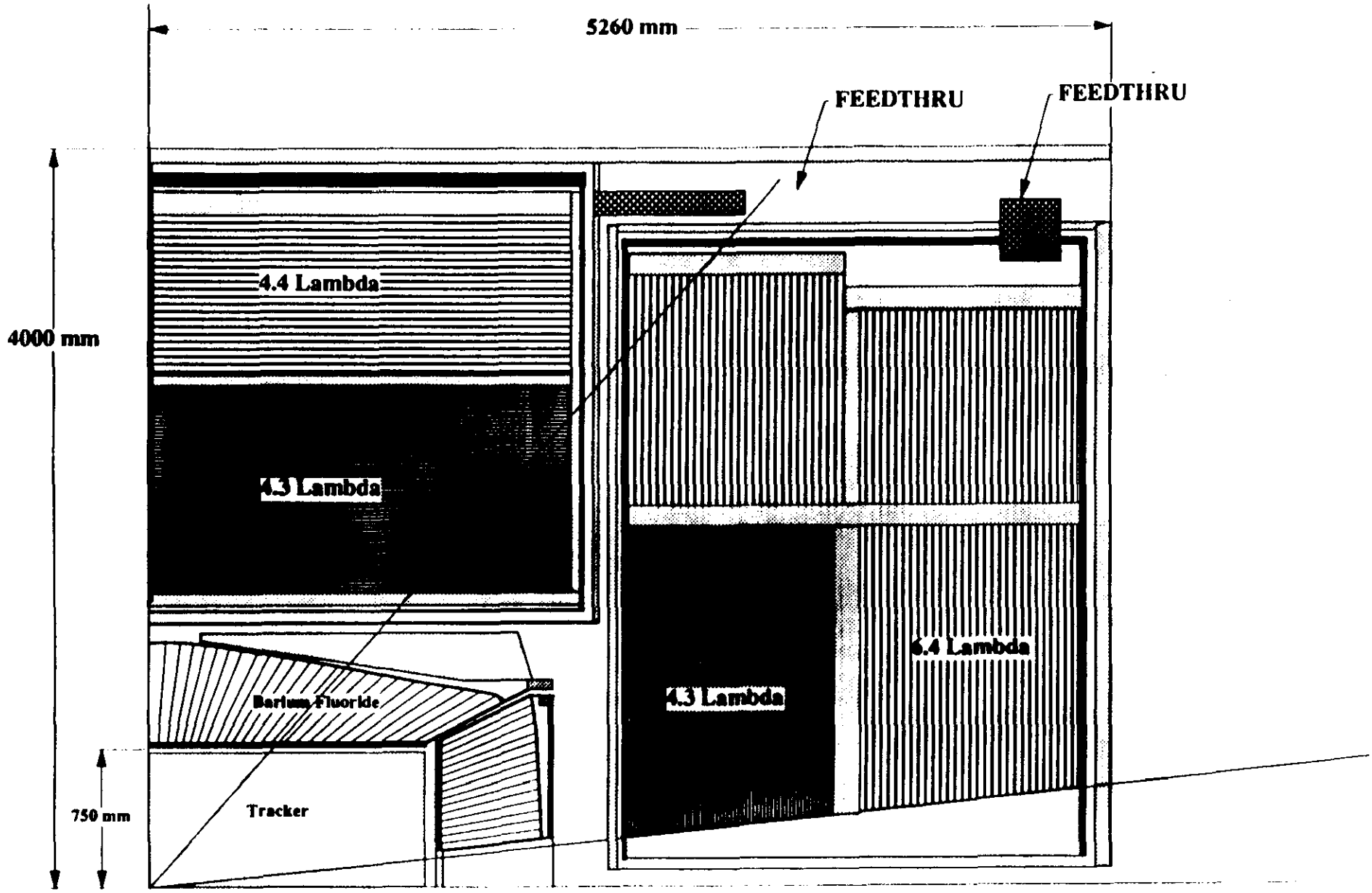

Total Thickness: 11 Lambda

G 03 1 A 00019

GEM
Liquid Argon Calorimeter
Barium Fluoride EM Section

Incomplete
Incomplete
Incomplete

Liquid Scintillator Hadron Calorimeter
Sampling structure scheme

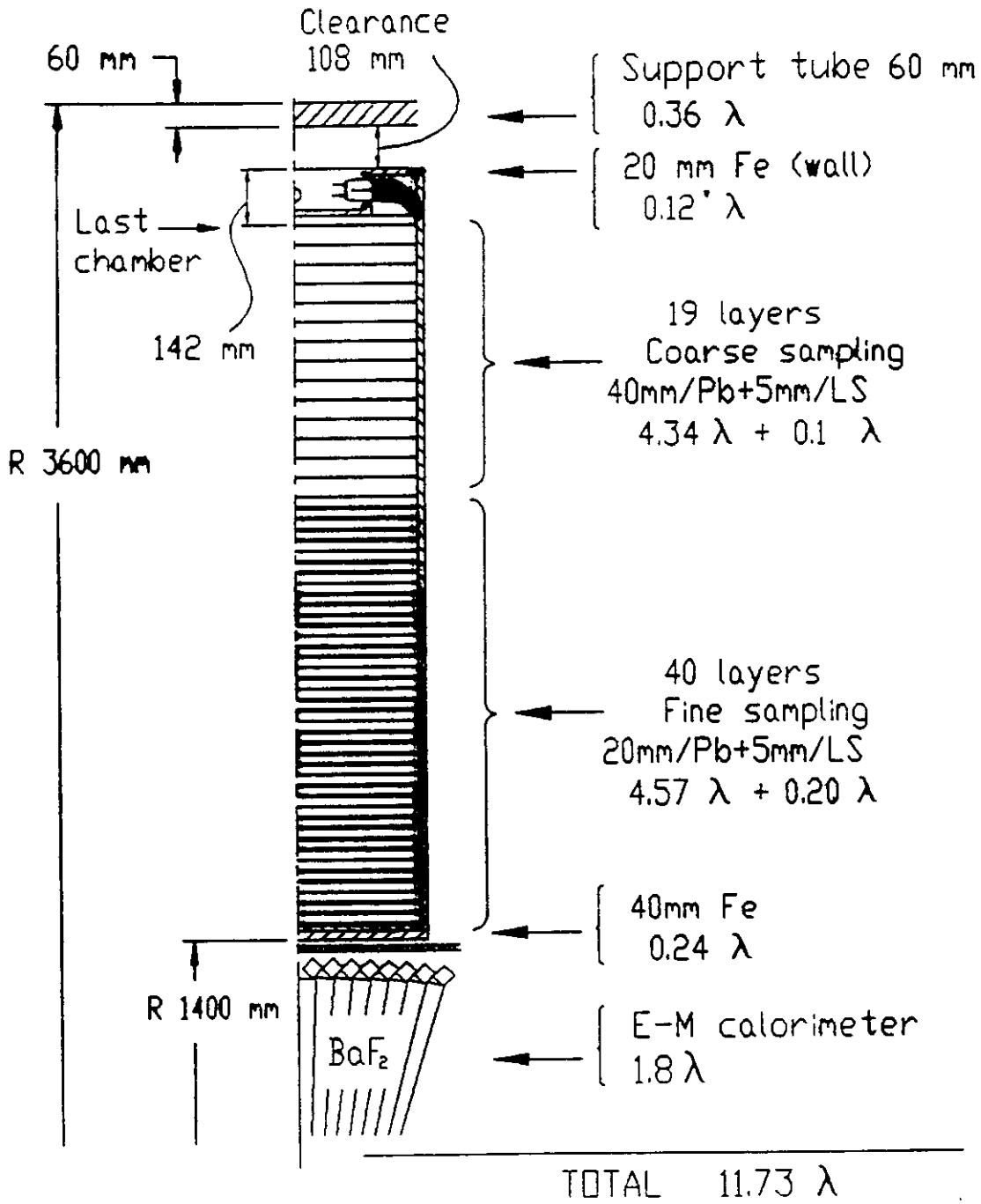

λ_{Pb} = 175 mm

λ_{Fe} = 168 mm

λ_{Scl} = 1000 mm

BaF_2 + HCAL CHOICE: PHYSICS QUESTIONS

SIMULATION STUDY COMPLETED By NOVEMBER:

- **Energy Resolution, Behind BaF_2 for 20, 100, 500, 1000, ... GeV Jets**
  - **Performance For Typical, Mostly-EM, and Mostly-Hadronic Jets:**
    - ⇒ **Reconstructed Energy Distribution**
    - ⇒ **Missing E_T Distribution**
- **Can Longitudinal Segmentation in the HCAL Improve the Muon Resolution ?**
- **Can Longitudinal Segmentation in the HCAL Improve the BaF_2 Electron and γ Resol'n ?**
- NUMBER of $\lambda \Leftrightarrow$ Performance

BaF_2 + HCAL CHOICE: ASSOCIATED EFFECTS and ISSUES

- **Systematic Effects:**
  - ⇒ **Magnetic Field (0.8 Tesla)**
  - ⇒ **Non-Uniformities in Cells or Towers**
  - ⇒ **Fiber Attentuation Length, Non-Uniformity**
  - ⇒ **Mechanical Structure, Walls, and Typical 'Dead Regions'**
- **Effective Compensation: Hydrogenous, Compensating or Overcompensating HCAL.***
- **Resolution as Function of e/h in EM Section, With Varying Reconstruction Algorithm.**
- **Transverse Segmentation Required by Physics**

* GEANT vs. HETC Study:
- Preliminary Results (ORNL)

Oct. 3, 1991

H. Gordon

Liquid "Argon" Approach to the Highest Resolution Calorimeter System for GEM

Accordion for EM (RD3)

Energy Resolution $\frac{\Delta E}{E} = \frac{10.1 \pm 0.4\%}{\sqrt{E}} \oplus (0.2 \pm 0.2)\%$

Linearity $<< 1\%$

Position Resolution $\Delta x = 4.4\,mm/\sqrt{E}$

Angular Resolution $\Delta\theta = 6.1$ mrad @ 120 GeV

Uniformity

NA31 $< 0.5\%$ (vs. time and position)

RD3 $< 0.4\%$

Fast shaping $\Rightarrow$ less sensitive to gap variations

Calibration - goal 0.1%

Hadronic

Parallel Plate Geometry (aka DØ, SLD, H.
with "electrostatic" transformer

Absorber choice Fe / Pb / DU

BNL results $\frac{\Delta E}{E} \cong 60\%/\sqrt{E}$

R+D Plans

EM – improve $\frac{\Delta E}{E}$ to $\frac{7\%}{\sqrt{E}}$

a) 1mm accordion + Argon

b) Krypton + 2mm accordion

Hadron – Construct + beam test prototype

Engineering

Integrated design

Energy Resolution

Fit: $\frac{\sigma}{E} = \frac{K}{\sqrt{E}} + c$

5x5 cluster

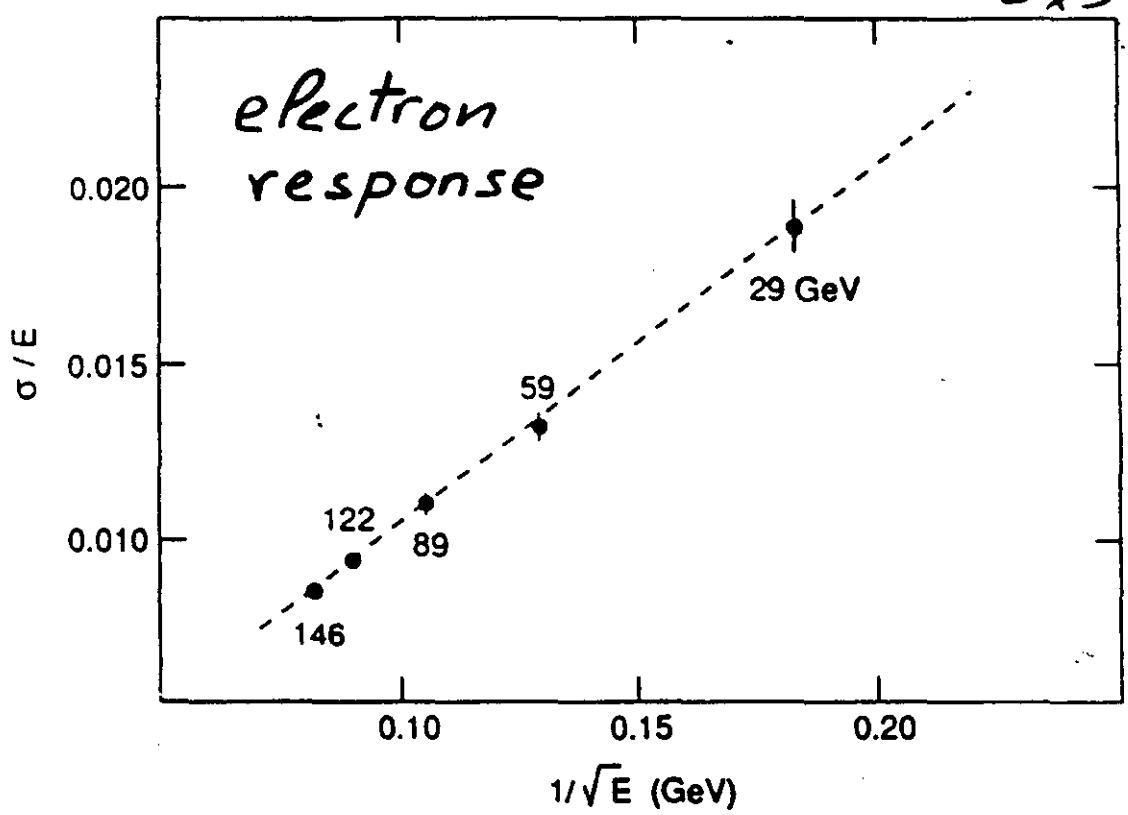

▲ 100% readou

'90 data

(5x5) = 13.6 x 12.5 cm²

$$\frac{\sigma}{E} = \frac{10.0 \pm 0.6}{\sqrt{E}} + (0.0 \pm 0.1)\ \%$$

$$\frac{\sigma}{E} = \frac{10.1 \pm 0.4}{\sqrt{E}} \oplus (0.2 \pm 0.2)\ \%$$

(3 x 3) = 8.1 x 7.5 cm²

compatible results

Accordion Waveforms 1991 Data

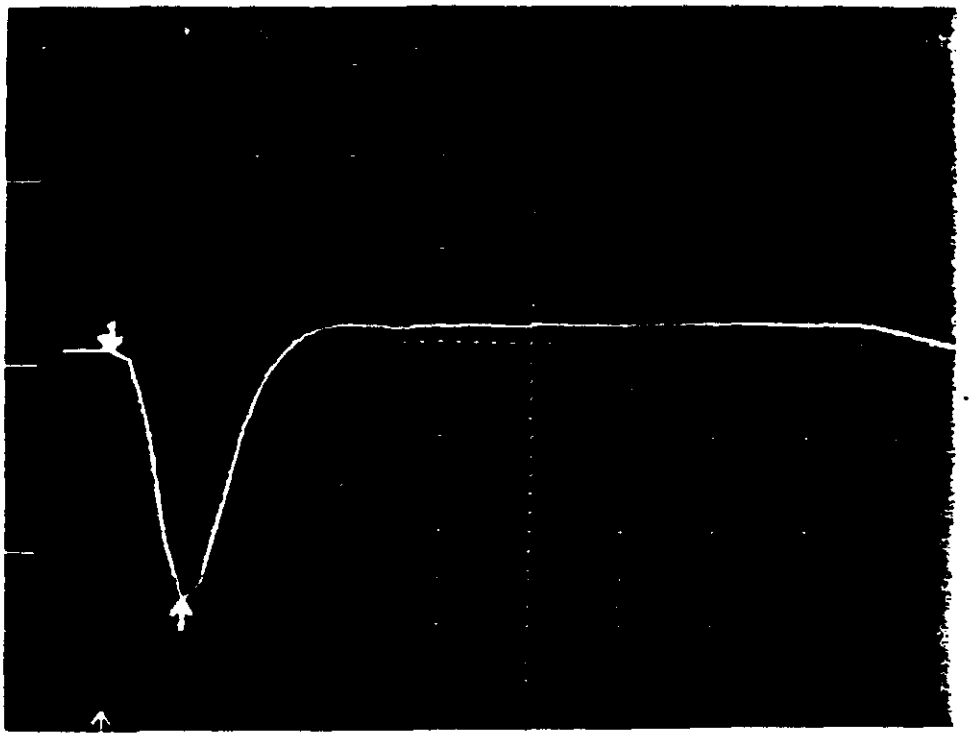

60G

2m

tp

scu

tri

50usec

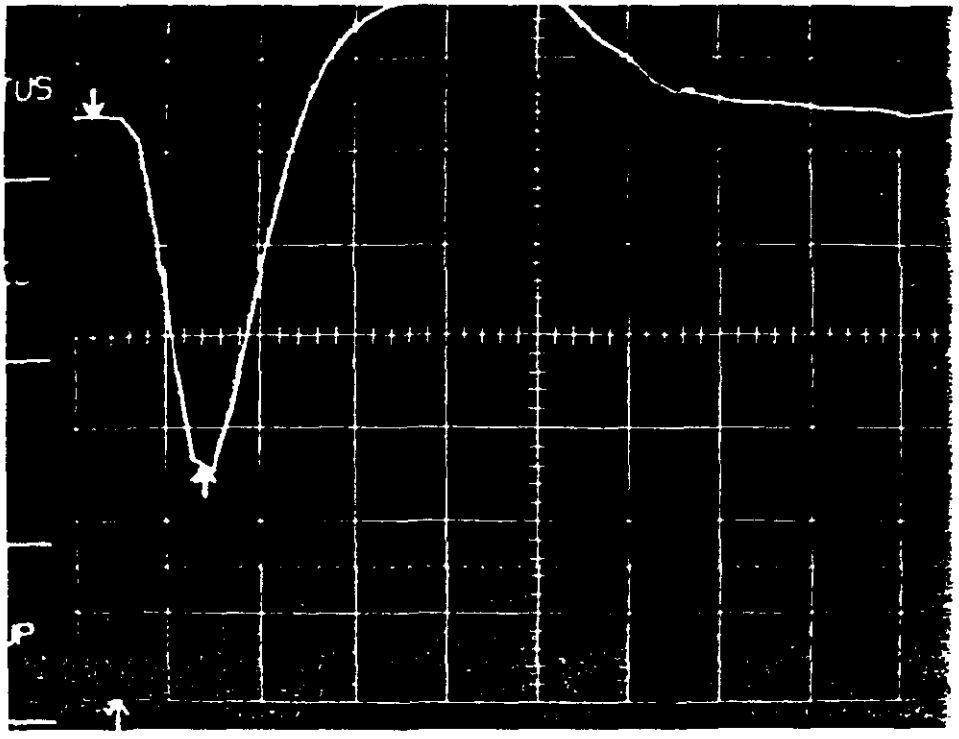

Pres

1mi

Linearity of the response (electrons)

- Electron data taken at several beam energies
  30, 60, 90, 120, 150, 175, 197 GeV

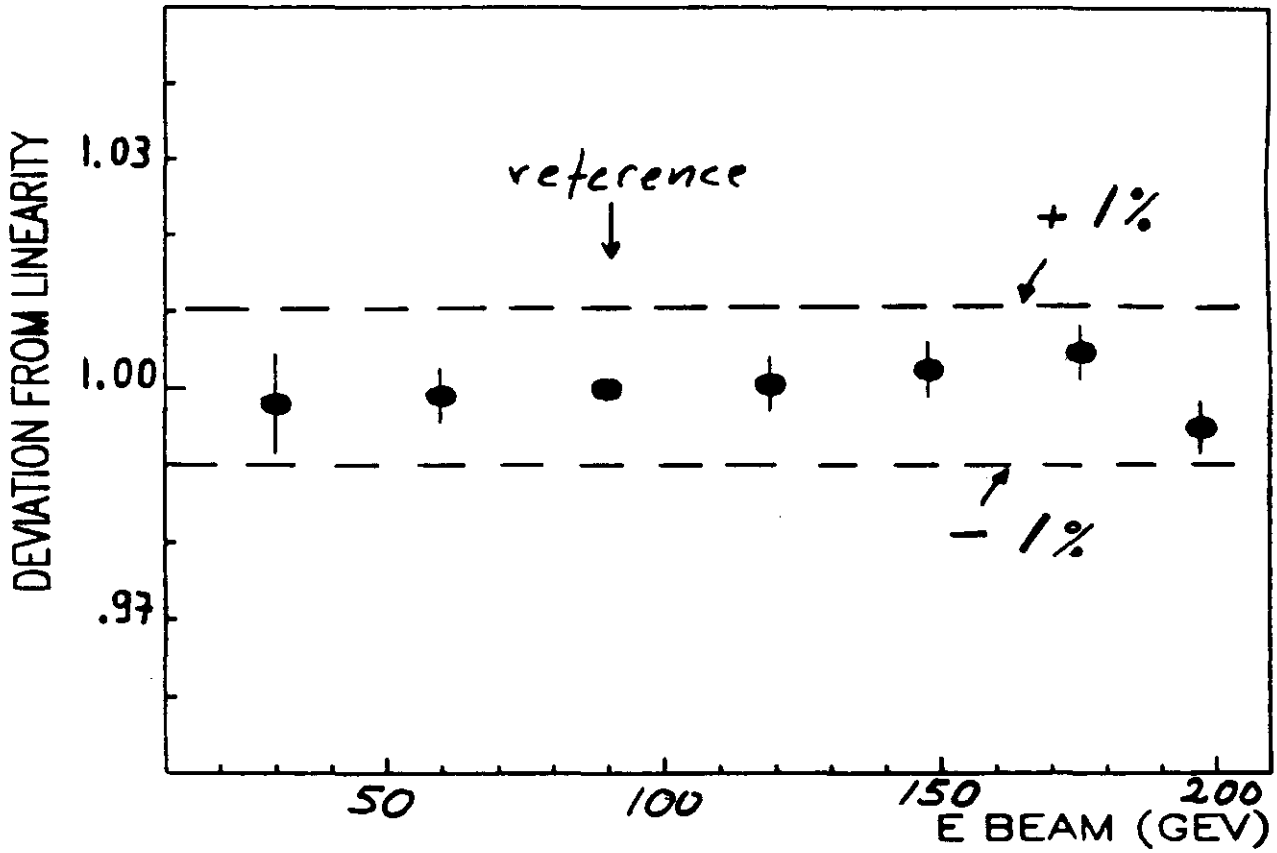

- for fast shaping (20ns)
- no longitudinal leakage corrections
- 3 x 3 clustering

Spatial resolution: along x (ACCORDION FOLDS)

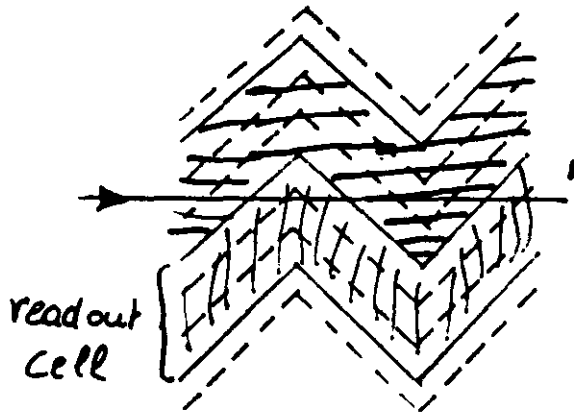

always 2 readout cells are involved

better energy sharing
⇕
better spatial resolution (c

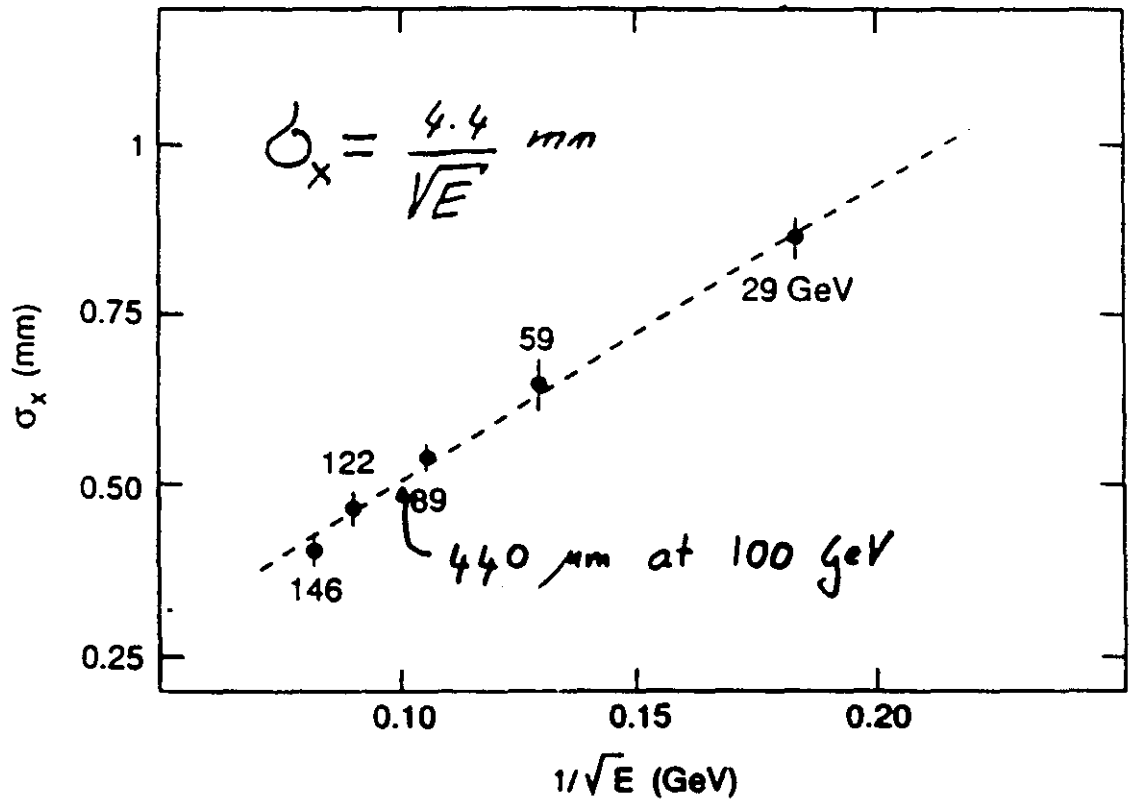

readou
100 ns

- same results with the fast shaping (20 ns)
- no bias $X_{calor} = X_{impact} \pm$ resolution
- in Y it behaves like a conventional pad detector $Y_{calor} = f(Y_{impact}) \pm$ resolution
- at 100 ns σ_x (muon) = 1.80 ± 0.05 mm

Angular resolution

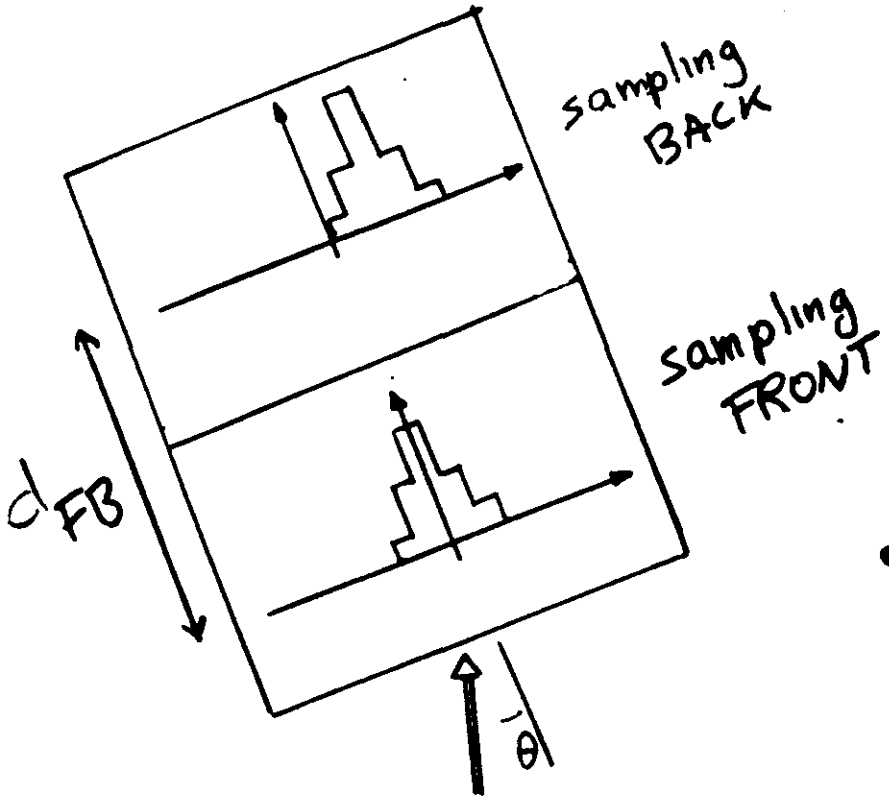

$$\theta = \frac{X_B - X_F}{d_{FB}}$$

- calibrated by rotating the calorimete on a platform

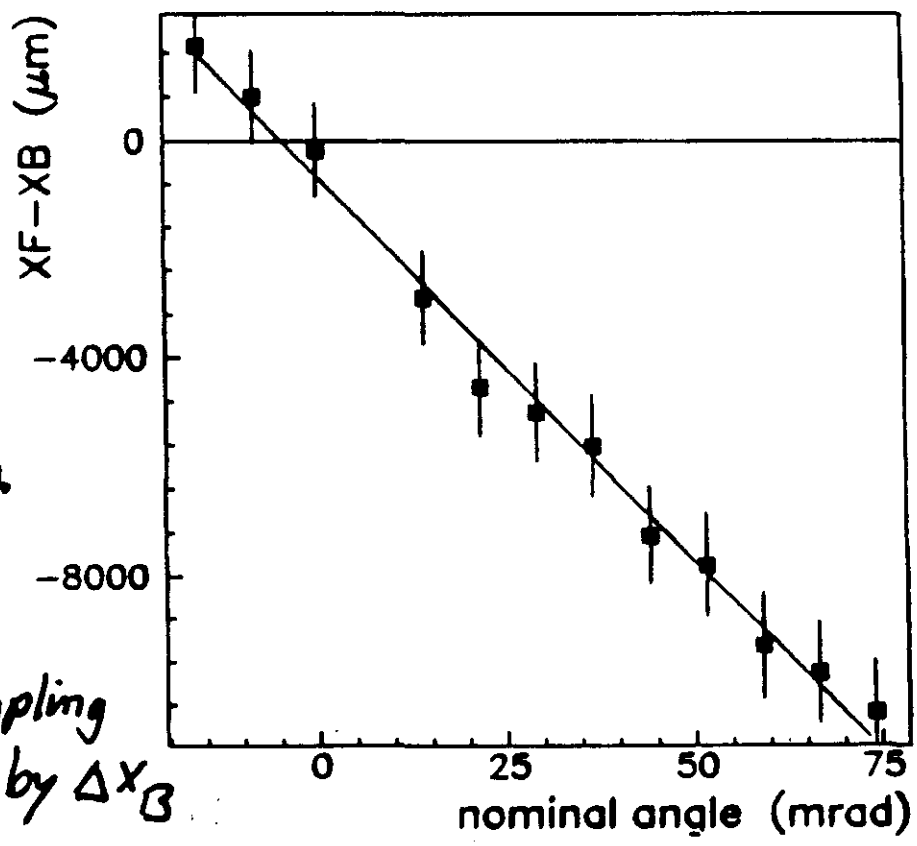

- $\Delta\theta = 6.1$ mrad at 120 GeV
- same result with the fast readout
- not optimized longitudinal sampling $\rightarrow \Delta\theta$ dominated by ΔX_B

Signal uniformity

cell [illegible]

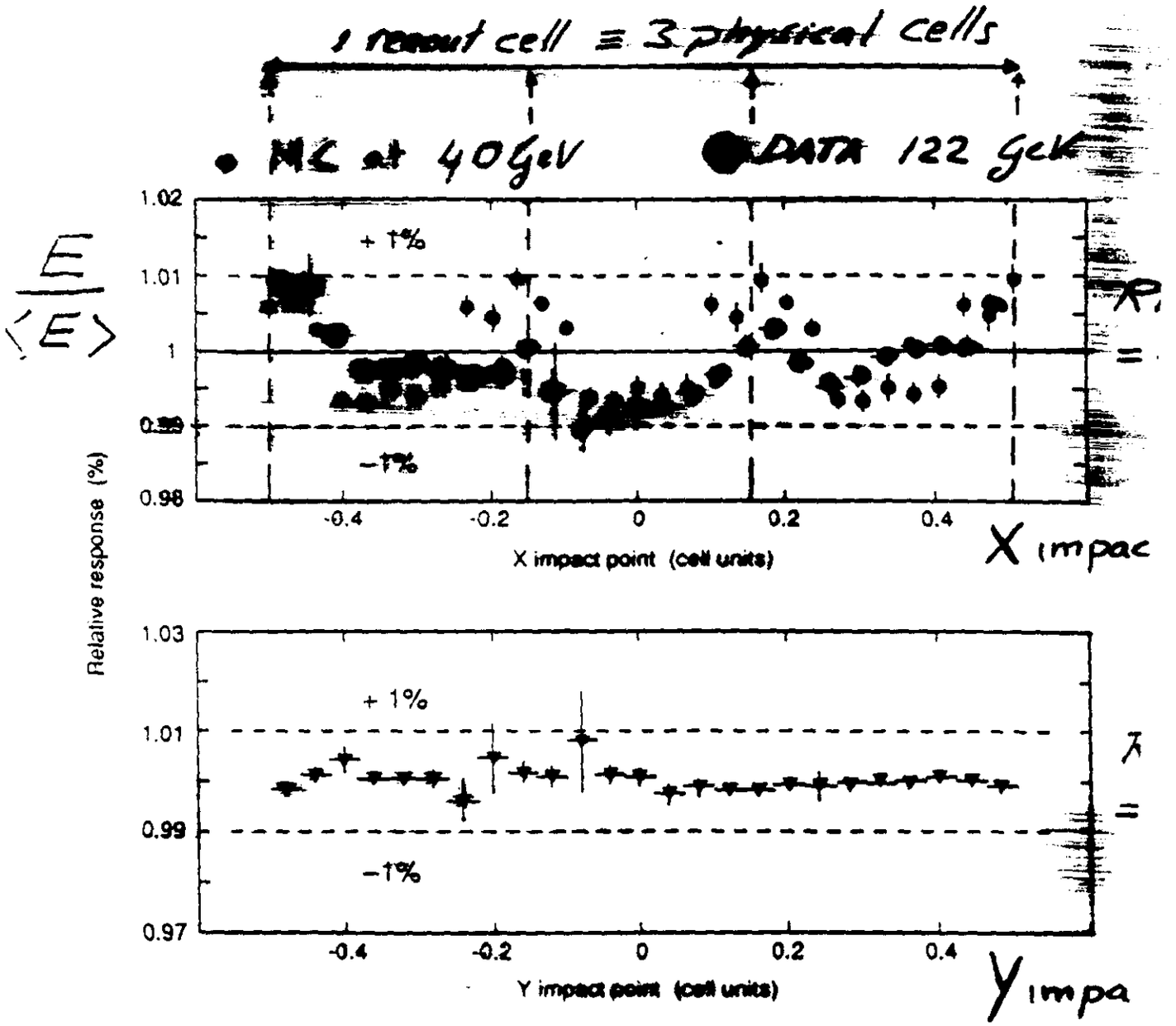

Pulse width

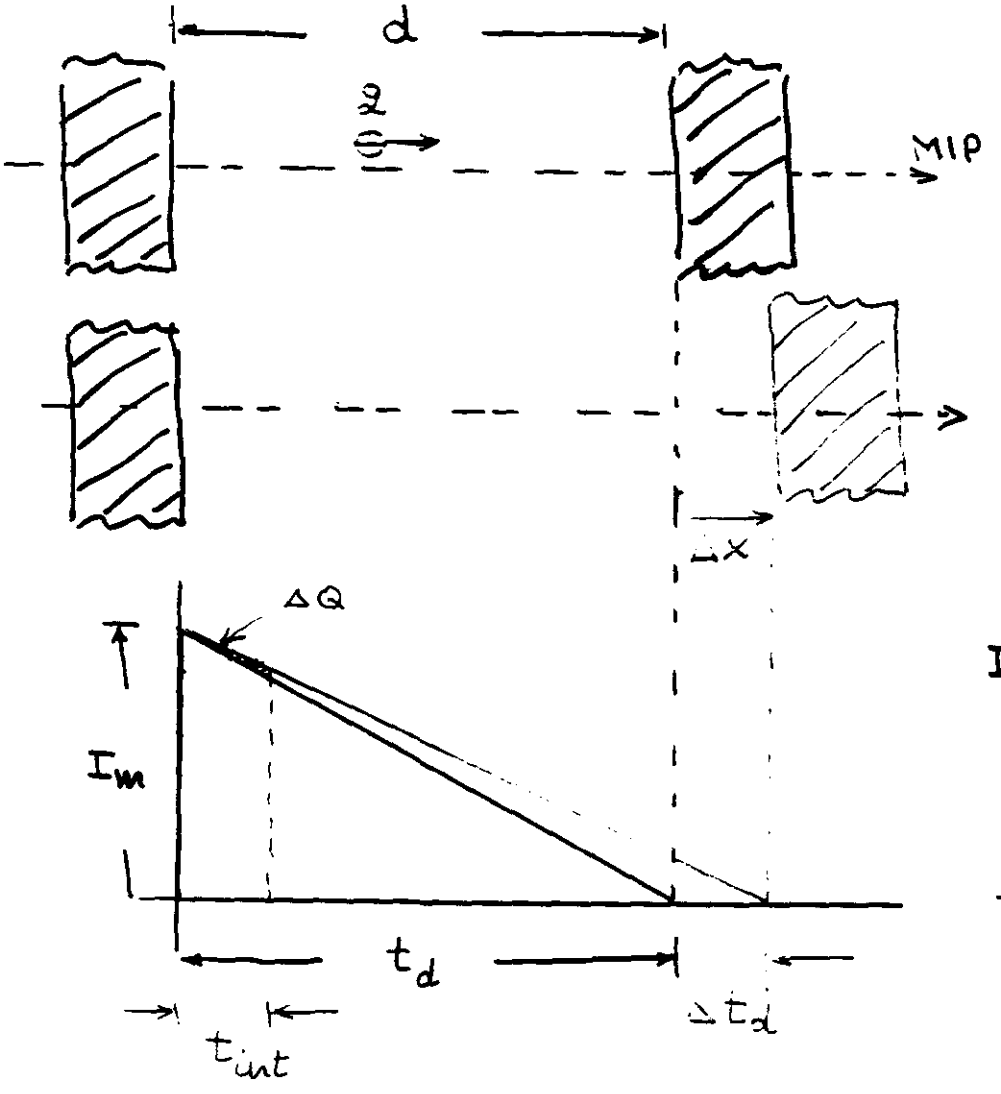

single carrier:

$$i = \frac{e}{t_d} = e\,\frac{v_e}{d}$$

MIP responce:

$$I_m = e\,\frac{dn_e}{dx}\,\frac{d}{t_d}$$

$$= e\,\frac{dn_e}{dx}\,v_e$$

I_m is independent of d!

long integration: $t_{int} > t_d$ $\quad Q_s = \frac{1}{2} I_m t_d$

Short integration: $t_{int} \ll t_d$ $\quad Q_s = I_m t_{int}\left(1 - \frac{1}{2}\frac{t_{int}}{t_d}\right)$

$$\frac{\Delta Q_s / I_m t_{int}}{\Delta t_d / t_d} = \frac{1}{2}\,\frac{t_{int}}{t_d} \approx \frac{1}{20}$$

for $d = 2$ mm (400 nsec), $t_{int} = 40$ nsec

∴ 20% gap variation results in 1% signal variation.

Calibration should be by I_m and not by $Q = \frac{1}{2} I_m t_d$!

1) $Q = C V_{cal}$

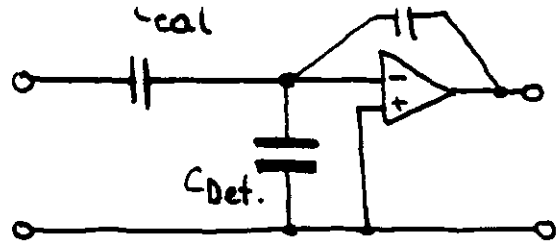

Conventional cha
calibration

$$\frac{\delta C_{cal}}{C_{cal}} \approx 1-2\%$$

2) $I_{in} = \frac{V_{cal}}{R_{cal}}$

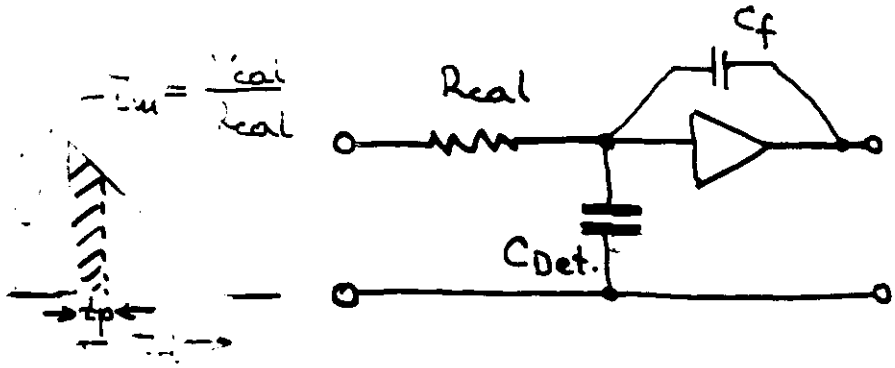

Current calibratic

$$\frac{\delta R_{cal}}{R_{cal}} \approx 0.1\%$$

- distribution o precisely contro pulses needed

3)

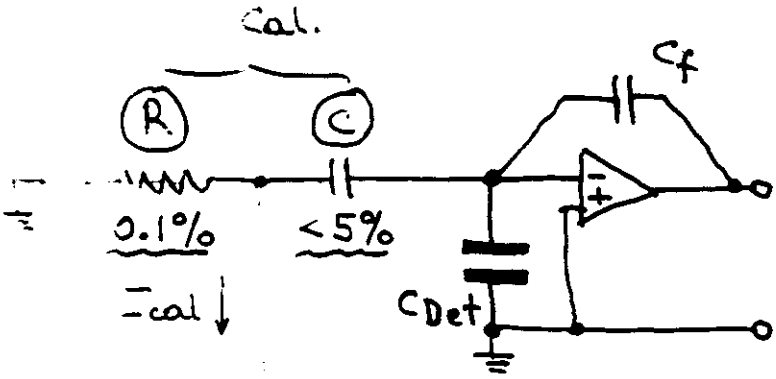

Current calibrati
by local pulse genere

- dc current distributed
- 5% in c's results in 0.12 calibration

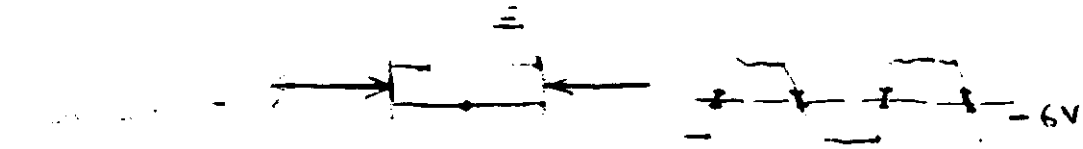

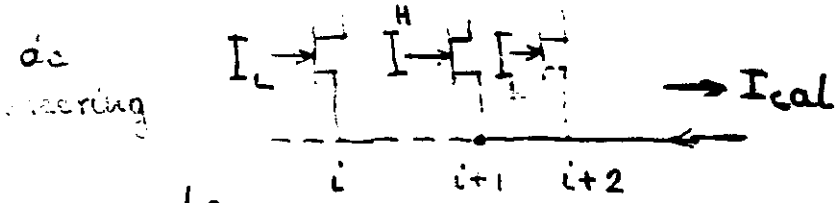

dc cal.
current (0 – 2.5 μA)
100 MeV ⟶ 2 TeV

leakag
pA
after
100 pA
0.1

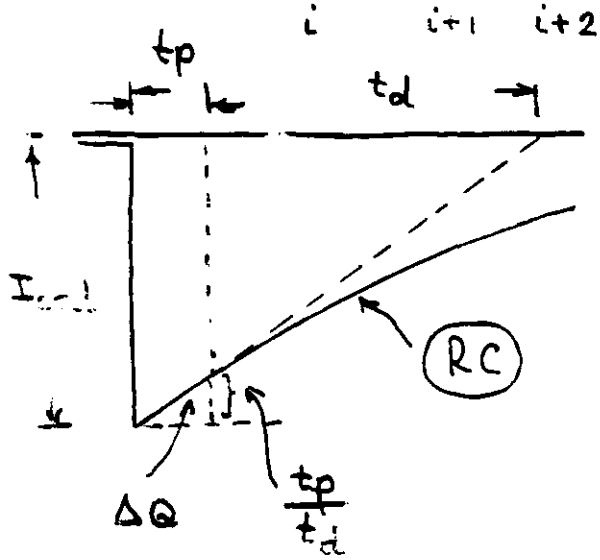

$$Q_{cal} = I_{cal}\, t_p \left(1 - \frac{1}{2}\frac{t_p}{t_d}\right)$$

$$\frac{\Delta Q}{Q_{cal}} = \frac{1}{2}\frac{t_p}{t_d} \approx \frac{1}{40}$$

$t_p = 20$
$t_d = 40$

$$\frac{\delta Q_{cal}}{Q_{cal}} \approx \frac{1}{40}\left(\frac{\delta R}{R}, \frac{\delta C}{C}, \frac{\delta(RC)}{RC}\right)$$

Switch parameters (V_t, noise, etc. do not influence calibration.

$I_{L} < 10^{-3} I$ (mini after radiation

PRELIMINARY RESULTS OF LIQUID ARGON TEST BEAM

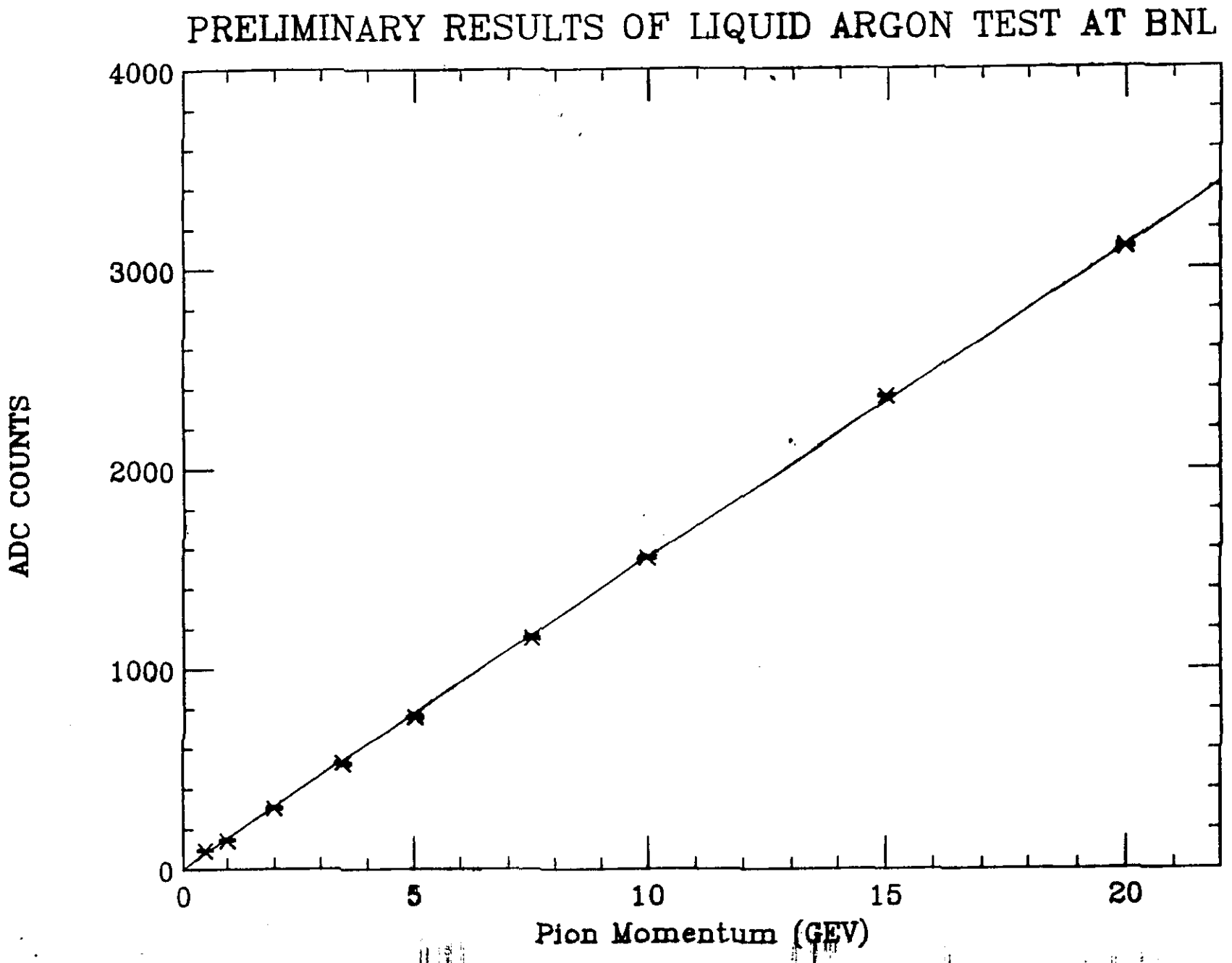
PRELIMINARY RESULTS OF LIQUID ARGON TEST AT BNL
ADC COUNTS
4000
3000
2000
1000
0
0
5
10
15
20
Pion Momentum (GEV)

Preliminary Results of Liquid Argon Test at BNL

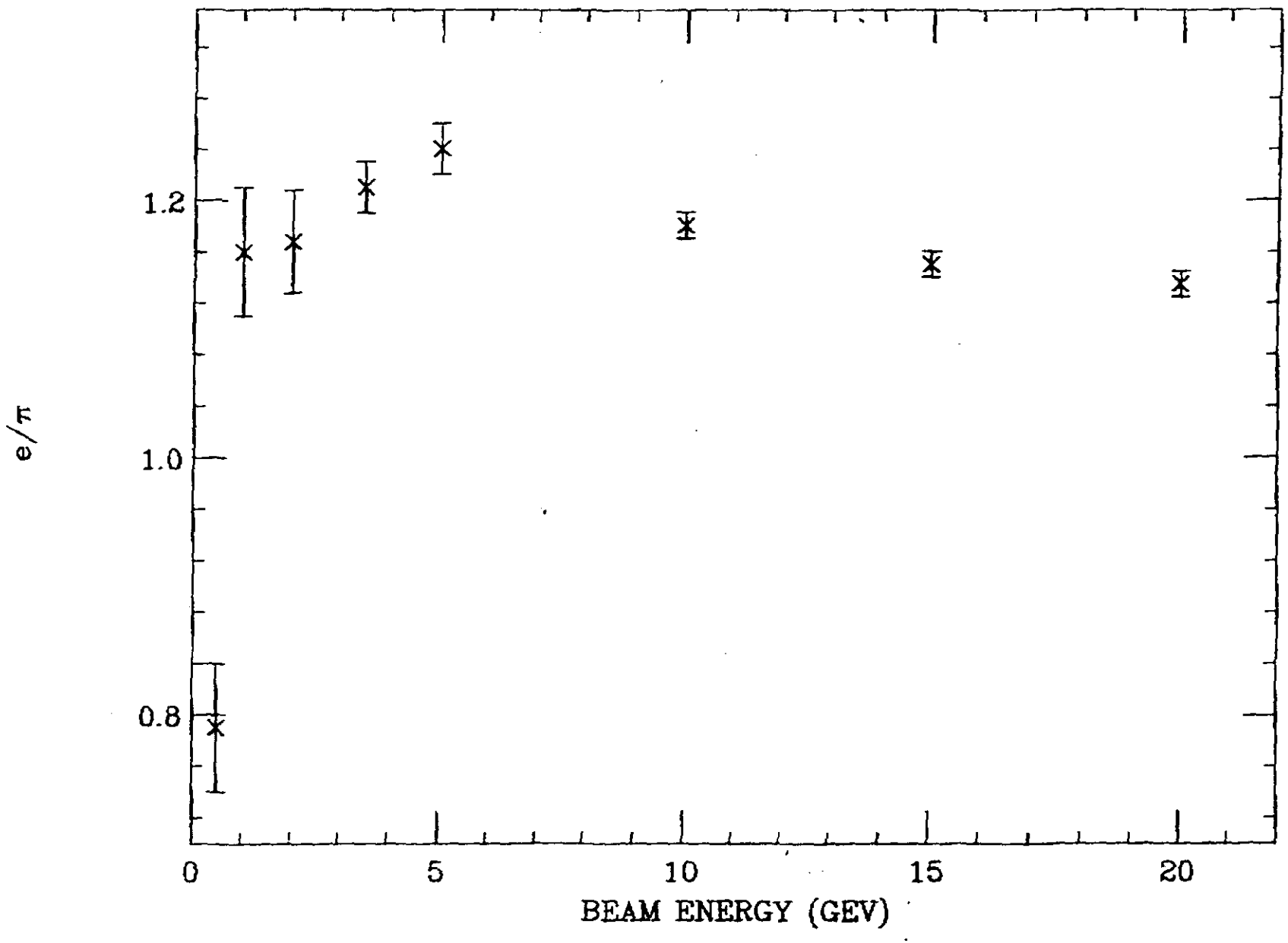

Liquid Argon Specs

EM

$\gtrsim 25 X_0$

$\Delta\eta \times \Delta\phi = 0.04$

3 longitudinal readouts

$\Delta E/E \lesssim \frac{7\%}{\sqrt{E}} \oplus 0.5\%$

$|\eta| < 3$

Hadron

$\sim 11 \lambda$ active

$\Delta\eta \times \Delta\phi = 0.08$

4 longitudinal divisions

$\frac{\Delta E}{E} \sim \frac{50\%}{\sqrt{E}} \oplus 2\%$

$|\eta| < 5.5$

$\sim 80{,}000$ channels

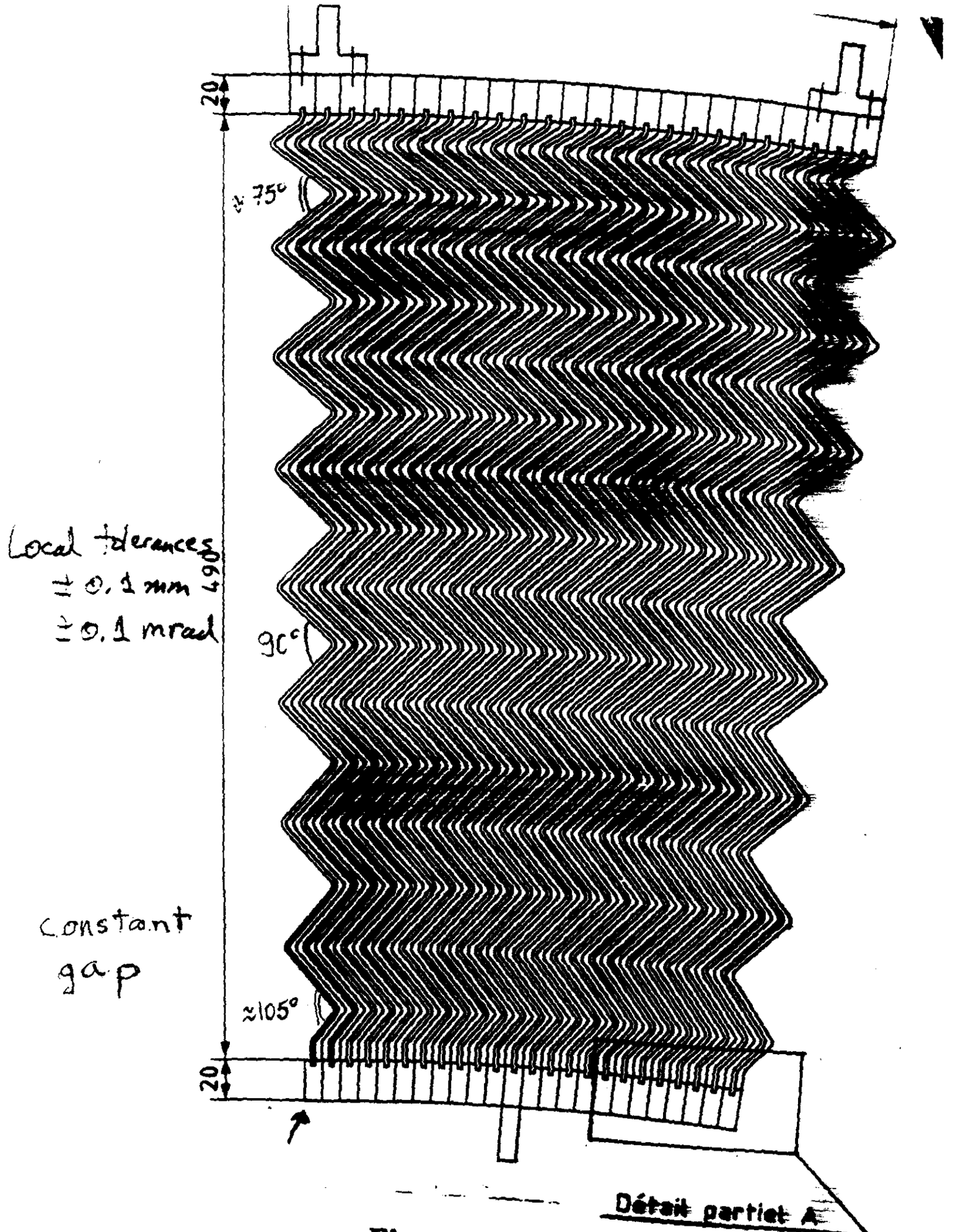
20
≈ 75°
Local tolerances
≃ 0.1 mm
≃ 0.1 mrad
490
90°
constant
gap
≈105°
20
Détail partiel A

Figure 12

EM Configuration

1mm OPTION

P=
X_0=
η=
Rs=21.1%
Cell=6.6mm

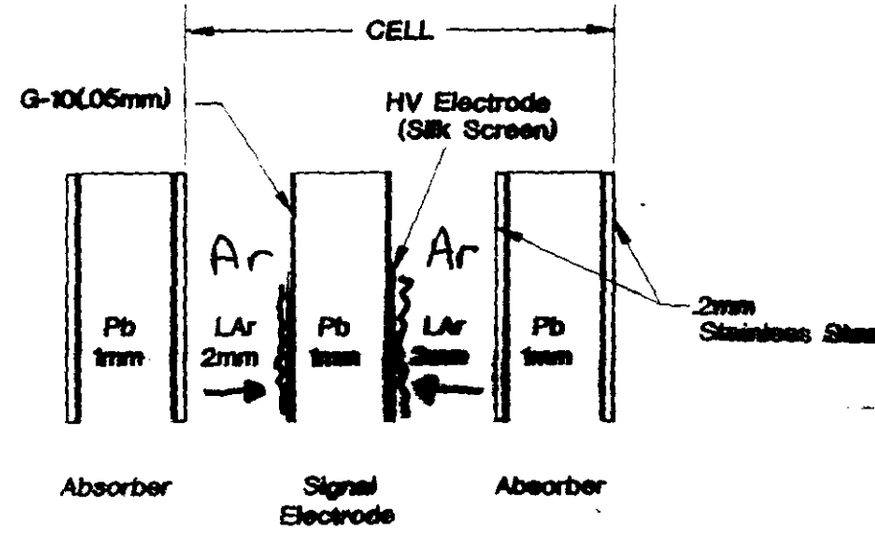

2mm OPTION

P=
X_0=
η=
Rs=22.8%
Cell=6.6mm

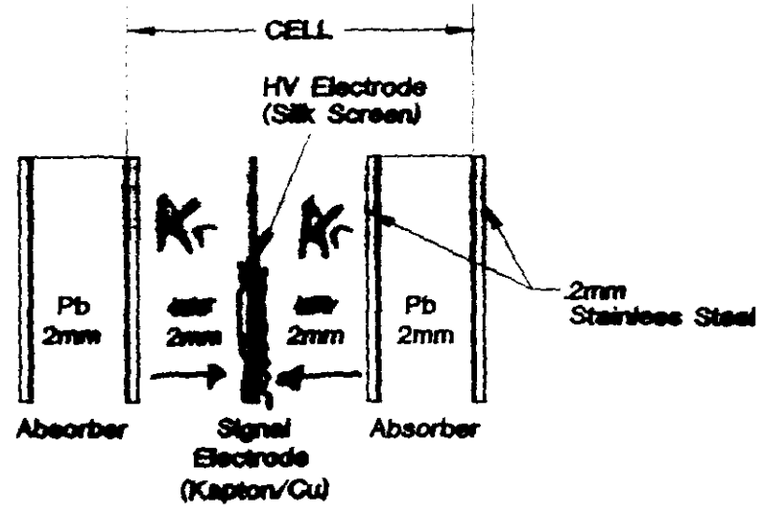

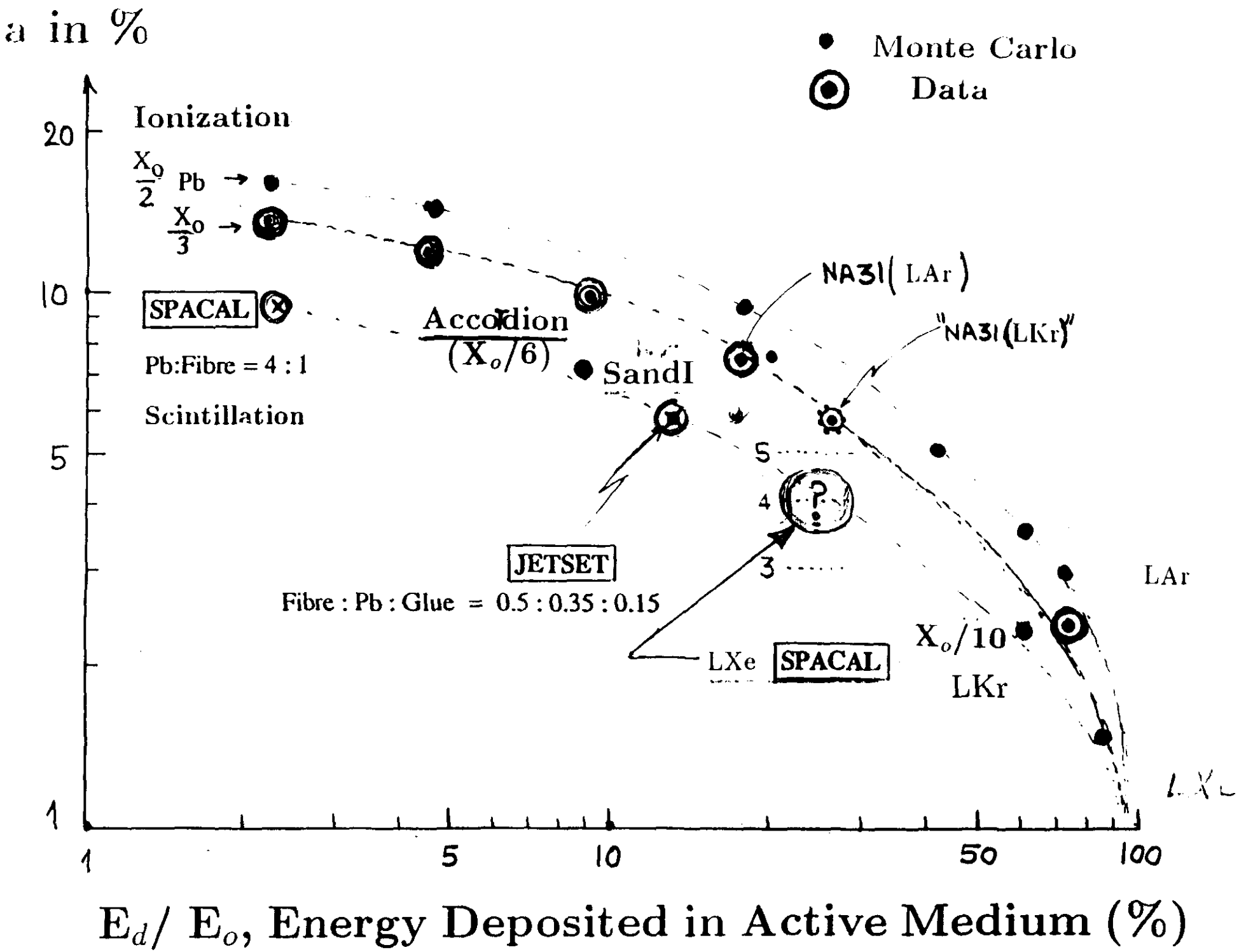
a in %
Monte Carlo
Data
Ionization
$\frac{X_o}{2}$ Pb
$\frac{X_o}{3}$
SPACAL
Pb:Fibre = 4 : 1
Scintillation
Accordion
$(X_o/6)$
SandI
NA31(LAr)
"NA31(LKr)"
JETSET
Fibre : Pb : Glue = 0.5 : 0.35 : 0.15
LXe
SPACAL
$X_o/10$
LKr
LAr
20
10
5
1
1
5
10
50
100
E_d/ E_o, Energy Deposited in Active Medium (%)

HADRONIC "Electrostatic" transformer

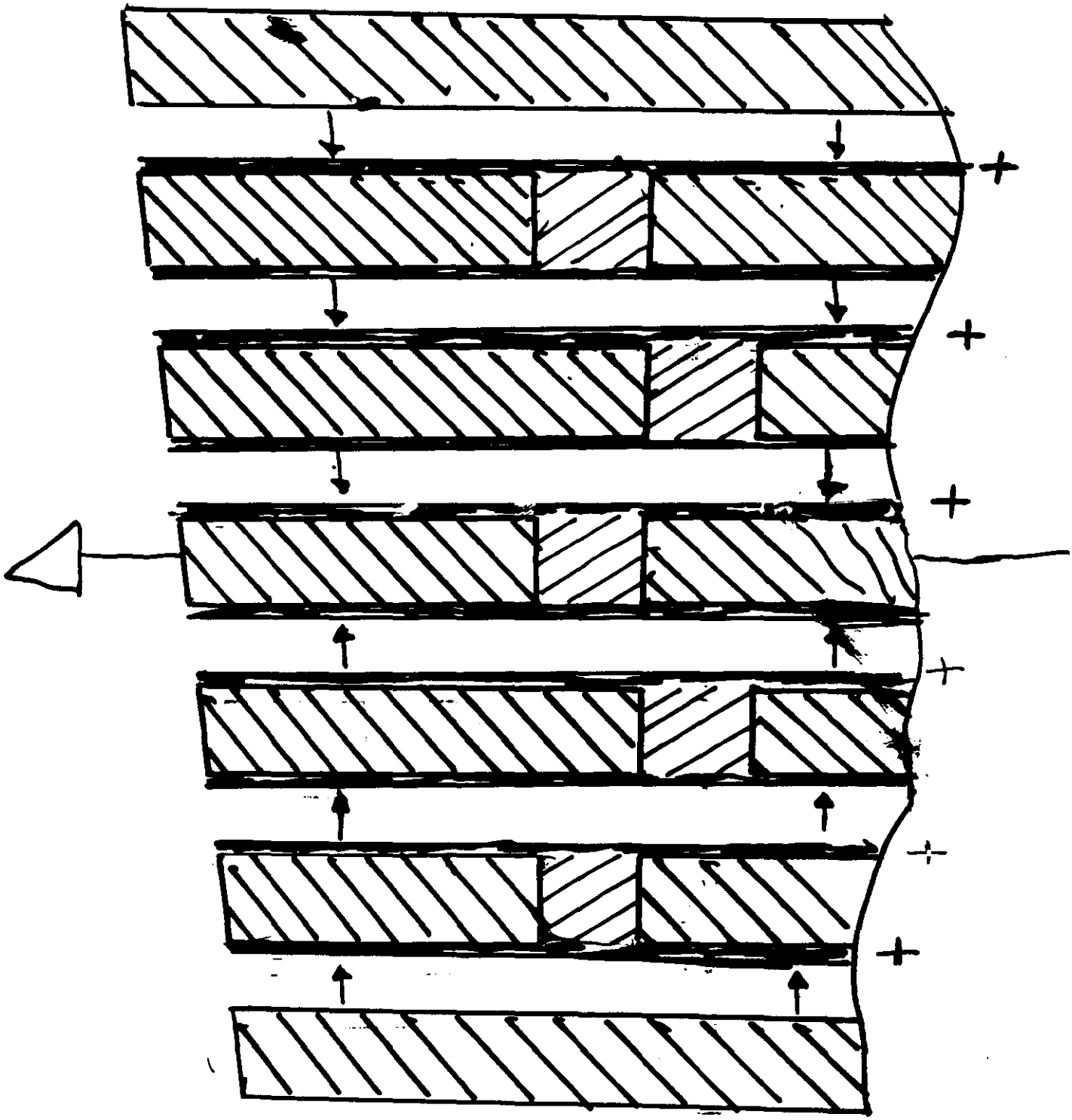

GEM [illegible] Configuration

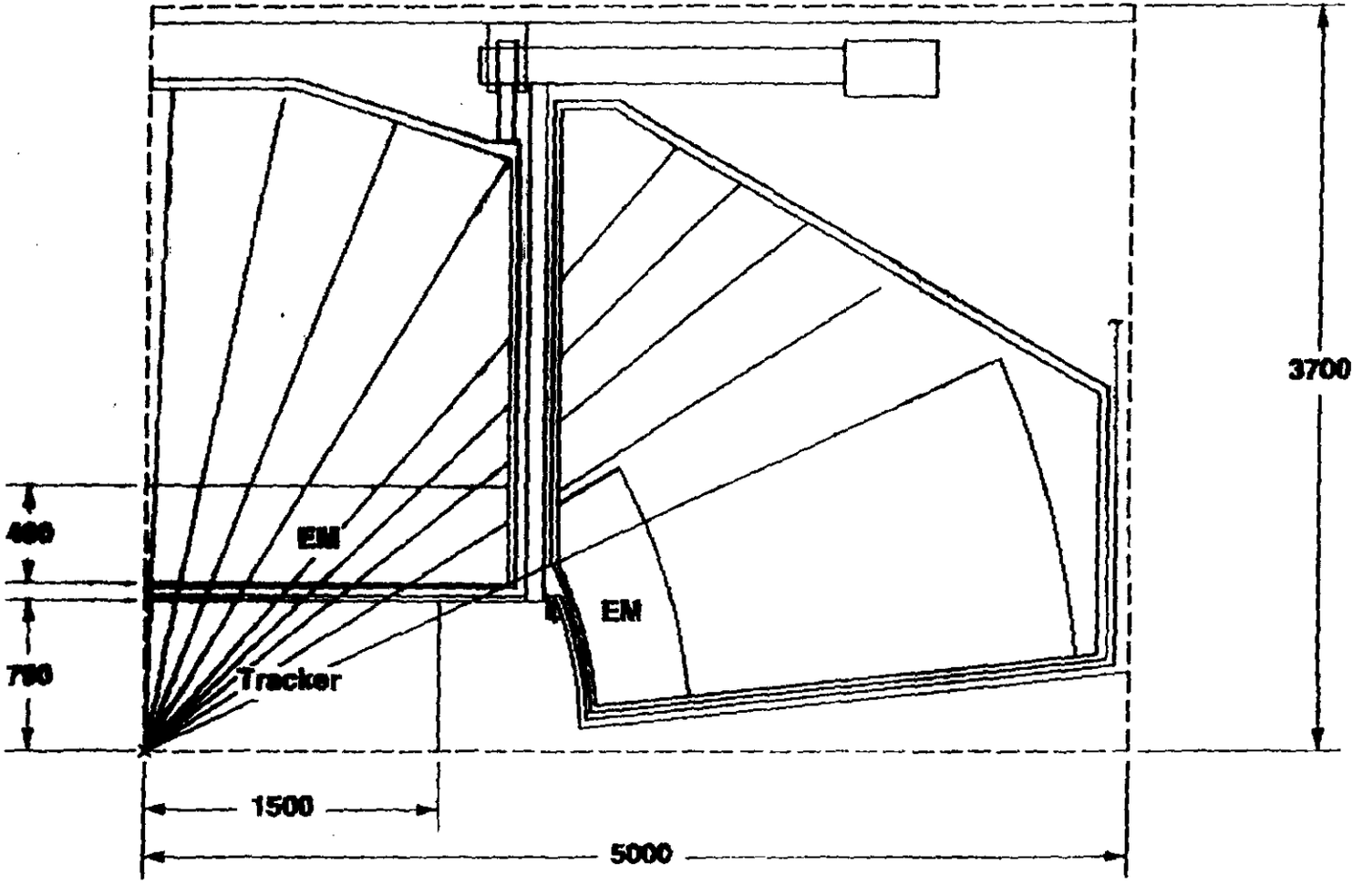

MARTIN MARIETTA

Options for Preradiator

Calorimeter alone can provide rejection

(γ/π^0) 4 $\epsilon_\gamma = 90\%$

(γ/π^0) 10 $\epsilon_\gamma = 80\%$

1) 2mm strips in argon $(3\text{-}4\ X_0)$
(with ganging preserve total number of ch

2) silicon strips insider or outside crye

3) silicon drift

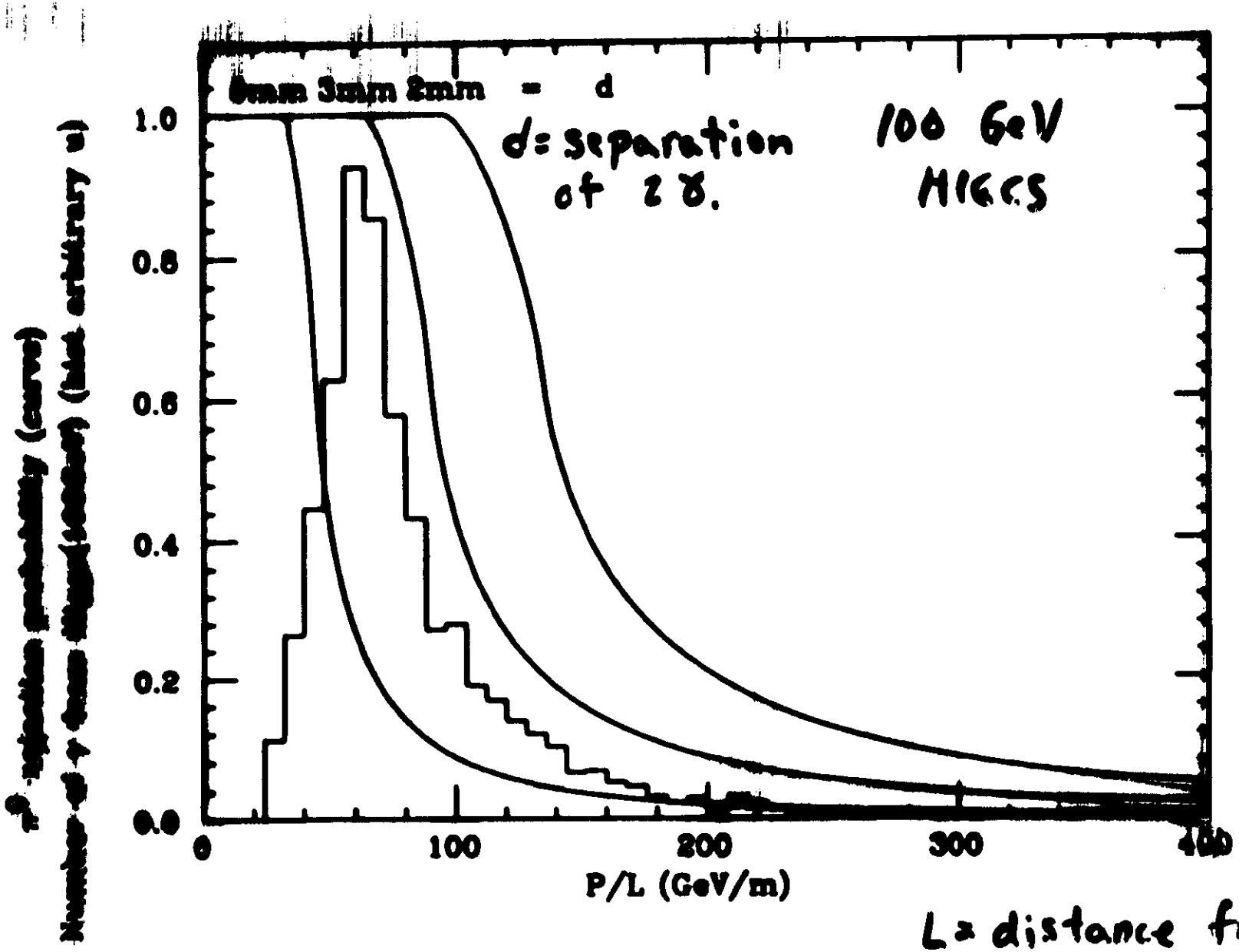

L = distance from interaction to P.R.

Figure V.2

2mm strips X + y in LAr

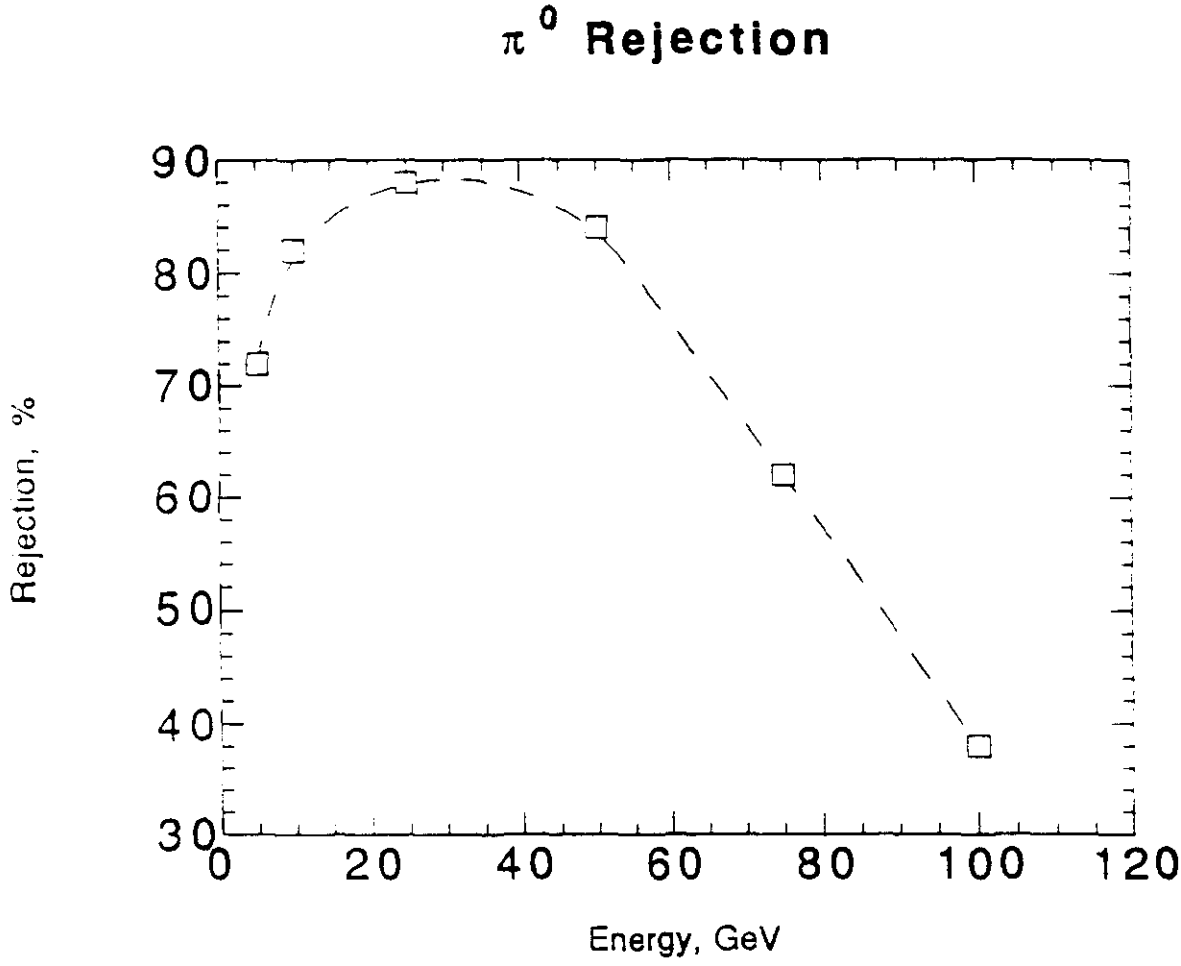

85 cm @ 90°

$\epsilon = 100\%$ for γ's

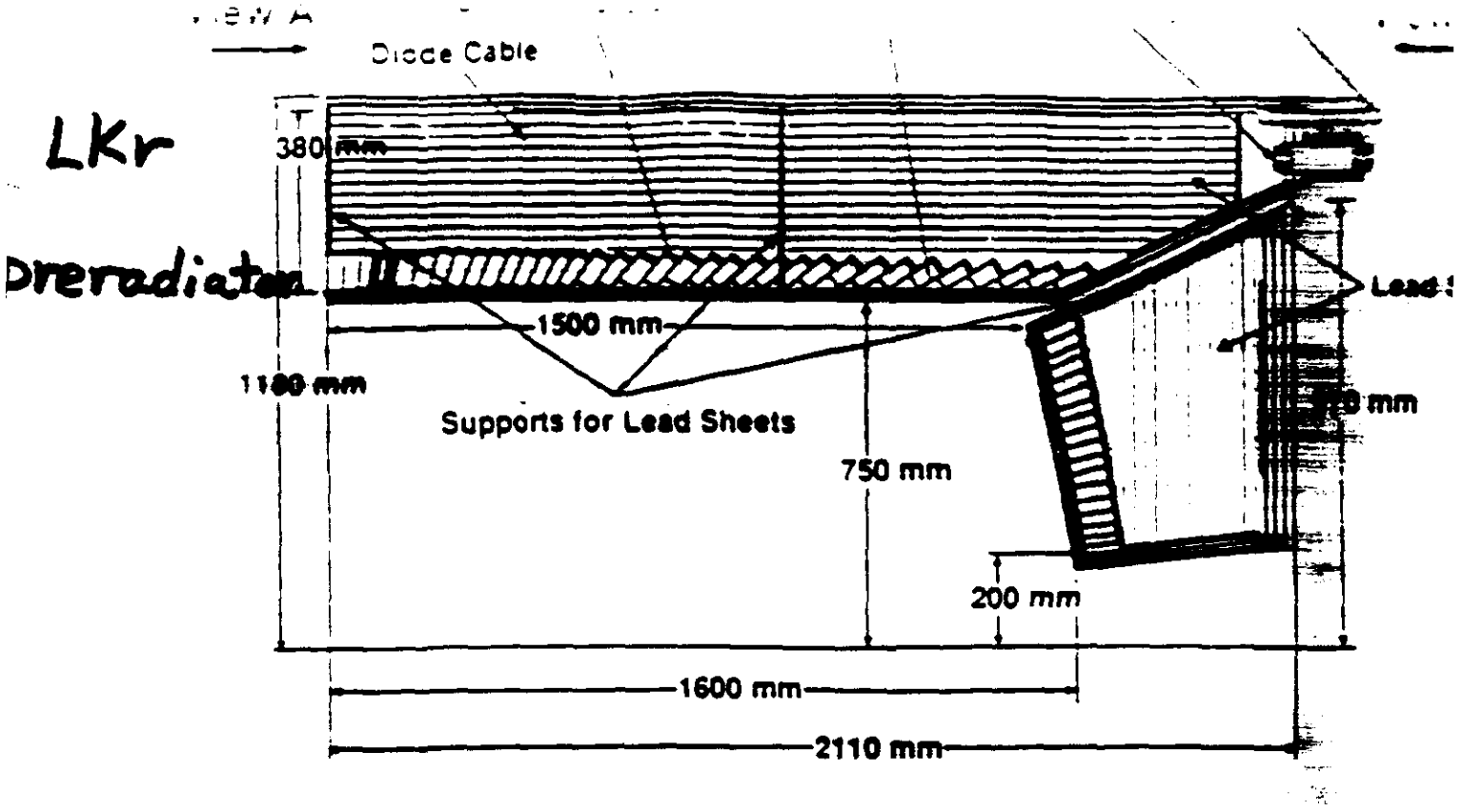

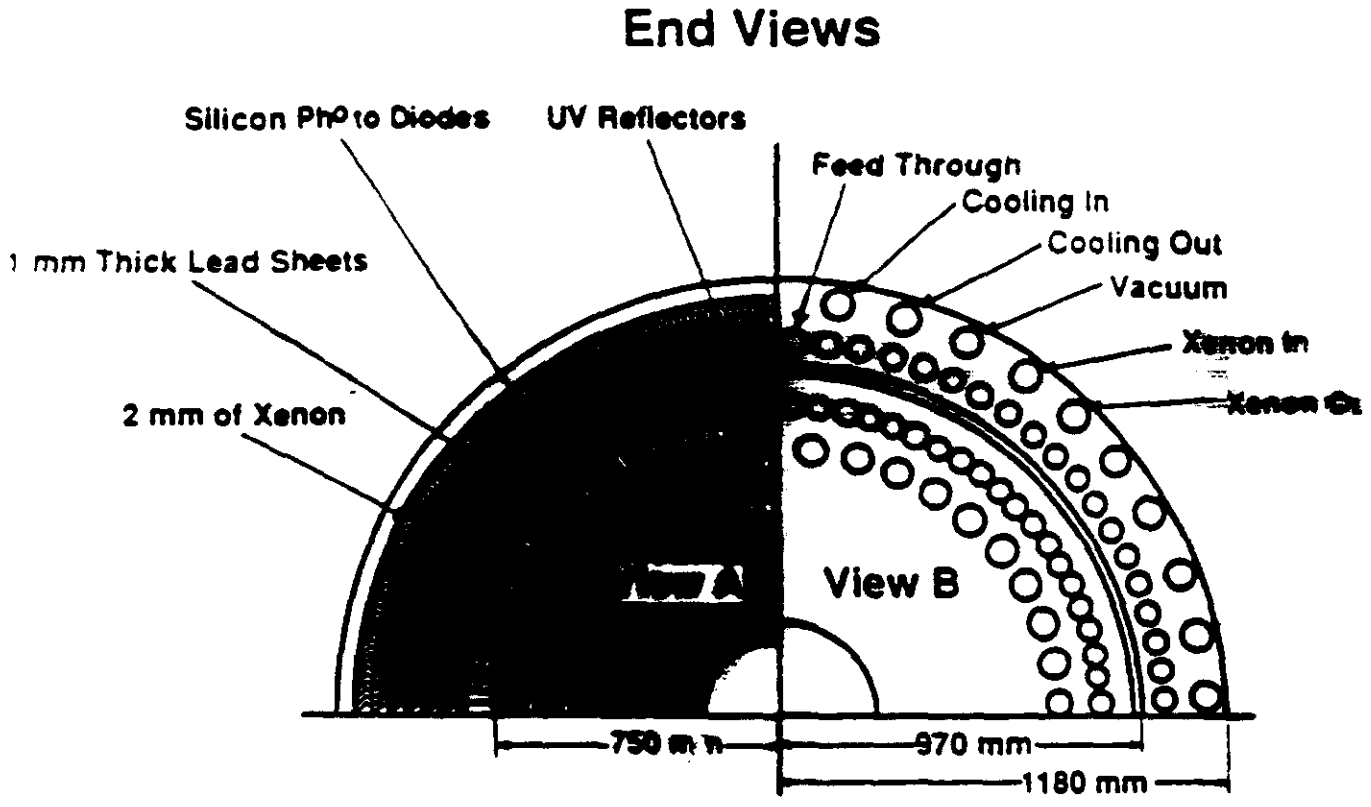

Figure 21: Side and end views of one quadrant of SandI electromagnetic detector using LKr + 5% LXe. SandI has a homogeneous section in the front, with a UV diode collecting scintillation light from the first 10 cm of the homogeneous noble liquid; followed by a drift diode to detect the positions of showers; and a sampling ionization calorimeter in the back (e.g. Accordion).

GEM CENTRAL TRACKING

Presentation to the SSC PAC

Oct 3-4, 1991

C. Baltay

– Baltay

PHYSICS GOALS OF TRACKER

MINIMAL GOALS: features that you need for the primary mission of GEM – γ, e, μ's

a) At $\mathcal{L} = 10^{33}$

i) Event vertex – separate event from pileup
ii) e/γ separation – presence of a charged track
iii) e, μ, γ isolation
iv) help with e/π separation: E – P comparison
v) electron sign selection

b) At $\mathcal{L} = 10^{34}$

Same as above, but iv) and v) may be hard

For most of the above, could do without full pattern recognition by interrogating tracker i.e. look for hits in a road extrapolated from calorimeter or muon chambers.

MORE AMBITIOUS GOALS for $\mathcal{L} = 10^{33}$

implement if we can afford it!

a) Secondary vertex finding
b) Tracking at low momentum with good $\Delta P/P$
c) Full event reconstruction

These are motivated by B and Top, etc.

Pattern recognition in tracker important for these

Electron Trigger?

DESIGN PARAMETERS FOR TRACKING

Occupancy ~ 1% (could be as high as 3%?)

1. Momentum Resolution

a) at high momenta - measurement limited

$$\frac{\Delta P}{P} \sim a \times 10^{-3}\, p(\text{GeV/c}) \qquad a = 1 \text{ to } 3$$

sign separation at 2σ to $\frac{500\ \text{GeV/c}}{a}$

b) at low momenta - multiple scatt. limited

$$\frac{\Delta P}{P} \sim b \times 1\% \qquad b = 2 \text{ to } 4$$

crossover at $P = b/a \times 10$ GeV/c

2. Vertex Resolution

$$\delta z \sim c\ \mu m \qquad c = \tfrac{1}{2} \text{ to } 2$$

4. Impact parameter resolution for 2nd vertex

$$\delta b \sim 50\ \mu \text{ at a few GeV/c}$$

5. Pattern Recognition

a) with stereo geometry (Si strips, straw
need ~ 40 layers (to within a factor of

b) with 3-D devices (pixels, pads, etc)
need ~ 15 layers ?

6. Coverage $\eta \lesssim 1 \sim 2.5$

GEM CENTRAL TRACKING

1. Baseline Design presented in EoI
   - Silicon Microstrips $12.75 \leq r \leq 35$ cm
   - Outer Tracker $45 \leq r \leq 75$ cm
     - 48 Layers of Straw Tubes
     - 12 Layers of Scint Fibers

2. Very similar to L* Tracker Design
   - Extensive Monte Carlo Simulation
   - Detailed Engineering Design
   - Careful Cost Estimate, "Thermiot"-ize
     ~ 40 M$

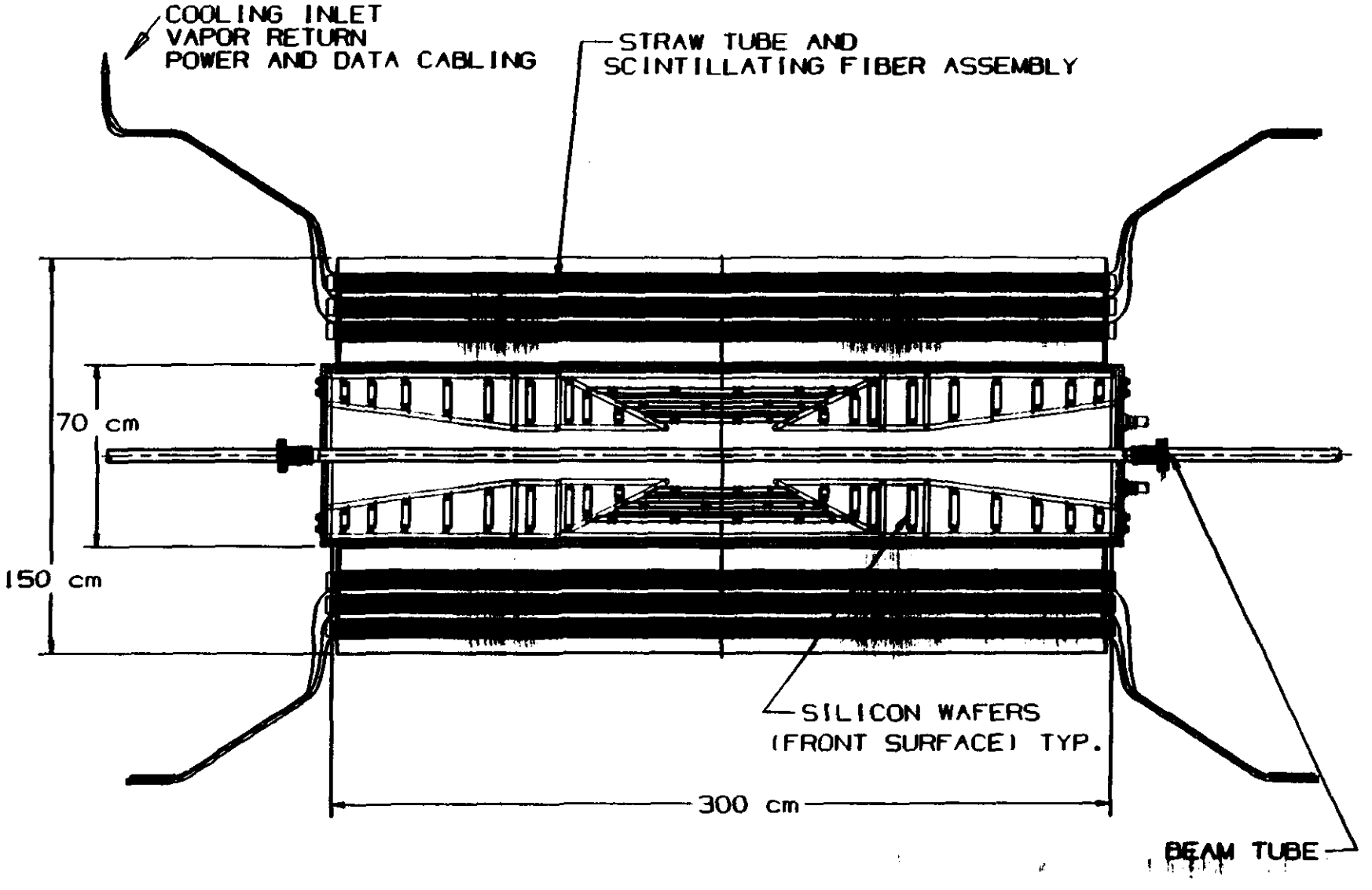
COOLING INLET
VAPOR RETURN
POWER AND DATA CABLING
STRAW TUBE AND
SCINTILLATING FIBER ASSEMBLY
70 cm
150 cm
SILICON WAFERS
(FRONT SURFACE) TYP.
300 cm
BEAM TUBE

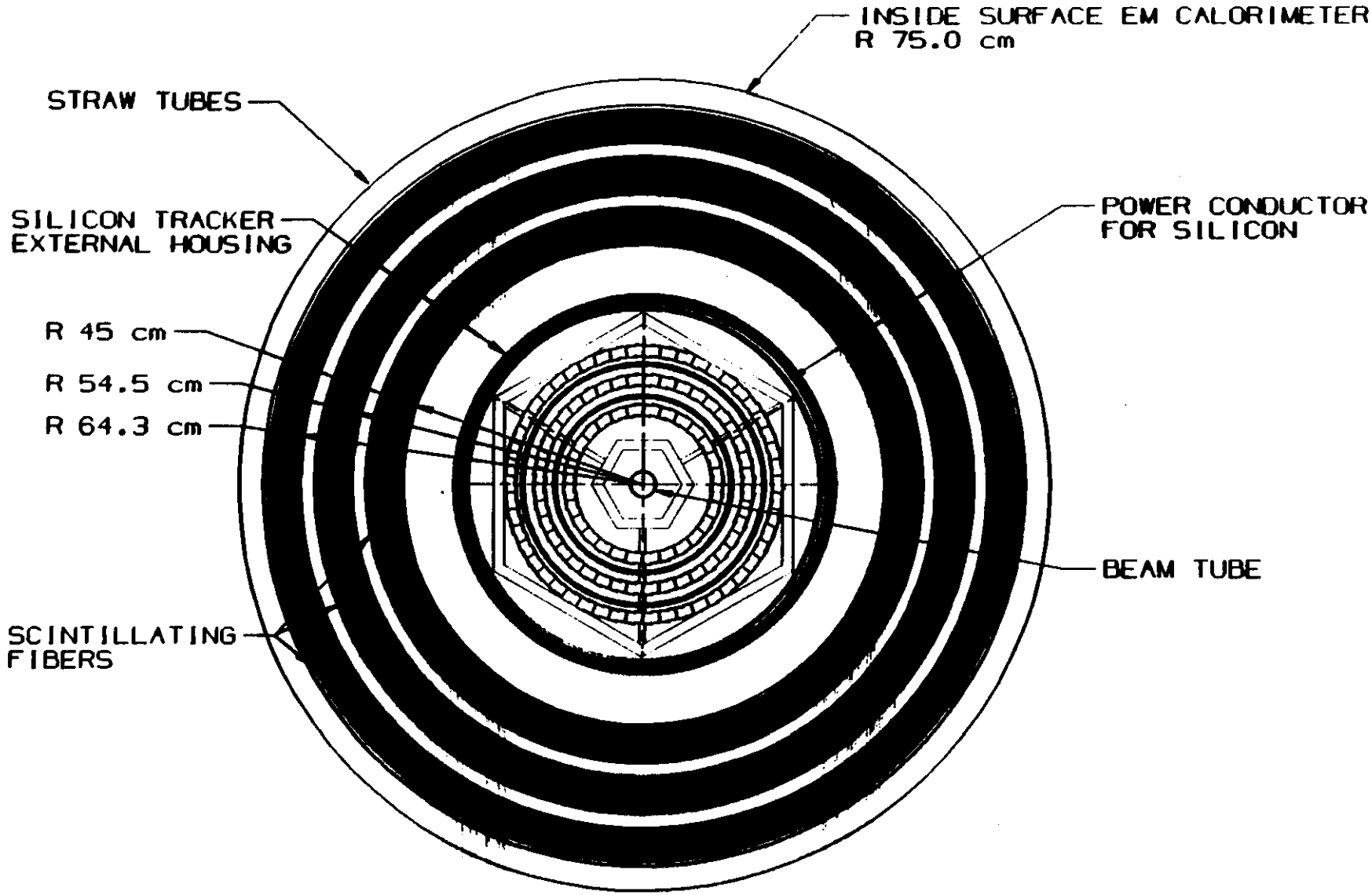
INSIDE SURFACE EM CALORIMETER
R 75.0 cm
STRAW TUBES
SILICON TRACKER
EXTERNAL HOUSING
POWER CONDUCTOR
FOR SILICON
R 45 cm
R 54.5 cm
R 64.3 cm
BEAM TUBE
SCINTILLATING
FIBERS

Reasons for Considering Alternate Design

1. Occupancy of straw tubes in Baseline Design is <u>calculated</u> to be

   $\sim 10\%$ at $\mathcal{L} = 10^{33}$

   Real Life will be probably worse

   Not very useful at $\mathcal{L} = 10^{34}$

2. Stereo Geometry of straws and fibers of Baseline Design. Pattern recognition and track reconstruction in a high multiplicity environment would be easier with a "3-D like" geometry

3. Three different technologies in baseline design. Two technologies would be better (One would be best but we have no good ideas how to do that

---

Consider only alternatives at a cost less than the Baseline Design Cost of 40M$

L. Dorway

A Possible Tracker Configuration

- Silicon Microstrips $\sim 10 \le r \le 25$ cm ~ 6 layers
- Interp. Pad Chambers $25 \le r \le 75$ cm ~ 12 layers
- Parameters:
  - Occupancy $\sim 1\%$ at 10^{33} in pads
    $\sim 1\%$ to $\sim 3\%$ at 10^{34} in 3 outer layers
  - Resolution $\sim 15\,\mu$ in silicon
    $\sim 50\,\mu$ in pad chambers
  - Total thickness 10 to 15 % of a rad length
  - $\frac{\Delta P}{P} \sim 2 \times 10^{-3}\, P(\mathrm{GeV/c})$
  - $\frac{\Delta P}{P} \sim 3$ to 4% at low momenta

- How many layers of pad chambers do we need for pattern recognition?
  How many layers can we afford?

GEM Central Tracking

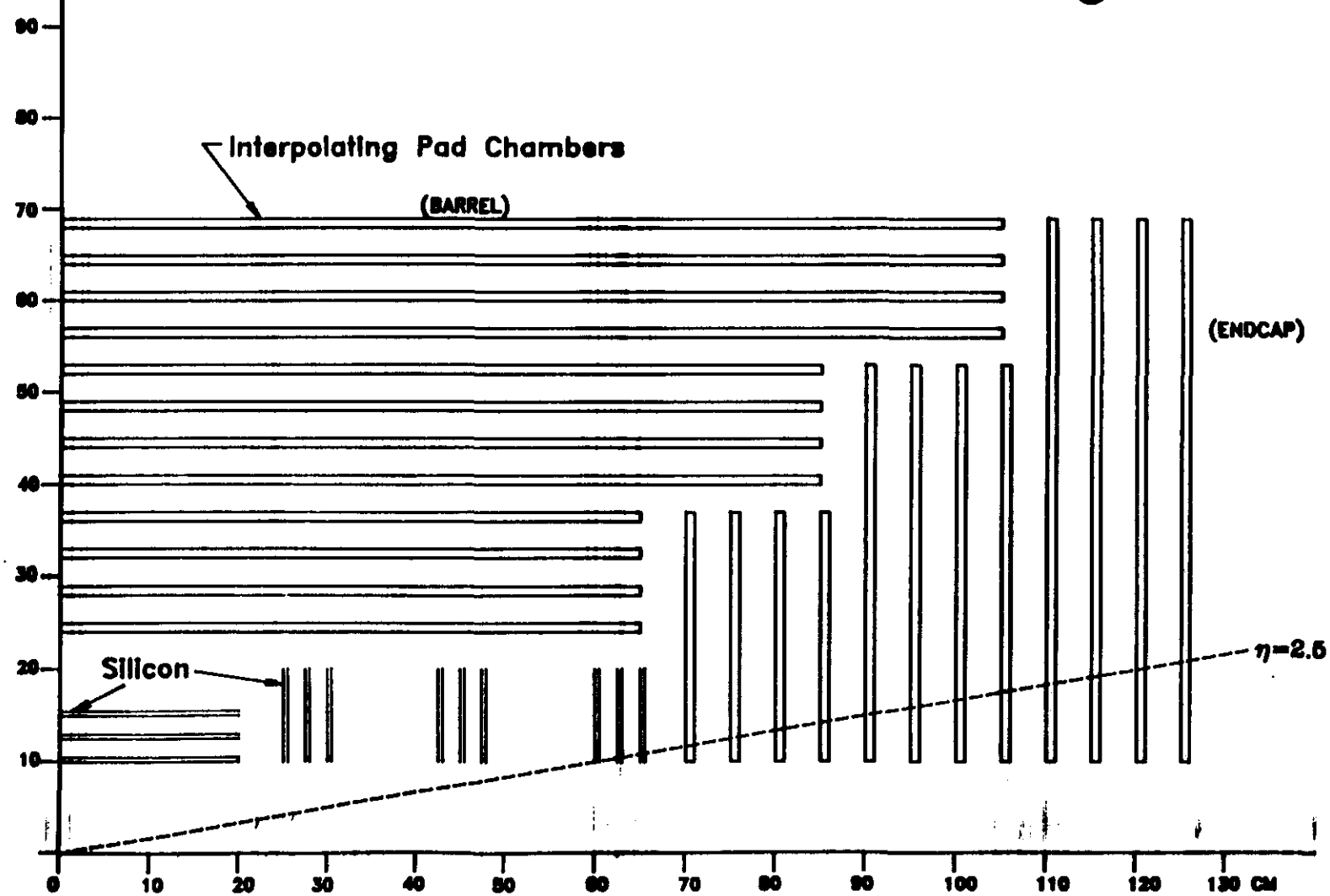

Silicon Microstrip Inner Detector

- 6 layers of double sided silicon detectors
- Strips 50 μ wide × 10 cm long

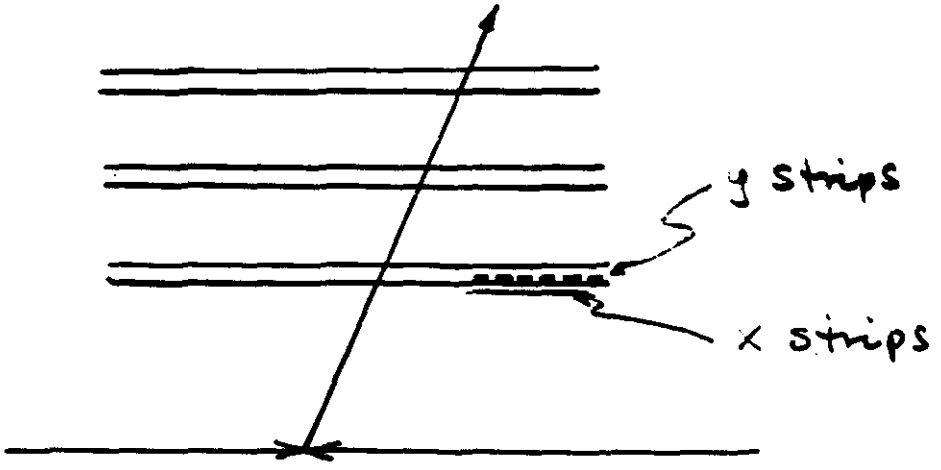

- Occupancy at innermost layer near 90°

  $\sim 2 \times 10^{-3}$

- Total area $\sim 6\ m^2$
- $\sim 10^6$ strips

  digital output, highly multiplexed

  ~2000 Readout channels

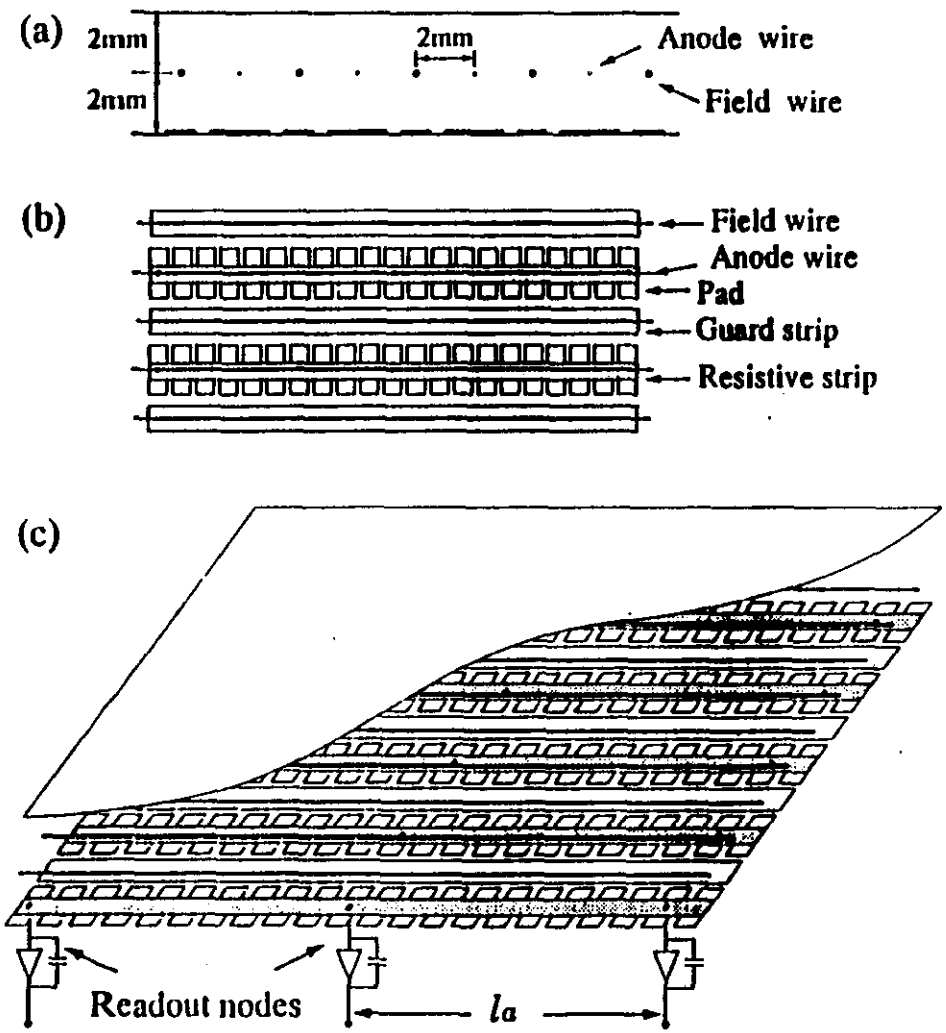

Figure 3.4.1: Schematic of a Pad Chamber. (a) Cell geometry viewed end-on to the anode/field wires. (b) Looking down onto the cathode plane. (c) "3-D" view of the Pad Chamber.

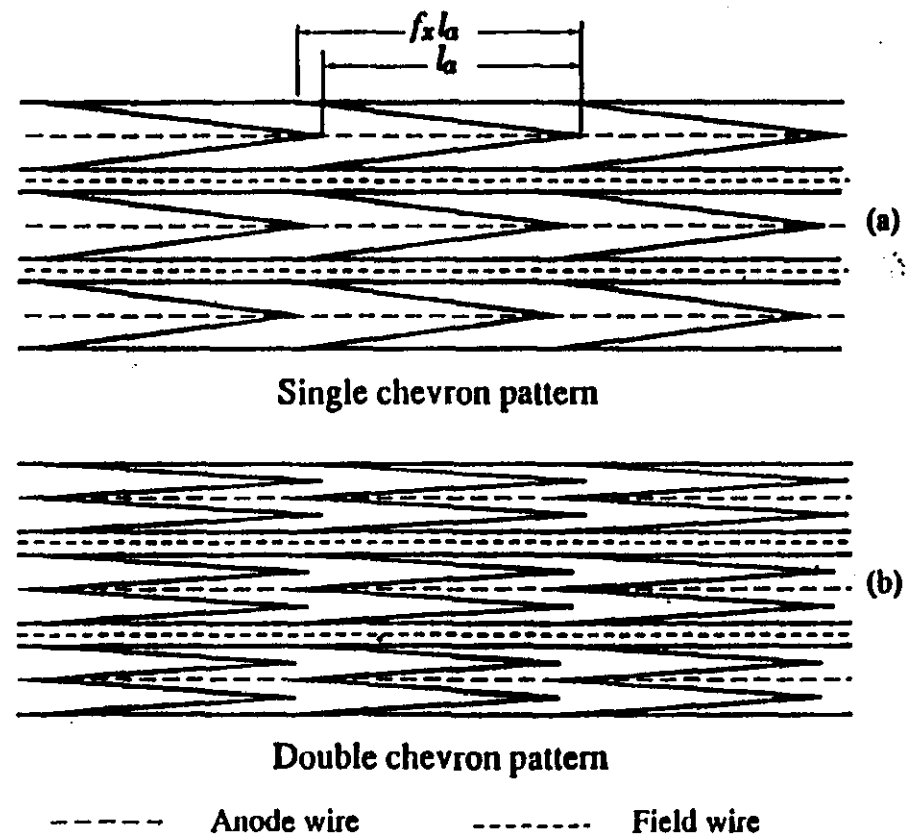

Figure 3.4.2: Two types of chevron pad cathode

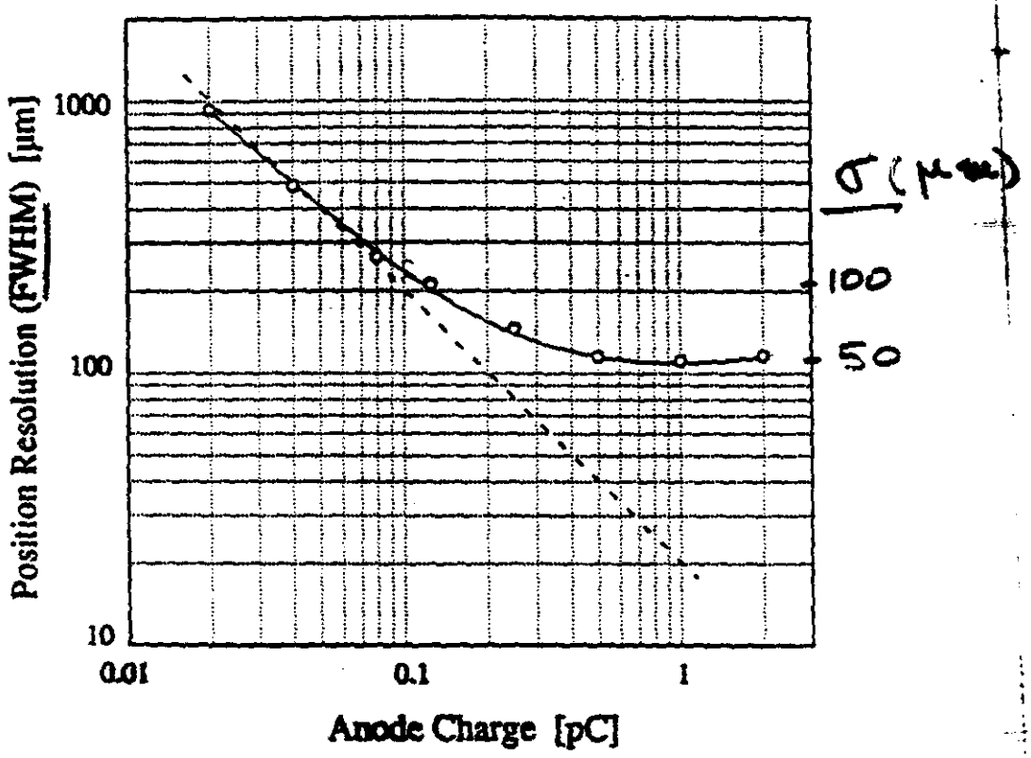

Figure 6: Position resolution vs anode charge, using centroid finding electronics

Pad Chamber Parameters

a) Barrel Chambers

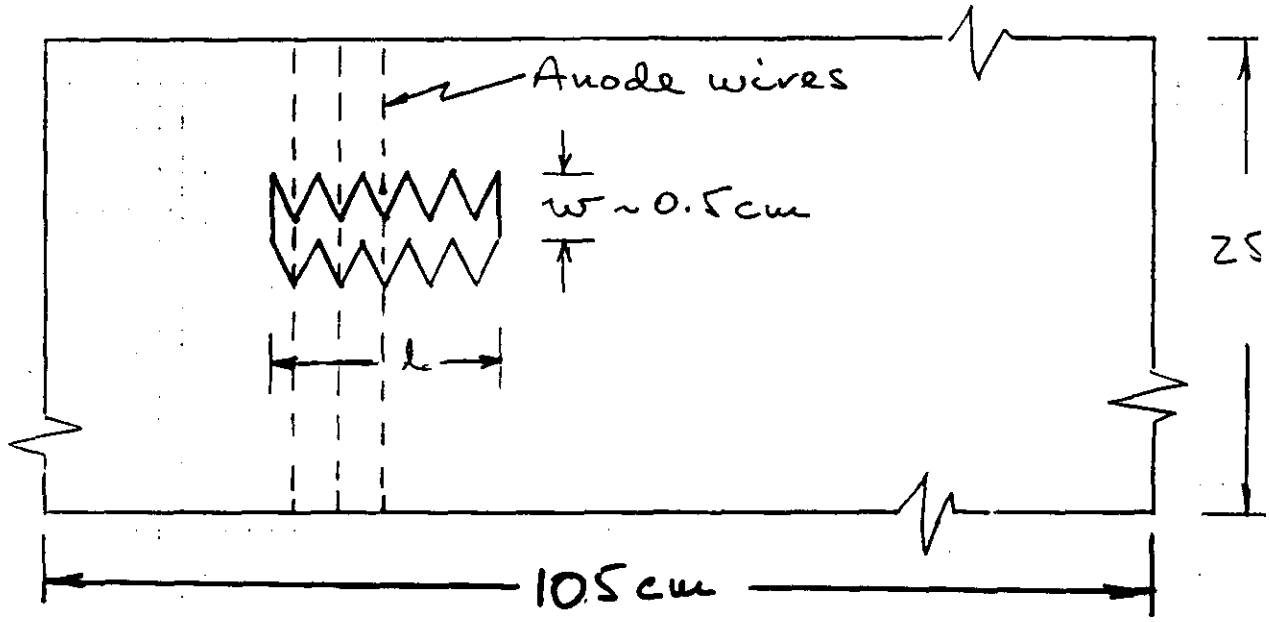

Resolution $\sigma \sim 1\%$ of $W \sim 50\mu$

Length of Pads $l \sim 3$ cm to 30 cm

Anode wire spacing ~ 3 mm

b) End Cap Chambers

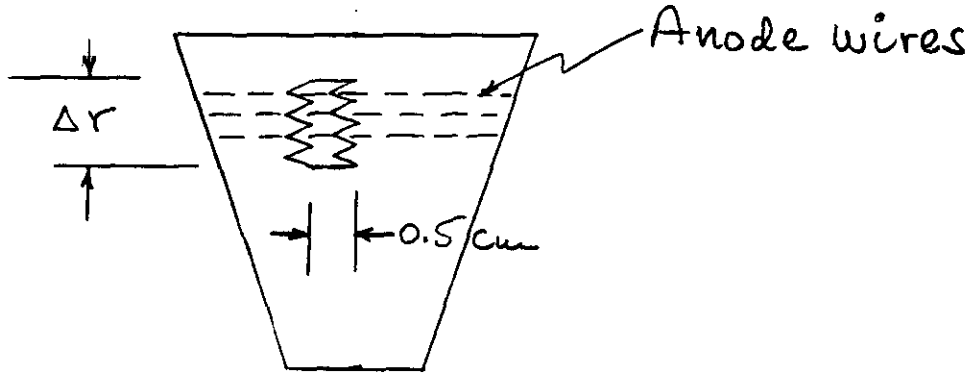

Keep 0.5 cm width for 50 μ resolution

Length of pads $\Delta r \sim 1$ to 8 cm

Occupancy at 10^{33}

From pileup of minimum bias events

$$\frac{dn}{d\eta\, d\phi} \sim 1 \text{ charged track per event}$$

If we assume pileup of 2 crossings at 10^{33}

$$dn/d\eta\, d\phi \sim 3$$

If we want occupancy of 1%, we need 300 cells per unit of $d\eta\, d\phi$, or

Cell size $\underline{\Delta\eta\, \Delta\phi \sim 0.003}$

For a central tracker of ± 2.5 units of η,

$$\Delta\eta\, \Delta\phi = (\pm 2.5)(2\pi) = 31.4 \text{ sq. units}$$

$\therefore$ we need $\frac{31.4}{0.003} \sim 10^4$ channels/layer

Near $90°$

$$\Delta\eta\, \Delta\phi \sim \Delta\theta\, \Delta\phi = 0.003 = 55\,\text{mr} \times 55\,\text{mr} = 3° \times 3°$$

Cell size for $\leq 1\%$ occupancy at various r

Radius r cm	Cell size at 10^{33}	Cell size at 10^{34}
20	$1\frac{1}{2}$ cm^2	
50	8 cm^2	
70	15 cm^2	1.5 cm^2

Numbers of Pads and Readout Channels

- 9 Layers with 10^4 pads/layer — 90,000
  1% occupancy at 10^{33}
- 3 Layers with 3×10^4 pads/layer — 90,000
  3% occupancy at 10^{34}
- Total no. of pads — 180,000
- Analog readout, highly multiplexed
  ~ 2000 readout channels

PROBLEMS WITH ALTERNATIVE DESIGN

1. Can we keep the total material in the chambers, the support structure, and the front end electronics below 10 to 15% of a radiation length?

2. Electronics cost of large no. of channels

3. How do we incorporate at least a few layers of the tracker into a level 2 electron trigger? How important is this for the physics?

4. How many layers do we need for pattern recognition with pads

5. How many layers of silicon microstrips do we need

6. How far out in radius and z should Silicon extend to?

etc

etc

R & D Effort Anticipated

1. Silicon Microstrips
   - Electronics - Radiation hardness, Pipeline details, Trigger design?
   - Mechanical Support Structure
   - Wafer design, fabrication, etc, etc
2. Interpolating Pad Chambers
   - Electronics - Readout, Trigger design?
   - Mechanical Design - chambers, supports
3. Scintillating Fibers
   - Readout - VLPC's, Multianode PMT's
   - Mechanical Support
   - Fiber Ribbon Fabrication
4. Straw Tubes
   - Readout Design
   - High Rate Test
   - End plate support structure design

+ Monte Carlo Simulations to evaluate and optimize design

GEM Trigger/DAQ/Computing

W. Sippach
Sept 25, 1991

TRIGGER AND DATA ACQUISITION SYSTEM

OVERVIEW

The system will have 3 levels of trigger processing. Level I will reduce the trigger rate to 100 KHZ and imposes about a 3 microsecond delay on the data acquisition systems. Level II will be a distributed, pipelined digital processor system, and Level III will be a processor farm.

Level I will use a reduced set of detector signals, encoded to a minimum number of bits, and is synchronous and pipelined with respect to the bunch crossings. A trigger from any detector subsystem will cause data from the entire detector to be transferred from data pipelines to event buffers. With the exception of the inner tracking, all data will be moved out of the detector to Level II. These event buffers must be at least 4 events deep in order to derandomize the data so that it can be digitized and multiplexed into the cable system during the 10 microsecond average Level I time. If an optical cable system can be developed, Level II can reside in the counting room.

Raw data from Level I will go to the Level II processor system and also to buffers for selective transfer of data to Level III.

CALORIMETER SYSTEM

Level I will use 5X5 (or 3X3) EMC and HAC analog sums with a set of energy thresholds with time discrimination for bunch association. These threshold bits are mapped into primitives for defining projective and global triggers.

Analog memories will sample charge for each bunch crossing to provide the delay and buffering functions. Seventeen bits of dynamic range will be achieved by splitting the input into a high gain and low gain channel. Twelve bit ADC's will encode up to 5 samples per signal for either the high or low gain channels. Digitized data will be multiplexed and sent to Level II with about a 10/1 reduction in cable count. In addition to forming physics triggers, Level II provides zero suppression and buffering for raw data for Level III.

MUON SYSTEM

Strip, pad, and drift chamber channels will use discriminators for Level I triggering. Discriminator hits will be projected on to look-up tables to define high PT candidates.

The low occupancy/channel should allow the pipeline delay principal to be replaced by a simpler discriminator driven sample and hold circuit. Zero suppression will take place on each chamber segment by scanning the data hits and assigning an address to the multiplexed data. Digitized data will be sent bit serially to the external Level II system.

CENTRAL TRACKING SYSTEM

We assume an inner silicon microstrip chamber that can only be read out after Level II, and an outer pad chamber with Level II readout. Both parts require analog memory for pipelining, with one level of buffering for the pads, and two levels for the microstrips. Local zero suppression will be required to reduce the output cable bulk.

TECHNOLOGY REQUIREMENTS

The calorimeter and tracking systems depend critically on the development of analog memory chips. We will depend heavily on the front end electronics development for SDC, work done at CERN at LHC, and work in progress within GEM.

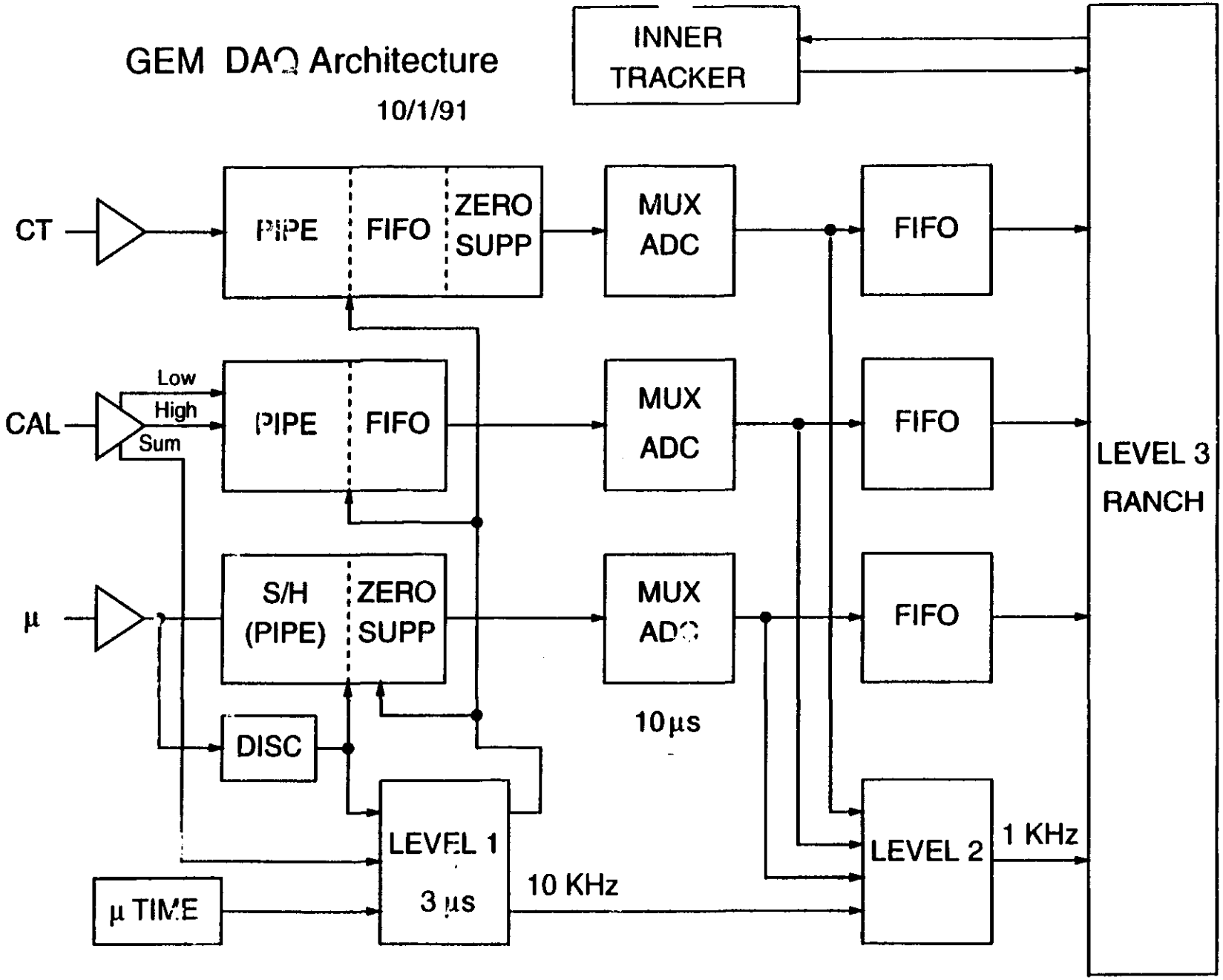
GEM DAQ Architecture
10/1/91
INNER TRACKER
CT
PIPE
FIFO
ZERO SUPP
MUX ADC
FIFO
CAL
Low
High
Sum
PIPE
FIFO
MUX ADC
FIFO
LEVEL 3 RANCH
μ
S/H (PIPE)
ZERO SUPP
MUX ADC
FIFO
10 μs
DISC
LEVEL 1
3 μs
10 KHz
LEVEL 2
1 KHz
μ TIME

GEM Trigger/DAQ Design Goals			
Level	Rate Out	Time/Event	Comments
1	10^4 Hz	$3\,\mu$s	Sync., Tags BX
2	10^3 Hz	$10\,\mu$s	Async., Monotonic
3	10^1 Hz	$100\,\mu$s	CPU Ranch

Calorimeter Readout

- Physics Goals (e.g. $H \rightarrow \gamma\gamma$) require
  - $\sigma_E/E \leq .1\%$
  - Full granularity at Level 2
  - High System Throughput

- Electrical Specifications
  - 16 ns sample rate.
  - Dynamic Range $\geq 2^{16}$
  - Resolution ≥ 8 bits
  - Total Conversion time $\leq 10\ \mu s$
    (for $\sim 2 - 5$ samples)

- Technology
  - Switched Capacitor Array (SCA) Baseline
  - Fully digital system also being studied

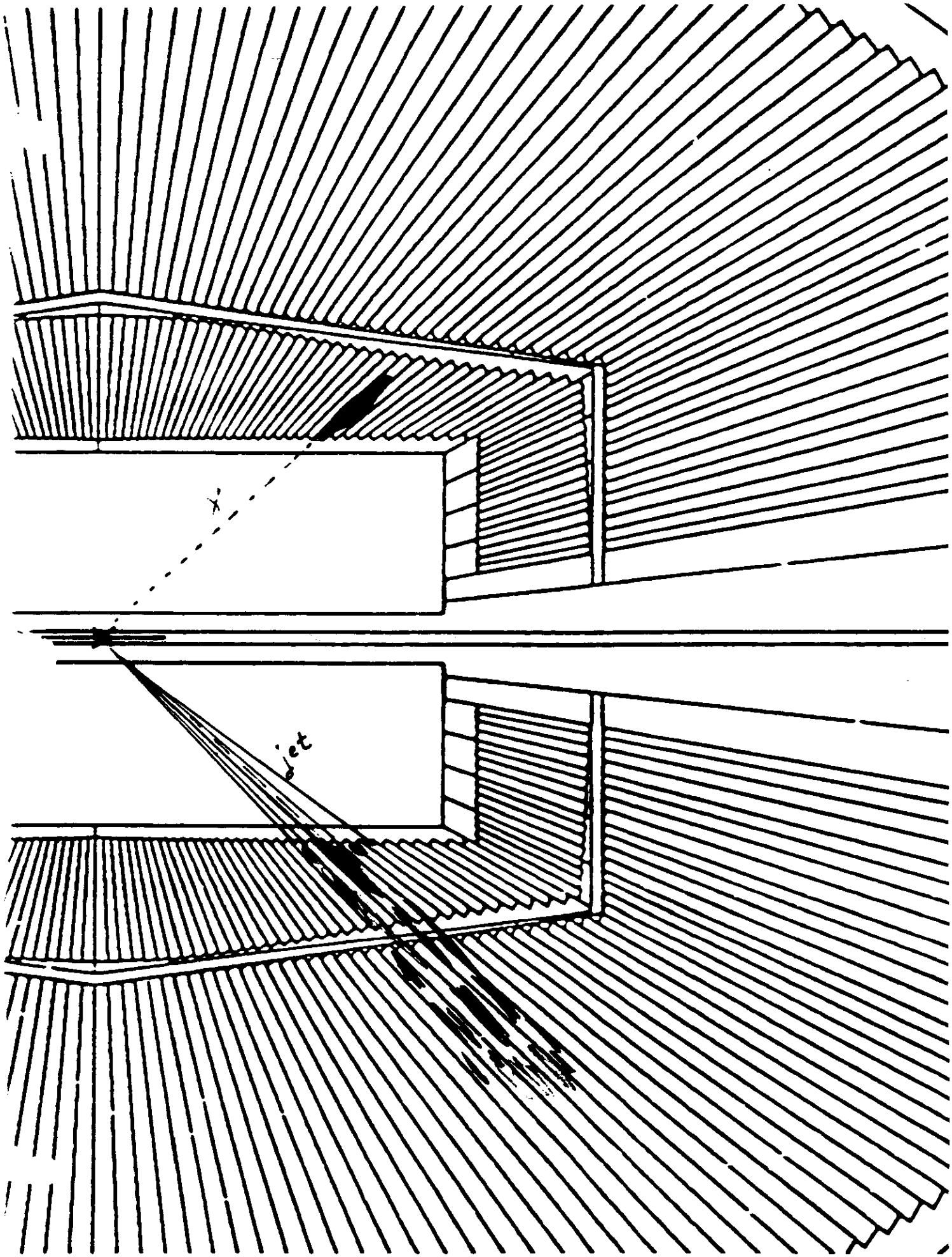
jet

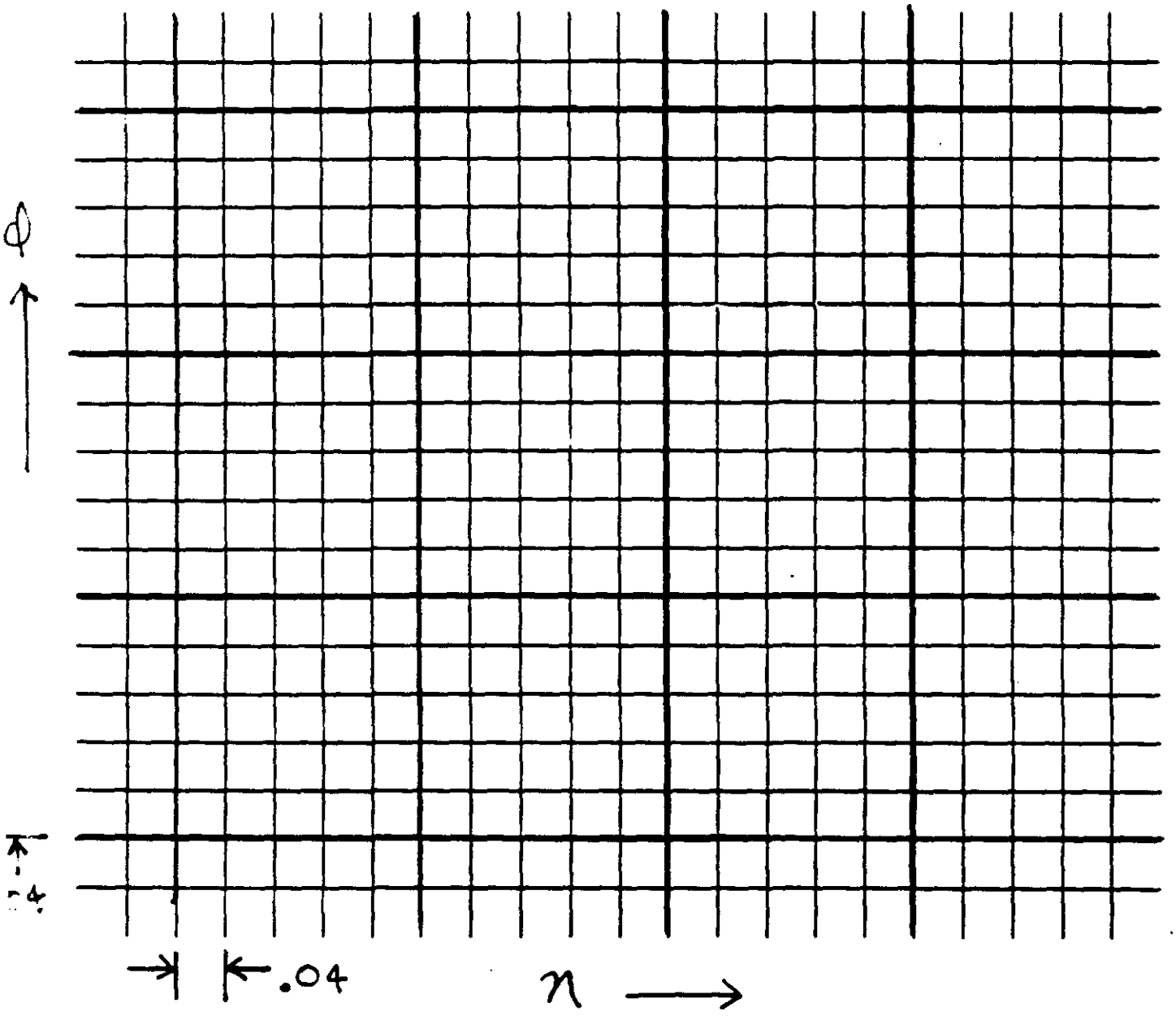

Trigger Cells $5 \times 5 \Rightarrow \Delta\eta \times \Delta\phi = .2 \times .2$

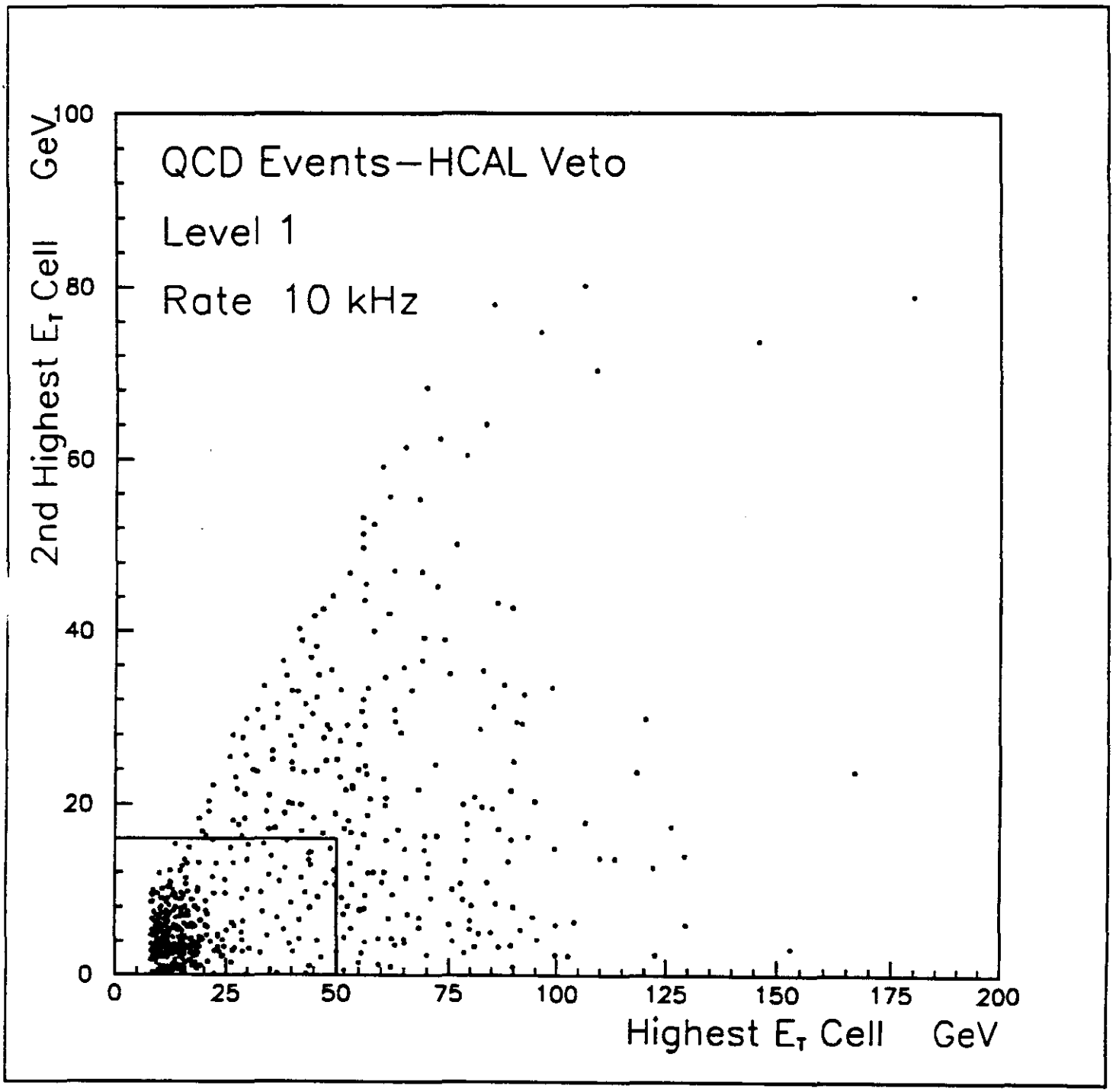
QCD Events—HCAL Veto
Level 1
Rate 10 kHz
2nd Highest E_T Cell GeV
Highest E_T Cell GeV
0
20
40
60
80
100
0
25
50
75
100
125
150
175
200

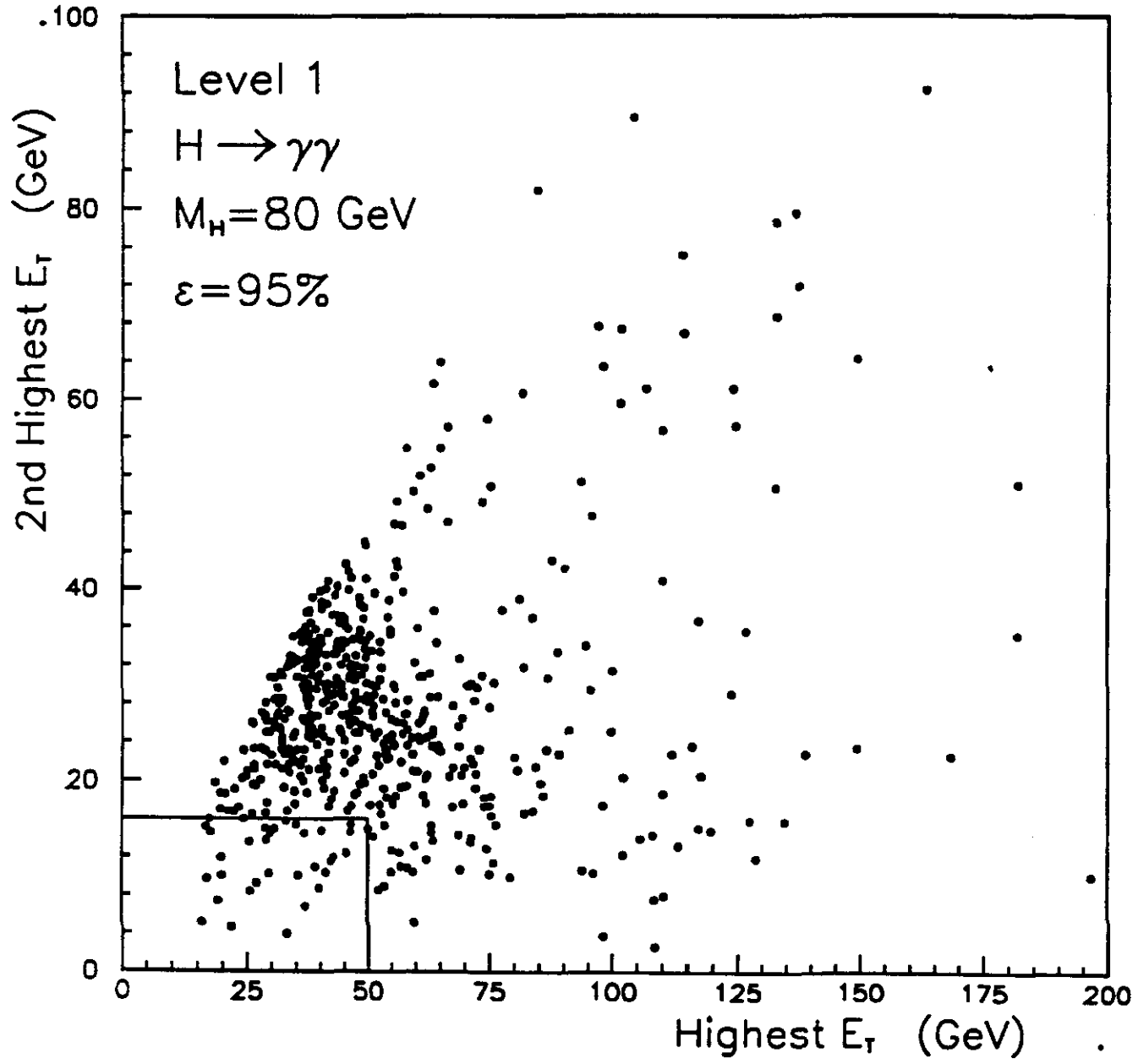
Level 1
H → γγ
M_H=80 GeV
ε=95%
2nd Highest E_T (GeV)
Highest E_T (GeV)
0
20
40
60
80
100
0
25
50
75
100
125
150
175
200

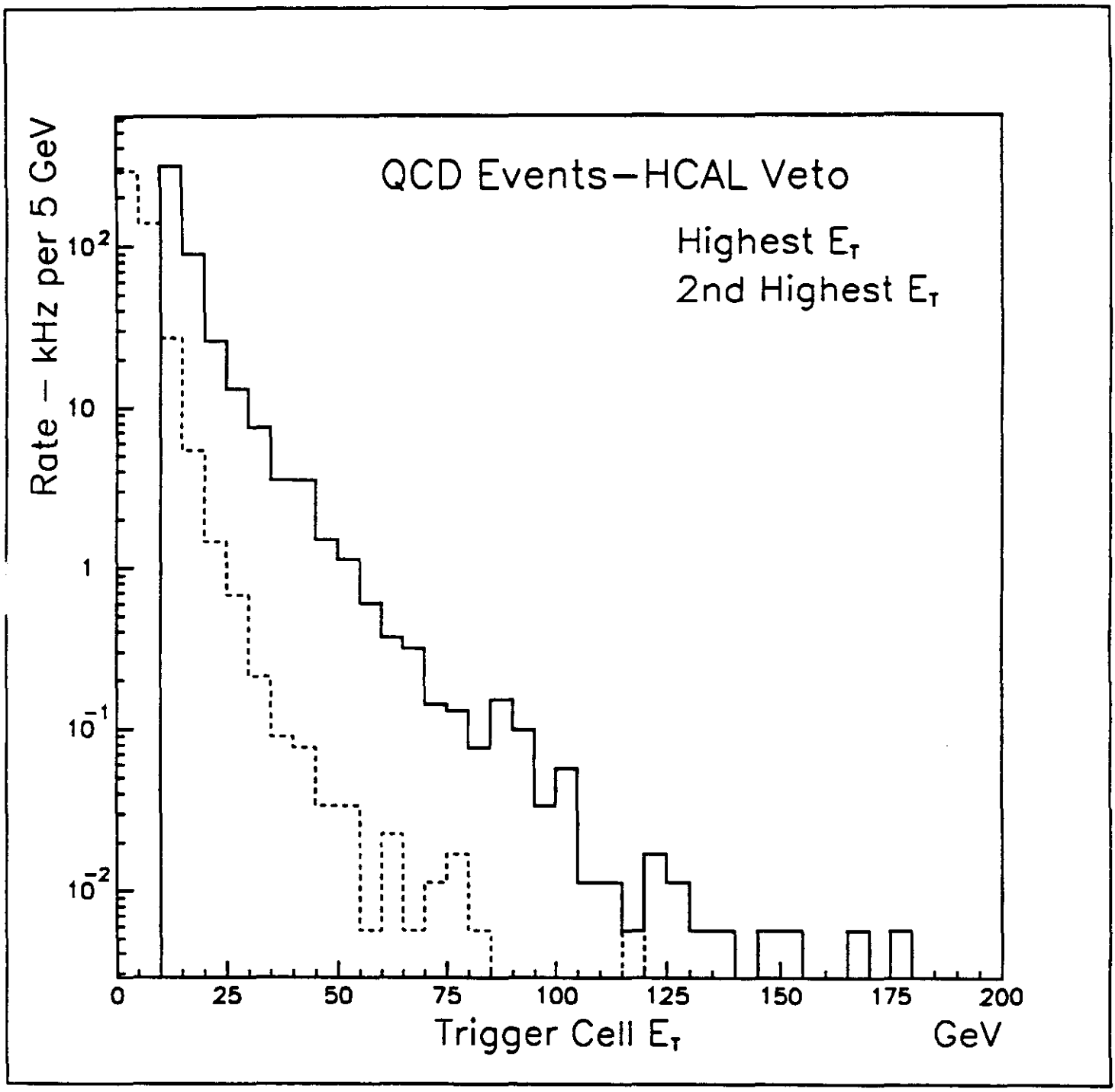
QCD Events—HCAL Veto
Highest E_T
2nd Highest E_T
Rate – kHz per 5 GeV
10^2
10
1
10^{-1}
10^{-2}
0
25
50
75
100
125
150
175
200
Trigger Cell E_T
GeV

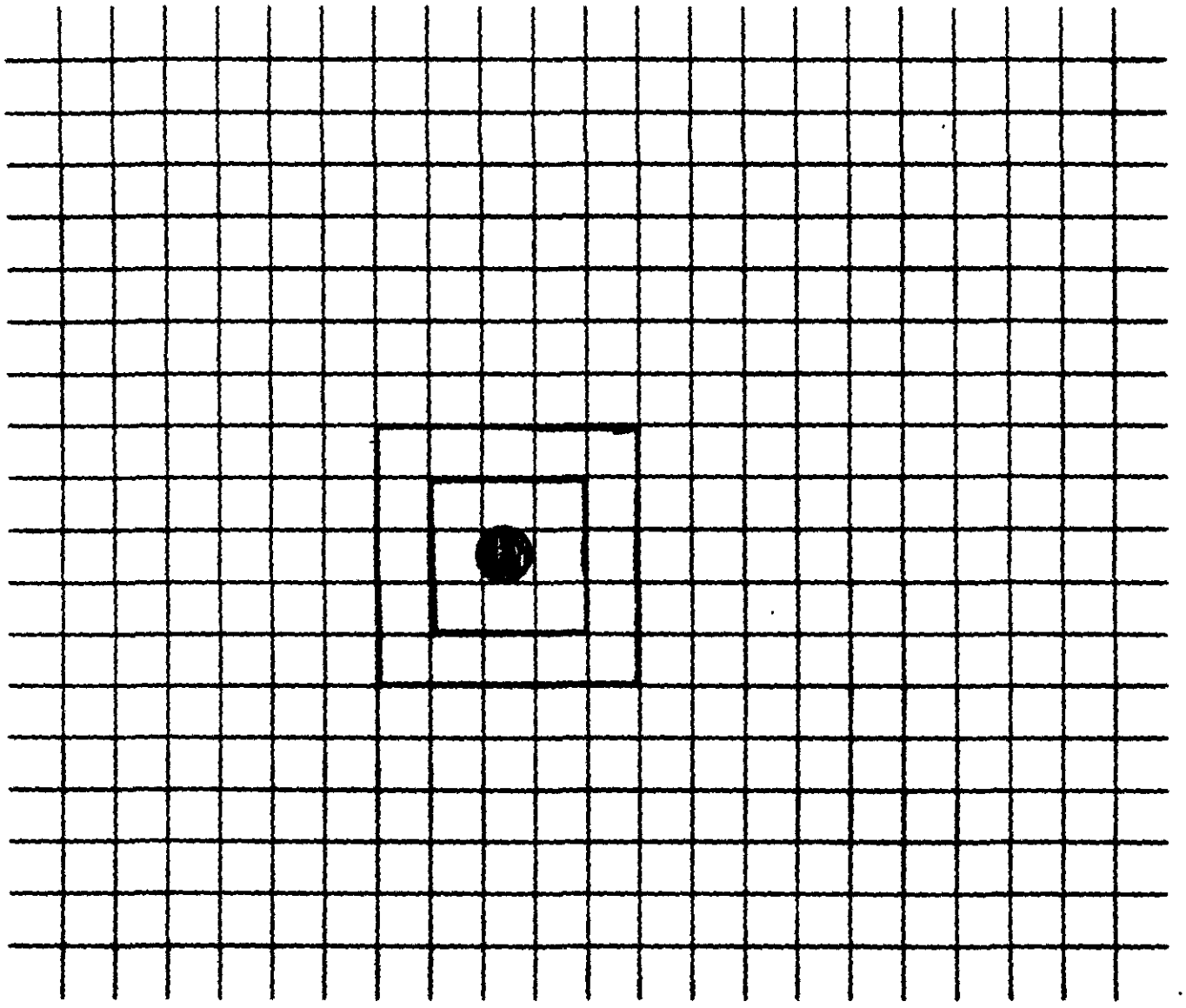

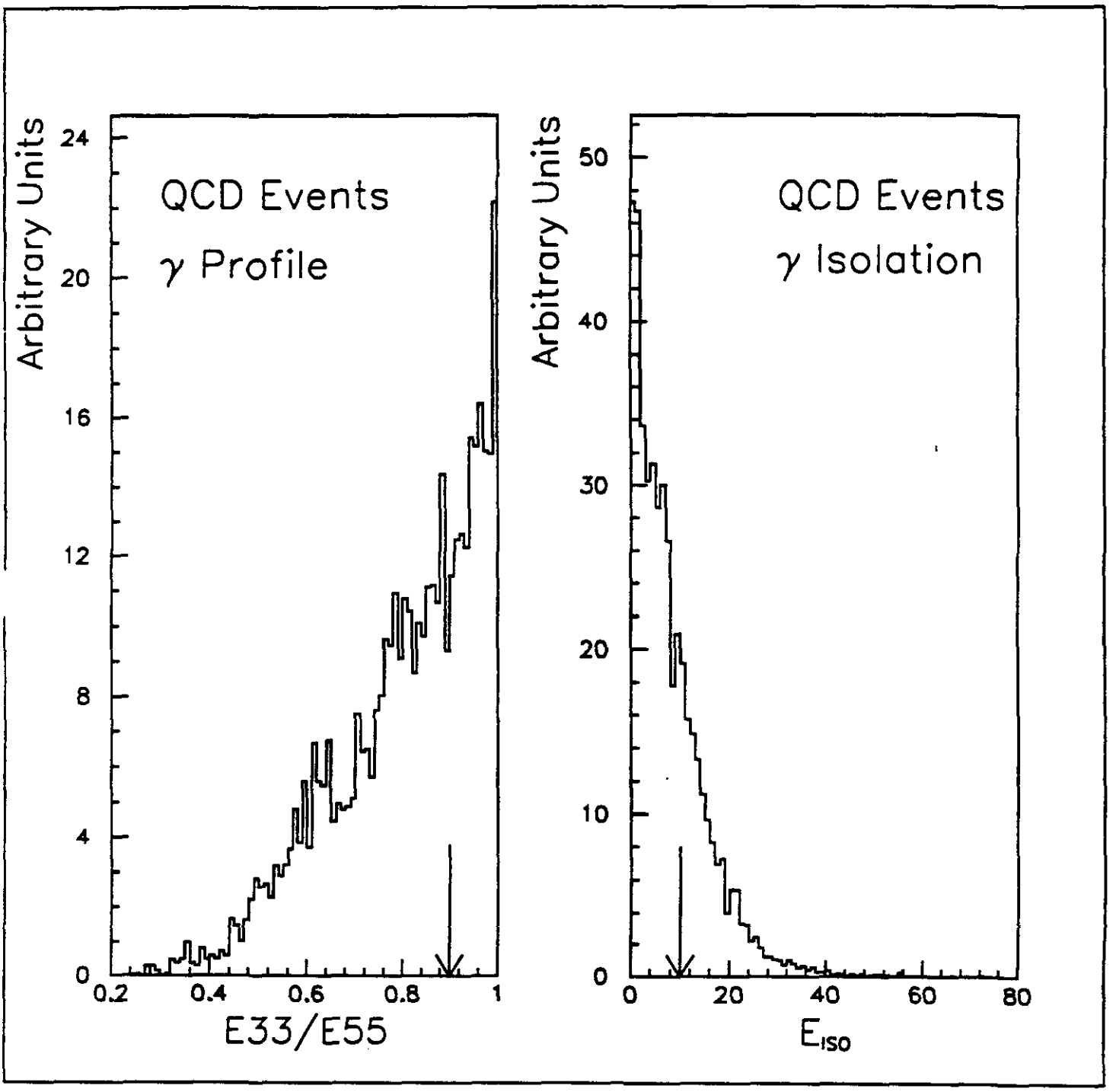
QCD Events
γ Profile
Arbitrary Units
0
4
8
12
16
20
24
0.2
0.4
0.6
0.8
1
E33/E55
QCD Events
γ Isolation
Arbitrary Units
0
10
20
30
40
50
0
20
40
60
80
E_ISO

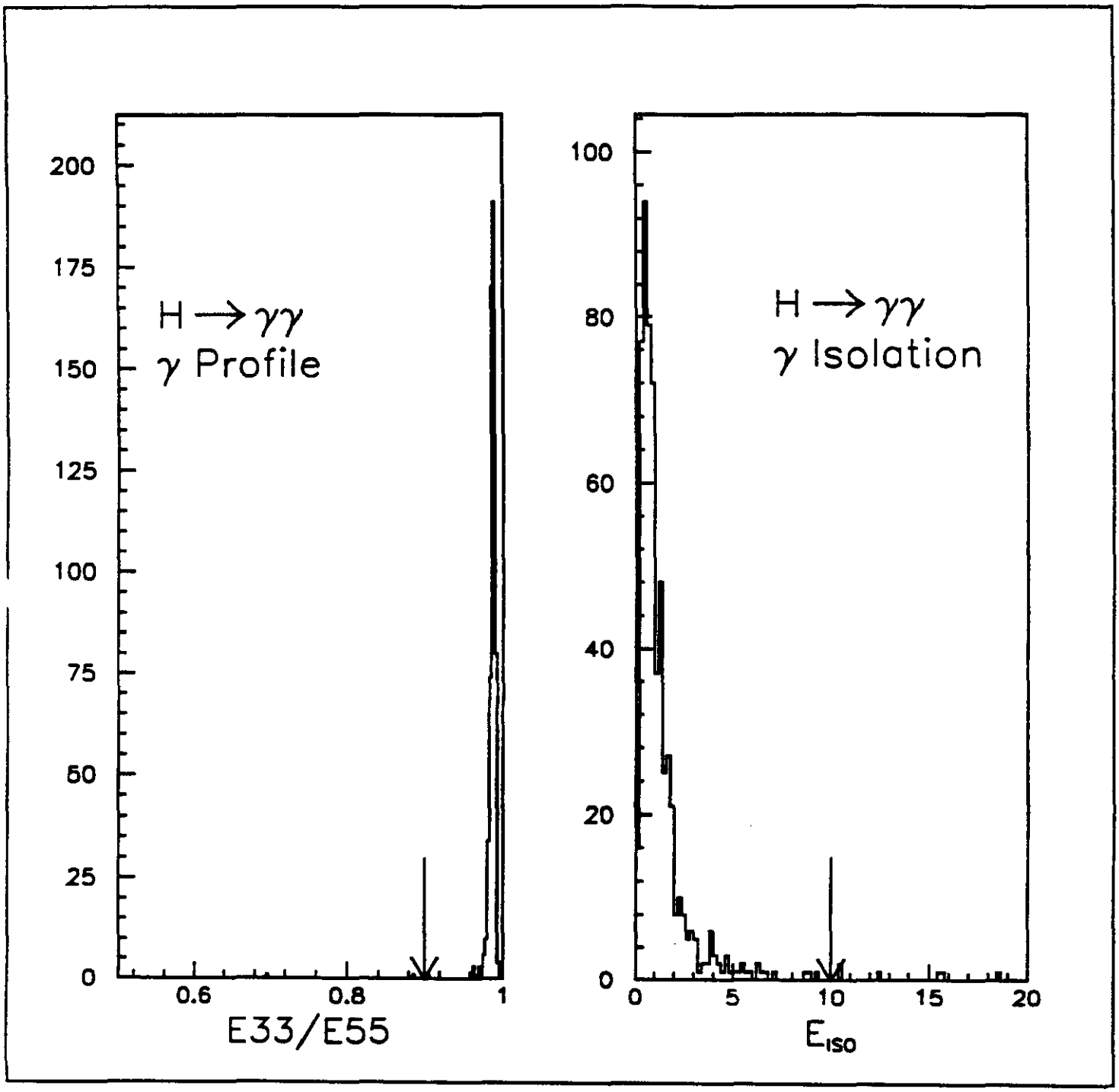
H → γγ
γ Profile
E33/E55
H → γγ
γ Isolation
E_ISO

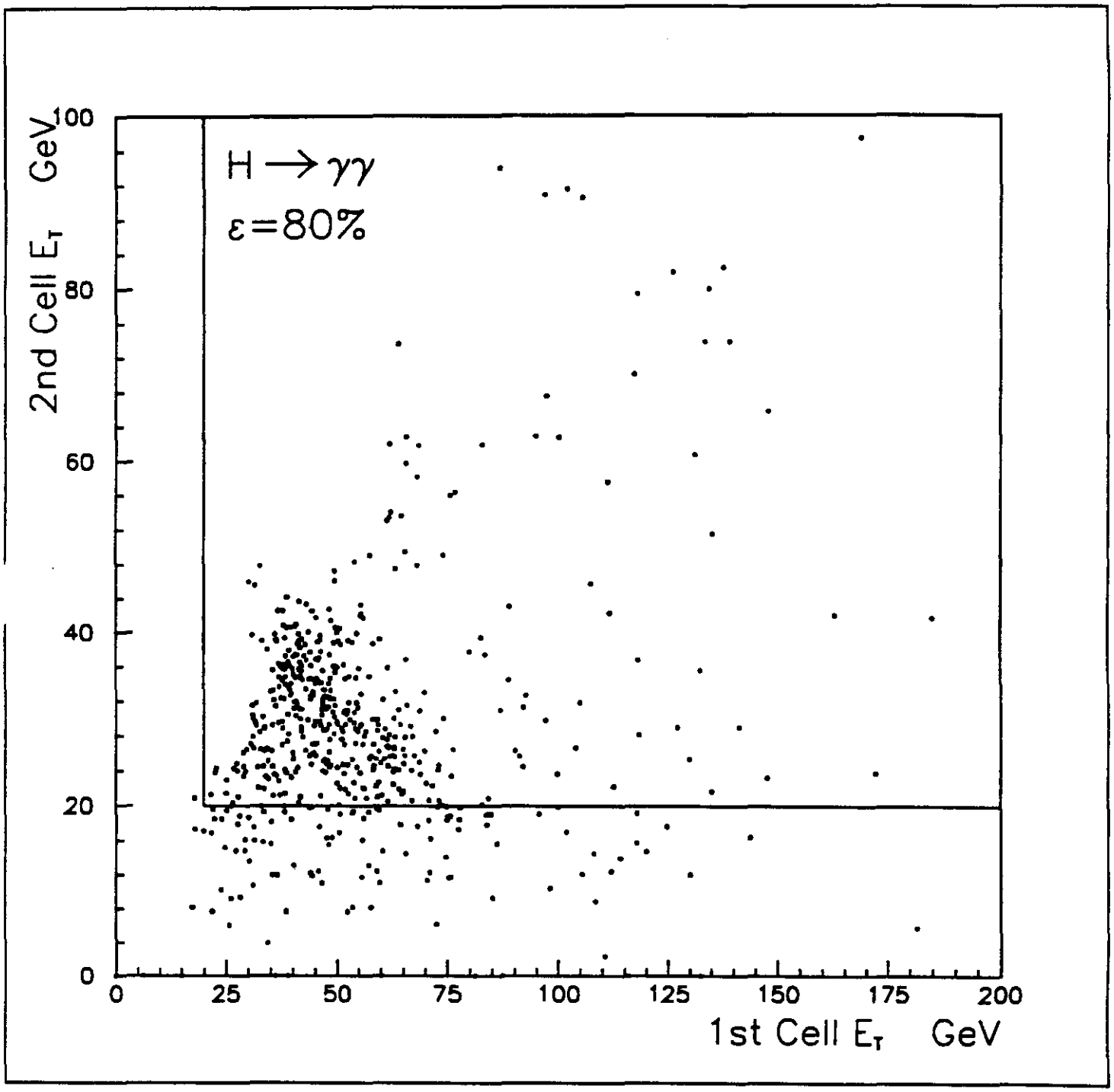
$H \rightarrow \gamma\gamma$
$\varepsilon = 80\%$
2nd Cell E_T GeV
1st Cell E_T GeV
0
20
40
60
80
100
0
25
50
75
100
125
150
175
200

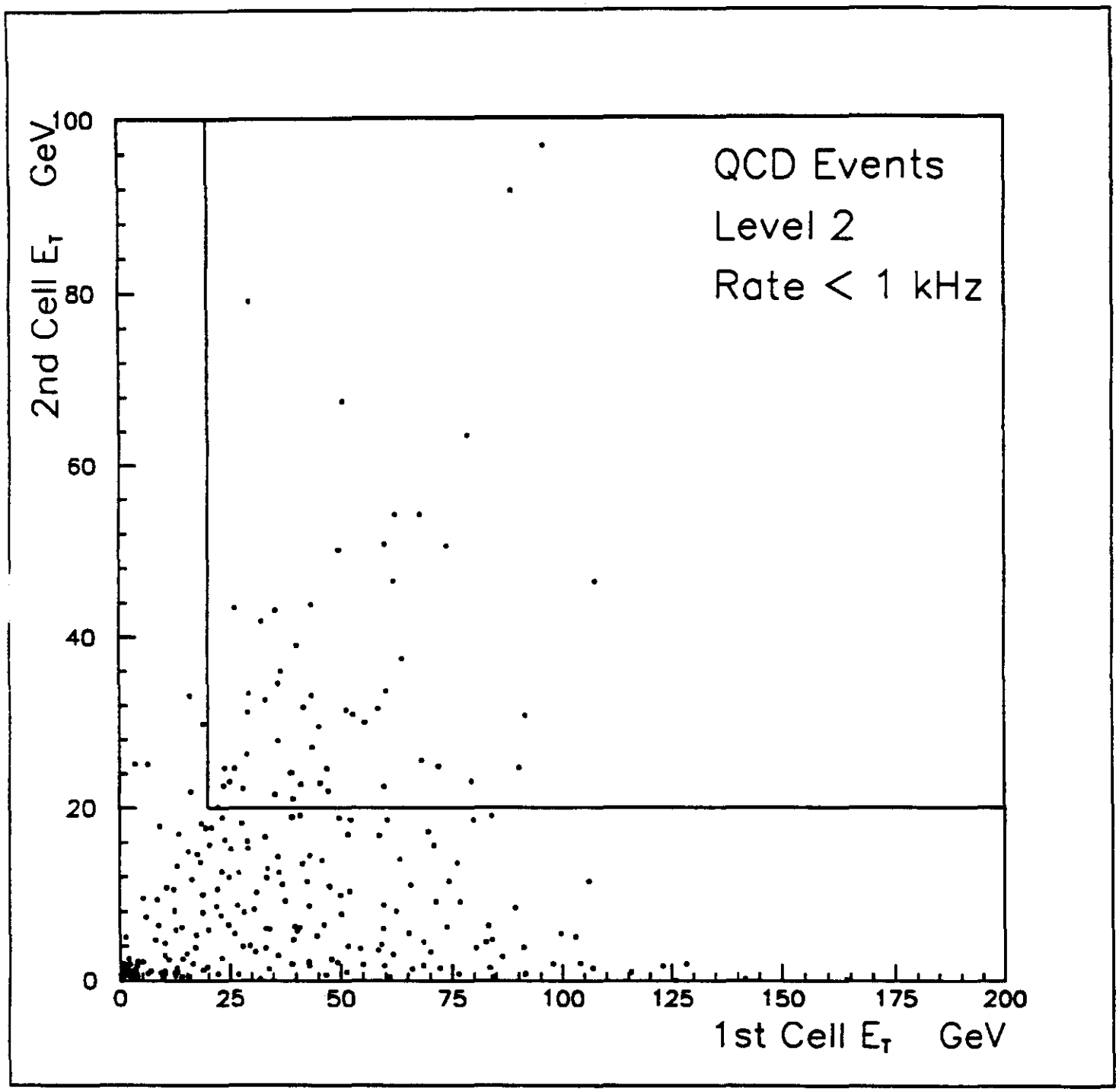
QCD Events
Level 2
Rate < 1 kHz
2nd Cell E_T GeV
1st Cell E_T GeV
0
20
40
60
80
100
0
25
50
75
100
125
150
175
200

D P H I AND RAYS TRIGGERS

***

D P H I IS A VALID TRIGGER IF THERE IS A COINCIDENCE BETWEEN PADS PHI3(i) AND ONE OF PHI2(i +/- thr)

WHERE thr = 0,1,2,3,....

***

R A Y S IS A VALID TRIGGER IF CALCULATED ANGLE BETWEEN RAY2 AND RAY3 IS SMALLER THAN A GIVEN THRESHOLD

GEM Trigger/DAQ/Computing 21/ 8/91

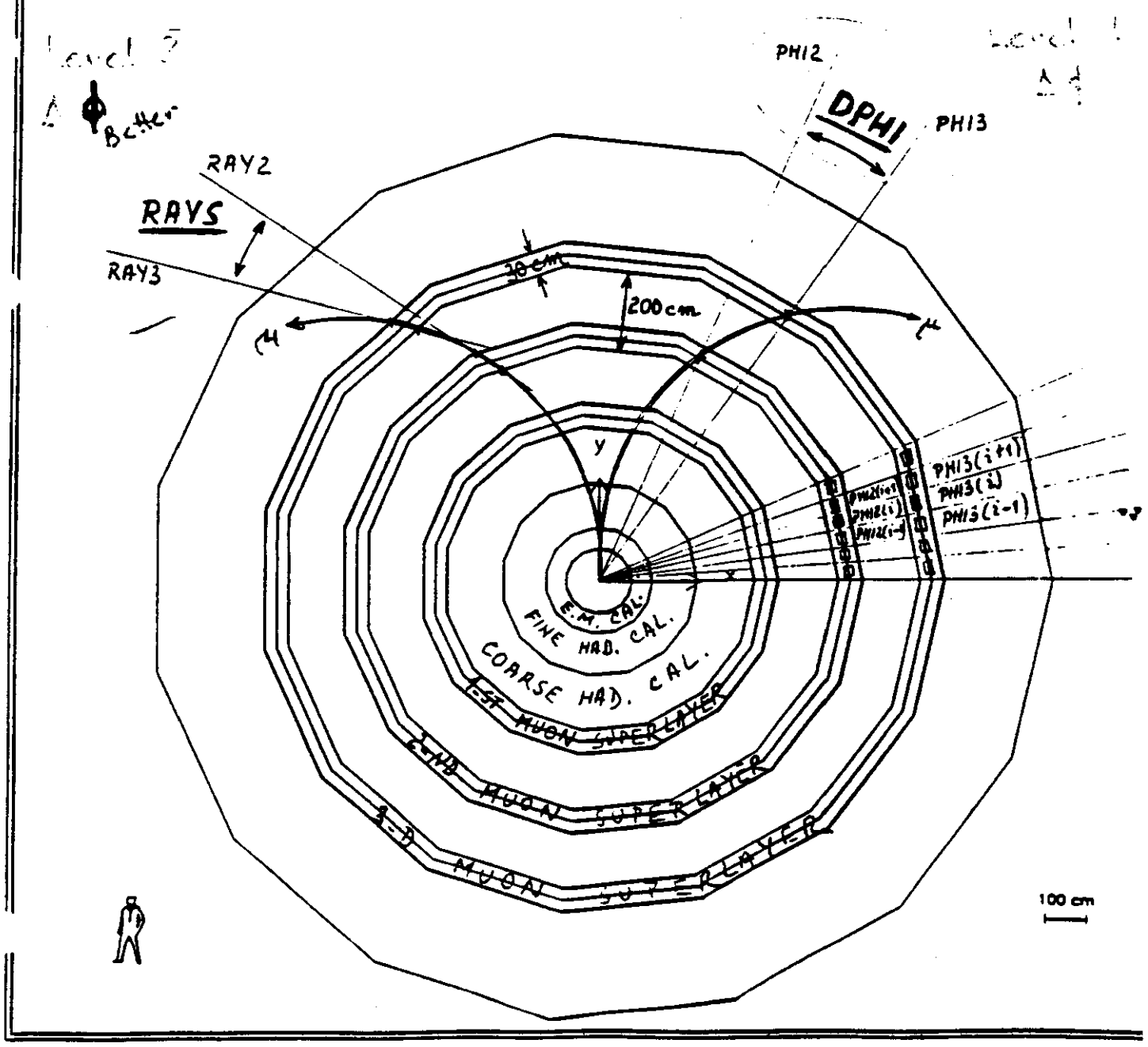

Fig. 21 Level 1 $\Delta\phi$ Trigger

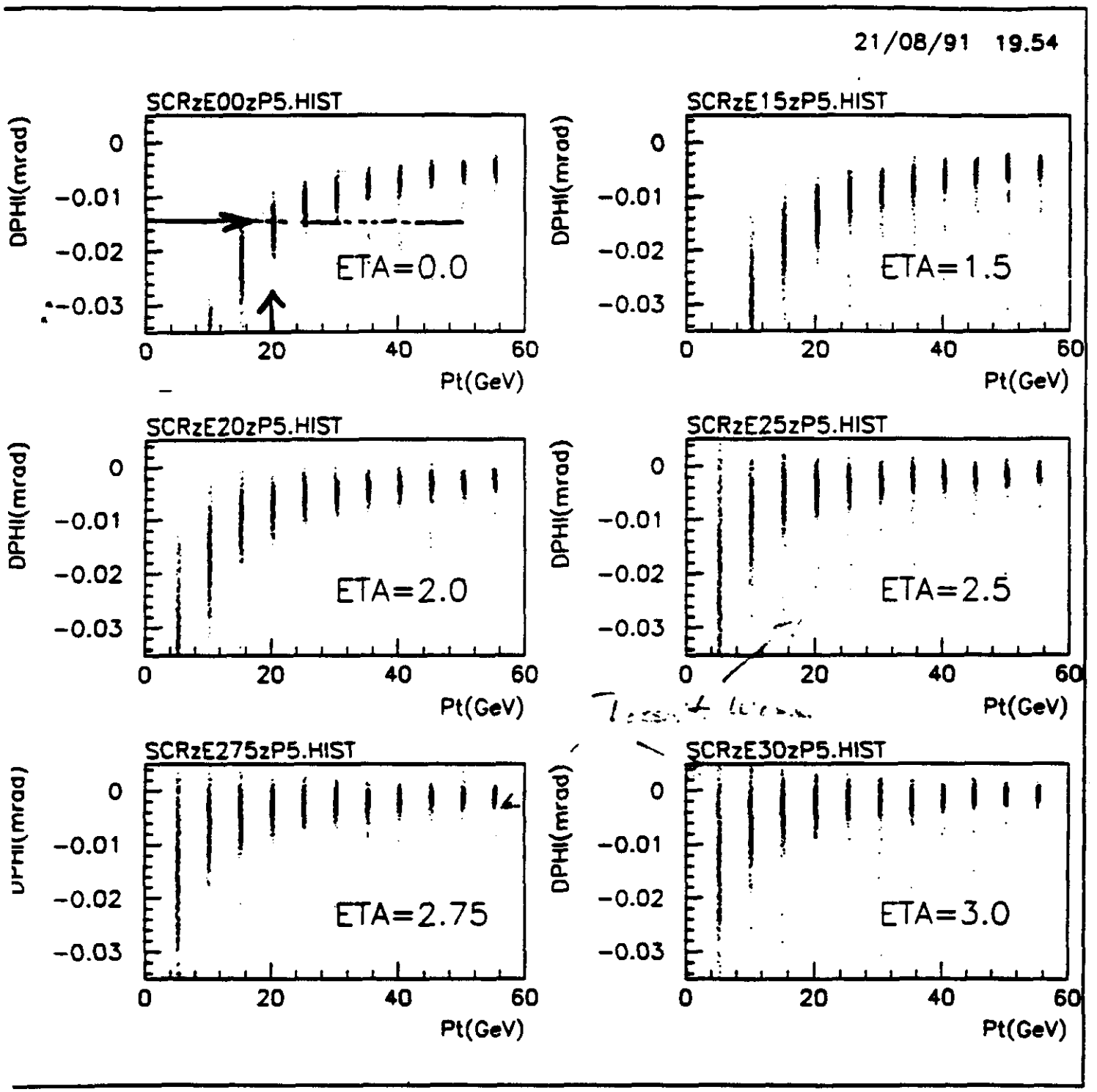

Level 2 "Ray Trigger"

$\Delta\phi$ Trigger

Better

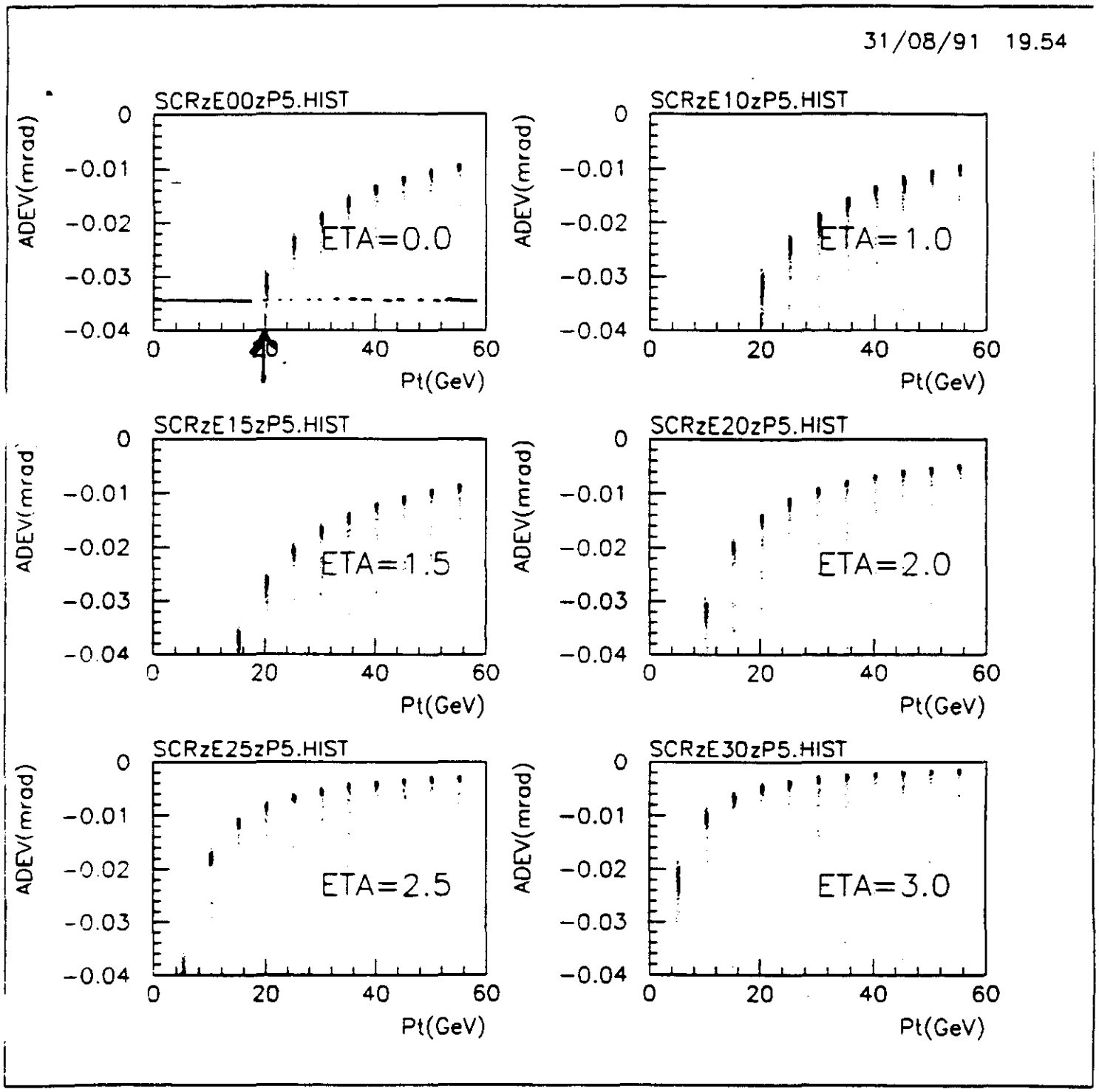

Muon Trigger Summary				
Level	Method	Region	Strip Size	Rates
			(cm)	(Hz)
1	$\Delta\phi$	$0 < \eta < 1.5$	3-5	< 10
	$\Delta\phi$	$1.5 < \eta < 2.0$	2-3	$10^2 - 10^3$
	$\Delta\phi'$	$2.0 < \eta < 2.5$	.2 - .5	$.2 - 2 \times 10^4$
2	$\Delta\phi'$	$p_T > 20$ GeV	$\sim .1$	200
	$\Delta\phi'$	$p_T > 50$ GeV	$\sim .1$	40

GEM Trigger/DAQ R&D

- System Issues
  - — Readout/Trigger Architecture
  - — Placement/Cabling Issues
  - — Clock Distribution
  - — Electron Charged Track Strategy
- Analog Pipeline (SCA) Design
  - — High Precision
  - — High Throughput
- Digital Pipeline
  - — FPADC (Wait to see results from FNAL)
  - — TI GaAs Feasibility Study
  - — Pipeline ADC
- Electro-optic Readout
  - — High Bandwidth/Low Density Readout
  - — Radiation Tolerant
  - — Cost issues remain to be resolved
- We will accelerate our efforts by using results of ongoing Subsystems R&D from LHC and SSC.

Online Computing

- Rate out of Level 2 $\sim 10^3$ Hz
- "Naive"* event size estimate $\sim$200 KBytes
- Consider system capable of handling 10^4 Hz of 2 MByte event

→ Requires $\sim$500 K SSCUF?

→ Projections show $\sim$500 SSCUF units will be available ⇒ 1000 units needed.

→ Such a system is "plausible".

- Similar projections hold for the offline analysis, where there are fewer events but more analysis.
- Storage Requirements: $\sim 3\times10^{15}$ Bytes/yr. This is daunting, but manageable.

* These are generally considered low. A more detailed analysis is in progress.

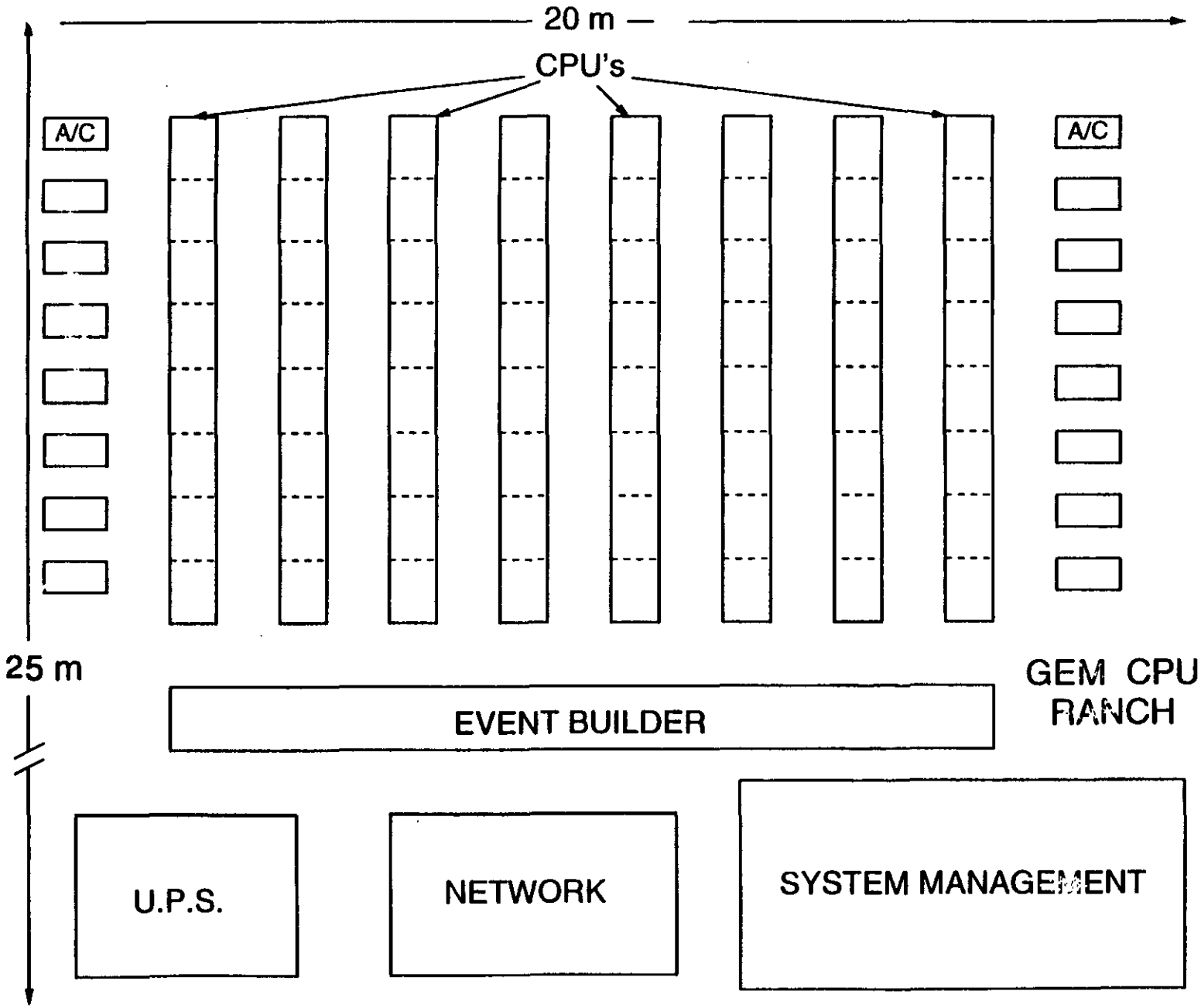
20 m
CPU's
A/C
A/C
25 m
GEM CPU
RANCH
EVENT BUILDER
U.P.S.
NETWORK
SYSTEM MANAGEMENT

Draft Requirements Document

Computing Space for GEM

K. McFarlane

September 26, 1991

1.0 COMPUTING SPACE FOR GEM

This is a brief note on computing space needs for GEM. It outlines some assumptions and computing requirements and sketches the resulting space requirements. Contingencies are yet to be develped.

1.1 TECHNOLOGY ASSUMPTIONS

The following will be available at installation time (1997-1998):

- Desktop boxes will be rated at 500 SSCUPS.

  The box will be 18" × 18" × 4" and consume 500W (750VA).

- Single board CPU's with the above capacity may be available.

- Magnetic disks will be > 10GB storage in a space of 12" × 12" × 4"

- Optical disks of 1TB capacity will be available at about the same size and power consumption as the magnetic disks.

- Network hardware at 2.5 Gbs^{-1} will be in volume production, with 9.95 GBs^{-1} in limited production.

- Mass storage will be available with 200 MBs^{-1} input rate, 15 PB total capacity in 100′ × 80′ floor area. Power consumption to be determined.

(Each of the items mentioned ~~above~~ below could be in a different area (item 5, is of course, off-site). They can also be in the same area. Particularly item 1 should be at the detectors.)

2.0 SYSTEM MODEL AND BREAKDOWN

Figure 1 shows a block diagram of the overall GEM computing system. It consists of six subsystem:

1. The event-builder and on-line computers (called Level 3). This overlaps with trigger and data acquisition.

2. The tertiary storage system ("tape system") for all raw data, calibrations, PASS1 output and data summaries ("DST").

3. The off-line computers.

4. The analysis activity, on-site.

5. The analysis activity, off-site.
6. Computing relevant to detector operations.
7. Back-up store for (raw) data.

3.0 COMPUTING REQUIREMENTS

3.1 ON-LINE

- CPU capacity of 500,000 SSCUPS, with wide-band networking (special purpose) and some local storage (~10 GB per CPU).
- Event builder capable of accepting and distributing 10 kHz of 1MB events.
- Output rate to storage of 200 MBs^{-1} substained rate.

3.2 TERTIARY STORAGE

- Capable of storing (near-line access) 3 PB of data for 5 years (15 PB). Substained I/O rate up to 300 MBs^{-1}

3.3 OFF-LINE

- CPU capacity of 600,000 SSCUPS, with wide-band networking.
- Secondary storage system capable of storing up to 50 data sets of 1 TB each, with 100 MBs^{-1} access (for off-line) use.

3.4 ENVIRONMENTAL

We assume air-cooled equipment. The equipment should be maintained between 10°C - 40°C, and 20% - 80% RH. This implies input of cold air at e.g., 60°F - 65°F at 80% RH.

Power should be 'clean' and 90 - 132 VAC at 47-63 HZ. 30 mins back up power should be available.

CRTs must be below 2 gauss or shielded. Disks and tape drives must be below 5 gauss or shielded.

CPU Boxes must be below 50 gauss or shielded.

4.0 ANALYSIS

Space should be provided in one or more locations for up to 40 people. This requires space for 40 workstations, printers, etc.

5.0 CONFERENCE

There should be space for conferencing, with computer and tele-video capabilities. This should include space at the IR and the West Campus.

6.0 SYSTEM MANAGEMENT AND REPAIR FACILITIES

Each of the major computing facilities will need space for system management and repair personnel and equipment.

7.0 SPACE REQUIREMENTS

7.1 ON-LINE

Assume the boxes and the network hardware are assembled in stacks, each stack containing 8 boxes and the network hardware. Space for the disks is shared between adjacent stacks.

See Figure 2. Figure 2a shows a smaller-footprint- stack assuming Single-brand computers (SBC's).

The stacks are then arranged in rows as shown in Figure 3, with event builder, networking, air-conditioning, and 30-minute backup power supply.

7.2 OFF-LINE

The off-line area would look roughly the same, without the event builder but with more disk space.

7.3 TERTIARY STORAGE AND BACK-UP

7.4 ANALYSIS AREA

7.5 CONFERENCE FACILITY USE OF 100 HBS^{-1}

Summary of Areas Required

NET AREAS (Approximate) (increase by 30% or more for gross)

System	Area	Cumulative Area
On-Line:	5,500 sq ft.	
Off-line:	5,500 sq. ft.	/11,000
Analysis area:	1,200 sq. ft. × 4 = 4,800 sq. ft.	/16,000
Conference:	1,200 sq. ft. × 2 = 2,400 sq. ft	/18,500
Main Tertiary Store:	8,500 sq. ft	/27,000
Back-up Tertiary Store:	5,500 sq. ft	

Time Scale

Costs

Model

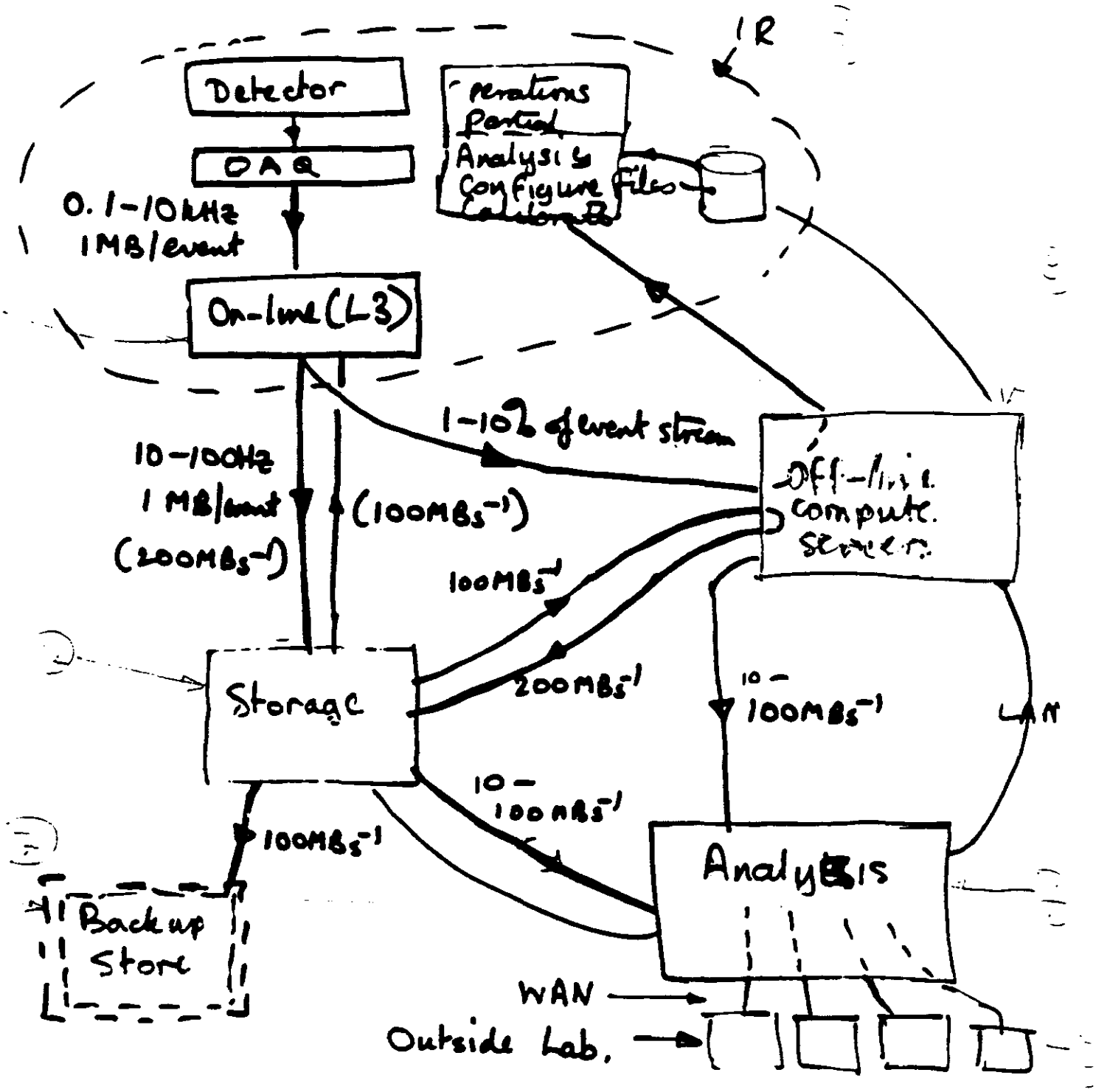

Up to 5 geographic locations. Prefer 2!

Fig. 1

Basic Stack

(16 CPU boxes)

SCALE

1" = 2'

1/2" = 1'

Plan

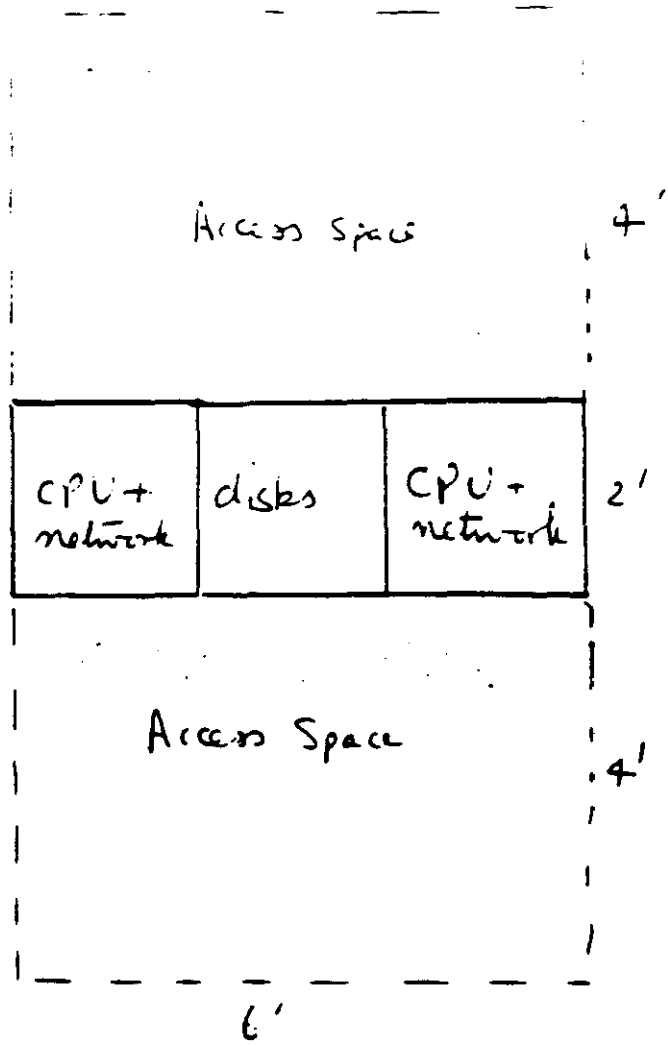

Elevation

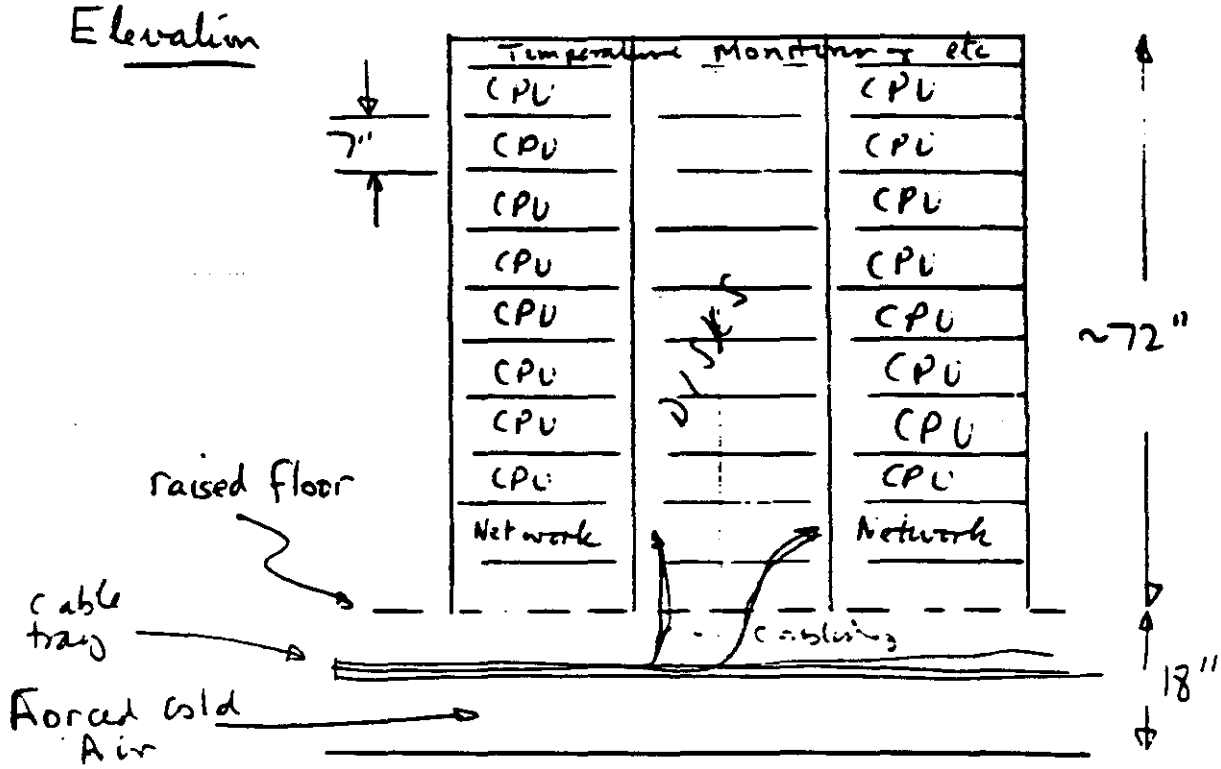

SCALE

$\frac{1}{2}'' = 1'$

$1'' = 2'$

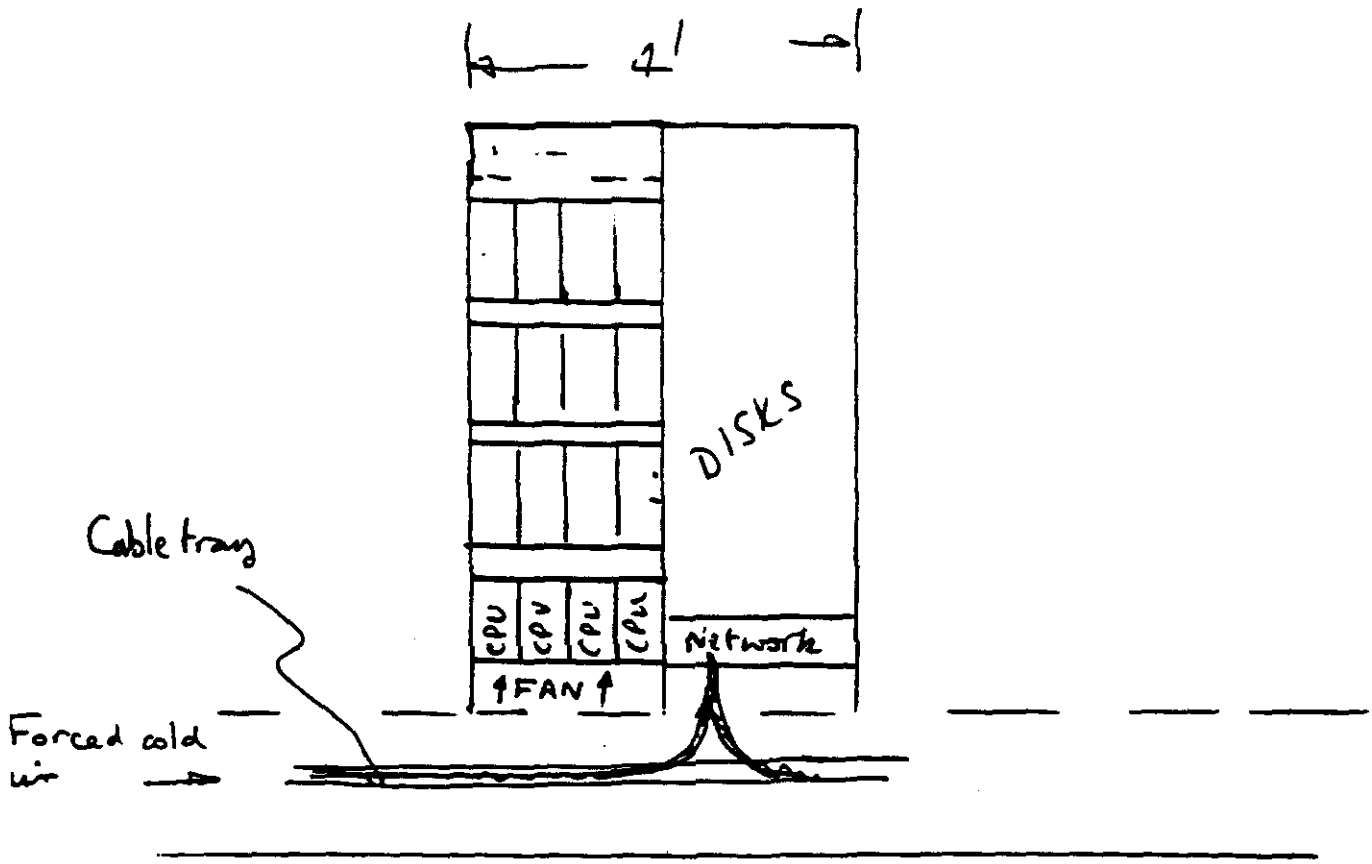

Fig 2a — Alternate Stack Using SBC's

Smaller (4') instead of 6') (9,000 SSCUPS per stack)

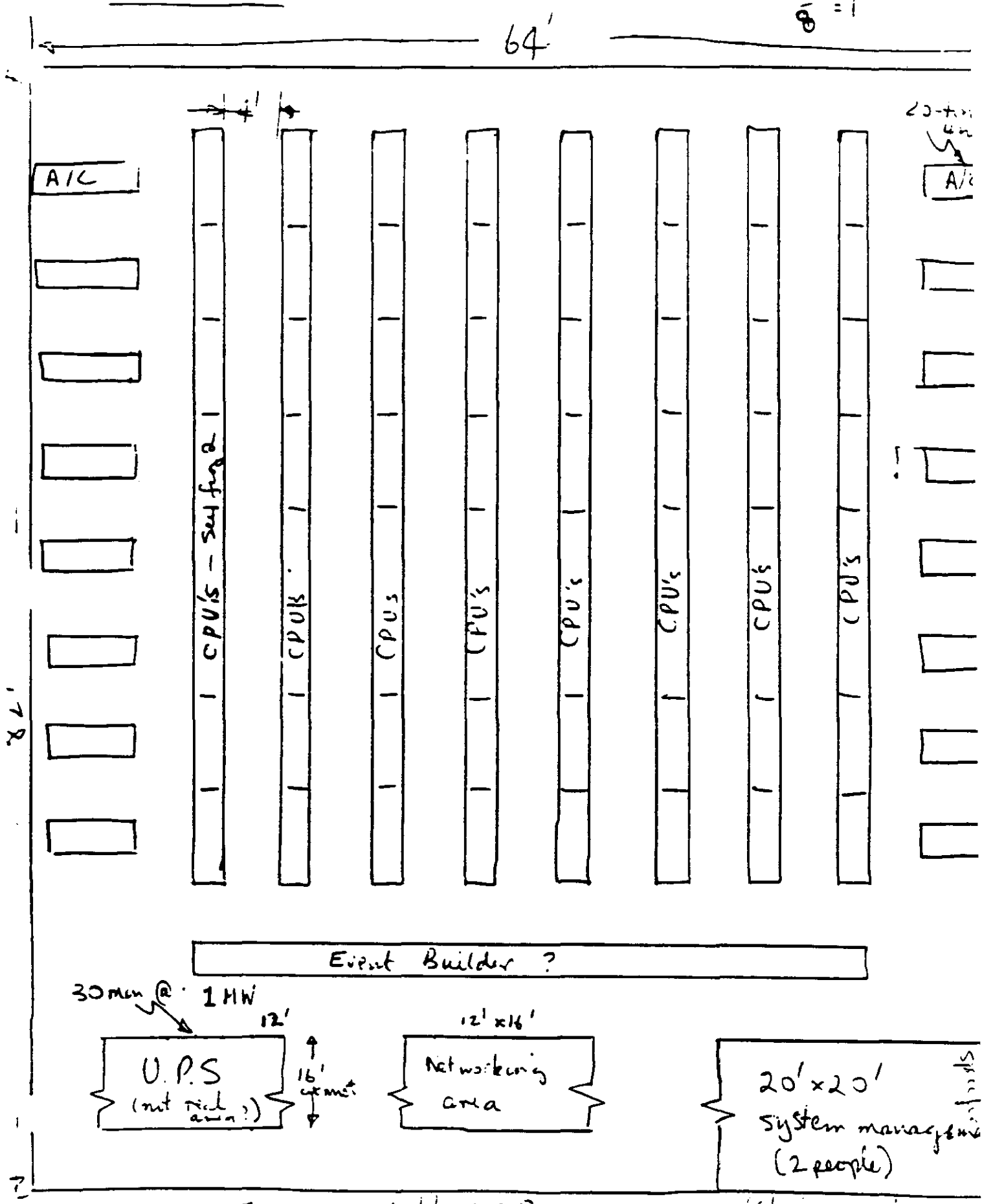

Fig. 3 – [illegible] 1-202 Support [illegible]

(1) Replace Exabytes with Disk arrays / optical disks

(2) increase number of disks in disk stack (no impact on floor space)

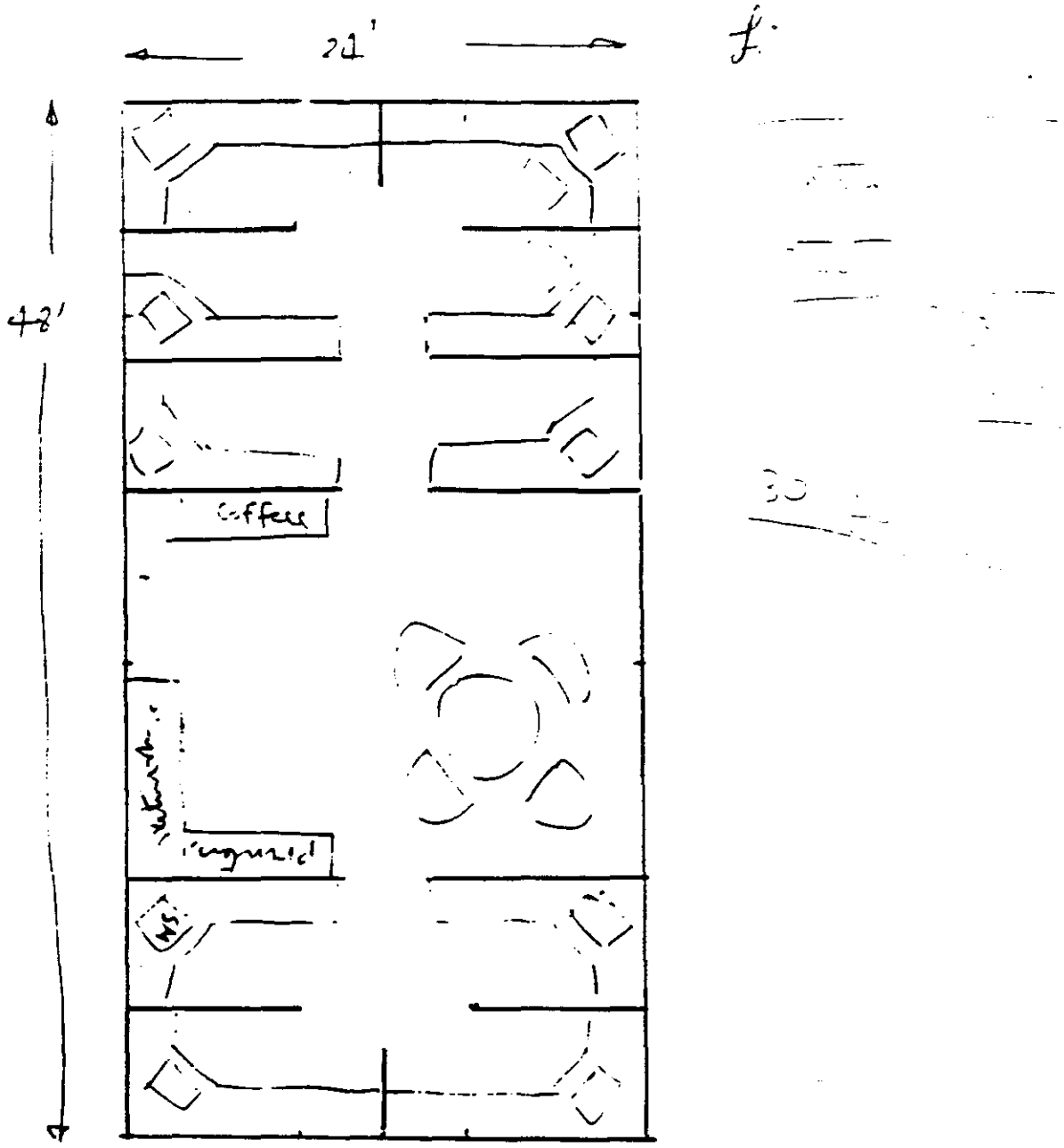

Fig 5 - Analysis Area for 10 people

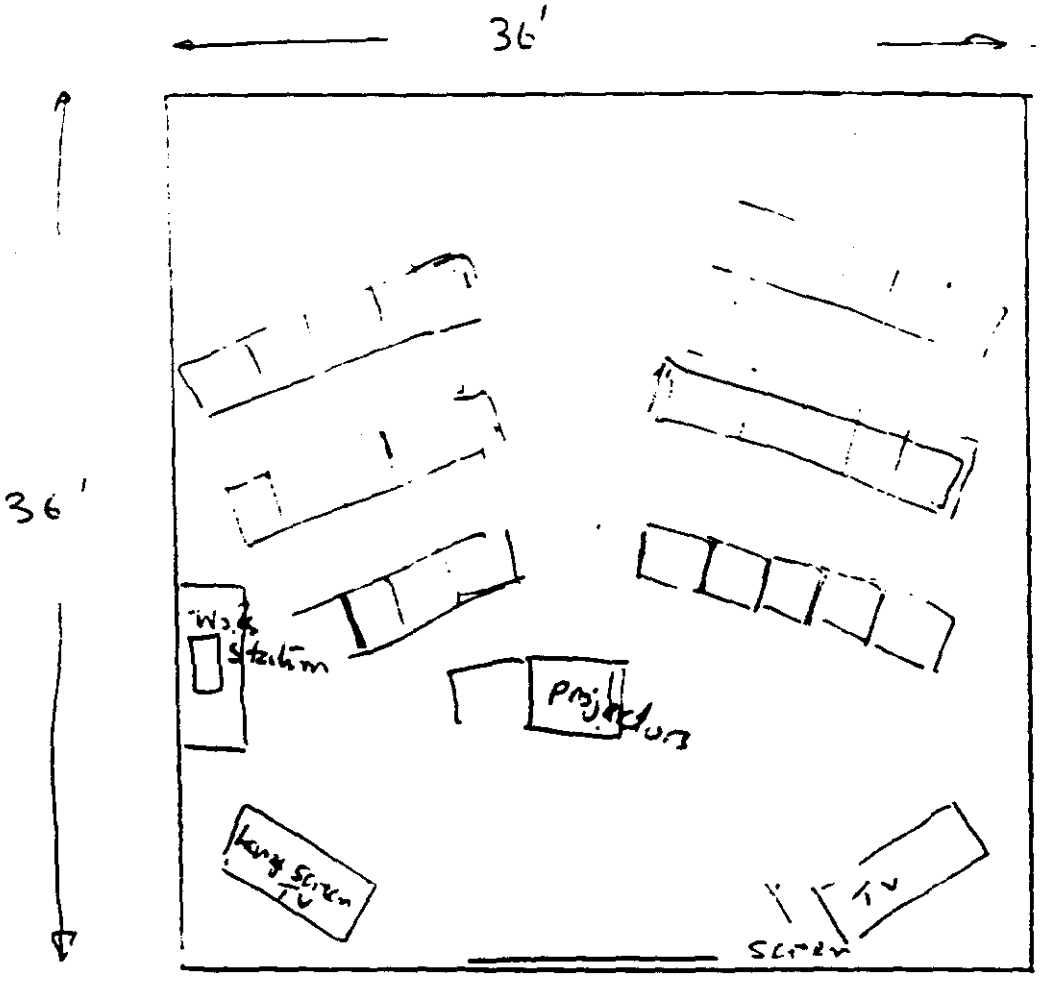

Aim is to have tele-video conference, plus ability to have large-screen output from workstation to discuss analysis.

(Tele/video) (30-40
Fixt → Conference Room → people)

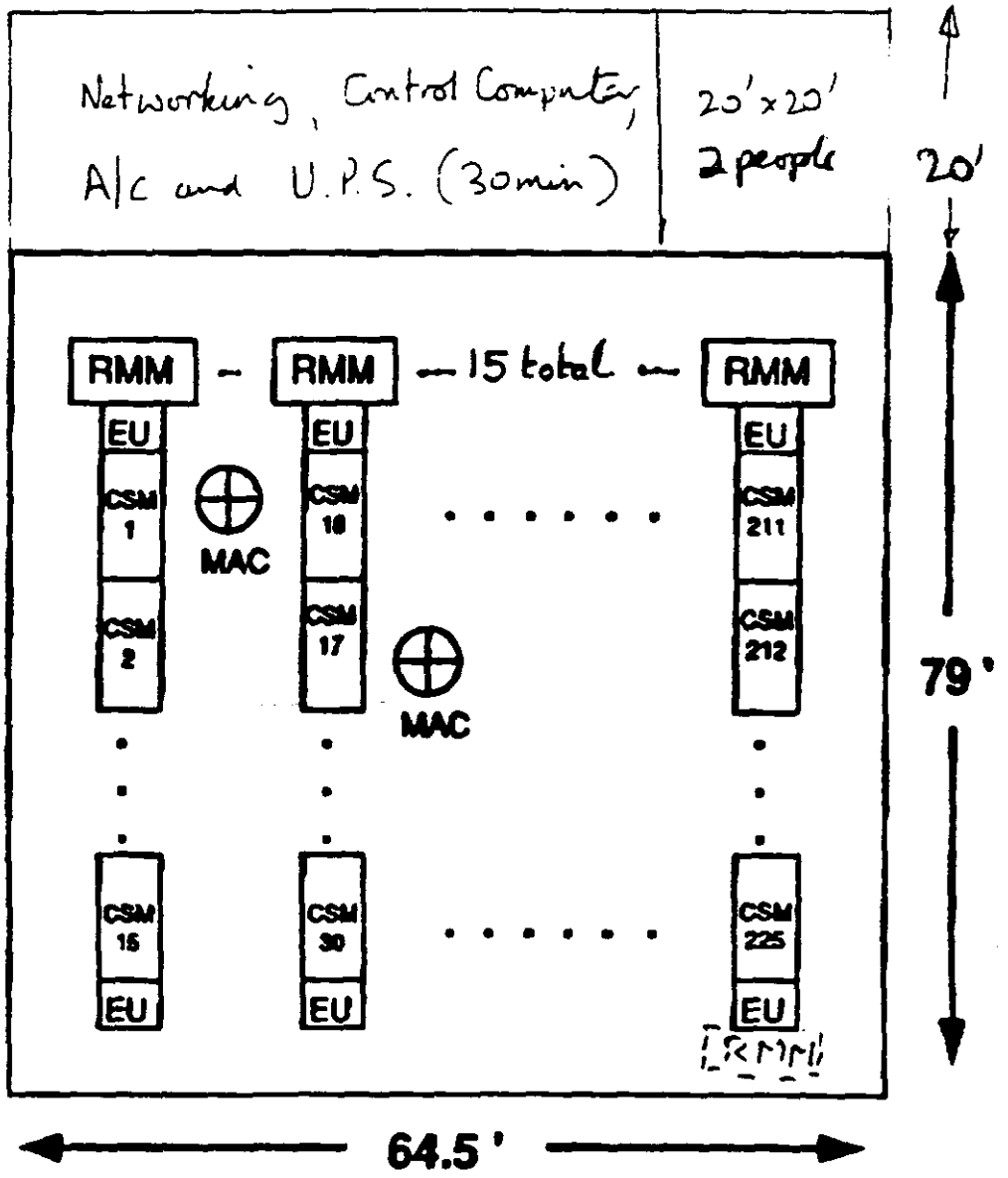

Fig. 7 Main Tape Store.

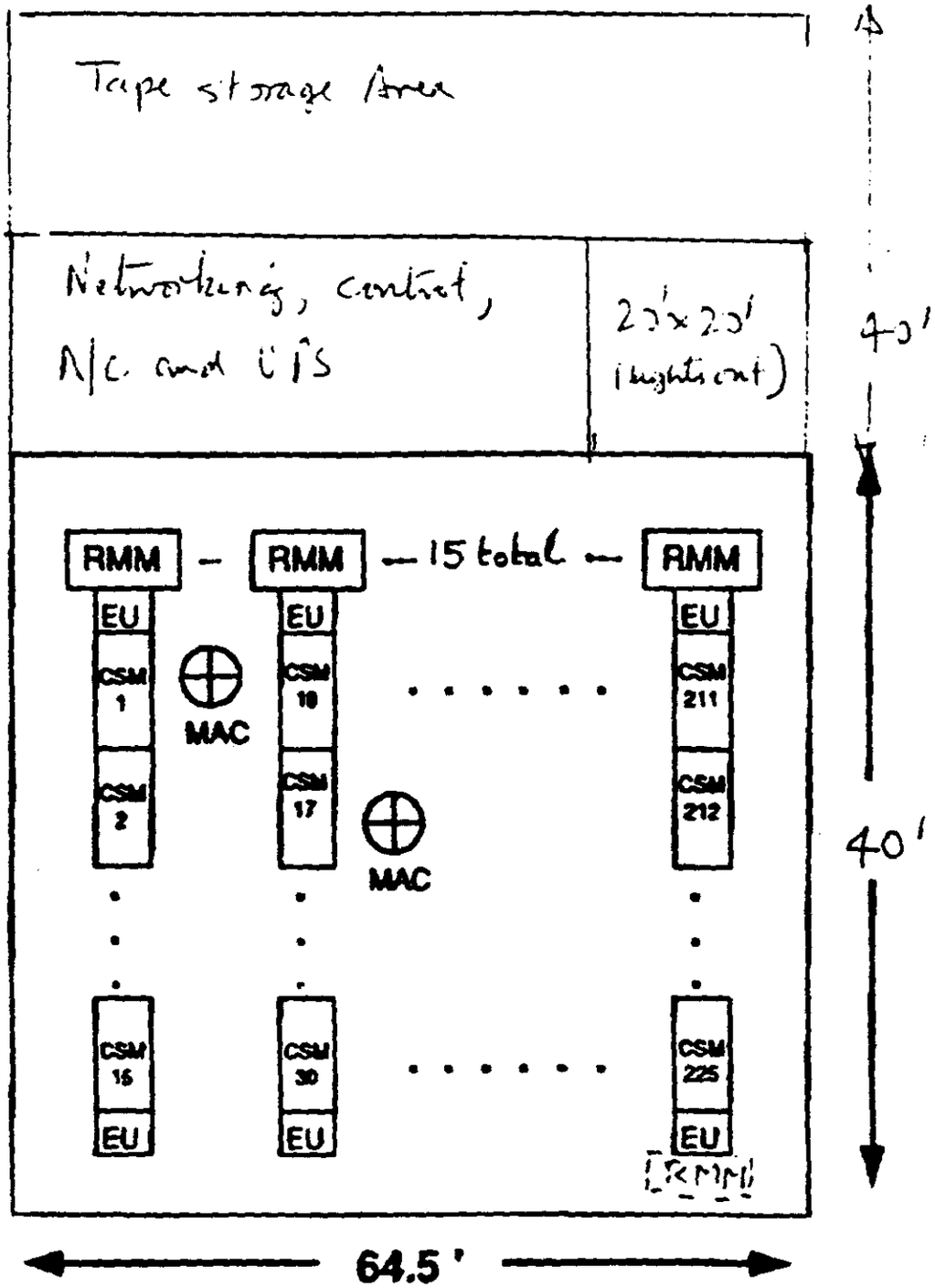

Fig 2 - Backup Tape Stor

GEM Physics

Physics Goals:

- Origin of electroweak symmetry breaking –
  - Higgs? SUSY-Higgs? Technicolor?
  Something else?? $\Lambda_{EWSB} \lesssim 1$ TeV

- Meaning of flavor –
  Why 3 identical generations?
  Are there more? Why $M_{\nu_4} \gg 0$?

- Origin of flavor symmetry breaking –
  - Arbitrary Yukawa couplings?
  Technicolor? q/ℓ Substructure?
  Something else?? $\Lambda_{FSB} = ?$

- Sensitivity to unknown & unexpected phenomena in the TeV-energy regime!

GEM DESIGN GOALS

- SUPERB MEASUREMENT OF γ, $e^{\pm}$, $\mu^{\pm}$, HADRONS AT NOMINAL AND ULTRA-HIGH LUMINOSITIES.

  → PRECISION EM & HADRONIC CALORIMETRY, WITH ADEQUATE CENTRAL TRACKING.

  → PRECISE, ROBUST $\mu^{\pm}$ MEASUREMENT IN A LARGE, OPEN MAGNETIC VOLUME

  → 800 GeV $H^0 \to \mu^+\mu^-\mu^+\mu^-$.

- COMPLEMENTARY TO SDC - TO ENSURE THAT THE FULL RANGE OF 1-TeV PHYSICS IS WELL-COVERED

→ EMPHASIZE GAMMAS, ELECTRONS, MUONS

•

•

•

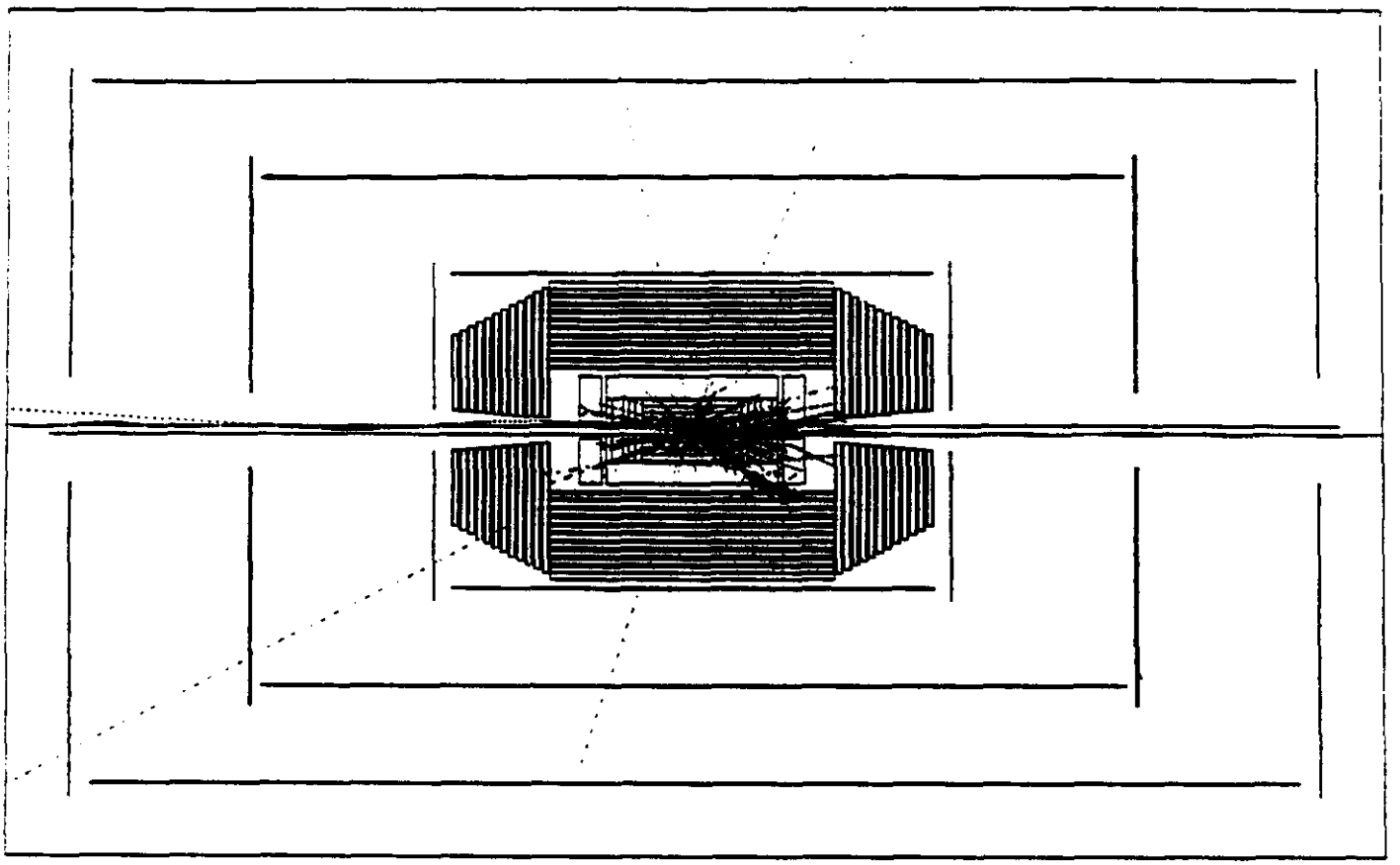

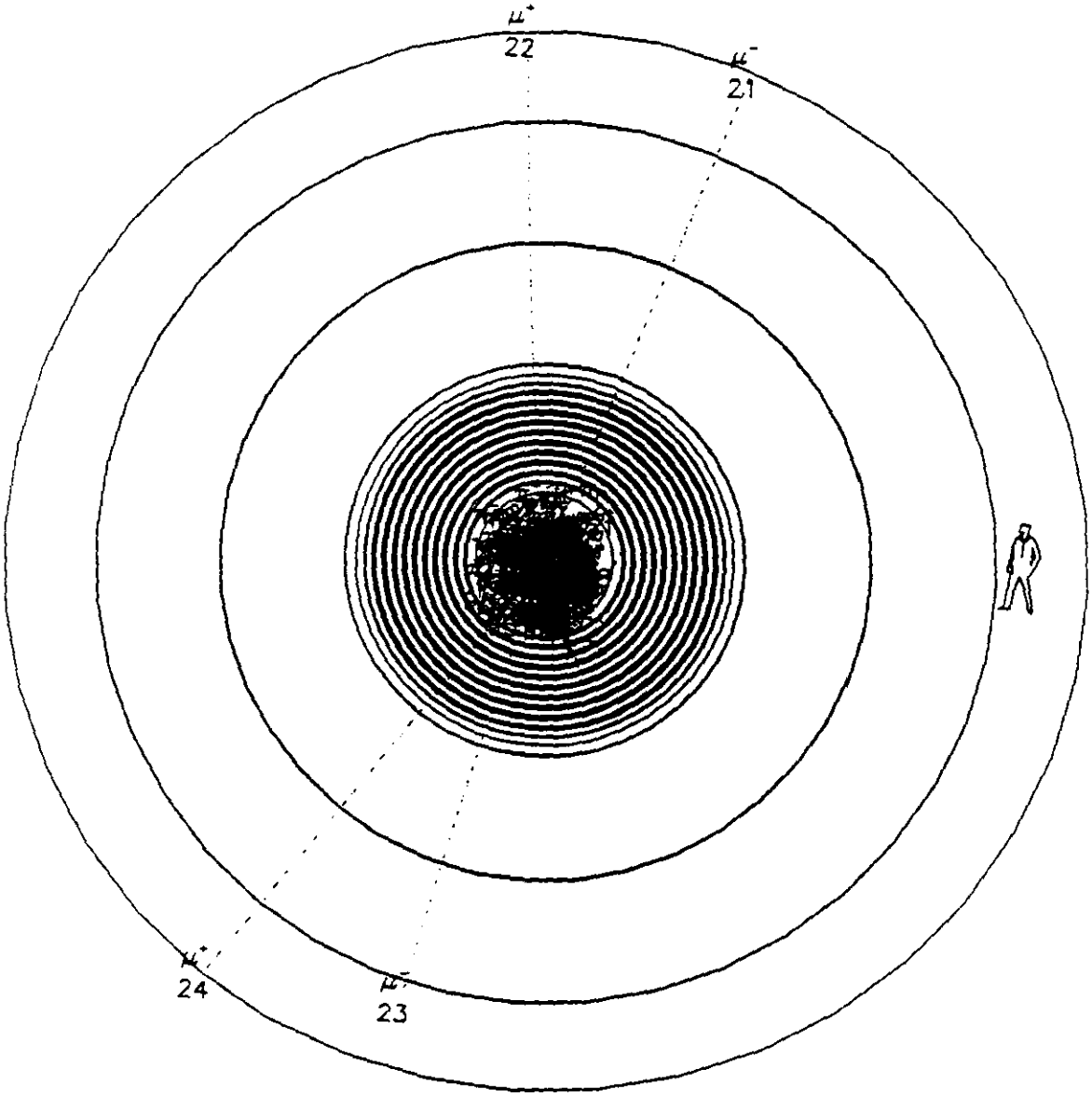
μ^+
22
μ^-
21
R
μ^+
24
μ^-
23

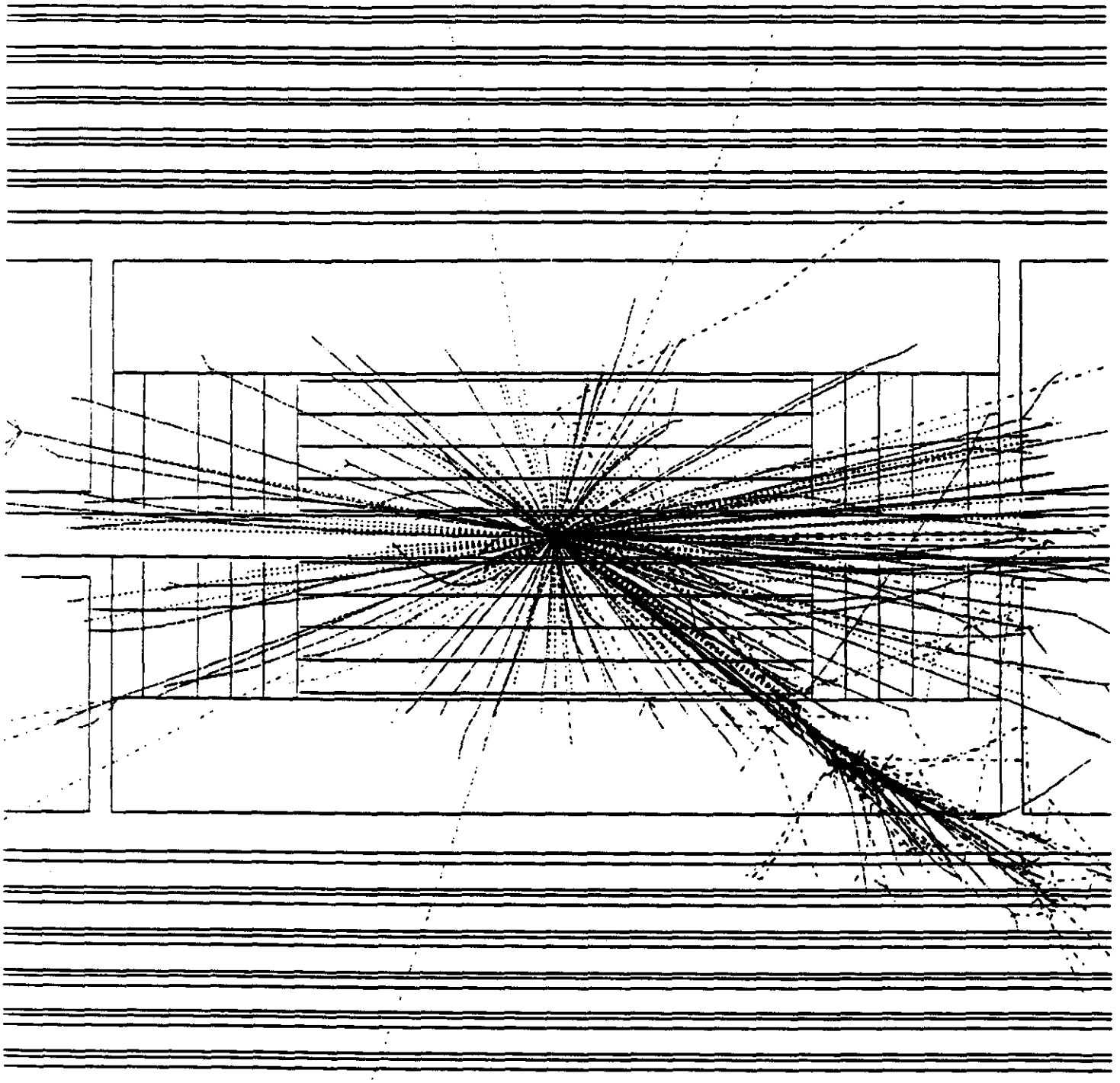

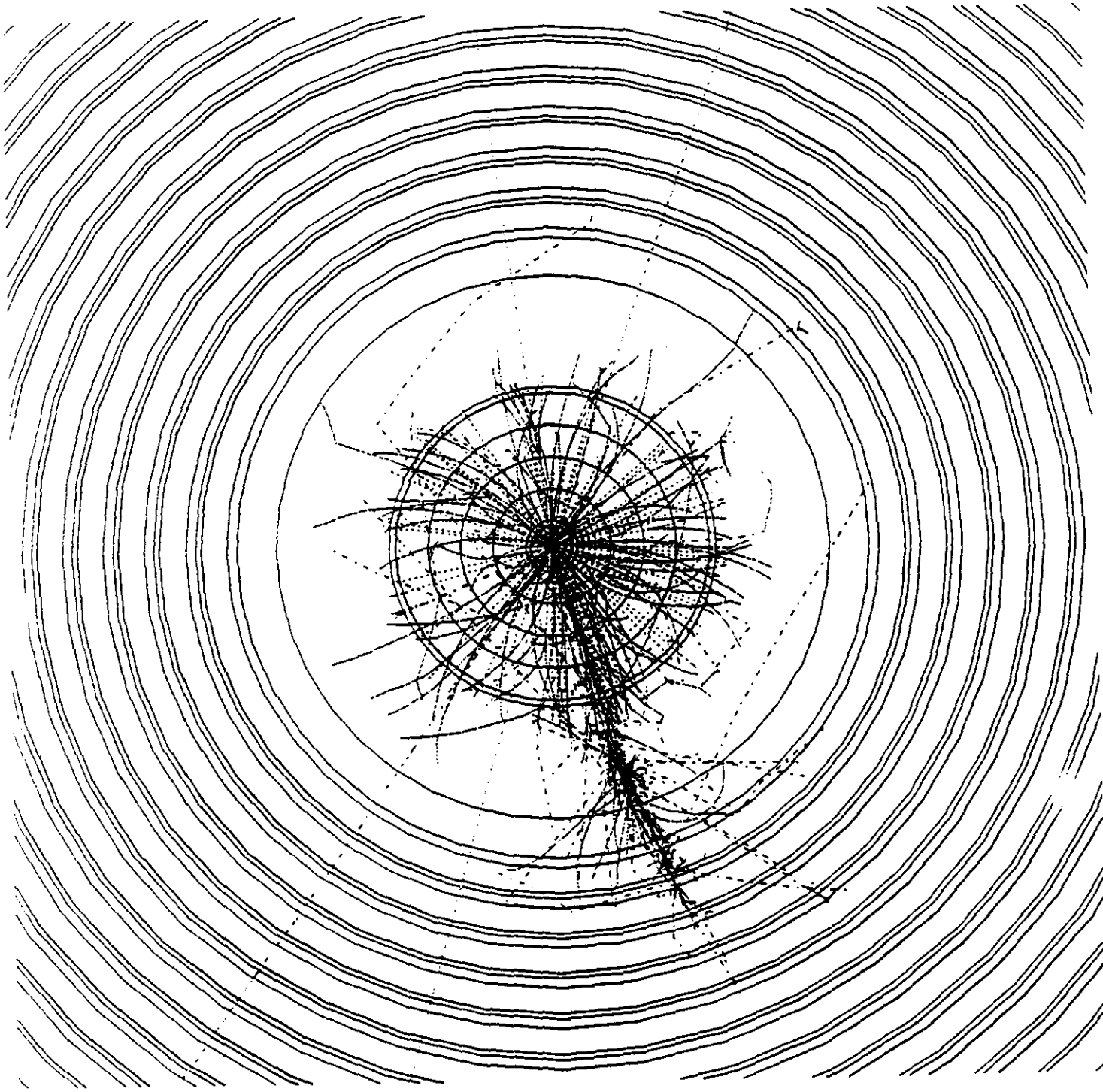

... WHAT ARE GAMMAS, ELECTRONS, MUONS GOOD FOR?

- H^0, h^0_{SUSY}, $\pi_T^0 \to \gamma\gamma$
- $H^0 \to ZZ^* \to \ell_1^+\ell_1^- \ell_2^+\ell_2^-$
- HEAVY $H^0 \to ZZ \to \mu^+\mu^-\mu^+\mu^-$ AT $\mathcal{L} \simeq 10^{34}$
- TAGGING b, $t \to b$ BY $\mu^\pm$ INSIDE JETS

  ➡ FLAVOR PHYSICS: HEAVY QUARKS, LEPTOQUARKS, CHARGED HIGGS, TECHNIPIONS,

- $Z' \to e^+e^-$ ➡ PRECISION $M_{Z'}$, $\Gamma_{Z'}$ } AT $\mathcal{L} \simeq 10^{34}$
- $Z' \to \mu^+\mu^-$ ➡ ASYMMETRY
- $\tilde{g}\tilde{g} \to \mu^\pm\mu^\pm + \not{X}$
- $\rho_T^\pm \to W^\pm Z^0 \to \ell^\pm\nu\,\ell^+\ell^-$ AT $\mathcal{L} \simeq 10^{34}$
- $\bar{q}q \to \mu^+\mu^-$ SUBSTRUCTURE – REACH, ASYMMETRY AT $\mathcal{L} \simeq 10$
- ETC., ETC., ETC.

GEM Parameters for Physics Simulation

Calorimetry

1. BaF_2 EMC with scintillation HC (Liq. Scint. or Spa

	EM	Hadron
$\Delta E/E$	$\frac{2\%}{\sqrt{E}} \oplus \frac{1}{2}\%$	$\frac{50\%}{\sqrt{E}} \oplus 2\%$
η_{max}	2.5	3.0
segmentation	.04 × .04	.08 × .08

2. LAr with Xe/Kr option

	EM1	EM2	Hadron
$\Delta E/E$	$\frac{7.5\%}{\sqrt{E}} \oplus \frac{1}{2}\%$	$\frac{2-7.5\%}{\sqrt{E}} \oplus \frac{1}{2}\%$	$\frac{63\%}{\sqrt{E}} \oplus 1.$
η_{max}	3.0	2.5	3.0
segmentation	.04 × .04	.04 × .04	.08 × .0

3. F/B Calorimetry: $3 < |\eta| < 5$, LAr parameters assum

Muon System

$B = 0.8\,T$; $\eta_{max} = 2.5$; $\left.\frac{\Delta p}{p}\right|_{500\,GeV} = 5\%$ at $90°$, 10% at $10°$

Central Tracker

$\eta_{max} = 2.5$, $\frac{\Delta p_T}{p_T} = \frac{p}{500}$ to $|\eta| = 1.5$, $\frac{1}{\sin^2\theta}$ beyond.

→ Resolutions

GEM Physics Simulations Group

Organizers - J. Branson, K. Lane, F. Paige, B. Zhou

Higgs Physics - B. Zhou*, J. Branson, R. Zhu, M. Chen, H. Ma, H. Yamamoto, M. Mohammadi, K. Furuno

Top Physics - S. Protopopescu*, H. Ma

Z_T Physics - F. Paige*, G. Folden, J. Rutherfoord, S. Kahn, M. Murtagh, K. McFarlane, A. Vaniyashin

Jet Physics - R. Frey, H. Ma

Complementarity to SDC + Beyond the Standard Model -
- K. Lane*, M. Golden, E. Simmons, E. Carlson, L. Randall, B. Zhou, H. Ma, R. Zhu, M. Chen, H. Yamamoto, F. Paige, S. Kahn

Tools - Isajet, Pythia, GEANT

SELECTED PHYSICS PROGRESS REPORTS

I. HIGGS PHYSICS – FEATURES EMC, MUON, HC

1. $H^0 \to \gamma\gamma$ FOR $80\,\text{GeV} \le M_H \le 150\,\text{GeV}$ (ZHU, YAMAM

BACKGROUNDS:

- QCD JETS $\longrightarrow$ ISOLATED "γ" + "γ"
- $q\bar{q}, gg \to$ JET + γ ; JET $\to$ "γ"
  - STUDIED EXTENSIVELY BY L^*, BUT NEEDS / GETTING FURTHER STUDY –
  - REJECTION OF ISOLATED π^0s : SHOWER SHAPE / PRESHA
- $q\bar{q}, gg \to \gamma\gamma$ – IRREDUCIBLE

EVENT SELECTION:

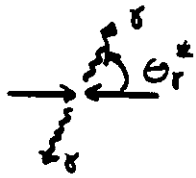

- $|\eta_\gamma| < 2.5$; $E_T^\gamma > 20\,\text{GeV}$;
- $|\eta_{\gamma\gamma}| < 3.0$ (REDUCE $q\bar{q} \to \gamma\gamma$)
- $|\cos\theta_\gamma^*| < 0.8$ (REDUCE $gg \to \gamma\gamma$)

CUTS TO REJECT QCD BACKGROUNDS:

- CHARGE VETO CUT IN 3×3 CELLS ABOUT γ
- ISOLATION CUT: $\sum_{R<0.6} E_T - E_T^\gamma < 5\,\text{GeV} + 0.1\,E_T^\gamma$
- SHOWER SHAPE (FOR MULTI-π^0)

➡ PLOTS OF SIGNAL + IRREDUCIBLE BACKGROUND
BACKGROUND-SUBTRACTED SIGNAL

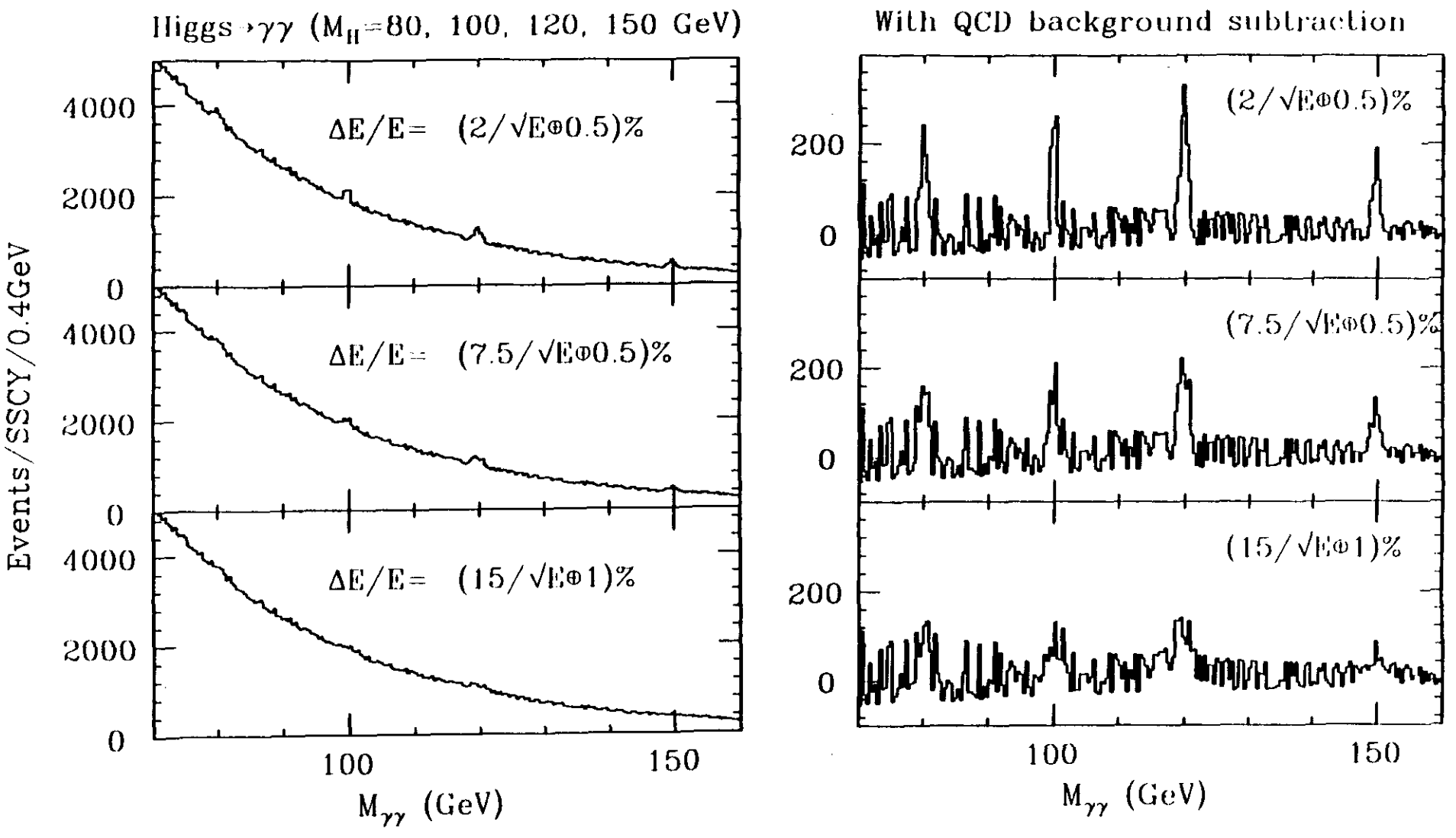
Higgs →γγ (M_H=80, 100, 120, 150 GeV)
With QCD background subtraction
Events/SSCY/0.4GeV
ΔE/E= (2/√E⊕0.5)%
ΔE/E= (7.5/√E⊕0.5)%
ΔE/E= (15/√E⊕1)%
4000
2000
0
200
0
100
150
M_γγ (GeV)

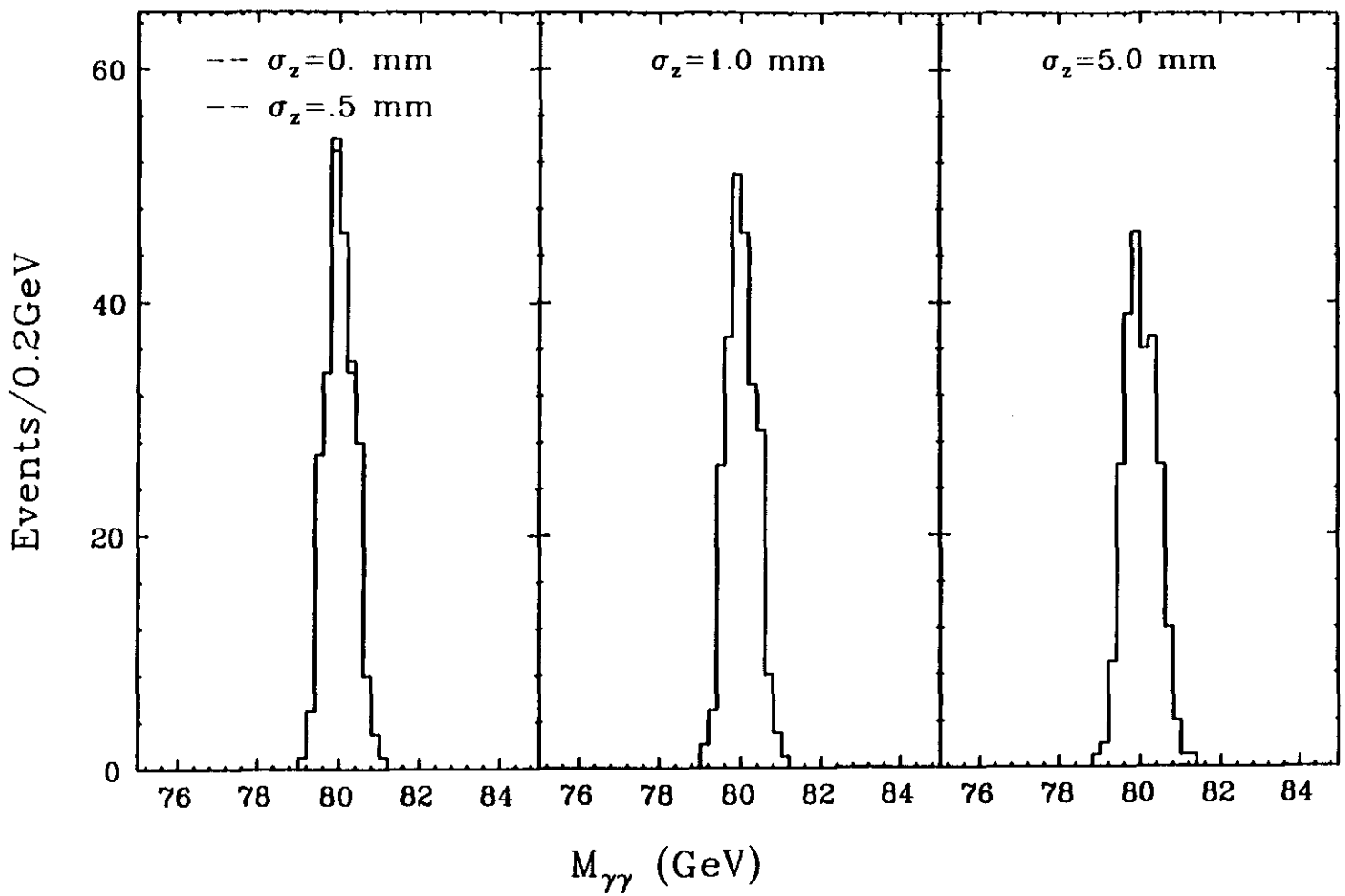
-- σ_z=0. mm
-- σ_z=.5 mm
σ_z=1.0 mm
σ_z=5.0 mm
Events/0.2GeV
0
20
40
60
76
78
80
82
84
$M_{\gamma\gamma}$ (GeV)

2. $H^0 \to Z Z^* \to l_1^+ l_1^- l_2^+ l_2^-$ FOR $140\ \text{GeV} \leq M_H \leq 170\ \text{GeV}$
(ZHOU)

BACKGROUNDS :

- QCD PROCESSES (e.g., $t\bar{t}$)
- $q\bar{q} \to Z Z^* \to l^+ l^- l^+ l^-$
- $q\bar{q} \to Z \gamma^* \to l^+ l^- l^+ l^-$
- $q\bar{q} \to Z + Q\bar{Q} \to l^+ l^- l^+ l^- + X$

EVENT SELECTION :

$|\eta_l| < 2.5$; $E_{T_l} > 5\ \text{GeV}$

ISOLATION : $\sum_{R<0.7} E_T - E_{T_l} < 5\ \text{GeV} + 0.1\, E_{T_l}$

$M_{ll} > 10$ GeV FOR ALL LEPTON PAIRS

→ PLOTS OF M_{4e} ; $M_{e^+e^-\mu^+\mu^-}$; $M_{4\mu}$
(GEANT - SIMULATED PARAMETERIZATIONS)

3. $H^0 \to W^+ W^- \to e^\pm \mu^\mp + X$ FOR $2M_W < M_H < 2M_Z$
(PAIGE)

SIGNAL + BACKGROUND (W^+W^-; $t\bar{t}$) UNDER STUDY — PRELIMINARY RESULTS "ENCOURAGING".

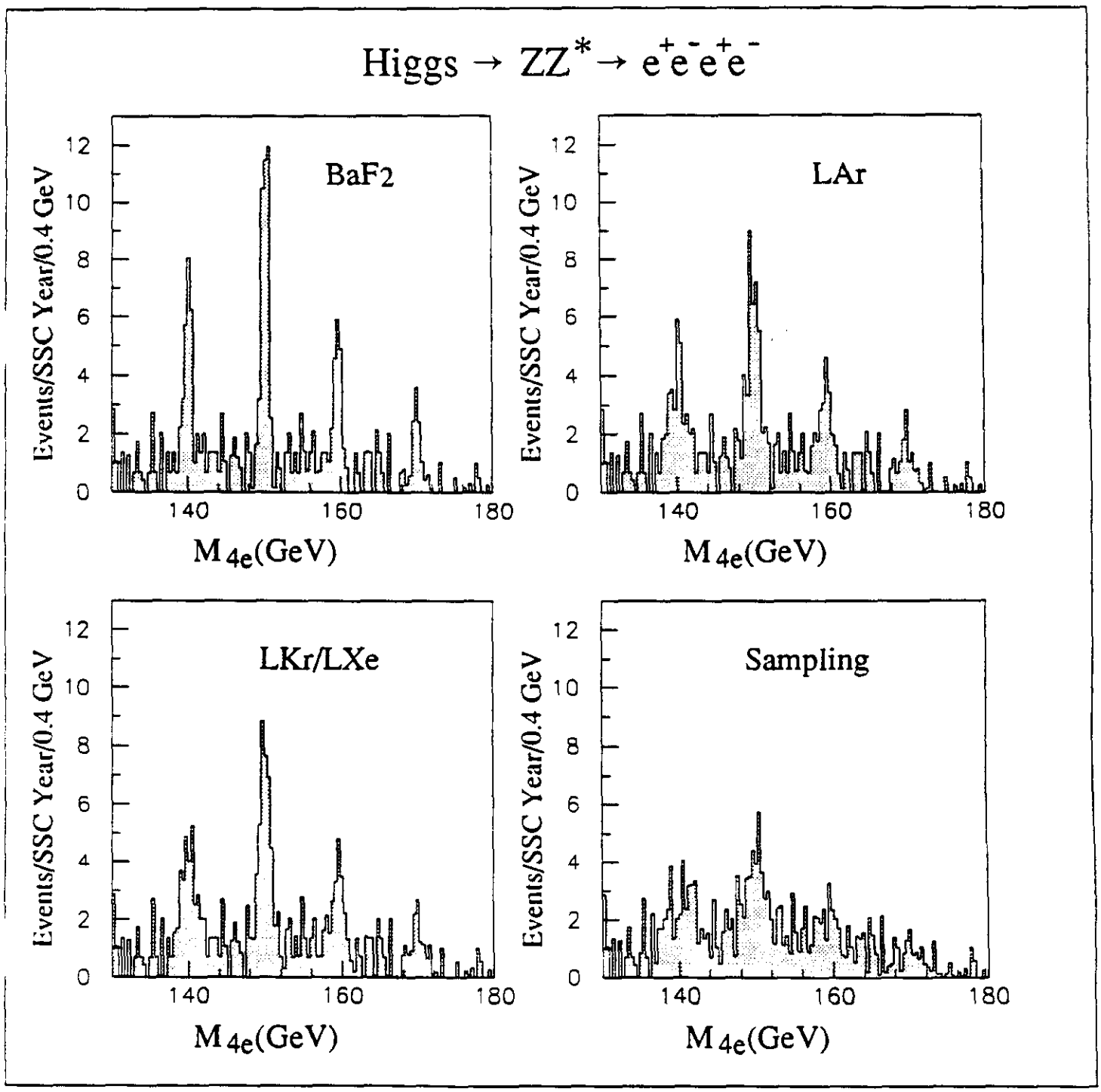
Higgs → ZZ* → e+e-e+e-
BaF2
LAr
LKr/LXe
Sampling
Events/SSC Year/0.4 GeV
M 4e(GeV)
0
2
4
6
8
10
12
140
160
180

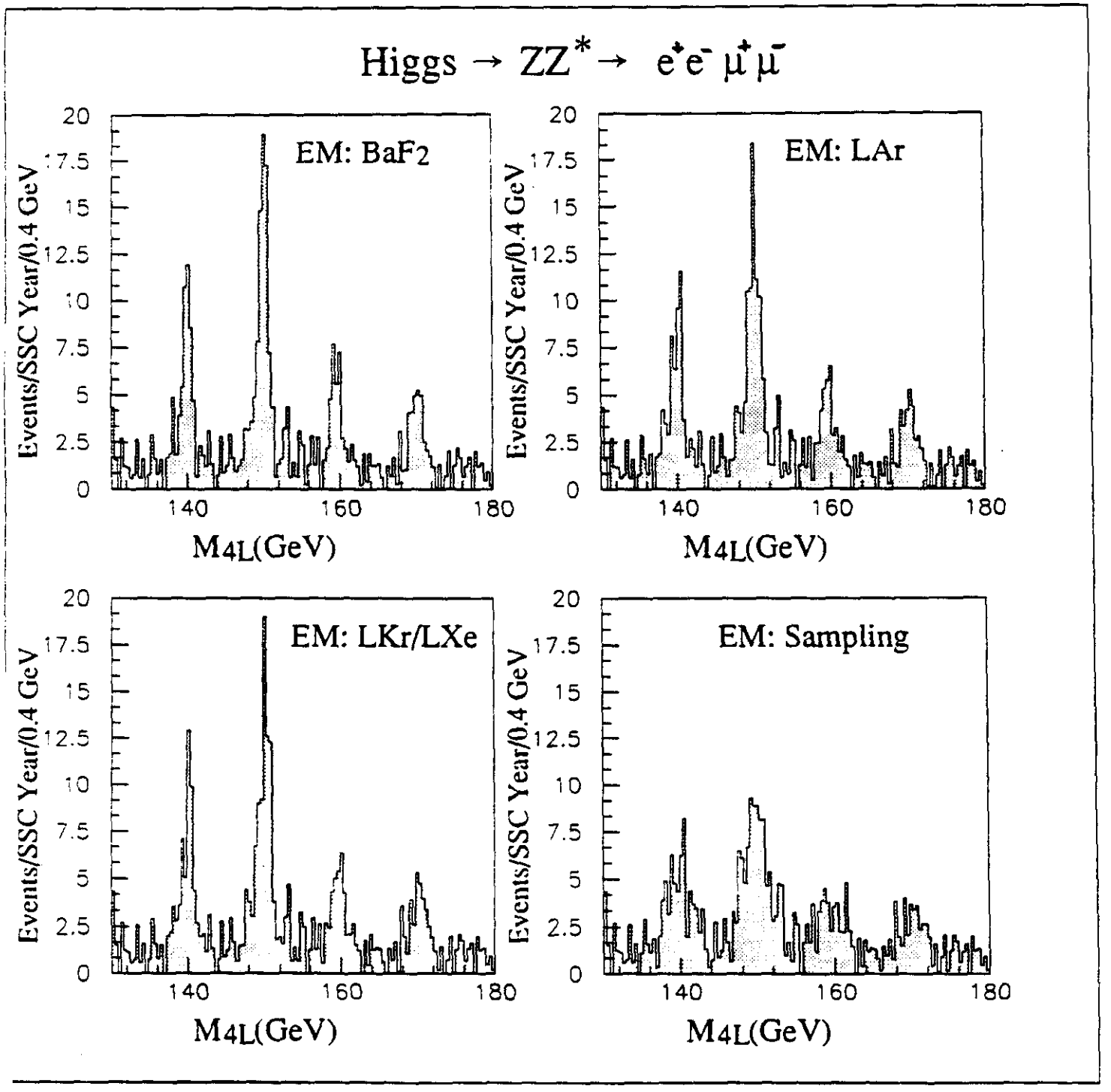
Higgs → ZZ* → e+e- μ+μ-
EM: BaF2
EM: LAr
EM: LKr/LXe
EM: Sampling
Events/SSC Year/0.4 GeV
M4L(GeV)
0
2.5
5
7.5
10
12.5
15
17.5
20
140
160
180

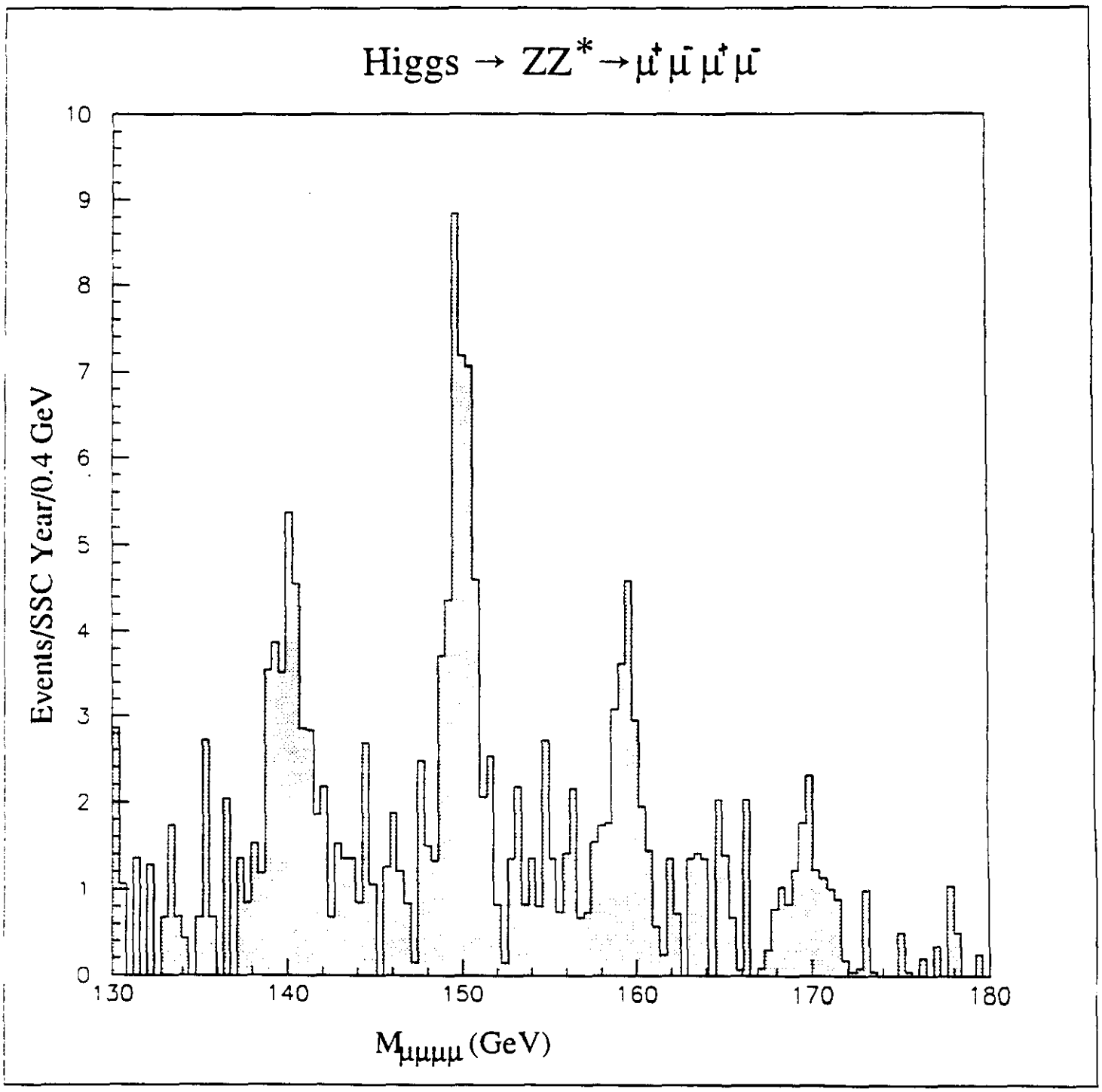
Higgs → ZZ* → μ+ μ- μ+ μ-
Events/SSC Year/0.4 GeV
0
1
2
3
4
5
6
7
8
9
10
130
140
150
160
170
180
Mμμμμ (GeV)

4. $H^0 \to Z^0 Z^0 \to l_1^+ l_1^- l_2^+ l_2^-$ FOR $200\ \text{GeV} \le M_H \le 800\ \text{Ge}$
(ZHOU, et al.)

STANDARD VARIATIONS ON THE ABOVE THEMES.

5. $H^0 \to Z^0 Z^0 \to \ell^+ \ell^- j j$ FOR $M_H = 800\ \text{GeV}$ (MA, ZHOU)

BACKGROUNDS :

- $Z^0 Z^0 \to \ell^+ \ell^- j j$
- $t\bar{t} \to \ell^+ \ell^- j j$
- $Z^0 j \to \ell^+ \ell^- j j$ - MAIN BACKGROUND.

EVENT SELECTION :

2 ISOLATED $\ell^+ \ell^-$ WITH $E_{T\ell} > 50\ \text{GeV}$, $|\eta_\ell| < 2.5$

$|\varphi_{\ell^+} - \varphi_{\ell^-}| < 100°$

$E_T(\ell^+\ell^-) > 240\ \text{GeV}$

$|M_{\ell^+\ell^-} - M_Z| < 2\ \text{GeV}$!

$E_T(jj) > 240\ \text{GeV}$

$|M_{jj} - M_Z| < 7\ \text{GeV}$

RESIDUAL $\Sigma E_T < 50\ \text{GeV}$

$M_{jj\ell^+\ell^-} = (800 \pm 200)\ \text{GeV}$

$\Rightarrow$ PLOTS OF M_{jj} AND $M_{jj\ell^+\ell^-}$

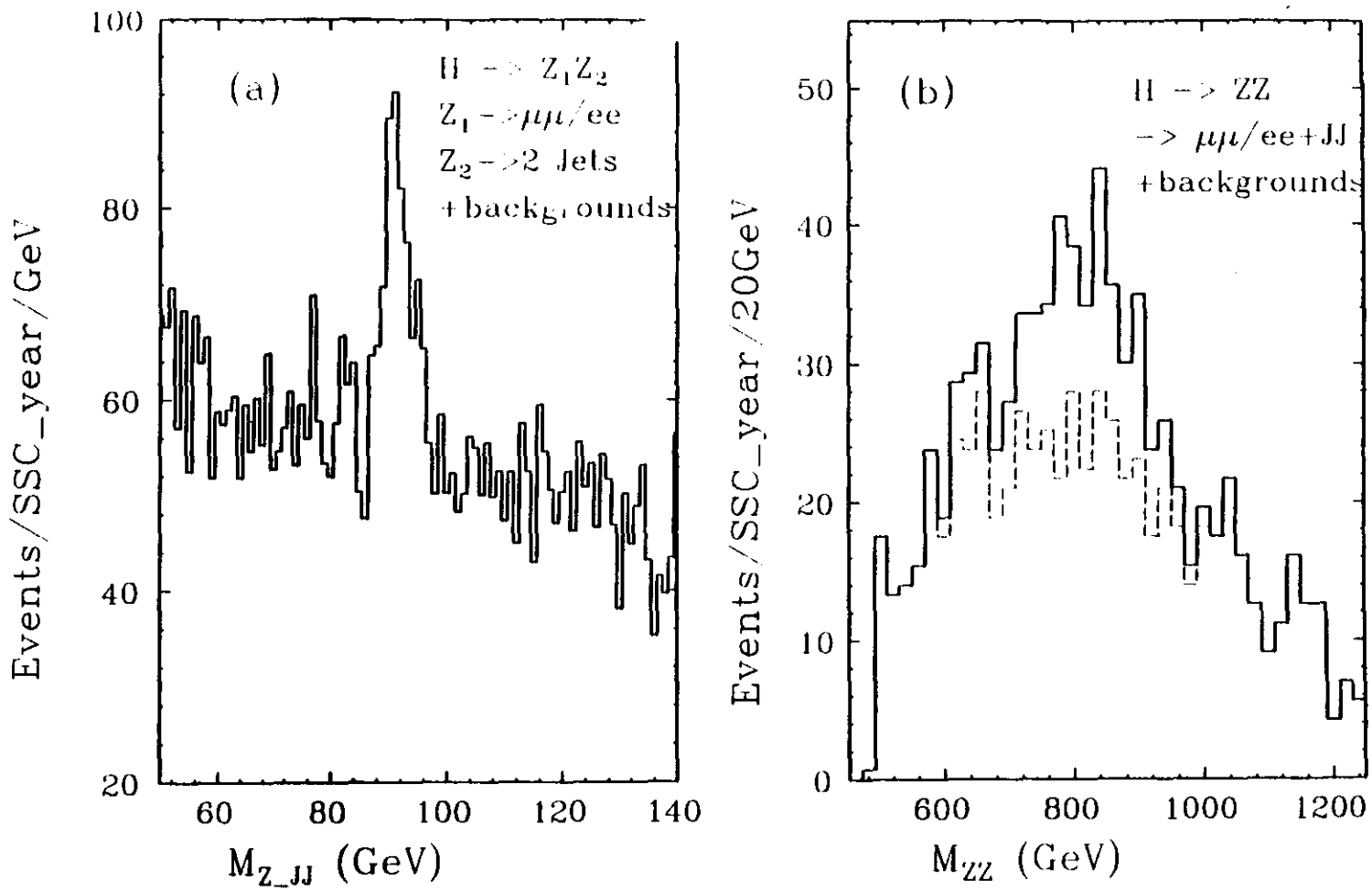
(a)
H -> Z1Z2
Z1 -> μμ/ee
Z2 -> 2 Jets
+backgrounds
Events/SSC_year/GeV
M_Z_JJ (GeV)
(b)
H -> ZZ
-> μμ/ee+JJ
+backgrounds
Events/SSC_year/20GeV
M_ZZ (GeV)

II. Heavy Top Quark (Protopopescu)

- Features Muon, HC

$$gg \to t\bar{t}$$

$t \to W^- + \bar{b}$, $W^- \to e^-/\mu^- + \nu$, $\bar{b} \to \mu^+ + \bar{c} + \nu$

$\bar{t} \to W^+ + b$, $W^+ \to jj$, $b \to j$

Tag: $W \to$ isolated e/μ.
$b \to$ nonisolated μ in c-jet.

Backgrounds - Negligible for $m_t \gg m_b$

Event Selection ($m_t = 250$ GeV):

Isolated e/μ from W, $E_T > 50$ GeV
Inclusive μ from b, $E_T > 40$ GeV
c-jet (excluding μ) has $E_T > 20$ GeV
≥ 3 additional jets, each $E_T > 20$ GeV
$|\eta_\ell| < 2.5$
$|\eta_j| < 2.5$ for m_t - determination

→ Plots of $M_{t \to Wb \to jjj}$ and $M_{W \to jj}$

$\int \mathcal{L}\, dt \simeq 100\ pb^{-1}$ (250 GeV) 2-3 days!
$50\ pb^{-1}$ (50 GeV)

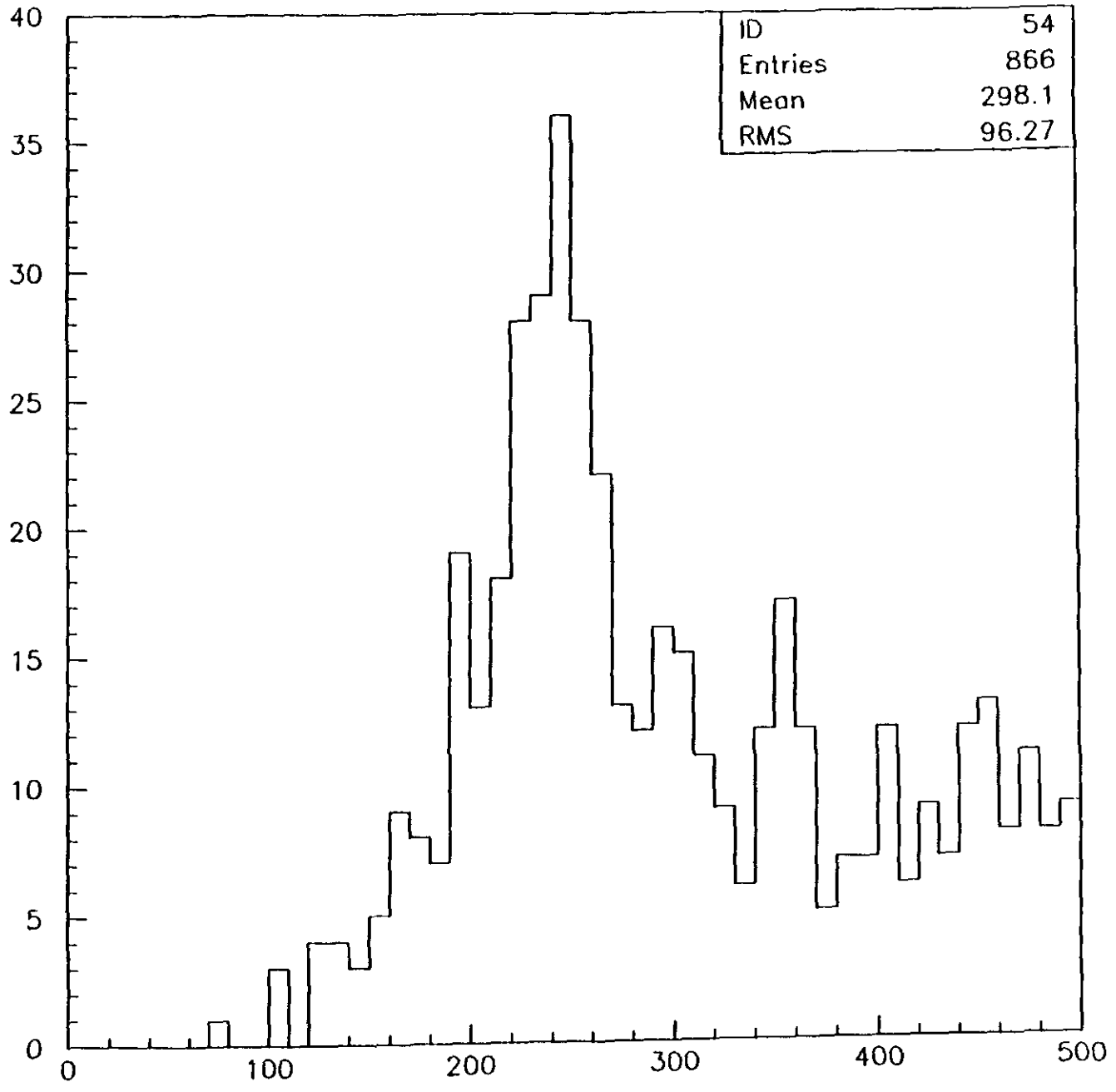
ID 54
Entries 866
Mean 298.1
RMS 96.27
0
5
10
15
20
25
30
35
40
0
100
200
300
400
500

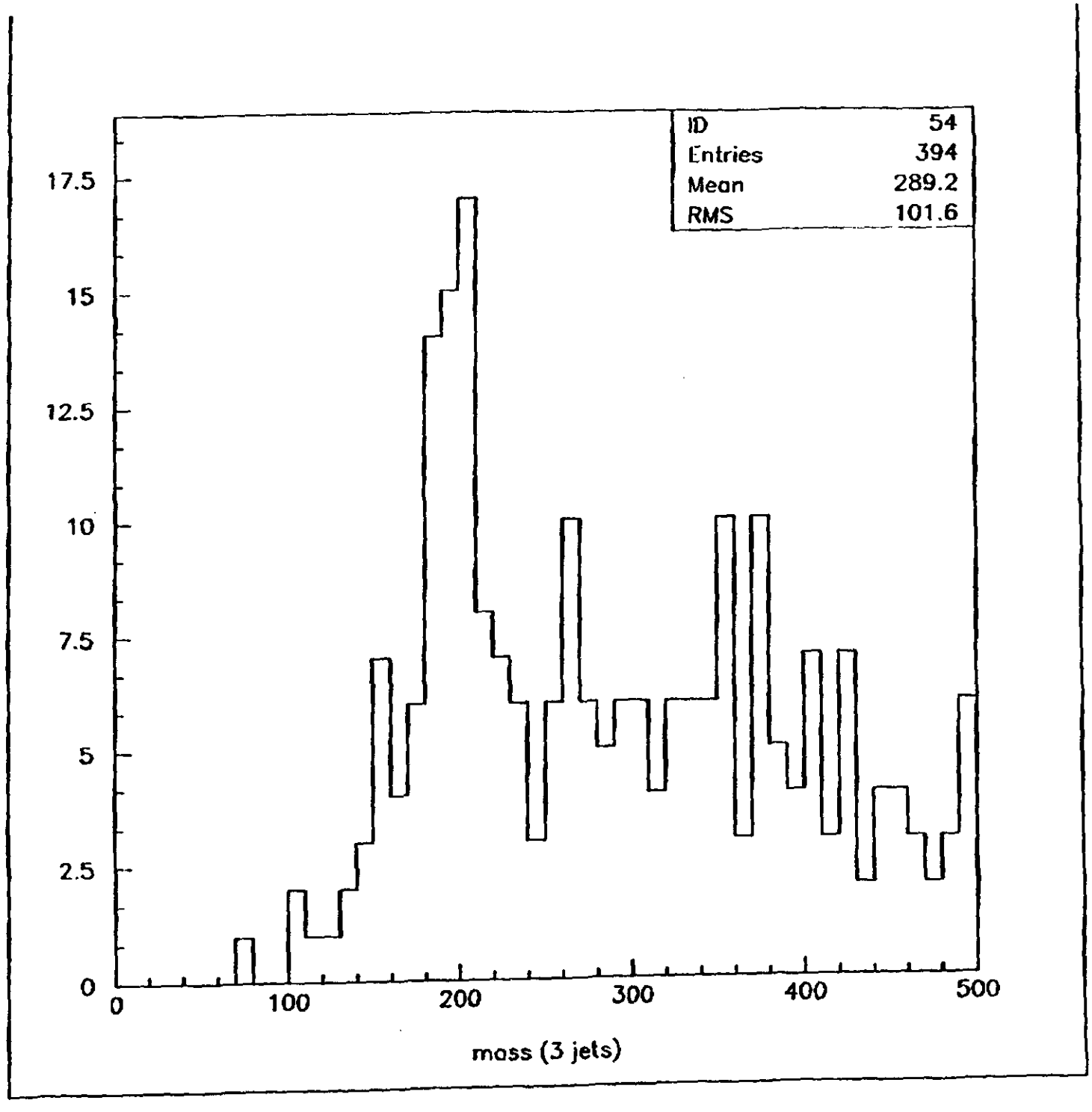
ID 54
Entries 394
Mean 289.2
RMS 101.6
17.5
15
12.5
10
7.5
5
2.5
0
0
100
200
300
400
500
mass (3 jets)

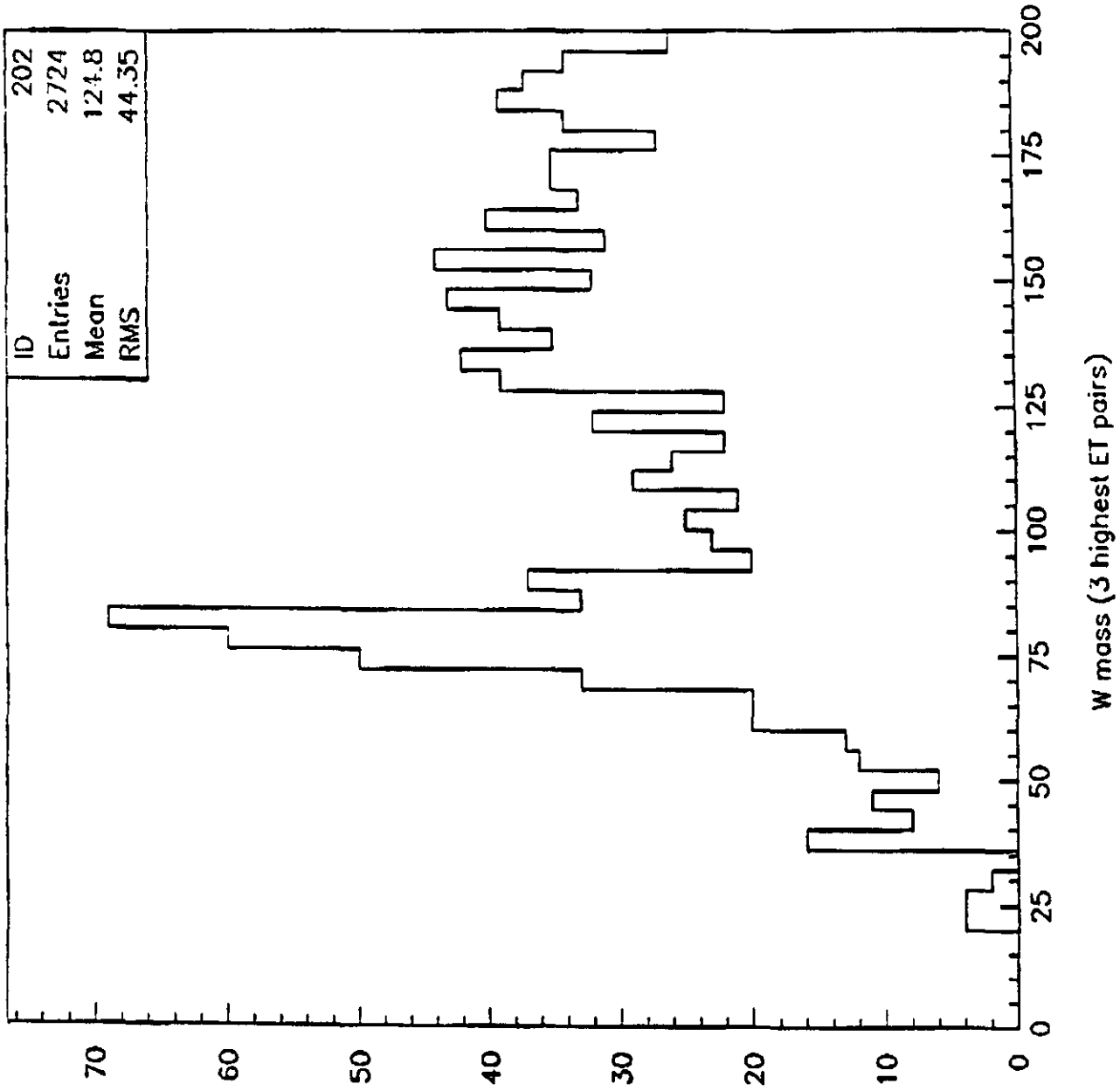
ID 202
Entries 2724
Mean 124.8
RMS 44.35
0
10
20
30
40
50
60
70
0
25
50
75
100
125
150
175
200
W mass (3 highest ET pairs)

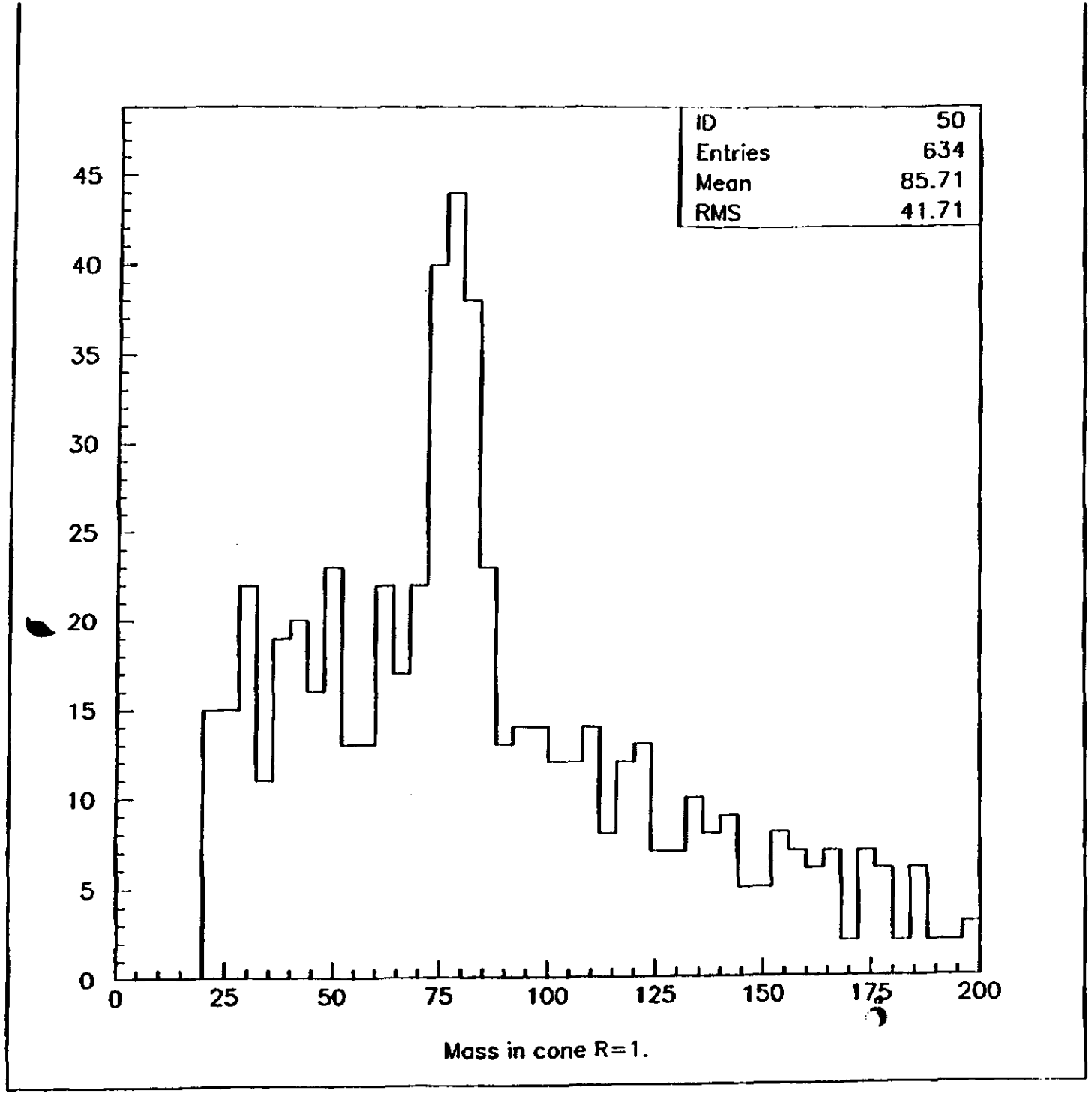
ID 50
Entries 634
Mean 85.71
RMS 41.71
0
5
10
15
20
25
30
35
40
45
0
25
50
75
100
125
150
175
200
Mass in cone R=1.

III. Complementarity – Reach Beyond the Standard Mode

- Features Muon ; EMC

Precision muon measurement outside calorimeter

➡ Flavor tagging

e.g., $\pi_{Q\bar{L}} \to b\mu$; $\eta_T \to t\bar{t}$

Increased reach at $\mathcal{L} \gtrsim 10^{34}$

e.g., $Z' \to \mu^+\mu^-$; $\bar{q}q \to \mu^+\mu^-$ M, asymme

Precision EMC ($\frac{1}{2}$% constant term)

➡ H^0, h, $\pi_T^0 \to \gamma\gamma$

$M_{Z'}$ reach, $\Gamma_{Z'}$; $\bar{q}q \to e^+e^-$ reach at $\mathcal{L} \gtrsim$

Many open questions:

EMC fast enough at $10^{33} - 10^{34}$?

Tracking – γ/e discrimination at 10^{34}?

EMC lifetime at 10^{34}?

⋮

q/ℓ Substructure in $\bar{q}q \to \mu^+\mu^-$ at 10^{34}

(Golden, Lane, Simmons)

Event Selection:

Highest-P_T μ^+, μ^- identified, charge well-measured

$P_{T\mu} > 100$ GeV

$M_{\mu\mu} > 1000$ GeV

μ^+, μ^- isolated

$|\varphi_{\mu^+} - \varphi_{\mu^-}|$ cut

Energy, cluster cuts

} To reject $\bar{t}t$, W^+W^-, Z^0Z^0, punchthrough, etc.

→ Plots (Very Preliminary)

$M_{\mu\mu}$ and $\cos\theta^*$ for

Standard Drell-Yan $\frac{d\sigma}{d(\cos\theta)} = a(1+\cos\theta)^2 + b(1-\cos\theta)^2$

"LL isoscalar" model $\frac{d\sigma}{d(\cos\theta)} = (1+\cos\theta)^2$

"Helicity non conserving" model $\frac{d\sigma}{d(\cos\theta)} = 1$

STANDARD DRELL-YAN $\bar{q}q \to \mu^+\mu^-$ xm12

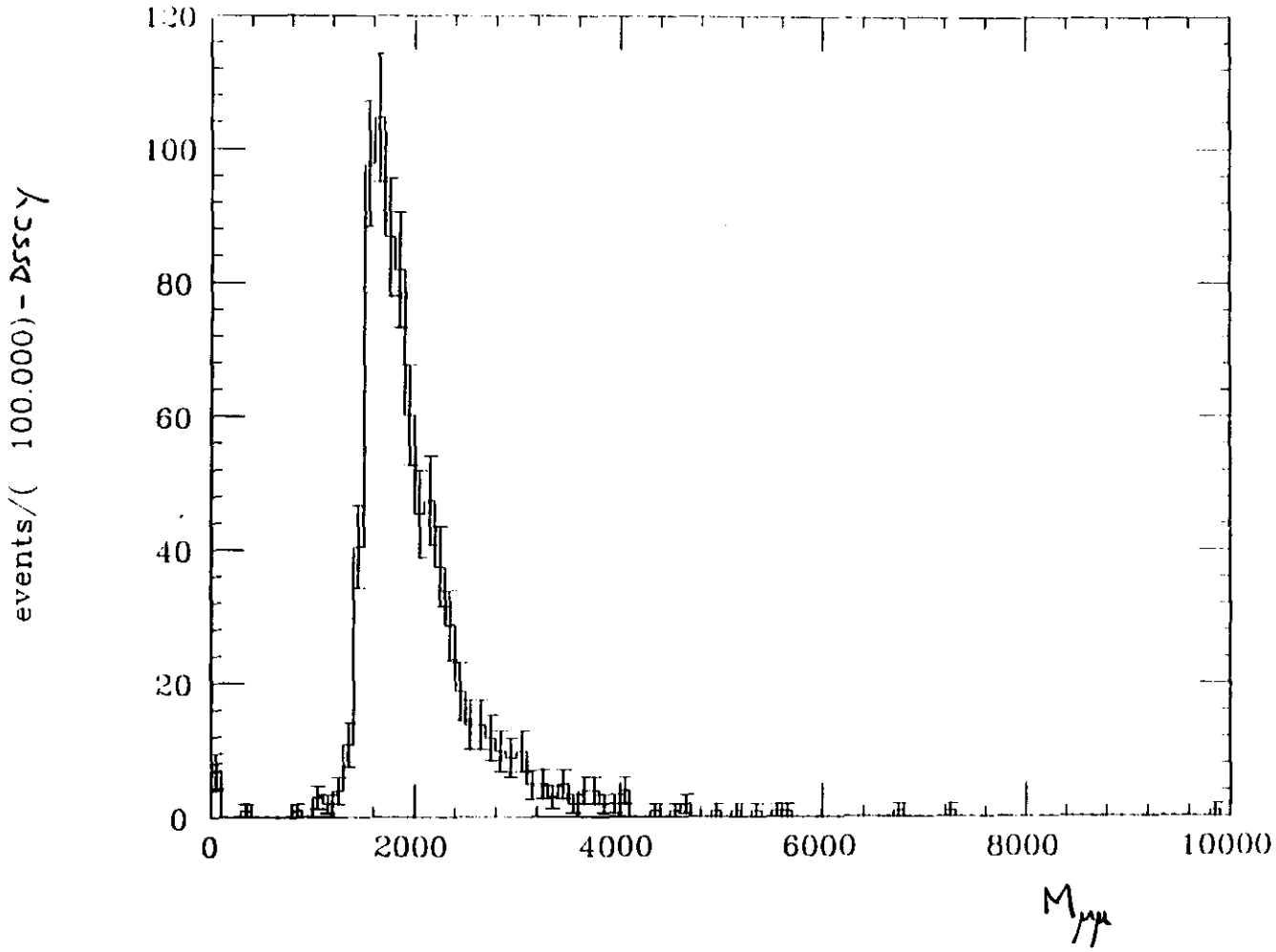

795 EVENTS

$\Lambda = 20$ TeV

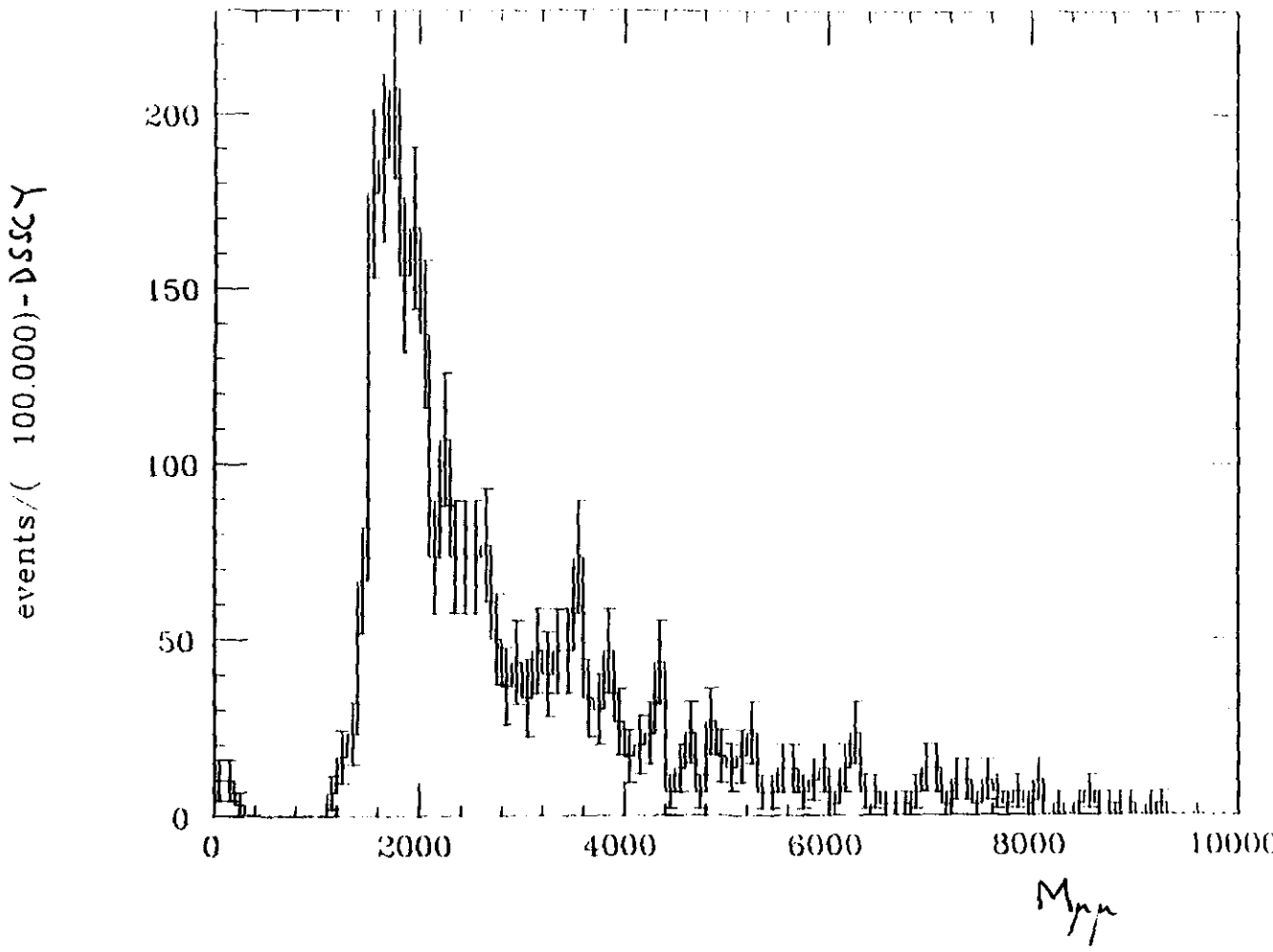

2556 EVENTS

HELICITY CONSERVING MODEL
$\Lambda = 20$ TeV

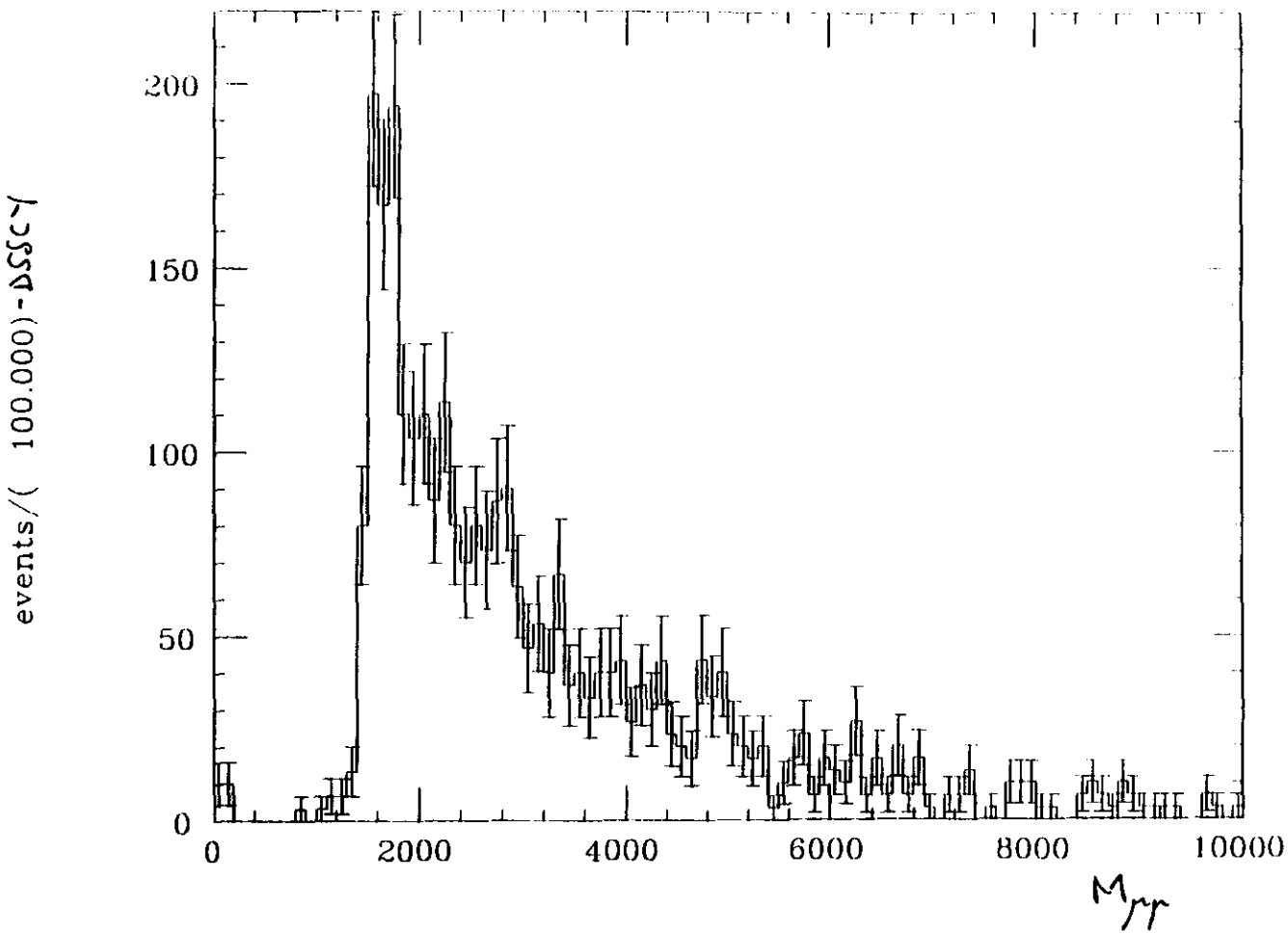

2959 EVENTS

STANDARD DRELL-YAN

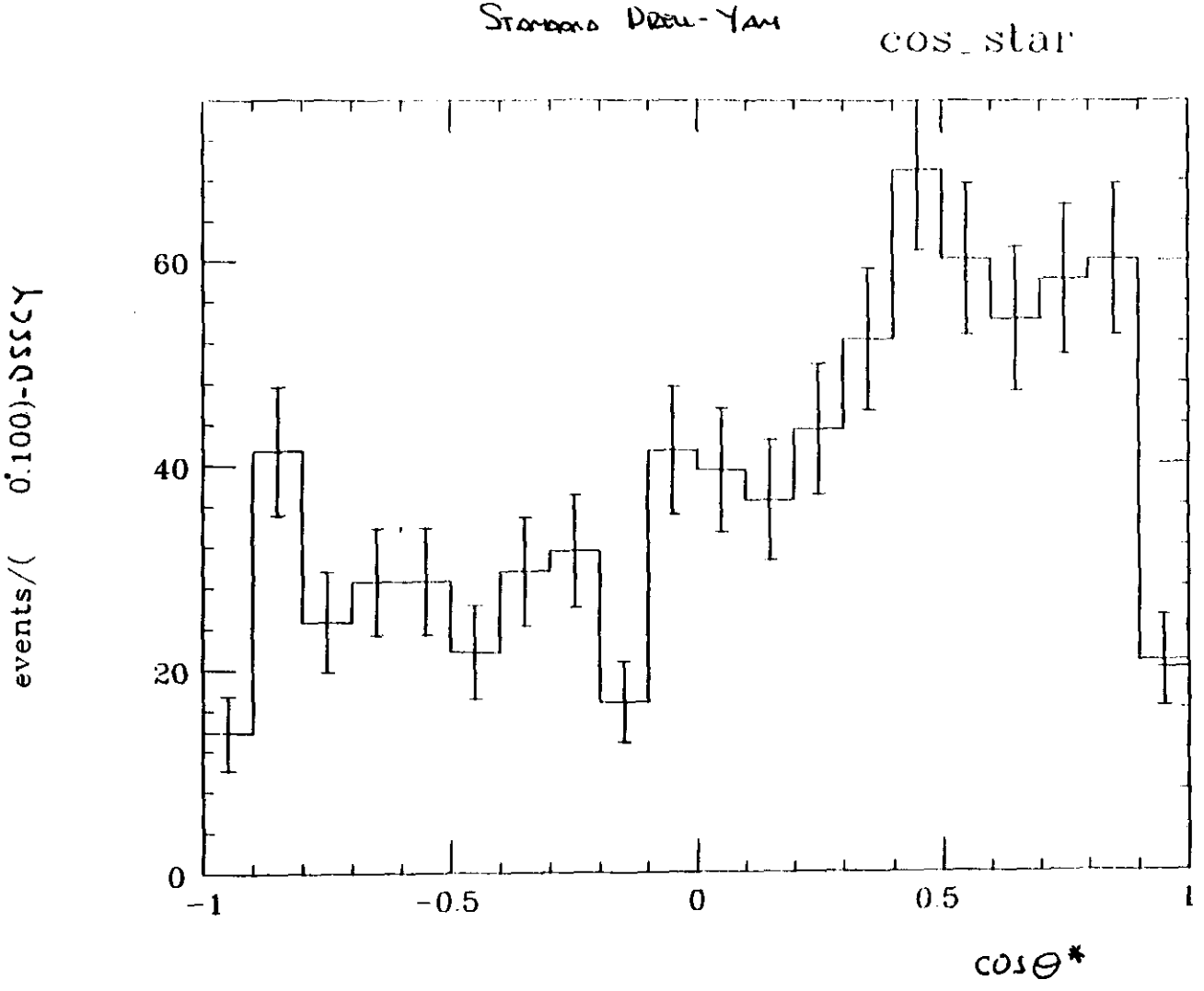

773 EVENTS

LL Is [illegible]
$\Lambda = 20$ TeV

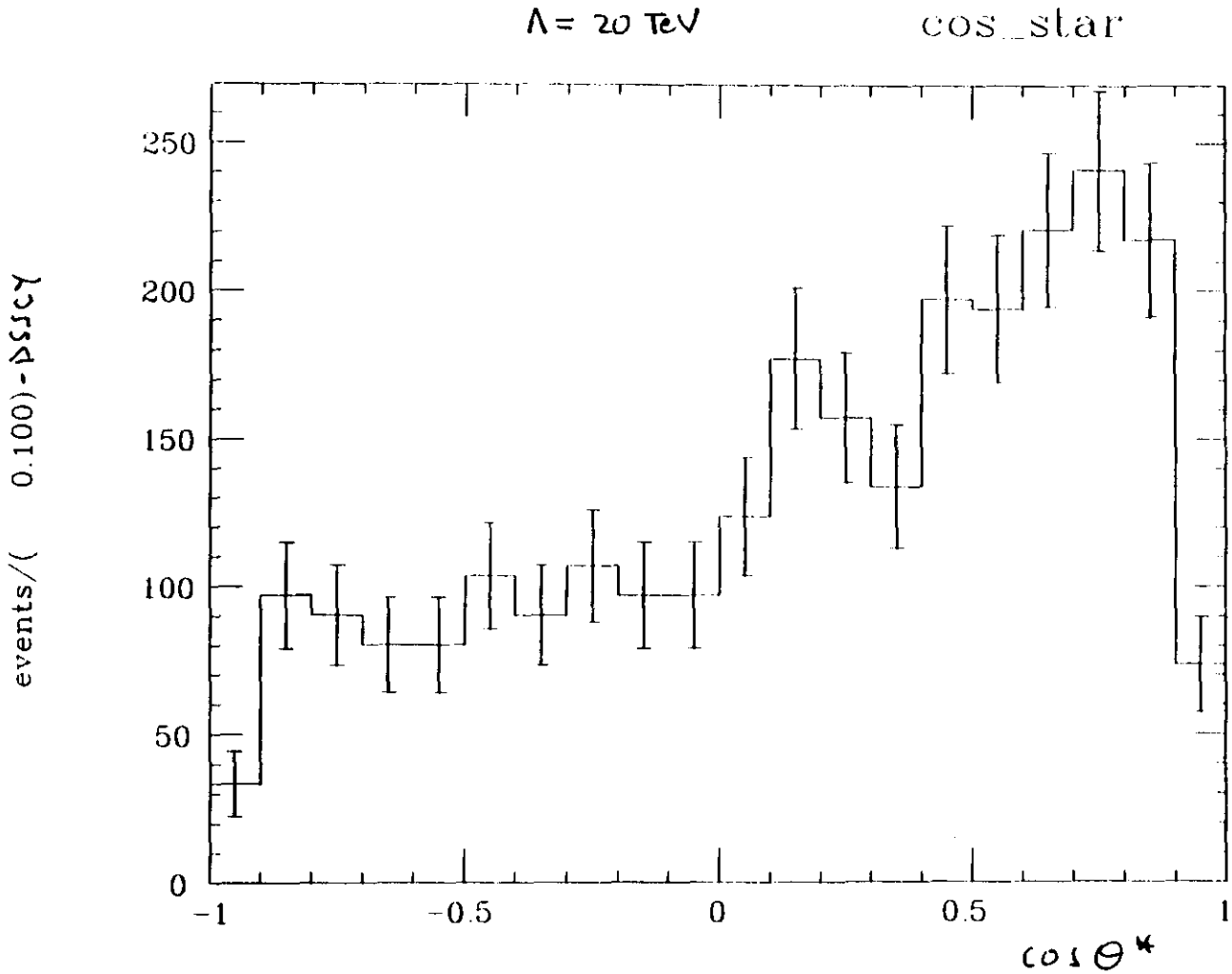

2438 EVENTS

GEM ENGINEERING/INTEGRATION

Status at EOI

1. Several descoped detector concepts were presented with costs scaled from Theriot panel reviewed costs.

2. Collaboration expressed its commitment to design to cost and schedule.

3. Engineering experience derived from L* and E/T engineering teams.

GOALS OF ENGINEERING/INTEGRATION EFFORT

SUPPORT OF FOUR TIME SCALES:

1. Subdetector trade studies (August-September 1991) - Support working groups on each subdetector.

2. Design/Cost/Schedule for Letter of Intent (August-November 1991) - Establish conceptual design for detector baseline, preliminary cost and schedule.

3. Engineering/Integration for Technical Proposal (August 1991-November 1992) - Organize engineering team, methodology and infrastructure to efficiently support Technical Proposal effort, avoiding possible reorganization following LOI review.

4. Support SSC Laboratory Experimental Facilities Definition (August 1991- ...) - Respond to SSC Laboratory requests for experimental facility user requirements needed for A/E design of conventional construction.

INITIAL ENGINEERING TEAM (Aug.-Sept. 1991)

1. PHYSICS COORDINATION - Gary Sanders, Michael Marx

2. ENGINEERING INTEGRATION - Coleman Johnson (LLNL); Brian Smith (LANL); Cliff Eberle (ORNL)

3. MAGNET DESIGN - Gary Deis, Coleman Johnson, ... (LLNL); Peter Marston, ... (MIT PFC)

4. MUON SYSTEM - Frank Nimblett, ... (Draper); Brian Smith, Jack Hanlon (LANL); Charles Grinnell (SSCL); Eric Hazen (Boston)

5. CALORIMETERS - Mark Rennich, Cliff Eberle, ... (ORNL); Francois Ayer, ... (Draper)

6. TRACKER SYSTEM - Ron Barber, Jan Boissevain, ... (LANL)

7. SSCL INTEGRATION - Mike Harris, Emil Sabin, David Etherton, Bob Richardson, Norm Gober, Marvin Hecht, Jon Piles, David Veal, Norm Wells, Ron Wooley, ... (SSCL)

RECENT PARTICIPATION

Dick Sumner (LeCroy), Lyle Mason (Martin Marietta Space Systems)

STATUS OF FOUR EFFORTS

1. Subdetector Trade Studies - Initial working group decisions made and, in some cases, being refined.

2. Design/Cost/Schedule for Letter of Intent - Baseline being established and study is beginning.

3. Engineering/Integration for Technical Proposal - Initial team organized and is being expanded. Some roles may evolve as subdetector choices are incorporated. Methodology for cost studies established. Future organization under discussion.

4. Support SSC Lab Experimental Facilities Definition - Draft of GEM Experimental User Facilities Requirements (GEFUR) in progress with first draft due late October, revision at end of calendar 1991.

Draft I

GEM Detector

Cost And Design Study For Scintillating Hadron Calorimeters

Oak Ridge National Laboratory

M. J. Rennich
C. L. Claffey
M. K. Singhal
C. C. Eberle

September 18, 1991

ENGINEERING/INTEGRATION INFRASTRUCTURE

1. Document Control System established.

2. Baseline cost targets established.

3. Interface Control drawings initiated.

4. Regular GEM/SSCL engineering coordination meetings scheduled and team established at SSC Lab with real presence.

5. First integration meeting held with physicists leading subdetector working groups.

6. Work Breakdown Structure (WBS) defined and adopted. Lessons learned from L* and E/T experience incorporated and external cost/schedule reviews accommodated in WBS.

7. GEM Cost Estimating Plan reviewed and adopted. Plan includes all cost book formats, definition of EDIA, contingency analysis methodology, labor rates, format for engineering basis presentations at reviews. Designed to facilitate frequent and detailed internal and external review and to insure uniform estimate quality across subsystems.

GEM COST TARGETS (29 JULY 1991)
($ MILLIONS)

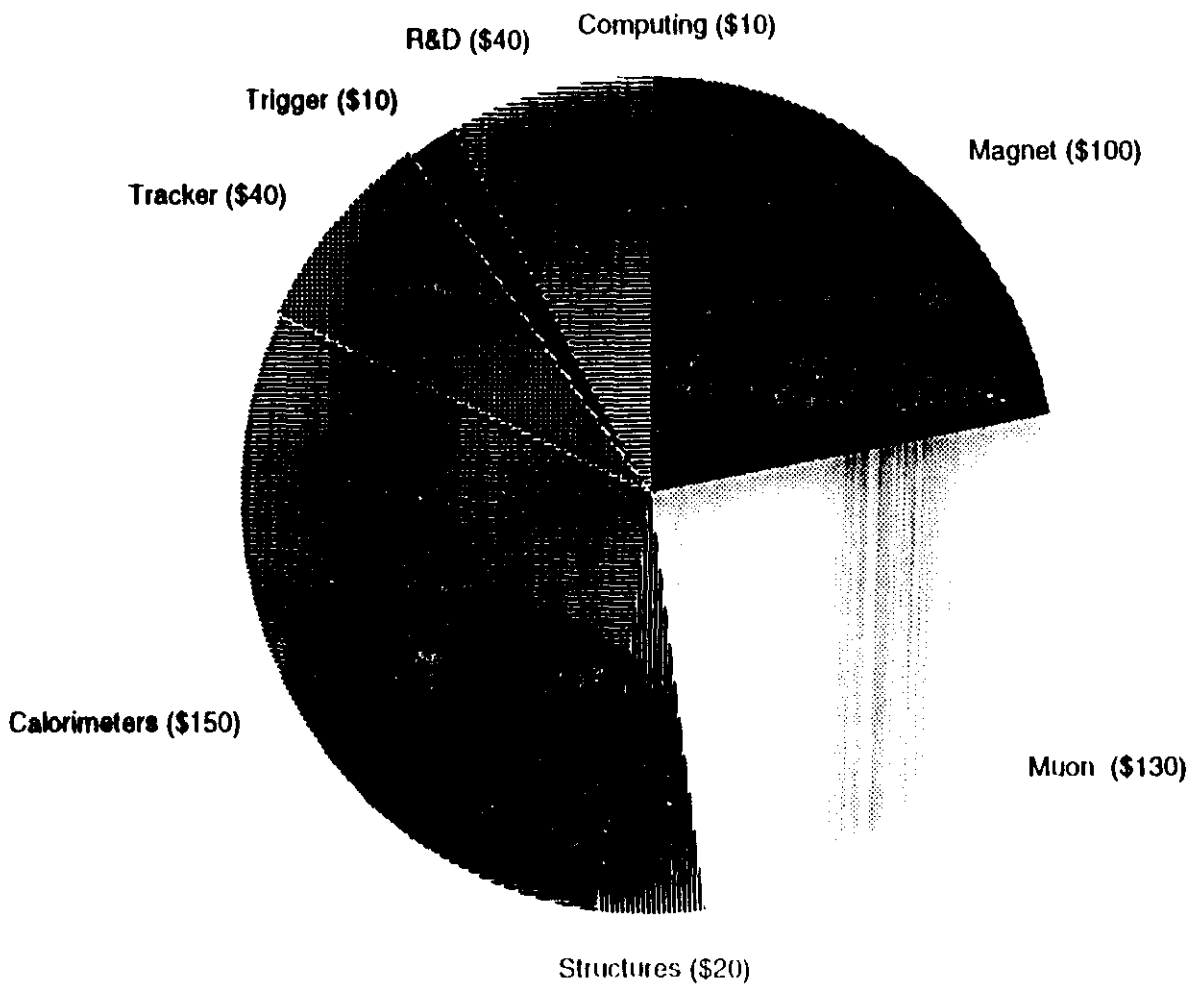

Approved by:

Ron Barber, LANL

Dave Etherton, SSCL

Tony Chargin, LLNL

Frank Nimblett, CSDL

Gary Deis, LLNL

Mark Rennich, ORNL

Dan Marlow, Princeton University

Prepared by:

Rick Sawicki, LLNL

Table of Contents

1.0 Scope
2.0 Objectives
3.0 Basis
4.0 Work Breakdown Structure
5.0 Cost matrix
6.0 Labor rates
7.0 Material costs
8.0 Risk Analysis/Contingency
9.0 Escalation
10.0 Supporting Documentation
11.0 Responsibilities
12.0 Review process
13.0 Schedule

Each WBS element shall be tagged with a cost basis descriptor which characterizes the type of estimate that was used. Acceptable data entries are as follows:

1) Bottom-up (BU)
2) Specification analysis (SA)
3) Parametric study (PS)
4) Revision update (RU)
5) Trend analysis (TA)
6) Expert opinion (EO)

5.2.2.3 Risk factors

The risk analysis described in Section 8.0 is used to calculate contingency. In the three columns provided in the SDT, technical, cost and schedule risk factors are input. Standard ranges for these parameters are as follows:

1) Technical risk - 1 to 10
2) Cost risk - 1 to 10
3) Schedule risk - 2 to 6

In some cases the standardized risk parameters may not be appropriate. Higher values may be used as described in Section 8.

5.2.2.4 Dates

Start dates and completion dates for all activities must be assigned to permit appropriate application of escalation factors to the base cost estimates. The month and year (numerical) shall be identified for the end dates of the four main functional categories, engineering./design, inspection/QA/administration, procurement/fabrication, and installation/assembly. These dates need only be input at WBS level 4. Costs at only this level will be used to escalate costs.

6.0 Labor rates

6.1 Estimators shall use their best discretion in selecting the labor rates that should be used for their GEM cost estimates. In making their decision, the estimators should determine where the work shall be performed and use the most accurate information available regarding the labor rates for that particular institution. Detailed backup information shall be provided in the cost book supporting any non-standard labor rate used. Rates used shall be fully burdened with all associated costs.

6.2 In many cases the exact source of labor will not be known. In these cases standard labor rates are provided below and should be used selectively as required.

6.2.1 National Laboratories

It is anticipated that the US National Laboratories will participate in many of the GEM subsystems. The following rates are average rates that may be used for work performed for any of these institutions. These rates include general overhead, support and payroll burden. If it is necessary to translate these rates to an hourly rate use 1800 hr/yr.

Type	Rate (k$/yr)
Manager	210
Secretary	60
Engineer/physicist	150
Designer/coordinator	90
Senior technician	100
Junior technician	75
Craft	65

6.2.2 National average rates

National average rates may be used for cases where the source of labor is completely unknown. If it is necessary to translate these rates to a yearly rate use 2080 hr/yr.

Type	Rate ($/hr)
Engineer/physicist	62.00
Senior technician	50.00
Junior technician	38.00
Craft	25.50
Machinist	25.50

6.2.3 SSC employees

Work performed by SSC employees shall be charged at the following rates which are fully burdened. If it is necessary to translate these rates to a yearly rate use 1800 hr/yr.

Type	Rate ($/hr)

SSC/GEM

Bottom-Level Work Breakdown Structure for the Muon Detector Subtask

Rev. 9

Todd Hamilton
Draper Laboratory

9/27/91
7:12

3.2.1.1.2.5.2 Assembly, Alignment & Testing
3.2.1.1.2.5.2.1 Off-site Assembly/Test
3.2.1.1.2.5.2.2 On-site Assembly/Test

3.2.1.1.2.6 Outer Layer
3.2.1.1.2.6.1 Assembly/Test Equipment
3.2.1.1.2.6.1.1 Assembly Tooling
3.2.1.1.2.6.1.2 Test Equipment

3.2.1.1.2.6.2 Assembly, Alignment & Testing
3.2.1.1.2.6.2.1 Off-site Assembly/Test
3.2.1.1.2.6.2.2 On-site Assembly/Test

3.2.1.1.4 Sector Support Structure
3.2.1.1.4.1 Final Design
3.2.1.1.4.2 Engineering Drawings Modifications/Generation
3.2.1.1.4.3 Assy/Process Instruction Modifications/Generation
3.2.1.1.4.4 Support Module
3.2.1.1.4.4.1 Truss Element Assembly
3.2.1.1.4.4.2 Truss Joint Assembly
3.2.1.1.4.4.3 Support Frame Assembly
3.2.1.1.4.4.4 Flexural Foot Assembly
3.2.1.1.4.4.5 Servo Motor/Spring Assembly
3.2.1.1.4.4.6 Kinematic Mounts
3.2.1.1.4.4.7 Insertion Rail Assembly
3.2.1.1.4.4.8 Assembly/Test Equipment
3.2.1.1.4.4.8.1 Assembly Tooling
3.2.1.1.4.4.8.2 Test Equipment
3.2.1.1.4.4.8.3 Dummy Chambers

3.2.1.1.4.4.9 Structure Assembly & Testing
3.2.1.1.4.2.9.1 Off-site Assembly/Test
3.2.1.1.4.2.9.2 On-site Assembly/Test

3.2.1.1.5 Alignment & Calibration Systems
3.2.1.1.5.1 Final Design
3.2.1.1.5.2 Engineering Drawings Modifications/Generation
3.2.1.1.5.3 Assy/Process Instruction Modifications/Generation
3.2.1.1.5.4 Sector Straightness Monitors
3.2.1.1.5.5 UV Laser Calibration System
3.2.1.1.5.6 Global Alignment Monitors

3.2.1.1.6 Sector Assembly Tooling/Facility Preparation
3.2.1.1.6.1 Assembly Tooling
3.2.1.1.6.2 Facility Preparation

3.2.1.1.7 Sector Assembly
3.2.1.1.7.1 Off-site Assembly
3.2.1.1.7.1.1 Mechanical Assembly
3.2.1.1.7.1.2 Electrical Assembly

3.2.1.1.7.2 On-Site Assembly
3.2.1.1.7.2.1 Mechanical Assembly
3.2.1.1.7.2.2 Electrical Assembly

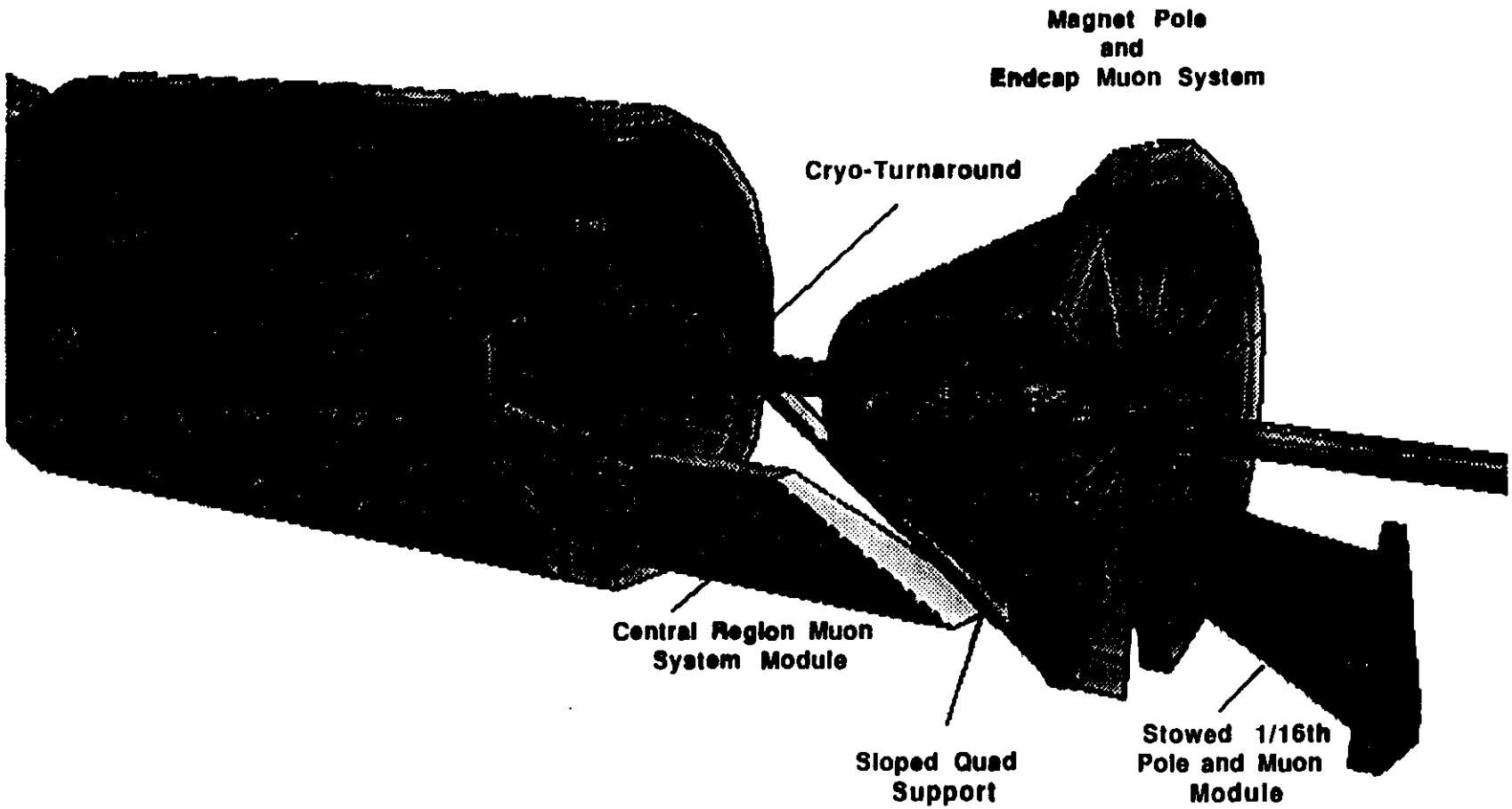

GEM
Muon System
Access

F. Nimblett
9/17/91

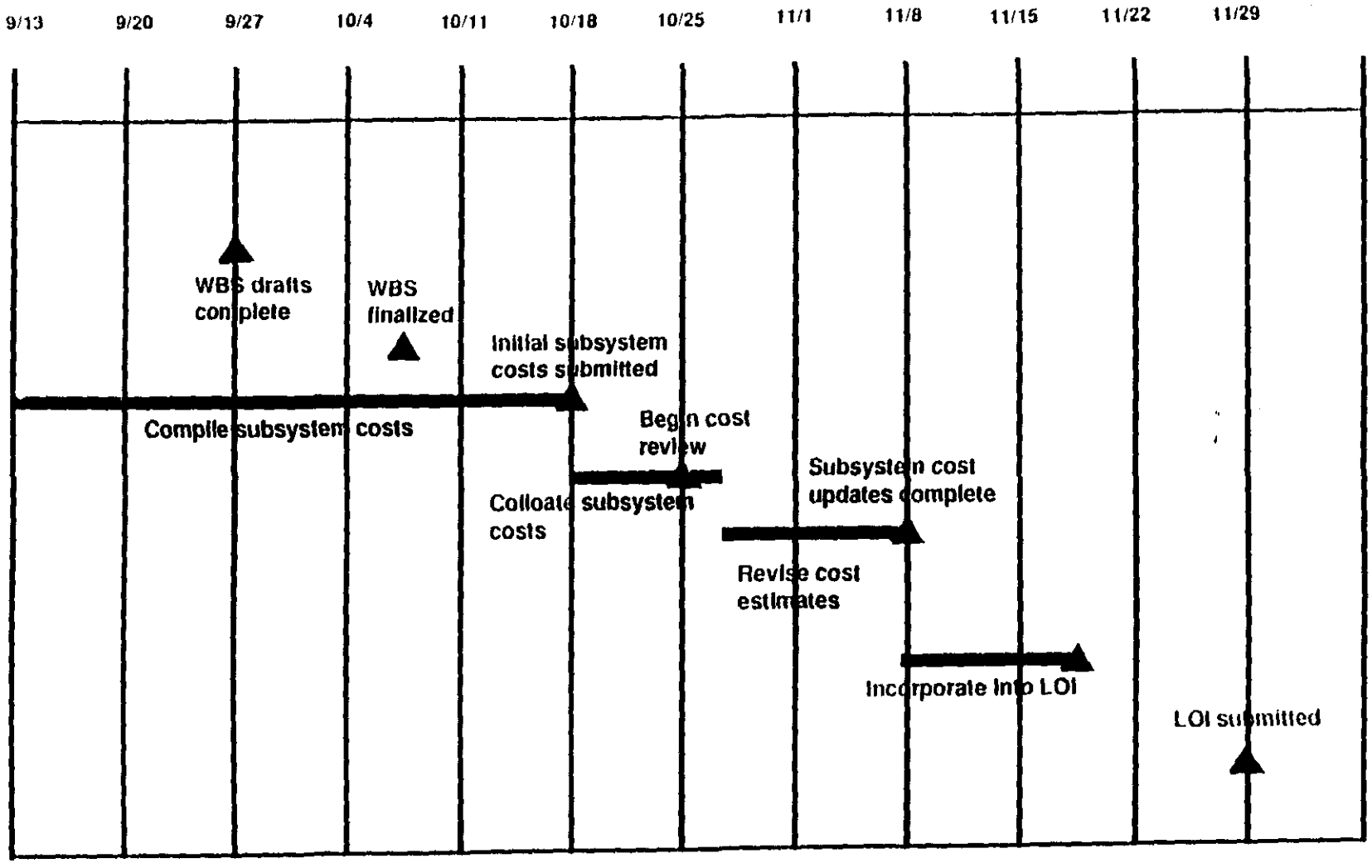

Table 4. Cost estimating schedule

COST ESTIMATE TIMELINE

GOAL: Cost estimate with basis of estimate advanced well beyond Theriot panel reviews of L* and SDC.

Based upon schedule followed in producing L* Cost Estimate, which began with a mature design and subsystem technologies identified well in advance, two months are required to produce full cost estimate.

For new technologies (muon drift tubes, accordion liquid argon calorimeter, pad chambers, spaghetti calorimeter, ...) an extra month is required for integrated conceptual design in order to reach same standard as L* cost estimate.

To advance major item estimates beyond Theriot panel, transmittal of estimate drawings to vendors and return of estimates will require one additional month.

System iterations may require additional time.

DELIVERABLES:

1. With Letter of Intent, cost estimate based upon engineering estimates, trend analysis, parametric study for technologies not previously included in L* or SDC reviews.

2. For full bottom-up analysis, inclusion of vendor/fabricator estimates, and system iteration, cost estimate available February 1, 1992.

MAIL> 40
#40 10-SEP-1991 12:10:44.62 MAIL
From: SSCVX1::MARX "MICHAEL MARX AT THE SSCL 214 708-6188"
To: BNLDAG::ATIYA,URHEP::SOLSEN,UCDHEP::LANDER
CC: @DEC.LST,MARX
Subj: Communique of GEM Decision Group to High Field Proponents

Response to the High Field Magnet Option
Proposed for the GEM Experiment

The GEM Decision Group
September 10, 1991

The High Field Option (HFO) Group has made a proposal to GEM to replace the large open magnet with a high field 5T magnet which encloses the calorimeters. The main advantages of this option are better resolution for high momentum muons, better coverage for all muons

Press RETURN for more...

MAIL>
#40 10-SEP-1991 12:10:44.62 MAIL
in the forward region (eta between 1.5 and 3), and less stringent alignment and precision requirements for the muon detectors. This option may also provide advantages in manufacturing of the magnet off-site, and in the reduction of fringe fields.

The GEM Decision Group expressed several key concerns with the new proposal:

(1) The HFO option presents major new problems which would have to be solved for the tracking and calorimetry systems, because of the high magnetic field. Examples are:

(a) The inability to use of vacuum photodevices, which appears to eliminate some of the principal calorimetry choices being considered by GEM, including: Barium Fluoride, scintillating fibers and liquid scintillator,

(b) The degradation of liquid ionization calorimeters because of

Press RETURN for more...

MAIL>
#40 10-SEP-1991 12:10:44.62 MAIL
interaction of the field with shower products in the inner vessel walls,

(c) The Lorentz angle, and systematics of coordinate reconstruction for chambers, particularly the first set of muon chambers in the high field region,

(d) The high occupancy levels in the tracking system generated by loopers.

(2) No specific physics example has been presented by the HFO group, to demonstrate the physics advantages are may result from the improved coverage and high-momentum muon resolution.

(3) The detector performance of the HFO is inferior to the GEM baseline design for low momentum muons.

These and related concerns would have to be investigated at a sufficient level of detail to provide confidence in the proper functioning

Press RETURN for more...

MAIL>
#40 10-SEP-1991 12:10:44.62 MAIL

of the complete experiment. The investigation would have to include a demonstration of both:

(a) The technical feasibility of operating various technologies in the high field, and

(b) The ability of GEM to achieve its main physics goals, given the new configuration, new systematic effects (e.g. in chambers), and possible reduced performance of some of the readout devices. This would involve both new device-performance studies, followed by simulation studies.

In addition to these specific concerns, there are the general concerns of the GEM Committee that:

(1) There has been little progress in the development of a plan for a complete experiment. The need to provide a complete experimental design was first discussed with the proponents in April. Since that time, there has been insufficient dialog between the HFO proponents and the

Press RETURN for more...

MAIL>
#40 10-SEP-1991 12:10:44.62 MAIL

various subsystems to expose the problems. The HFO group itself has not demonstrated any examples of viable alternative approaches, to allow the GEM subsystems to function in the presence of difficulties such as those listed above.

(2) There is insufficient basis to judge the feasibility of the HFO magnet, including issues of cost, technical and schedule risk. In particular, a plan to manufacture the magnet off-site, then transport it to the SSC, resulting in a substantial cost and/or time savings, has not been provided.

In summary, there was an overriding concern that a decision now to change the baseline magnet would result in an unacceptable delay of the experiment. This delay would result from (1) the severe narrowing of choices, (2) the inability to use much of the R&D on these systems which has already taken place (3) a complete reordering of our priorities and schedules for selecting the subsystems, and (4) our inability

to reconsider, recompile, and present a complete case for a superior experimental design to the PAC within a sufficiently short time.

Press RETURN for more...

MAIL>
#40 10-SEP-1991 12:10:44.62 MAIL

In the light these considerations, the Committee concluded that it would not be constructive to ask the HFO group to provide "answers" to the many specific concerns. It is the consensus of the group that the High Field Option would not be accepted as the basis of the GEM design at this time.

The GEM Collaboration may, however, reconsider the High Field option fully if some major technical obstacle arises which jeopardizes the implementation -- within the cost constraints, and on schedule -- of the baseline magnet. The cost and schedule of the baseline magnet is expected to be well-understood by the time the Magnet Review Committee finishes its work in early October.

In conclusion, the GEM Decision Group has considered the substantial potent
ial
advantages of the High Field Option, and has tried to weigh these advantages against the specific technical problems which it entials. We also have tried to consider the possibilities for incorporating it into GEM. We greatly appreciate the work and merit of the ideas presented by the

Press RETURN for more...

MAIL>
#40 10-SEP-1991 12:10:44.62 MAIL
proponents of the HFO, and now hope that they will join us on GEM, to work together towards our common physics goals. In addition to future work on the high field magnet option, we suggest that we work together to integrate the proponents of the HFO into several aspects of the principal GEM baseline activities. We also propose that if we decide to adopt the HFO as the basis of the GEM design at some future date, that we all join together with the HFO group to develop it into a complete experiment.

MAIL>

High Quality Muon Detection for GEM—an Alternative to the GEM-baseline Approach

M. Atiya, T. Kycia and M. Tannenbaum
Brookhaven National Laboratory, Upton, LI, NY 11973

Winston Ko, R. Lander and P. Yager
University of California at Davis, Davis, CA 95616

R. McNeil
Louisiana State University, Baton Rouge, LA 70803

C. Bromberg
Michigan State University, East Lansing, MI 48824

Q. Fan, G. Fanourakis, T. Ferbel, S. Kanda, S.L. Olsen,
P.F. Slattery, K. Ueno and M. Zielinski
University of Rochester, Rochester, NY 14627

M. Mohammadi
State University of New York at Stony Brook, Stony Brook, NY 11794

C. Rosenfeld and J. Wilson
University of South Carolina, Columbia, SC 29208

W. Vernon
University of California at San Diego, La Jolla CA 92093

J. Ritchie and A. Yamashita
University of Texas, Austin, TX 78712

A. Abashian, N. Morgan and L. Piilonen
Virginia Polytechnic Institute and State University, Blacksburg, VA 24061

P. Cushman, S. Hou and V. Singh
Yale University, New Haven, CT 06511

October 3, 1991

Abstract

We present an alternative approach for muon detection at the SSC based on a high field magnet (B = 5 Tesla) of "moderate" dimensions (radius = 3.5 m; overall length = 15 meters). A precision determination of a muon's momentum is made using a point-slope method, where the point is the interaction point and the slope is the direction of the muon's track as it exits the magnet coil. Momentum resolutions on the order of $\Delta p_t/p_t \simeq 4\%$ are possible over large solid angles for muon momenta as high as 1 TeV with rather modest alignment ($\sim 200\mu$m) tolerances, with standard drift chamber resolutions ($\sim 100\mu$m), and with no reliance on the performance of an inner tracking system. Robustness is provided by additional momentum measurements in the inner tracker and in a solid iron spectrometer based on the magnet's return yoke. The total cost of the system, including a proper magnetic shielding for the magnet and a forward-backward iron-core toroid muon detection system with $\Delta p/p \simeq 9\%$, is comparable to that of the low-field GEM-baseline approach without a magnetic flux return and with no forward-backward muon system. The magnet leaves the same amount of space for inner detector items as does the large, low-field L*-type system, while providing a substantially higher magnetic field in the inner tracking volume.

1 INTRODUCTION

1.1 Review of the GEM-baseline Scheme for Muon Measurements.

The central theme of the GEM-baseline detector design is its emphasis on precise measurements on gammas, electrons and muons. The detector concept, as presented in the group's Expression of Interest (EOI) [1], is dominated by a large (inner radius = 8.5 m; overall length = 28 m), relatively low-field (B = 0.8 Tesla) solenoid magnet that supports an air-core muon spectrometer situated radially outside of an inner tracker system and electromagnetic and hadronic calorimeters. All detection elements are inside the coil. The muon spectrometer, which extends radially from R = 3.6 m to 8.5 m, determines muon momenta by a measurement of the sagitta of the muon's trajectory in the solenoid's magnetic field (see Fig. 1). The alignment tolerances of the muon spectrometer system are controlled by the requirement of a precise measurement of the trajectory's sagitta δ, where

$$\delta(\mathrm{mm}) = \frac{0.3B(\mathrm{Tesla})L^2(\mathrm{m})}{8p_t(\mathrm{TeV/c})} \simeq \frac{0.75\ \mathrm{mm}}{p_t(\mathrm{TeV/c})}.$$

Thus, a $\Delta p_t/p_t \simeq 5\%$ measurement at $p_t = 0.5$ TeV/c requires a $\sim 75\mu$m resolution on the sagitta measurement, placing strict requirements on the alignment of the various elements in the muon spectrometer. These precise alignment tolerances for large chambers separated by large distances ($\Delta R \sim 5$m) result in a muon system that accounts for the largest part of the estimated cost for the GEM-baseline detector.

While the proposed muon spectrometer gives the desired 5% resolution (at $p_t = 0.5$ TeV/c) over the central region of the detector (i.e., for $|\eta| < 1.4$), the resolution for larger $|\eta|$ values rises rapidly, as can be seen in Fig. 2. Improvements in the resolution in the forward direction will require systems that cover very large areas. The GEM-baseline magnet provides a rather modest field of only 0.8 T in the inner tracking region. As a result, the EOI projects a momentum resolution for the inner tracker of $\Delta p/p \simeq 130\%\ p(\mathrm{TeV/c})$, which precludes, for example, the ability to measure electron charges reliably for momenta above $\sim$ 200 GeV/c. Moreover, the size of the magnet makes the provision of a proper path for returning its magnetic flux difficult. Three approaches for dealing with the magnet's return field have been suggested:

1. a passive iron return, which would require approximately 25,000 metric tons of iron and an increase in the radial dimension of the detector by $\sim$ 2m;
2. a second superconducting coil of even larger radius, whose sole function is to return the field;
3. no flux return at all.

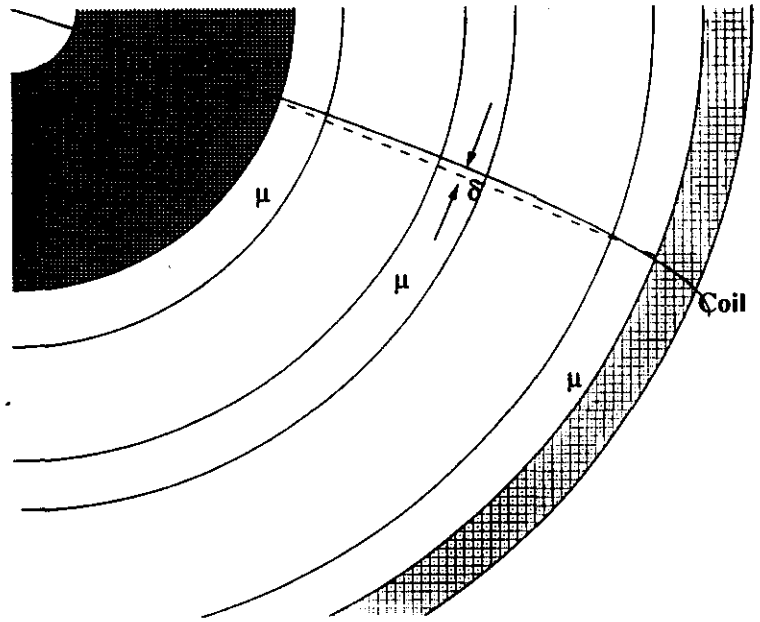

Figure 1: A cross section of the GEM-baseline detector illustrating the sagitta technique used for muon momentum measurements.

The first two approaches add substantially to the cost of the detector and interaction hall (Δcost$\geq$ \$50M), and the last approach results in significant magnetic fields extending for some distance above ground level near the detector area.

1.2 The Proposed High Field Option

In light of the limited η coverage for muons, the momentum resolution of the inner tracking system, and the flux return concerns of the GEM-baseline detector arrangement, we propose an alternative approach to muon detection, one that emphasizes excellent resolution for very high momenta over a larger solid angle, and is based on detection elements with alignment tolerances that are an order-of-magnitude less demanding than that of the EOI concept.

Our proposed system, illustrated in Fig. 3, is based on a high-field (B = 5 Tesla) magnet with dimensions (inner radius = 3.5 m, overall length = 15 m) selected to have minimal interference with the other detection systems. We estimate that the costs of our proposed system, which includes a properly shielded magnet and iron-core-toroid muon spectrometers covering the forward-backward regions ($|\eta| \leq 3.5$), are comparable to those of the GEM-baseline system.

1.2.1 Point-Slope Measurements of Muon Momenta

In our proposed high-field scheme, we abandon the reliance on a sagitta measurement for the determination of muon momenta and employ instead a point-slope measurement. For the point, we exploit the precisely known transverse position of the interaction point; for the

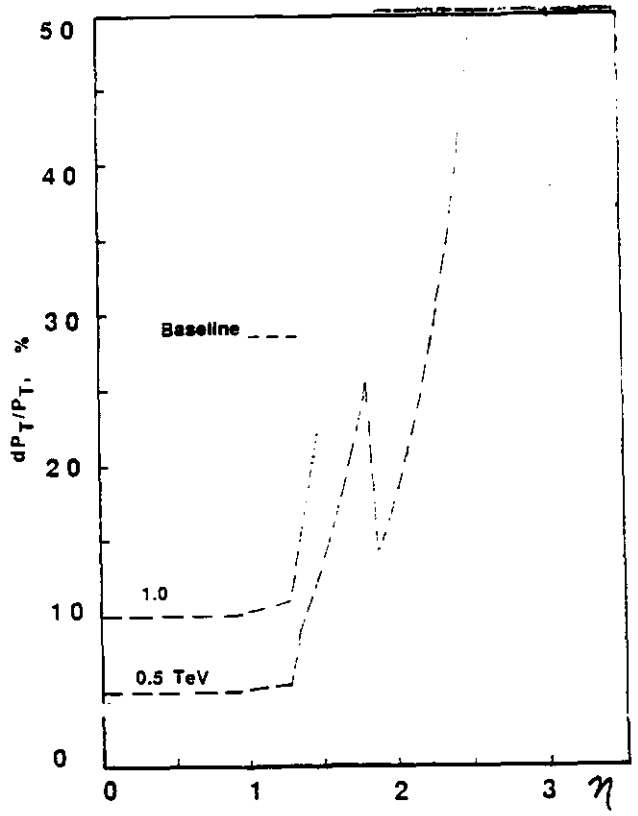

Figure 2: $\Delta p_t/p_t$ *vs* $|\eta|$ for the GEM-baseline detector.

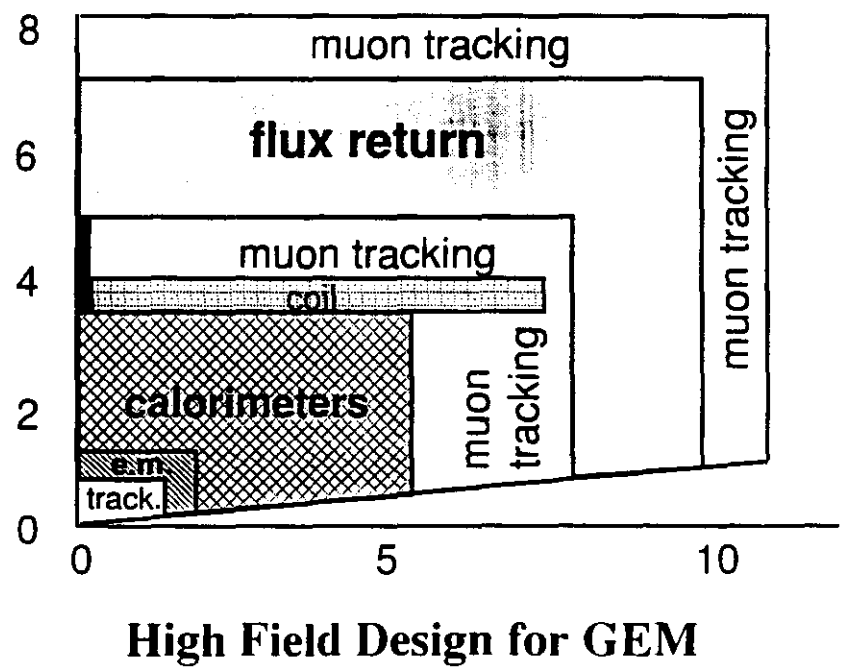

Figure 3: The proposed high field detector arrangement.

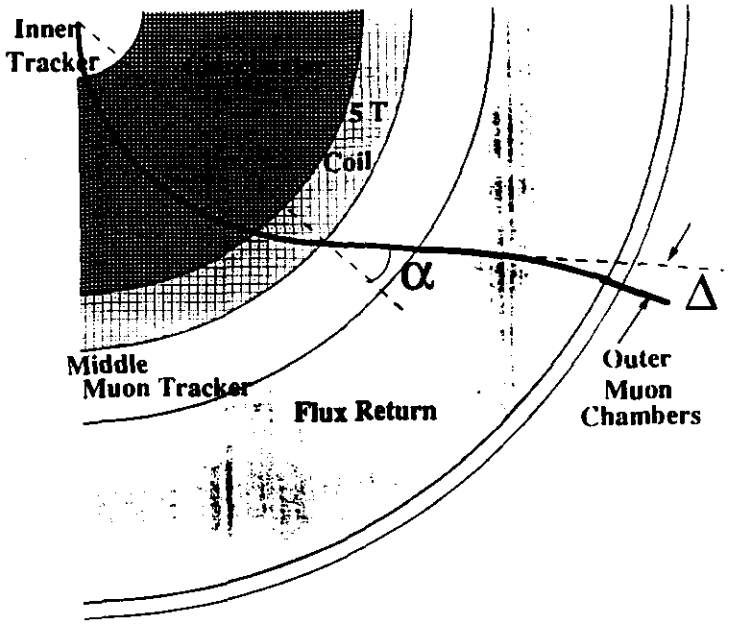

Figure 4: A cross section view of the proposed system illustrating the technique used for muon momentum measurements. The angle α is inversely proportional to the muon's transverse momentum.

slope, we use the angle of the muon's trajectory (relative to the radial direction) as it emerges from a solenoid coil situated radially outside of the inner detector, as illustrated in Fig. 4. We estimate that a 15 m-long superconducting coil with inner radius $R = 3.5$ m (about the same as the inner radius of the inner muon chambers of the GEM-baseline design) can have a field of $B = 5$ Tesla for approximately the same cost as the large (28 m-long, $R = 8.5$ m) low-field ($B = 0.8$ Tesla) magnet described in the GEM group's EOI. A magnet coil of this size leaves the dimensions of the inner detector essentially unchanged.

The momentum of the muon can be directly inferred from the angle between the track vector and the radial direction (the angle denoted as α in Fig. 4) as:

$$\alpha(\text{mrad}) = \frac{0.3B(\text{Tesla})R(\text{m})}{2p_t(\text{TeV/c})} \simeq \frac{2.7\text{mrad}}{p_t(\text{TeV/c})}.$$

The fundamental limit on the precision of this measurement derives from the multiple scattering of the muons in the material of the inner detector, given by the rms multiple-scattering angle θ_{ms}, where

$$\theta_{ms} \simeq \frac{0.014(\text{GeV})}{p}\sqrt{\frac{x}{x_{rl}}}.$$

Here, x/x_{rl} is the amount of material in the inner detector and magnet coil in units of radiation lengths. For the inner detector, we take the the amount of material at $\theta = 90°$ to be $x/x_{rl} \simeq 130$, which allows for a 30 x_{rl} EM calorimeter, an 8λ ($\simeq 80x_{rl}$) stainless-steel radiator hadron calorimeter and a $20x_{rl}$ "thick" superconducting coil and cryostat. In this

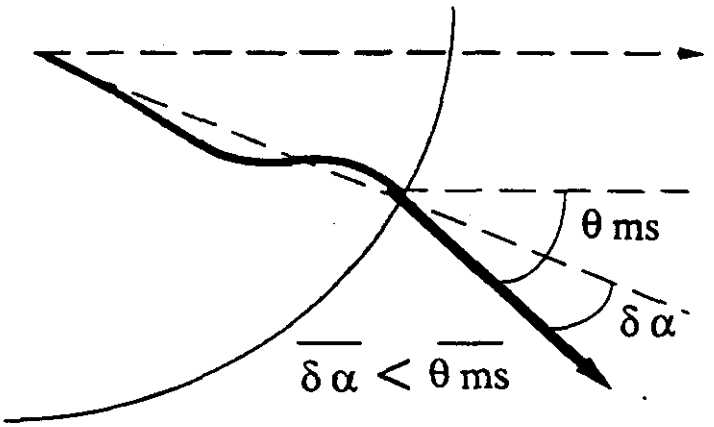

Figure 5: An illustration of the correlation between the multiple scattering angle θ_{ms} and the error in the radial direction caused by the multiple scattering induced transverse displacement of the trajectory. The resulting error in α is smaller than θ_{ms}.

configuration, the multiple scattering uncertainty is

$$\theta_{ms} \simeq \frac{0.16mrad}{p_t(TeV)},$$

and a simple estimate of the limiting precision on $\Delta p_t/p_t$ is given by

$$\frac{\Delta p_t}{p_t} \simeq \frac{\theta_{ms}}{\alpha} = 0.06,$$

which (at $\theta = 90°$) is independent of p_t. In fact, a more precise calculation indicates that the situation is somewhat better than this. Multiple scattering, in addition to introducing an uncertainty in the angle α, produces a transverse displacement that is correlated with the multiple scattering angle. This translation results in a change in the inferred radial direction that partially compensates the uncertainty in α, as illustrated in Fig. 5. The α distribution for a complete GEANT simulation of a sample of 1 TeV/c muon tracks, including, plural- as well as multiple-scattering, is shown in Fig. 6. Here the multiple-scattering limit on muon momentum resolution is just the rms width of the distribution, which is $\Delta p_t/p_t = 4.1\%$. Simulations for 100 GeV/c muon tracks yield the same multiple scattering limit on the resolution.

The multiple scattering limit sets the scale of precision required for measurements—for measurements up to $p_t \sim 1$ Te/V/c, the angle of the track exiting the coil must be measured with a precision that is ≤ 0.1 mrad, This can be readily done in a radial space of $\Delta R \sim 1$ m using conventional tracking systems. The track's exit position from the coil relative to the interaction point is used to define the radial direction and must be known with a precision of $< 350\mu$m. This sets the scale for relative alignment requirements. Thus, systems with conventional alignment tolerances will provide an excellent momentum resolution of $\Delta p_t/p_t \simeq 5\%$ for p_t up to ~ 1 TeV/c! (For p_t values above 1 TeV/c, the ~ 0.1 mrad measuring precision results in a gradual deterioration in $\Delta p/p$.) The above

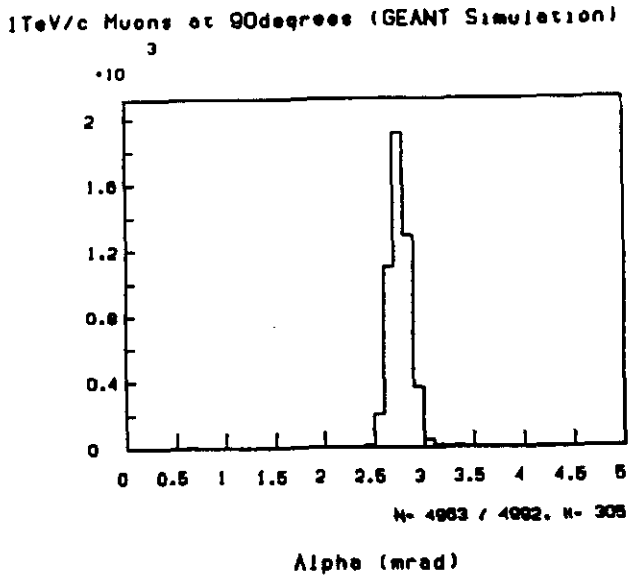

Figure 6: The distribution on α from a simulation of 1 TeV/c muons. The rms spread is 0.11 mrad.

discussion is for $\theta = 90°$. The results of an analysis of our proposed system extended over all angles and for a variety of muon momenta are shown in Fig. 7. Also shown are the expectations for the GEM-baseline design.

(If, in addition to the external measurements, a single position measurement, with a spatial precision of $\sigma \sim 50\mu$m , is used from the outer region of the inner tracker, the resolution can be further improved to the ~3% level. In Fig. 8, we show the expected resolution for the case where an inner tracking coordinate at $R = 75$ cm with a precision of ~50μm is incorporated into the momentum measurement. Of course, if the complete track is found in the inner tracker, a totally independent momentum measurement can be made and used to improve the overall resolution.)

1.2.2 Forward-Backward Muon Coverage

If one is to accomplish the physics goals of a high-p_t detector at the SSC, momentum resolutions must not deteriorate at $|\eta| \sim 1.5$, as it does in Figs. 7 and 8. For example, Fig. 9 shows the efficiency for detecting all four muons from the reaction

$$pp \longrightarrow Higgs + X; \qquad Higgs \longrightarrow Z^o Z^o \longrightarrow \mu^+\mu^-\mu^+\mu^-,$$

for different Higgs' masses as a function of the maximum $|\eta|$ value of the muon acceptance [2]. From the figure it is clear that there is a premium on having good muon detection down to $|\eta| = 3 \sim 3.5$, particularly for lighter Higgs' masses. If one is restricted to $|\eta| \leq 1.4$, the efficiency for this reaction is limited. (This is particularly true for Higgs masses below $2M_Z$, where the Higgs$\longrightarrow Z^o Z^*$ decay channel is important. Here, since the Higgs is relatively light, it tends to be produced in the forward direction, and, since the branching ratio is small, event rates are small and good efficiency is important.)

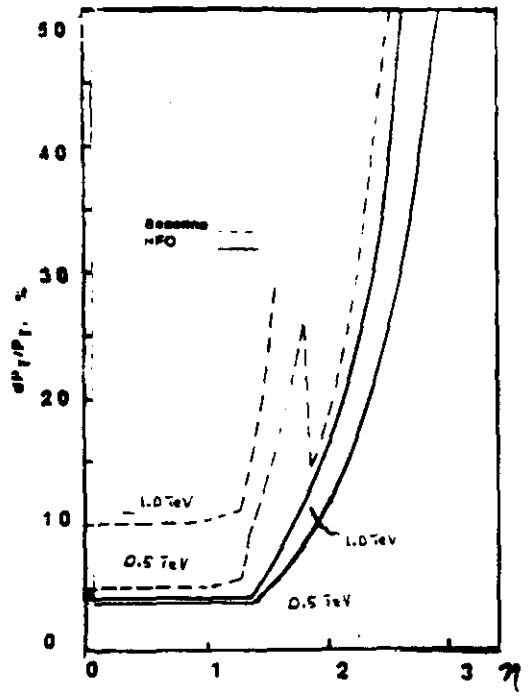

Figure 7: The expected transverse momentum resolution ($\Delta p_t/p_t$) for the proposed system from measurements in the middle tracker only.

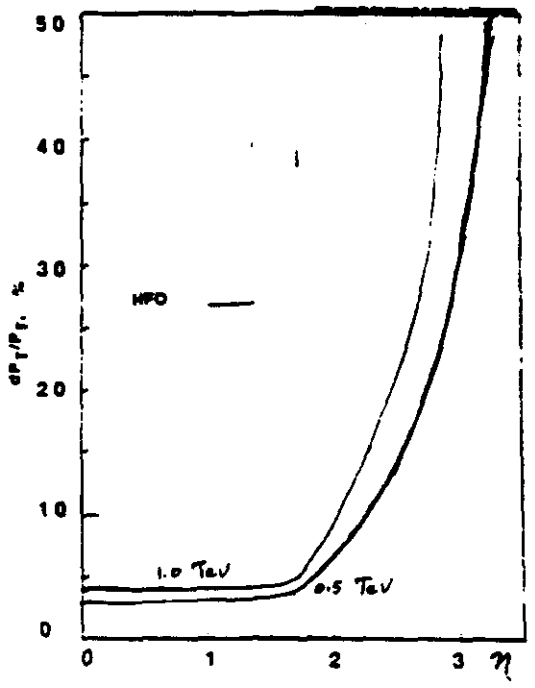

Figure 8: The expected transverse momentum resolution ($\Delta p_t/p_t$) for the case where one point from the inner tracker is used assuming a resolution of $\sigma = 50\mu$m at $R = 75$ cm.

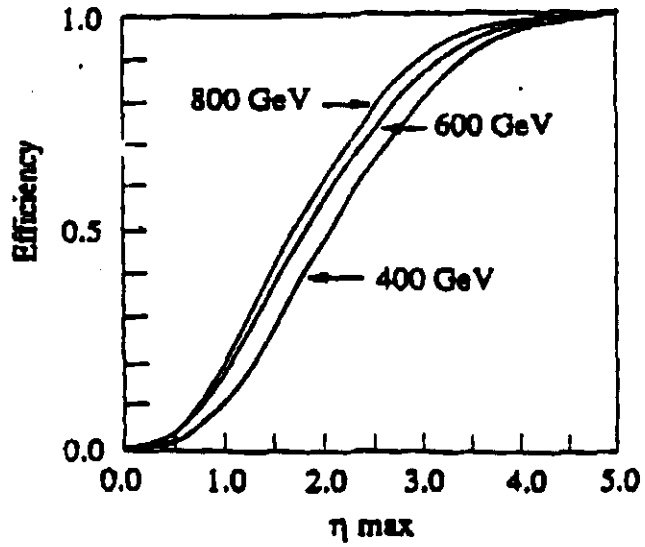

Figure 9: The efficiency for Higgs$\longrightarrow \mu^+\mu^-\mu^+\mu^-$ *vs* the maximum $|\eta|$ of the muon acceptance (from ref. 2).

To provide adequate momentum resolution in the forward-backward region, we propose to incorporate iron-core toroids covering the $2 \leq |\eta| \leq 3.5$ region, as indicated in Fig. 10. Two 2-meter thick toroids at each end of the detector will provide a multiple scattering limited momentum resolution in this region of $\Delta p/p \simeq 9\%$. Here, the relative compactness of the high field system allows this to be done with $R \simeq 5$ m toroids; each toroid weighs about 1.2 ktons. With this system, we get reasonable muon coverage out to $|\eta| \leq 3.5$. Figure 11 shows $\Delta p_t/p_t$ *vs* $|\eta|$ for the complete system.

1.2.3 "Robustness"

The measurement of a single, straight-line track segment by itself would hardly qualify as a "robust" measurement. A low-momentum track could scatter through a large angle and emerge from the coil near the radial direction, faking a high momentum track. Therefore, the track segment measurement must be tightly constrained by other measurements in the system, both at the trigger level and beyond. In our proposed system, we use the measurement outside the coil to infer the position of hits both in the inner-tracking system and in a second outer-tracking system located behind the iron flux return of the magnet.

Comparison with Measurements in the Inner Tracker The track coordinates and momentum determined in the tracking system just outside of the coil (which is subsequently referred to as the "middle tracker") can be used to extrapolate to the inner tracking device and correlated with measurements of the same track there. This is similar to the constraint used in the GEM-baseline design. (This is the only constraint in the baseline system.) All

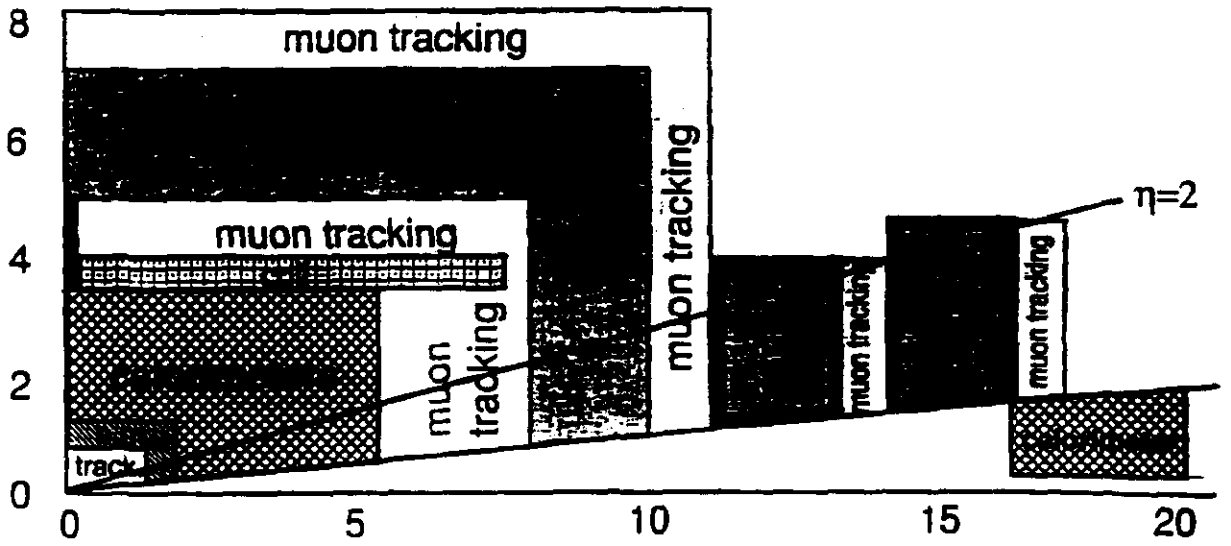

High Field Design for GEM with Forward Toroids

Figure 10: A plan view of the proposed high field system including the forward-backw iron-core toroid systems.

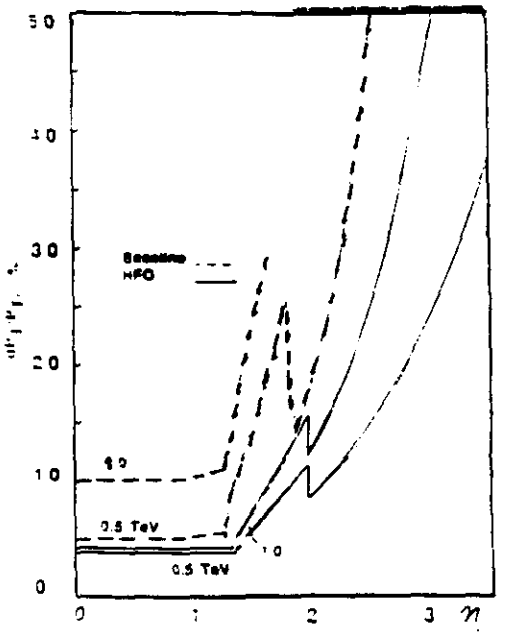

Figure 11: $\Delta p_t/p_t$ *vs* $|\eta|$ for the complete system, including the forward-backward iro toroid system.

things being equal, the comparison in the high-field system is more meaningful because the higher magnetic field will facilitate a better momentum resolution in the inner tracker.

Comparison with Measurements in the Outer Tracker At very high luminosities (e.g., in excess of $10^{34}\mathrm{cm}^{-2}\mathrm{s}^{-1}$) the performance of the inner tracking device may be compromised. Therefore, we place our emphasis on constraints that are independent of the inner tracking system.

In our proposed system, the magnetic flux produced by the superconducting coil is returned through an iron yoke with a radial thickness of $\Delta R = 2.25$ m, as shown in Fig. 3. The magnetic field in the iron is around 2 Tesla and is approximately perpendicular to radial particle trajectories for $|\eta| < 1.75$ ($\theta > 20°$). Thus the flux return is well suited for use as the bending element of a second muon spectrometer. A tracking system situated outside of the return yoke (the "outer tracker") measures the exit position and slope of the muon's trajectory as it exits the iron.

Measurements of a muon's position and angle in the middle tracker uniquely predict the position and slope of the track when it emerges from the iron return yoke. A high momentum muon will emerge from the iron yoke very near the radial direction; multiple scattering in the 2.25 m (125 x_{rl}) thick iron smears the exit angles by about 0.15 mrad/p(TeV/c). The exit position (in the bend plane) of the track from the iron return can be used to make a second determination of the momentum: the difference between the straightline extrapolation of the track in the middle tracker and the measured exit position (i.e., Δ in Fig. 4) is

$$\Delta(\mathrm{mm}) = \frac{0.3B(\mathrm{Tesla})L(\mathrm{m})^2}{2p(\mathrm{TeV/c})} \simeq \frac{1.9\mathrm{mm}}{p_t(\mathrm{TeV/c})}.$$

Multiple scattering smears the exit position of the muon introducing an uncertainty of $\Delta_{ms} \simeq 270\mu\mathrm{m}/p(\mathrm{TeV/c})$, which limits the resolution of the second momentum measurement. If the exit position is measured with a precision of 200μm, the second momentum measurement will have a resolution of $\Delta p/p \simeq 18\%$ for 1 TeV/c muons; for 500 GeV/c and below, the effect of the measurement error becomes negligible and the resolution is $\simeq 15\%$. This measurement can be compared with the measurement of the angle α in the middle tracker, providing a powerful constraint. The results of a GEANT simulation for the exit angle and position for 1 TeV/c tracks when they emerge from the iron return yoke are shown in Figs. 12 (a) and (b), respectively. The width of the Δ distribution in Fig. 12 (b) reflects the multiple-scattering limits on the second momentum measurement as discussed above. (The simulation includes single and plural scattering.) The results of a simulation of a sample of $p = 100$ GeV/c muons produced the expected results with no surprises.

Measurements in the outer tracker are performed in a very quiet environment—the material between the interaction point (25λ at 90° and more at smaller angles) and the outer tracker reduce the particle fluxes in the worst locations to $\sim 1\mathrm{Hz/cm}^2$. The requirement that the measured exit position agree with the value predicted by the middle tracker with an rms precision of 270μm provides a powerful (two-dimensional) constraint. While these

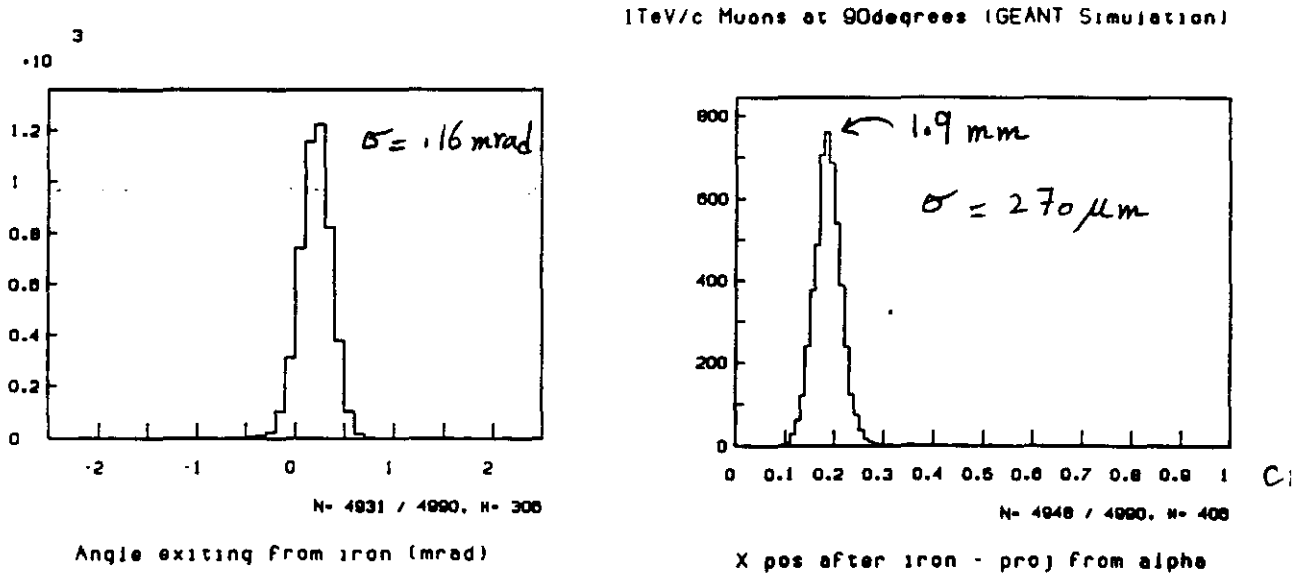

Figure 12: (a) The distribution in angle of 1 TeV/c muons emerging from the iron return yoke (at 90°). (b) The distribution in the displacement Δ of the muon's trajectory from its straight line extrapolated position for a sample of 1 TeV muons.

constraints provide powerful handles for rejecting background, they correspond to rather comfortable precision requirements on the angle ($\leq$ 100mrad) and position ($\leq 200\mu$m) measurements in the outer tracker. The relative alignment requirements between the middle- and outer-tracker are about an order-of-magnitude less demanding than is the case for the relative alignment of the different muon chambers in the GEM-baseline system.

In summary, "robustness" is provided by redundant measurements of the track parameters in the inner tracker, the *only* constraint available to the GEM-baseline system, and by the correlations with the position and angle of the track as it emerges from the magnetized iron return yoke of the solenoid. The latter constraints, which do not obtain in the GEM-baseline design, will be available in the event of high luminosity running, when the operation of the inner tracker may be severely compromised.

Further questions that relate to robustness, such as the expected particle rate at each detector element, the "corruption" of muon trajectory measurements by accompanying delta rays and electromagnetic "debris," and estimates of the effectiveness of the track constraints are being studied. These studies are discussed in more detail in Section 2 below.

1.2.4 Triggering

The simplicity of the muon measurement scheme, namely the measurement of straight-line track segments in the middle and outer trackers, allows one to generate simple but powerful triggers both at Level-1 and Level-2. The angle α is inversely proportional to the muon's transverse momentum; a requirement that $\alpha \leq 270$ mrad corresponds to a transverse

momentum selection of $p_t \geq 10$ GeV/c. Using ISAJET, we estimate that the requirement that $\alpha \leq 270$ mrad, corresponding to the indication of a particle track in a coarse (~ 27 cm wide) radial road, together with the presence of some hits nearby in the outer tracker provides a Level-1 trigger that is efficient for $p_t \geq 10$ GeV/c muons and has a rate of 1 KHz at the SSC design luminosity of $10^{33}\text{cm}^{-2}\text{s}^{-1}$. Since this is an order-of-magnitude lower than the rate necessary for a Level-1 trigger at the SSC, the same scheme should be applicable for operation at luminosities of $10^{34}\text{cm}^{-2}\text{s}^{-1}$.

For Level-2, the position of the muon track in the outer tracker can be correlated with the extrapolated position from the middle tracker measurement to make a more precise selection of the muon's transverse momentum. A ± 5 cm correspondence is equivalent to a selection of $p_t > 40$ GeV/c, which will have a rate of a few hundred Hertz at a luminosity of $10^{33}\text{cm}^{-2}\text{s}^{-1}$.

1.2.5 Effects on the Rest of the Detector

While the dimensions of the inner detector elements have not been changed, the presence of the stronger field in the inner detector region necessarily has significant effects. We discuss a few of them.

Effects on the Physics Capabilities of the Inner Detector The presence of a stronger field will have a beneficial effect on the capabilities of the inner tracking system. As noted above, the anticipated momentum resolution of the inner tracker for the 0.8 Tesla field in the GEM-baseline design is $\Delta p/p \simeq 130\% p(\text{TeV/c})$. In the high field case, if a similar tracking precision is obtained, the momentum resolution in the inner tracking system will improve by a factor of six to $\Delta p/p \simeq 22\% p(\text{TeV/c})$. With such resolution, reliable ($> 5\sigma$) measurements of charge can be made up to momenta of 900 GeV, permitting, for example, the use of electron decay channels in the study of the production of high-p_t W^+W^+ and W^-W^- pairs, the so-called guaranteed discovery reaction at the SSC [3]. Here reliable charge determination is needed to distinguish like-sign W-pairs, where the signal dominates, from unlike-sign pairs, which are dominated by background processes. The ability to use the electron and muon decay modes provides a nominal factor of four improvement in event rate over the case where only muons can be used. The rates for these processes are marginal. The improved efficiency provided by the electron channel is crucial for accessing this important area of physics. This reaction is discussed below in Section 4.5.

A potential problem in a detector with a high magnetic field is the spreading of the charged particles in a hadron jet before they enter the calorimeter, thereby reducing the effectiveness of jet clustering algorithms and particle isolation cuts. We have studied this in some detail and have concluded that it does not present a significant deterioration on the physics performance of the detector. This is discussed below in Section 4.3.

Effects on the Performance of the Inner Detection Elements Our proposed system places a number of constraints on the elements of the inner detector. For example, the

momentum resolution in the muon system is limited primarily by multiple scattering in the material of the hadron calorimeter. Thus, we prefer that the calorimeter's radiator be a relatively low-Z material such as iron (stainless steel) or copper, rather than lead or uranium. The high field probably precludes the operation of vacuum photodiodes for reading out scintillation light. Thus, for the case of the BaF option for EM calorimetry, alternative readout systems, such as proportional-wire readout using TAME, would have to be employed (assuming that the systematic calibration effects inherent in this scheme are resolved). We have investigated the effects on resolution of cryogenic liquid calorimeters, caused by the curling up of secondary particles produced in the entrance window before they reach the sampling medium, and see only a small degradation between 0.8 and 5 Tesla (see the discussion in Section 4.2). For a tracking radius of 75 cm, a 5 T field will cause an increase in the number of curling tracks. Moreover, the increased Lorentz angle results in longer drift times in gas drift devices such as straw tubes. The combination of these effects results in serious occupancy problems for straw-tube-type inner tracking elements. We discuss problems in the inner tracking system in Section 4.1, where we argue that, at least for operation at $10^{33}\mathrm{cm}^{-2}\mathrm{s}^{-1}$, silicon strip and gas microstrip detectors will function well in the 5 Tesla environment.

1.3 Summary

In the following sections we provide supporting evidence for the claims made in this introduction and compare the capabilities of our proposed system to those of the GEM-baseline configuration.

To summarize, we list some attributes of our proposed high field system:

- An iron return yoke is provided, eliminating magnetic fields at the earth's surface.
- Excellent muon momentum resolution, particularly at high momentum (better than that of GEM-baseline for muons with $p_t > 300$ GeV).
- Good muon coverage down to $|\eta| \simeq 3.5$.
- Significantly relaxed alignment requirements.
- Very robust muon detection:

  $\Delta p/p \simeq 4\%$ without reliance on the inner detection system;

  redundant measurement of muons behind the iron return yoke.
- Simple muon triggering (behind $\geq 25\lambda$ of material).
- A high magnetic field for the inner tracker system

2 Muon Detection Simulation

In this section we consider the details of the design of the post-coil muon tracking system. An important consideration in the design of a muon spectrometer for SSC detectors is the effect of showers induced by the muon traversing material (muon radiation and delta-ray production). These accompanying showers may obscure the muon track and worsen the effective resolution of the system and have the potential for producing fake high p_t triggers. In order to optimize the cell size and the number of layers required for accurate and redundant measurements, the nature of these backgrounds must be well understood. We are studying these effects in our proposed geometry by means of a GEANT simulation.

As can be seen in Fig. 4, there are three separate muon track measurements, the "inner tracker" surrounding the interaction point, the "middle tracker" in the region between the coil and the iron flux return, and the "outer tracker" beyond the iron yoke. Here we summarize initial results from a study of the effects of muon-induced showers on the ability to measure the angle α in the middle tracker. If a particle accompanying the muon as it passes through a drift chamber element is closer to the wire than the muon, it results in an incorrect position measurement and a worsening of the resolution. (Not yet considered in this program is the effect on pattern recognition and triggering of extra cells in a layer that may be hit. While this has to be studied in detail, we expect that our proposed geometry, with its three separate muon track measurement, has an advantage over that of GEM-baseline both in resolving the track ambiguities and rejecting the fake triggers introduced by such particles.)

The uncertainty in the measurement of the angle α has a contribution from multiple scattering in the calorimetry (here we assume a thickness of $110x_{rl}$) and coil ($20x_{rl}$) of $\sigma \simeq 0.11\text{mrad}/p_t(\text{TeV/c})$, provided that the exit position is well measured. Thus, for a measurement to be limited by this multiple scattering uncertainty, the muon system must not provide any significant additional contribution to the determination of α. For a 1 TeV/c muon over $\sim$ 1m tracking length this amounts to a spatial position resolution at the track ends of 50μm or better. Assuming the typical single cell resolution is near 100μm, a minimum of 4 layers of cells at the exit of the coil and 4 layers of cells before the flux return are required. However, because of muon-induced showers, hit measurements can be compromised by an accompanying particle. These extraneous hits can be recognized by the track fitting algorithm and removed from the fit, but at the cost of reducing the number of cell layers in the fit and worsening of the resolution. The frequency of occurrence of these compromised cells and/or its impact on the measurement can be reduced by decreasing the cell size, or increasing the redundancy of the system by adding more layers of cells. Ultimately one has to optimize both the cell size and numbers of layers.

2.1 The Simulation

To understand backgrounds from muon-induced showers, it is very important to simulate in detail the final layers of material before the muon system as well as the muon system itself.

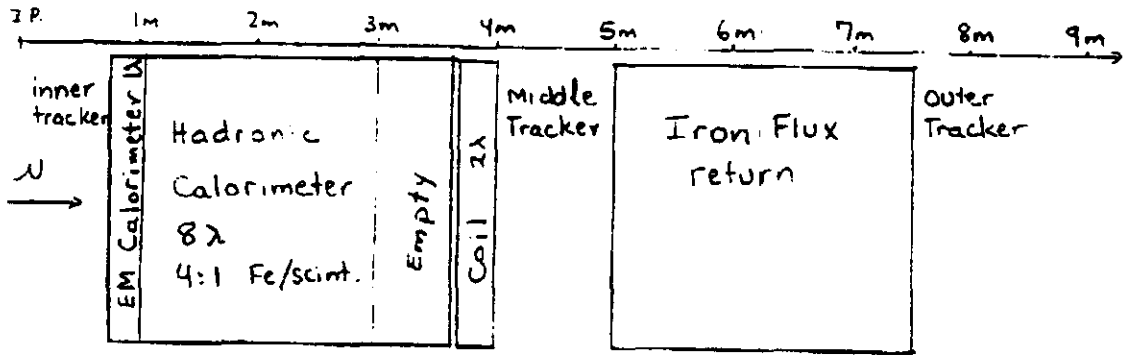

Figure 13: The muon chambers layer geometry used in the simulation

For this study the simulated calorimeter was a homogeneous mixture of absorber (Pb in the electromagnetic portion and Fe in the hadronic section) and scintillator. The details of the coil and chambers used for the simulation are shown in Fig. 13. For the muon chambers, the cell design proposed by L. Osborne et al. [4] is used. The cells have 2 mm thick Al walls (it was recently proposed to reduce this), and 2.5cm square drift cells with a sense wire down the center. The resolution of these cells has been demonstrated to be $\sigma \sim 80\mu m$ [5]. We use the GEANT program, a GEANT simulation of showers induced by 0.5 TeV/c muons was found to be consistent with experimental measurements in a Fermilab muon beam. For the material of the calorimeter, coil and flux return, the energy cutoffs in GEANT for electrons and gammas were set to 1 MeV, since charged particles with energy below this would not penetrate the 2 mm thick Al walls of the drift chambers. However, in the material of the drift chamber walls and in the Ar-isobutane cell gas, 10 KeV cutoffs were used in order to simulate the sensitivity of the drift chamber cells to very low energy charged particles.

A configuration of two superlayers with each superlayer consisting of 8 layers of cells was positioned in the middle tracking region as shown in Fig. 13. By adjusting the thickness of the flux return iron, the field strength in the middle tracking region can be "tuned" from zero to a few kG. To consider the benefit of a field in this region, the simulation was performed both at zero field and 2 kG field in the middle tracker, with the field direction along the length of the cells. Single muons with incident momenta of 1 TeV/c (at the I.P.) are propagated through the detector. Only a 90° incidence angle has been thus far simulated. The position and 4-momentum is recorded for particles in the chamber layers as they cross the plane containing the wires (mid-point of the cell). After the GEANT simulation, the event records are then read back by an analysis routine which constructs the response of individual cells. The cells in even-numbered layers are offset by 1/2 cell width from those in the odd-numbered layers. The positioning of the entry point of the muon relative to the "wire" in the first layer of the first superlayer can be adjusted. As a test, the entire configuration of cells was shifted with respect to the muon entry point by 0.62 cm in the X direction with no discernable change in the results.

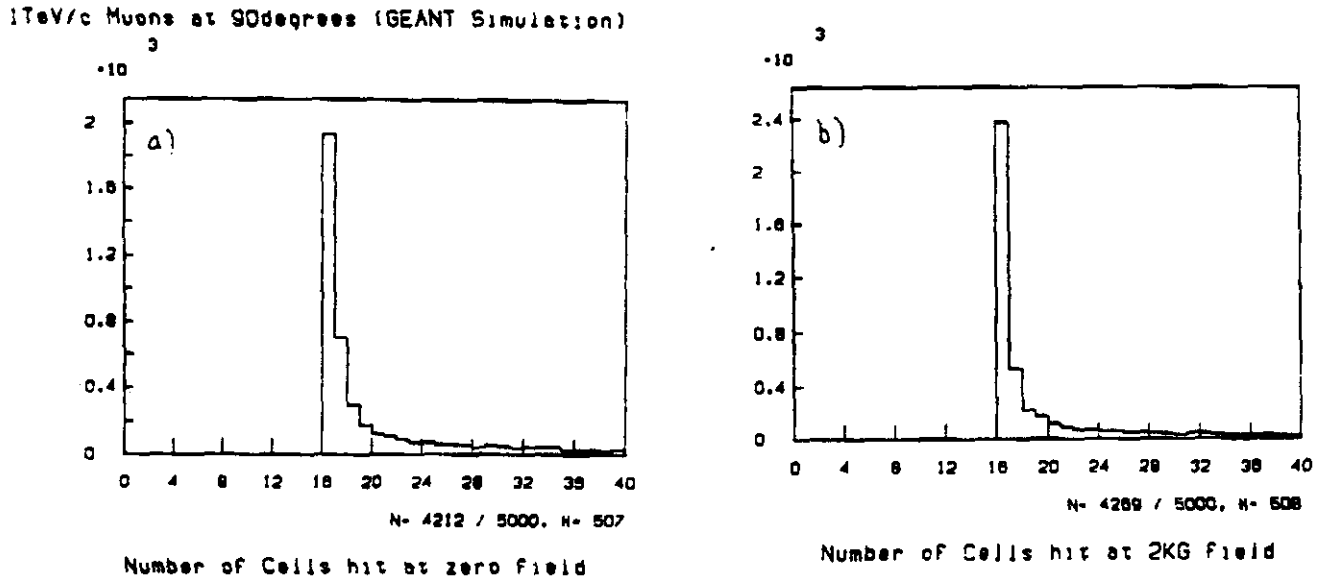

Figure 14: The distribution of the total number of cells in the middle tracker which are hit by the 1 TeV/c incident muon and its accompanying particles.

2.2 Results

Figure 14 shows, both for $B = 0$ (a) and $B = 2$ kG (b), the distribution of the total number of cells in the middle tracker that are hit by the 1 TeV/c incident muon and its accompanying particles. As expected, this distribution peaks at 16 (total number of layers in the middle tracker) with a tail at larger values coming from muon-induced showers. As noted above, this study only concerns itself with the 16 cells which the muons traverse. Figure 15 shows the number of total layers (out of 8) in each superlayer in which the muon was the particle that came nearest to the wire ("good hit") in the cell it traversed. The probability that all 8 layers in a superlayer are "good" ranges from 67% - 69% for zero field to 70% - 76% for 2 kG field. As expected, the presence of some magnetic field in the tracking region serves to suppress the background from muon-induced delta-rays by sweeping them out. Also as expected, the superlayer farther away from the material of the coil is somewhat cleaner.

As noted above, the required spatial resolution can be obtained with a minimum of four cell layers in each superlayer. To consider this requirement in detail we can examine the probability of having at least four "good" hit layers in the first N layers of a superlayer where N = 4,5,6,7,and 8. This is plotted in Fig. 16. As can be seen the probability for at least four "good" cells increases from 80% (86% at 2kG) for N=4 layers to 94% (96% at 2kG) for N=8 layers. Finally it was found that for a middle tracker with eight layers of chambers in each of two superlayers, 92.5% (94.9% at 2 kG) of 1TeV/c muons produce at least four "good" hits in each superlayer.

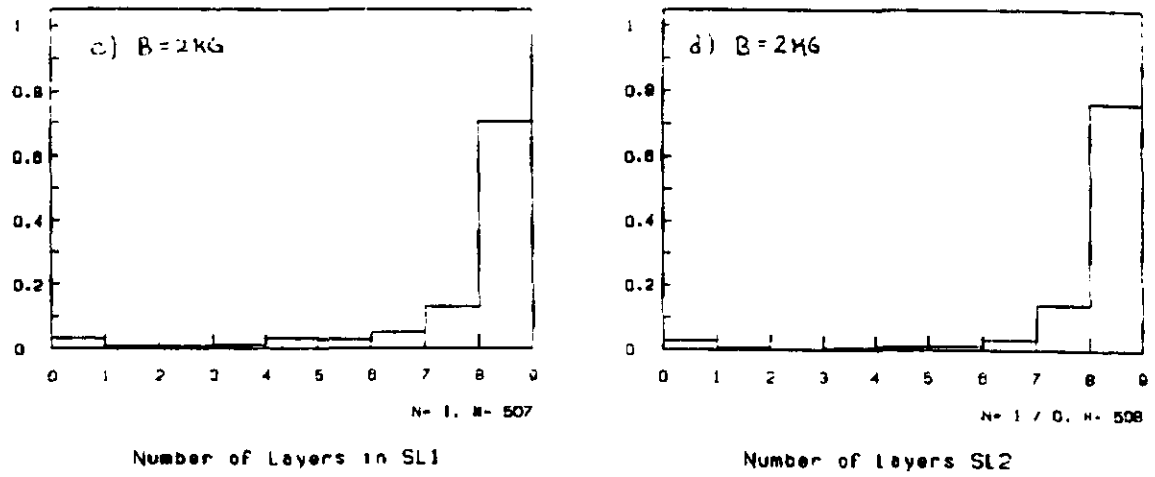

Figure 15: The number of total layers per superlayer (out of 8) in which the muon came nearest to the wire ("good hit") in the cell it traversed.

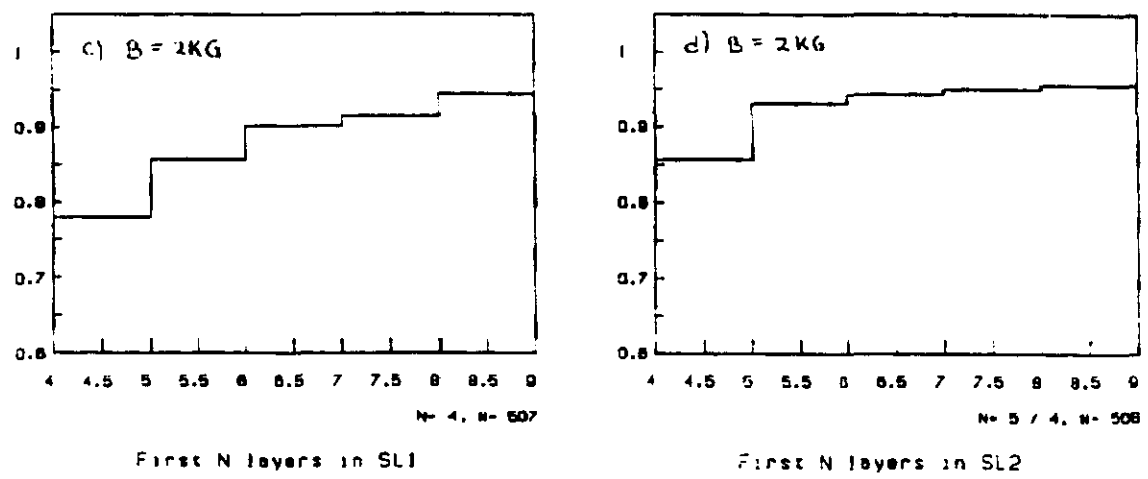

Figure 16: The probability of having at least four good hits in the first N superlayers, where N=4,5,6,7, and 8

2.3 Conclusions

Of order 16 layers of 2.5 cm cells will provide sufficient redundancy for efficient muon measurements in the middle tracker. With multi-hit electronics, the number of compromised muon cells could be further reduced, allowing for further reduction in the number of layers and corresponding reduction in the channel count and cost. Further simulation will continue to consider other candidate technologies for muon detector components in GEM and to consider pattern recognition in the high track multiplicity events, where the linkage between the track in the outer tracking region to that in the middle tracker will be used to help identify the actual muon hits.

3 Magnet and Mechanical Support

Our proposed geometry offers significant simplification in the mechanical support system and the coil. The iron flux return serves as an excellent structural element for supporting the muon tracking systems. Coupled with the less stringent alignment requirements for these systems, this offers potential cost and scheduling advantages. In addition, the coil is sufficiently small to allow for transportation to the laboratory site, thus de-coupling the magnet production schedule from land acquisition, factory construction, and other activities. We are undertaking two studies on the mechanical support and the magnet coil. We report preliminary, but encouraging results.

3.1 Magnet

The superconducting magnet has an inner radius of 3.5 m to keep the the dimensions of the inner tracker and calorimetry the same as for the current GEM-baseline design, and a total length of 15 m to enhance the η acceptance of the central muon system. The current choice of the central field of $B = 5$ T is a parameter in our study. For this design the total number of ampere-turns is 6.1×10^7 with a total stored energy of 6.1×10^9 Joules. Iron is provided for the flux return, bringing the fringing field at 60 m from beam to less than 4 gauss. The current structural design calls for two separate half-coils and supported from the iron by a diaphragm as shown in Fig. 17. The diaphragm also supports a stainless steel cylinder within which are mounted the calorimeter and inner tracker. The "barrel" iron, as shown in Fig. 18, can be built in either eight or sixteen sectors, with eight preferred for reasons of economy (fewer welds, supports, bolts etc.).

Figure 19 shows a field map for the configuration discussed above. Figure 20 shows how the magnetic field drops off with radius. The cost of the coil has been estimated as between \$70-100M [6]. We are currently undertaking a study to make a more thorough estimate of both the cost and schedule of magnet construction.

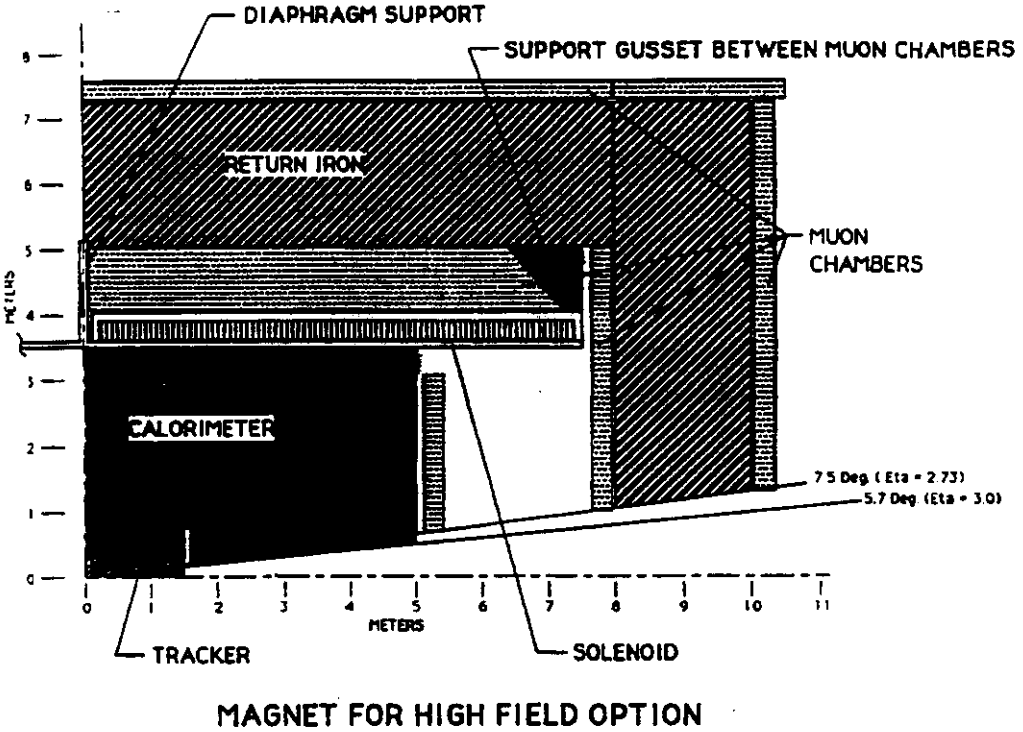

Figure 17: A view of the High Field Coil showing the diaphragm support in the middle of the coil.

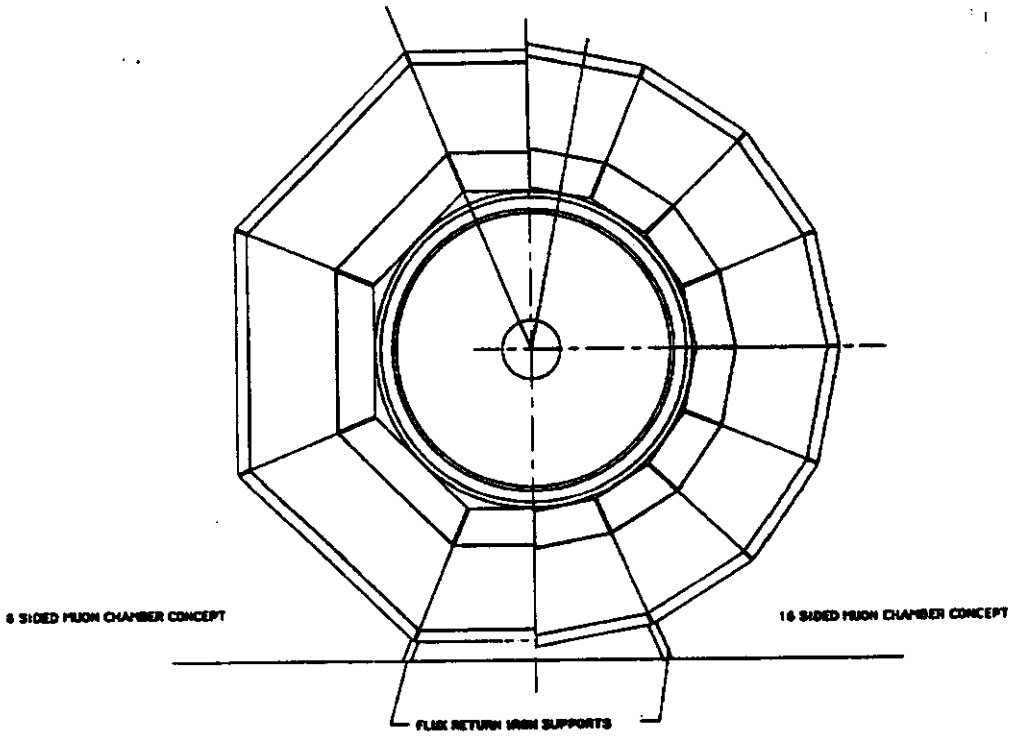

Figure 18: An end view of the barrel iron showing the overall support.

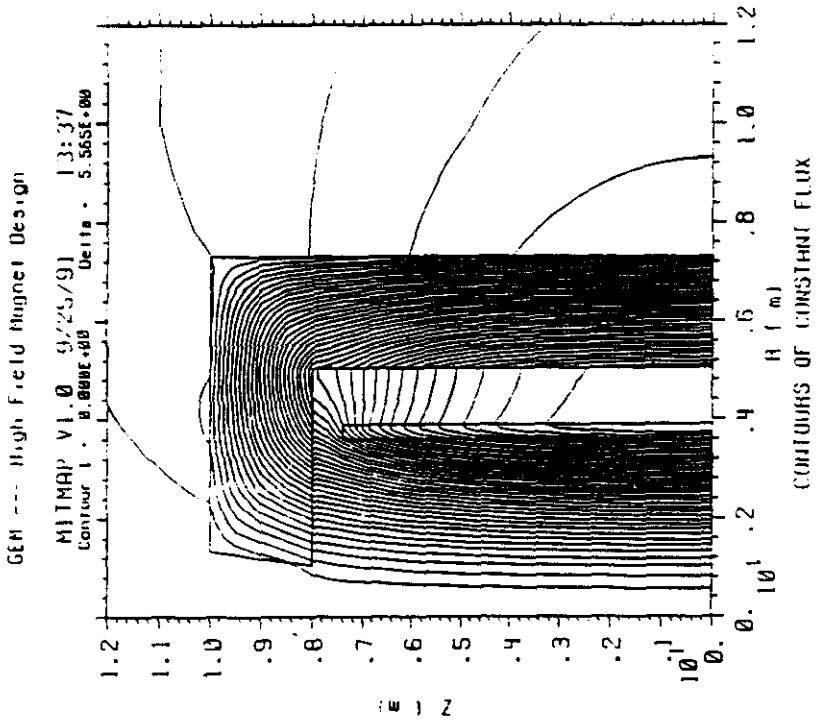

Figure 19: A field map showing the field lines for the High Field coil.

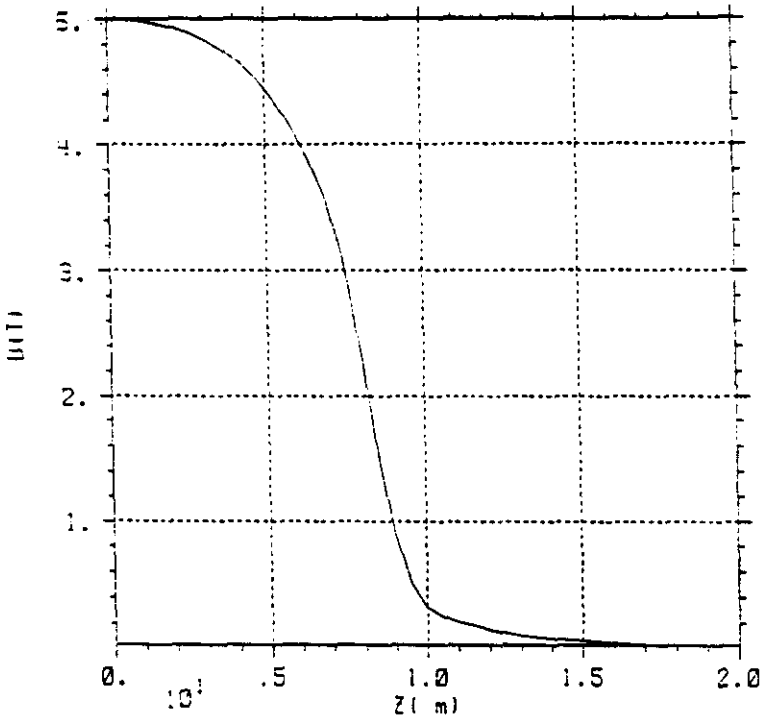

Figure 20: The Z dependence of the magnetic field in the High Field Magnet. (The Z scale is in units of 10 m.)

3.2 Mechanical Assembly and Support

The inner detector is assembled into a cylinder that captures the superconducting coil and is supported from its ends and by a mid-plane diaphragm as shown in Fig. 17. While the study of mechanical design is in a preliminary stage, one can draw some conclusions about the advantages of our proposed geometry over that of the GEM-baseline configuration:

1. The schedule for the construction and implementation of the coil is relatively independent of the rest of the detector.
2. The total size of the detector is considerably smaller that the planned experimental hall, allowing for flexibility in installation and maintenance of the detector.
3. The alignment tolerances are less stringent.

4 Effects of the High Field on Physics and Detectors

We discuss here a few of the effects of the high field on the detector performance and physics signals. For the sake of brevity we will discuss only those issues where the increased magnetic field has been thought to have a negative impact on the detector performance, as well as at least one important physics signal where the enhanced performance provided by the high field is of crucial importance.

4.1 The Effect of the Field on the Inner Tracker

The increased magnetic field in the inner tracker causes an increase of the Lorentz angle and drift time for all drift devices. In addition, the higher field results in an increased number of low p_t particles with closed orbits in the inner tracker, i.e., "loopers." These two effects combine to increase the occupancy in straw tube-type trackers to uncomfortable levels.

In an 0.8 T field, a 2mm straw tube will have a drift velocity of 40μm/nsec. For a collection time of 50 nsec the inner tracker will have 12% average occupancy at standard luminosity. In a 5 T field, the effective drift velocity is slower, about 25μm/nsec, causing the average occupancy to rise to 38%. More seriously, 13% of the events will have an average occupancy of 63%. This appears to preclude the use of straw-tubes with the 5 Tesla field.

There are, however, other likely technology choices for the inner tracker, among them silicon (strip or drift) devices and gas microstrip chambers (GMC), which can function well in the high field environment.

Silicon strip detectors necessarily have small cells in order to achieve good resolution, and drift distances of only a few hundred microns. Our simulations indicate that even in the 5 T field, a standard silicon strip detector will have an average occupancy of only 0.19%, which

should not pose a serious problem. In silicon drift devices the Lorentz angle is relatively small (20 degrees) and could, in principle, be compensated by a re-orientation of the devices, although a full mechanical design has yet to be worked out. The high field configuration will benefit from current R&D on silicon strip and silicon drift within the GEM collaboration.

Various attempts have been made to develop devices which are insensitive to looping tracks, foremost among them are the gas microstrip chambers proposed by the L* LOI [7] and independently at CERN by F. Udo [8]. In principle, these devices solve the three major problems of tracking in high magnetic fields at standard-to-high luminosity: large Lorentz angles, long drift times and "loopers". The Lorentz angle effect is minimized by using low mobility high drift velocity gas (DME/CO_2) and drifting axially within 20° of the magnetic field direction. The drift time is minimized by using a 3 mm gap with a collection time of 15 to 30 nsec depending on the incident angle. The strips can be arranged to be preferentially sensitive to radial tracks and have reduced sensitivity to wide angle, looping tracks.

A typical GMC is a 10 by 10 cm glass substrate (150 microns thick) covered by a thin metal film upon which microstrips are etched in the form of cathodes and anodes with 200 micron pitch. Tracks are incident nearly normal to the strips and pass through a 3 mm gas volume which is sealed by aluminized mylar. The devices are arranged so that the strips are oriented nearly radially so that high p_t radial tracks deposit all of their ionization on one or two microstrips while large angle tracks spread their ionization over many strips, leading to a reduced pulse height on any given strip. Analog, or possibly digital (yes/no), readout of strips is possible and the discriminator threshold can be set to reject loopers. Measurements reported by F. Udo [9] showed resolutions of $\sigma = 44\mu m$ and a 98 % efficiency. Small angle stereo can be obtained with 1 mm radial resolution by tilting adjacent 10 by 10 sections by ± 20 milliradians. An arrangement suitable for the inner tracker will have about 10,000 elements (10 cm by 10 cm each) and several million readout channels. The cost of the readout can be minimized by using digital readout of the channels. The obtained resolution would be comparable to the current GEM-baseline inner tracker resolution.

In conclusion, the increased magnetic field may make it necessary to use either silicon or Gas Microstrip detectors as the primary elements of the inner tracker. While more R&D is needed, there are of strong efforts in both of these areas proceeding in a number of laboratories. However, our proposed system, unlike the GEM-baseline scheme, does not rely on the inner tracker for a second muon measurement, thereby alleviating some of the risks associated with the general problem of tracking at the SSC.

4.2 The Effect of the Field on the Endcap Region of the Middle Tracker

The middle tracker elements in the endcap regions must function in a 5 Tesla magnetic field. These chambers are, however, shielded from the interaction point by about 14λ of material and we estimate that the rates in this region are a rather manageable few Hz/cm^2. Thus, drift chambers can operate in this region without the occupancy problems that exist in the

inner tracking region.

Some of the proponents of this proposal have considerable experience with the operation of drift chambers in the $B = 3$ Tesla field of the AMY detector. There we find that with care, the effects of large Lorentz angles and complex drift trajectories can be understood and spatial resolutions comparable to those obtained in the absence of a field can be acheived [10]. The AMY experiment has recently installed drift chamber arrays in the endcap regions in a configuration quite similar to that required for the end cap region of the middle tracker. Experience with the AMY endcap chambers will be directly applicable to the design and operation of the chambers required for this proposal.

4.3 The Effect of the Field on Calorimetry

The 5 Tesla magnetic field places constraints on the use of phototubes for light readout. However, many of these constraints are also present at the 0.8 T level. Cryogenic calorimetry (e.g. liquid argon and liquid xenon), which is among the final list of options being considered by GEM, can work in large magnetic fields. The readout of a liquid argon calorimeter (in an "accordion" configuration) is unaffected by the field.

It has been suggested that the increased field might have a detrimental effect on the energy resolution of the electromagnetic calorimeter due to the fact that the low energy shower particles initiated in the cryostat wall will curl up and vanish in the cryostat material prior to depositing their energy in the sampling medium. We are studying this effect for a cryostat with a 2 cm thick room temperature Al wall, a 1.5 cm vacuum space and a 2 cm thick cold wall. The calorimeter is taken to be a repeating pattern of a 1.75mm Pb radiator, followed by two 2mm argon gaps and a 3mm G-10 electrode. The mean energy deposited in argon is about 15.5%.

The following table lists the values of the magnetic field, the incidence angle of the electron, the effective resolution (or the sampling term divided by the $\sqrt{E}$), the average and rms spread of the energy lost both due to back scatter and to the cryostat wall. The amount of backscattered energy and the amount deposited in the front cryostat (dead) material increases somewhat with magnetic field, as expected, but the effect on the overall resolution is still not very large for normal entry. For large entry angles (60 degrees), the resolution for both the $B = 0$ and $B = 5$ T cases drops by about 1.5, which is consistent with change expected from sampling. There are detectable, but small (order 10%) changes in resolution when the field is turned on and off, but these are also close to the current statistical uncertainty of the EGS results. Consequently, our preliminary conclusion is that the effect of magnetic field, as such, is not very large (no more than a 15% degradation on the resolution). These studies are continuing.

Electromagnetic response for a 4 cm thick Aluminum cryostat wall									
Field	*No*	*Energy*	*Type*	*Theta*	*Effective*	*Backscatter*		*Front Alum*	
(T)	*Events*	*(GeV)*	*e/γ*	*Deg*	*Resolution*	*% E lost*	*RMS*	*% E lost*	RMS
0.0	100	25	e	0	1.29	0.06	0.02	0.14	0.07
5.0	90	25	e	0	1.27	0.33	0.12	0.25	0.08
0.0	100	25	e	60	1.58	0.51	0.11	0.70	0.24
5.0	74	25	e	60	1.78	1.01	0.21	1.02	0.28

4.4 The Effect of the Field on Jet Detection

The detection of hadron jets at the SSC will rely primarily on calorimetry. A potential harmful effect of the high magnetic field is the "spreading" of particles in the jets with potential deterioration of jet energy and angular resolution. We have studied this effect for jets with momenta ranging from 20 to 5000 GeV. The relevant parameters are the fraction of the jet's "potentially observable energy," i.e., the energy of the parent parton minus the energy of neutrinos, that is contained with an R cone of some value, and the rms fluctuations of this fraction. We define R in the standard fashion as

$$R = \sqrt{\phi^2 + \eta^2}.$$

The fluctuations are important because even with no magnetic field one does not generally detect all the jet energy and an R- and energy-dependent correction factor must be applied. Figure 21 shows the ratio of the energy fraction contained within various R cones in a 5 T field to that with no magnetic field. Figure 22 shows the actual energy fractions and the rms fluctuations of these fractions for an R value of 0.8. The conclusion is that for low energy jets, a high field reduces the energy in an R cone relative to the no field case. However, the rms fluctuations are very nearly the same in both cases. Thus, although the higher field results in a larger correction factor, the jet resolution is not seriously compromised.

4.5 The Effect of the Field on Isolation Cuts

Another concern is the effect of the field on isolation cuts of leptons outside the jet. There is the potential for the field to "sweep" particles from the jet nearer the otherwise isolated lepton and destroy the efficacy of the isolation cut. As a stringent test we chose to study the decay

$$pp \longrightarrow t\bar{t} + X; \qquad t\ \bar{t} \longrightarrow W^+\ b\ \ W^-\ \bar{b} \longrightarrow \mu^+\mu^-\ jets,$$

for a t-quark mass of 200 GeV/c^2. The dominant backgrounds to this signal are the muons from the decays of b and c quarks. In Fig. 23 we plot the muon p_t spectra for the $t\bar{t}$ signal events (dotted line), the background from b and c decays prior to any cuts (solid line), and

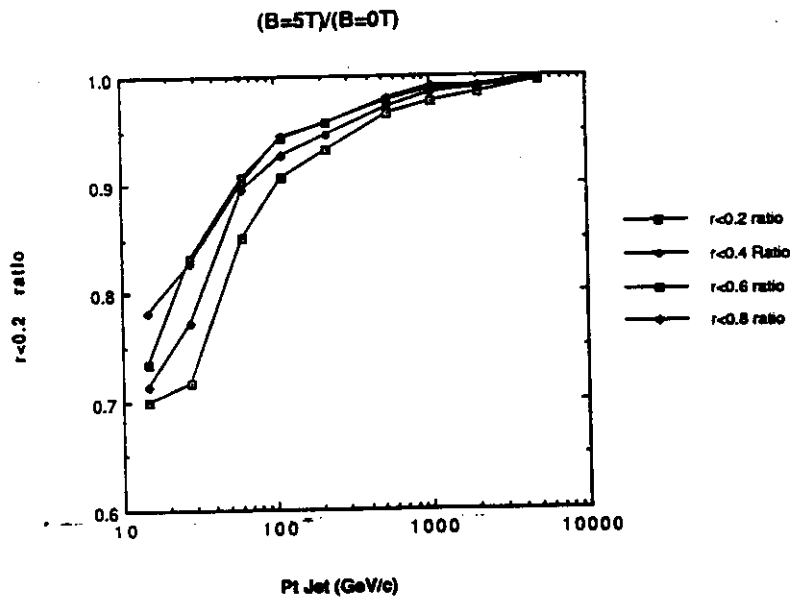

Figure 21: The ratio of the jet energy contained in a cone R for $B = 5$ T to that contained in the same size cone for $B = 0$ *vs* the jet energy for various R values.

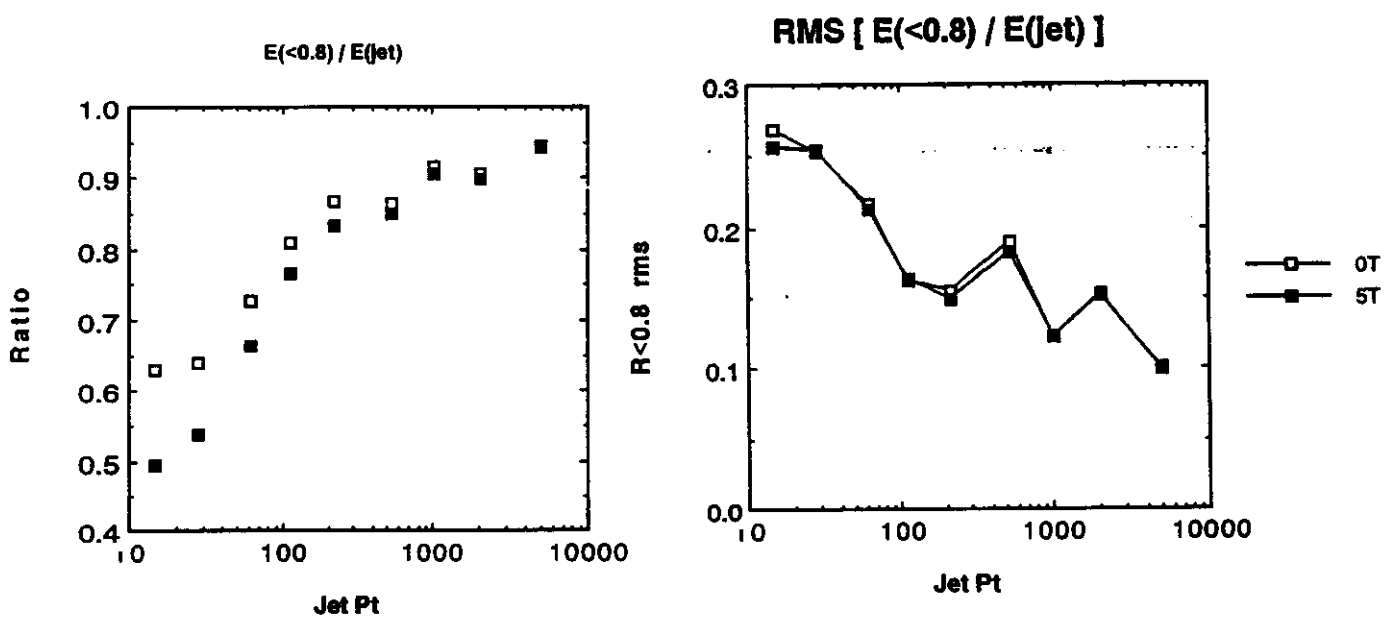

Figure 22: The actual jet energy fractions and the rms fluctuations of these fractions for an R value of 0.8 for $B = 0$ and $B = 5$ T.

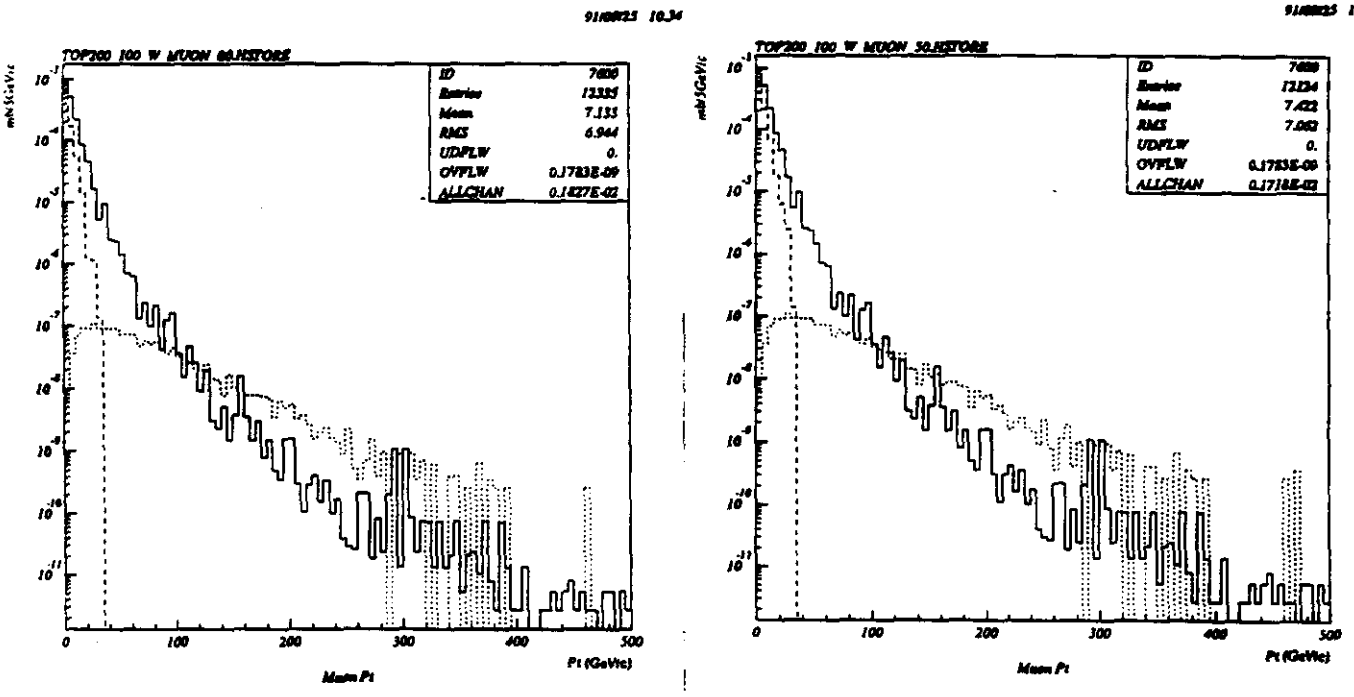

Figure 23: The transverse momentum distribution of the isolated lepton from a 200 GeV top decay (dotted line), c and b quark decays (solid line) and c and b quark decay after isolation cut (dashed line) for (a) no magnetic field, (b) a 5 T field.

the b and c background after the application of the isolation cut requiring the total transverse energy in an $R = 0.4$ cone around the muon be below 10 GeV (dashed line). (This is the cut used in many simulated top analyses for SSC experiments.)

Figure 23 shows the effect for no magnetic field (a) and effect for a 5 T field (b). The figure of merit is where the signal level intersects the background, around 40 GeV in both cases. We conclude that the 5 T field has no significant effect on isolation cuts aimed at observing the isolated leptons.

4.6 $pp \longrightarrow W_L{}^+W_L{}^+ X$

The reaction $pp \longrightarrow W_L{}^+W_L{}^+ X$ is central to the study of electroweak symmetry breaking at the SSC. In models with dynamical symmetry breaking the cross section for this reaction is enhanced. It has been shown on rather general grounds that if there is no Higgs particle with a mass that is accessible at the SSC, the interactions of longitudinally polarized W's (and Z's) must become strong for W-W cm energies above 1 TeV [3]. (Indeed, this is the flip side of the SSC's "promise to elucidate the nature of electroweak symmetry breaking" [11].) In this event, the cross section for the reaction $pp \longrightarrow W_L{}^+W_L{}^+ X \longrightarrow \mu^+(e^+)\mu^+(e^+)$ has been estimated to be between 5-10 fb, corresponding to only 50-100 events per SSC year with no acceptance factors [12]. Figure 24 shows the momentum (a) and η (b) distribution of like-sign leptons from the $pp \longrightarrow W_L{}^+W_L{}^+ X$ interaction and the opposite-sign leptons from WW production. Not shown is the momentum distribution of the like-sign lepton pair background from $W^+t\bar{t}$ production, which is estimated to be comparable to the $pp \longrightarrow W_L{}^+W_L{}^+ X$

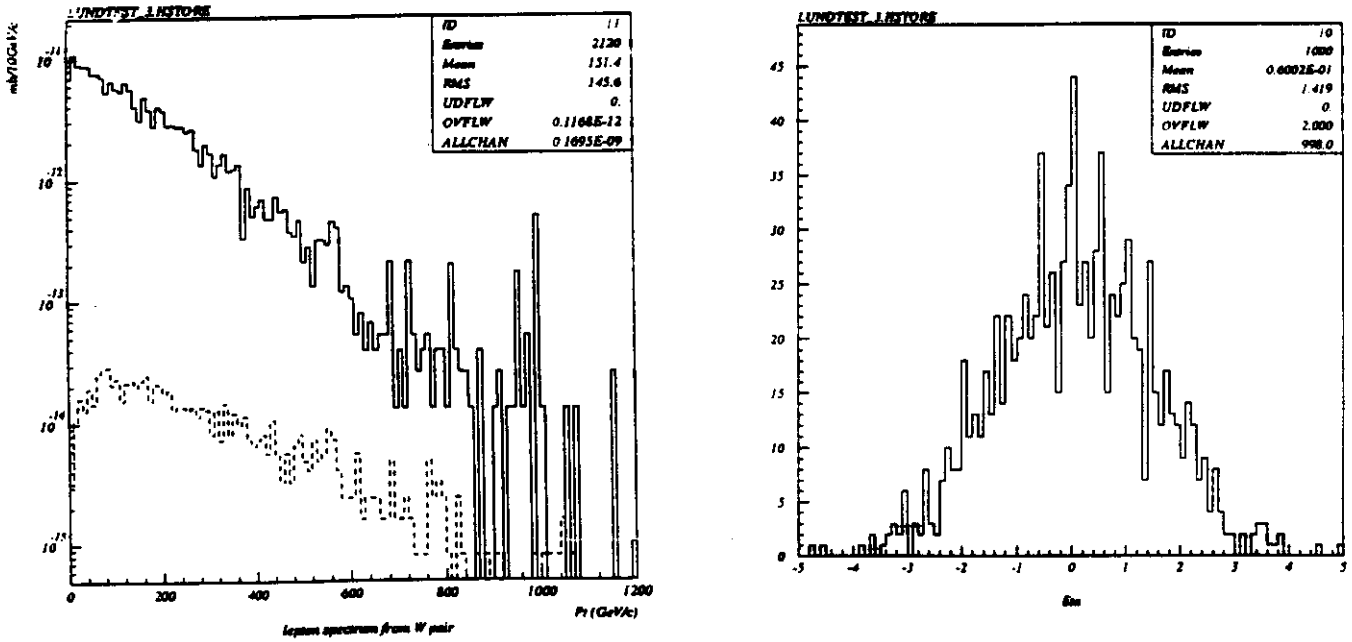

Figure 24: (a) Momentum and (b) η distribution of like-sign leptons from the $pp \longrightarrow W_L{}^+W_L{}^+ X$ (dashed) interaction and the opposite-sign leptons from WW production (solid).

signal [12]. Backgrounds in the opposite sign lepton pair channels from $t\bar{t}$ decays and $q\bar{q} \longrightarrow W^+W^-$ are of order $10^2 \sim 10^3$ times higher than the signal, and preclude the use of the unlike-sign channel for these studies. In order to avoid contamination of the like-sign signal from misidentified unlike-sign backgrounds, one needs excellent sign determination. To preserve a measureable rate, this capability is needed for *both* electrons and muons with energies up to ~ 1 TeV and for $|\eta|$ values as large as 3.0. The high field in the inner tracking region extends the momentum range for electron sign determination by a factor of six over the GEM-baseline design (from ~ 150 to ~ 1000 GeV/c). In addition, our proposed geometry covers a larger $|\eta|$ region for muons—the GEM-baseline design has a factor of 2 lower acceptance for two muons from $pp \longrightarrow W_L{}^+W_L{}^+ X$ than the high field proposal. The combined effect of the additional electron momentum and muon $|\eta|$ coverage results in a difference of about a factor of four in the efficiency for these events. Thus, the proposed high field configuration addresses a serious deficiency in GEM's ability to observe this crucial physics mode.

5 Conclusions

In this report we present the current status of our evaluation of the capabilities of a high field option for GEM. In it we provide preliminary results of our investigations into the questions raised by the GEM Decision Group in its memo of Sept. 10, 1991. Our current evaluation of the results derived to date is that although a considerable amount of further study and optimization is needed, there are no obvious fatal deficiencies in our proposed system. Moreover, the potential for significantly better momentum resolution in the inner

tracker and the better η coverage of the muon system should allow for investigations that appear to be inaccessible in the GEM-baseline design.

Work in progress includes:

1. The preparation of a conceptual design, a cost estimate, and a fabrication plan and schedule for the magnet coil.

2. The development of a detailed scheme for assembling and supporting the detector.

3. The complete simulation of a range of physics processes in the detector. This includes: the completion of the $pp \longrightarrow W_L{}^+ W_L{}^+ X$ study mentioned above; a comparative evaluation between the baseline and high field designs capabilities for the reactions $H \longrightarrow Z^\circ Z^* \longrightarrow l^+l^-l^+l^-$ and $H \longrightarrow \gamma\gamma$; the detector's capabilities for t-quark physics; etc.

4. The optimization of the muon detection systems and comparative study of different muon detection elements.

5. The completion of studies of B-field effects on calorimetry.

6. A full evaluation of an inner tracker for $B = 5$ T, and the development of an R&D plan for gas microstrip detectors.

7. A detailed cost estimate for our proposed system is in progress.

References

[1] R.V. Steiner et al., *An Expression of Interest to Construct a Major SSC Detector*, SSC Laboratory EOI-0020 (1991).

[2] J. Bensinger, E. Wang and H. Yamamoto, *Proceedings of the Workshop on Computing for SSC Experiments*, 1990.

[3] M. Chanowitz and M.K. Gaillard, Nucl. Phys. **B261**, 379.

[4] L. Osborne, presentation to the GEM Muon System Meeting, Boston University, August 23,1991.

[5] A. Korytov, presentation to the GEM Muon System Meeting, Boston University, August 23,1991.

[6] E. Bayham, presentation to the Workshop on Magnets for LHC Detectors, CERN, May 13, 1991.

[7] The L* collaboration LOI, SSCL 1990.

[8] F. Udo, LHC workshop, CERN 90-10, Volume III, P. 219.

[9] See for example F. Udo, CMS meeting notes, CERN CMS-Gen/91-02.

[10] K. Ueno et al., *The Central Drift Chamber of the AMY Detector*, to be published.

[11] *Report of the 1990 HEPAP Subpanel on SSC Physics*, S. Drell, chairman; DOE/ER-0434 (January, 1990).

[12] V. Barger, K. Cheung, T. Han, R.J.N. Phillips, Strong W^+W^+ Scattering Signals at pp supercolliders, Preprint University of Wisconsin MAD/PH/556. Also references within.

List of Figures

1 A cross section of the GEM-baseline detector illustrating the sagitta technique used for muon momentum measurements. 4

2 $\Delta p_t/p_t$ *vs* $|\eta|$ for the GEM-baseline detector. 5

3 The proposed high field detector arrangement. 5

4 A cross section view of the proposed system illustrating the technique used for muon momentum measurements. The angle α is inversely proportional to the muon's transverse momentum. 6

5 An illustration of the correlation between the multiple scattering angle θ_{ms} and the error in the radial direction caused by the multiple scattering induced transverse displacement of the trajectory. The resulting error in α is smaller than θ_{ms}. 7

6 The distribution on α from a simulation of 1 TeV/c muons. The rms spread is 0.11 mrad. 8

7 The expected transverse momentum resolution ($\Delta p_t/p_t$) for the proposed system from measurements in the middle tracker only. 9

8 The expected transverse momentum resolution ($\Delta p_t/p_t$) for the case where one point from the inner tracker is used assuming a resolution of $\sigma = 50\mu$m at $R = 75$ cm. 9

9 The efficiency for Higgs$\longrightarrow \mu^+\mu^-\mu^+\mu^-$ *vs* the maximum $|\eta|$ of the muon acceptance (from ref. 2). 10

10 A plan view of the proposed high field system including the forward-backward iron-core toroid systems. 11

11 $\Delta p_t/p_t$ *vs* $|\eta|$ for the complete system, including the forward-backward iron toroid system. 11

12 (a) The distribution in angle of 1 TeV/c muons emerging from the iron return yoke (at 90°). (b) The distribution in the displacement Δ of the muon's trajectory from its straight line extrapolated position for a sample of 1 TeV muons. 13

13 The muon chambers layer geometry used in the simulation 17

14 The distribution of the total number of cells in the middle tracker which are hit by the 1 TeV/c incident muon and its accompanying particles. 18

15 The number of total layers per superlayer (out of 8) in which the muon came nearest to the wire ("good hit") in the cell it traversed. 19

16 The probability of having at least four good hits in the first N superlayers, where N=4,5,6,7, and 8 19

17 A view of the High Field Coil showing the diaphragm support in the middle of the coil. 21

18 An end view of the barrel iron showing the overall support. 21

19 A field map showing the field lines for the High Field coil. 22

20 The Z dependence of the magnetic field in the High Field Magnet. (The Z scale is in units of 10 m.) 22

21 The ratio of the jet energy contained in a cone R for $B = 5$ T to that contained in the same size cone for $B = 0$ *vs* the jet energy for various R values. 27

22 The actual jet energy fractions and the rms fluctuations of these fractions for an R value of 0.8 for $B = 0$ and $B = 5$ T. 27

23 The transverse momentum distribution of the isolated lepton from a 200 GeV top decay (dotted line), c and b quark decays (solid line) and c and b quark decay after isolation cut (dashed line) for (a) no magnetic field, (b) a 5 T field. 28

24 (a) Momentum and (b) η distribution of like-sign leptons from the $pp \longrightarrow W_L{}^+ W_L{}^+ X$ (dashed) interaction and the opposite-sign leptons from WW production (solid). 29

Contents

1 INTRODUCTION 3

1.1 Review of the GEM-baseline Scheme for Muon Measurements. 3

1.2 The Proposed High Field Option 4

1.2.1 Point-Slope Measurements of Muon Momenta 4

1.2.2 Forward-Backward Muon Coverage 8

1.2.3 "Robustness" 10

1.2.4 Triggering 13

1.2.5 Effects on the Rest of the Detector 14

1.3 Summary 15

2 Muon Detection Simulation 16

2.1 The Simulation 16

2.2 Results 18

2.3 Conclusions 20

3 Magnet and Mechanical Support 20

3.1 Magnet 20

3.2 Mechanical Assembly and Support 23

4 Effects of the High Field on Physics and Detectors 23

4.1 The Effect of the Field on the Inner Tracker 23

4.2 The Effect of the Field on the Endcap Region of the Middle Tracker 24

4.3 The Effect of the Field on Calorimetry 25

4.4 The Effect of the Field on Jet Detection 26

4.5 The Effect of the Field on Isolation Cuts 26

4.6 $pp \longrightarrow W_L{}^+ W_L{}^+ X$ 28

5 Conclusions 29